THERMODYNAMIC STUDIES OF OXYGEN IN LIQUID METALLIC SOLUTIONS.

A thesis submitted to the
University of London
for the degree of
Doctor of Philosophy

by

Kalarackel Thomas Jacob
Nuffield Research Group in Extraction Metallurgy
Royal School of Mines
Imperial College of Science and Technology

July 1970

ABSTRACT

The object of this research was to study dilute solutions of oxygen in molten metals and alloys. Solid oxide galvanic cells of the type

Pt, Ni-NiO / CaO - ZrO_2 / $[O]_{Metal}$, Cermet, Pt.

have been used to study the activity coefficient of oxygen in copper at 1100 and 1300°C and in lead at 1100°C and also to determine the free energy of formation of Cu_2O and PbO from 500 to 1200°C.

When a third element is added to a solution of oxygen in a solvent metal in the above cell, the change in e.m.f. is a measure of the effect of the additive on the activity coefficient of oxygen, provided there is no exchange of oxygen between the solution and the atmosphere around it and the additive does not cause the formation of an oxide phase. A technique based on this principle has been used to study the activity coefficient of oxygen in Cu-Ag, Cu-Sn and Cu-Pb alloys at 1100°C, Ag-Pb alloys at 1000°C, Pb-Sn alloys from 500 and 1100°C, and copper containing phosphorus from 1150 to 1300°C.

The oxygen concentration in copper and copper-silver alloys were determined by measuring the weight loss on reduction with hydrogen. Oxygen content of lead and lead rich alloys were determined by Baker's method, where the pressure of H_2O formed on reduction with hydrogen is measured manometrically.

The results obtained have been used to test the general applicability of proposed solution models for predicting the activity coefficient of oxygen in binary metallic solution. When the ratio of the activity coefficients of oxygen in two pure metals is less than 10, Belton and Tankin's random approximation has been found to give a good fit to experimental data on the activity of oxygen in the whole range of alloys formed by the two metals. However the temperature coefficients of the activity of oxygen indicate that the partial entropy and

enthalpy of oxygen in the alloys is very different from that predicted by the model. An alternative treatment is proposed which adequately explains the observed behaviour. When the ratio of the activity coefficients of oxygen in the pure metals is greater than 10, none of the proposed quasichemical models have been found to be satisfactory for all the systems, although Alcock and Richardson's equation adequately forecasts the behaviour of oxygen in copper - silver and lead - tin solutions.

CONTENTS.

INTRODUCTION

Many pyrometallurgical processes involve selective oxidation of impurities from multicomponent metallic solutions. At the high temperatures involved chemical kinetics is unlikely to be rate controlling[1] and, although the reaction rates are often determined by mass transport steps, the overall feasibility of the process can be assessed from chemical thermodynamics. A knowledge of the activity coefficients, especially of oxygen, in metallic solutions is therefore of great interest to extraction metallurgy. Several authors[2-6] have proposed models to predict the activity coefficient of oxygen in ternary solutions from a knowledge of the activity coefficients in the three binary solutions.

Although high temperature equilibria can be described quantitatively in terms of the free energies, the free energy function is of restricted value for the systematic consideration of stability, the derivation of thermochemical rules and the estimation of thermodynamic data. The quantities of fundamental importance are the partial enthalpies and entropies of components in solution. To test critically the models proposed for predicting oxygen activity coefficients, a knowledge of partial enthalpies and entropies of oxygen in ternary solutions would be helpful.

Galvanic cells incorporating solid oxide electrolytes are finding increasing use in the metallurgical industry as oxygen monitors in liquid metals[7-10]. In order to correlate the chemical potential of oxygen, obtained from the electromotive force (e.m.f.) of such cells, with the oxygen content in the metallic solution, a knowledge of the activity coefficient of oxygen is essential.

The main objective of the present study has been to generate accurate thermodynamic data which would enable a clearer understanding of the behaviour of oxygen in metallic solutions to be obtained, and provide information of practical utility. A critical evaluation of the models proposed to predict the activity coefficient of oxygen can be undertaken on the basis of the data obtained. In the past, the provision of precise

data has led to the development from ideal to regular and then quasichemical models of solution. It is believed that the present study and others of a similar type will not only provide data but will contribute to a further development of theoretical models.

CHAPTER I

THERMODYNAMICS OF METALLIC SOLUTIONS.

A large amount of data has been obtained on the thermodynamics of binary and ternary metallic solutions[11-12]. Yet the understanding of the variations in thermochemical functions on alloying has not advanced sufficiently to permit accurate prediction of these properties for uninvestigated systems to be made. The development of the theoretical treatments of alloy thermodynamics has been along three basic approaches: the electron theory of alloys, the statistical bond models and empirical relationships. A brief review is presented below. A more detailed discussion of some aspects of alloy thermodynamics has been published by Oriani[13] and Alcock[14].

ELECTRON THEORY OF ALLOYS.

On the basis of the free electron theory, the cohesive energy of pure metals can be expressed as a function of 'valence' (number of free electrons per atom), lattice parameter (or density), and the ionisation energy. Apart from the interactions of free electrons with the ion core and with one another, there exist pairwise interactions between neighbouring ions. The van der Waals attractive interaction is due to the mutual polarisability of ions, while the repulsion between ions is due to the overlap of the closed electron shells of the atoms. The cohesive energy can therefore be expressed as a sum of electronic contributions and pairwise interaction energies between ion cores. The cohesive energy of pure metals calculated from the free electron model agrees reasonably well with experimental values especially for the elements of Group IA of the periodic table. For other elements the agreement is poor, partly due to errors in the estimation of constants used in the calculation. Bolsaitis and Skolnick[15] have suggested the use of correction factors to obtain agreement between calculated and observed values for the cohesive energy of pure metals.

The energy changes on alloying may be viewed as resulting from a redistribution of electron densities around the ions and changes in the pairwise interactions between neighbouring ions. Bolsaitis and Skolnik[15] have used the electronegativities of metals as a measure of the electron

attracting power of ions and the difference in electronegativities as the driving force for changes in electron energy on alloying.

The cohesive energies of noble metal alloys calculated from the free electron model agree very well with the measured values. However, in alloys of polyvalent metals the agreement is less satisfactory, probably because the model does not treat factors such as binding of valence electrons, the differences between s and p electrons and the energy changes that may arise from the hybridisation of the s and p bands when a metal with electrons in the p band is alloyed with another metal with an unfilled s band. Also the model is not applicable to systems with covalent or ionic contribution to bonding. Considering that the heat of mixing (1 to 5 k cals) is obtained as the difference between the cohesive energy of the alloy and that of the pure components (20 to 80 k cals), the results of such calculations appear promising, especially in view of the possibilities for further refinements. The main drawback of this treatment is that the constants used in the calculations are available only for a few alloy systems. This treatment has not been developed for ternary solutions. The main success of the model has been the illustration of the importance of electronic contributions to the cohesive energy of alloys, this being ignored in chemical bond approximations. However, as in the chemical bond models, the exchange interaction energy between ion cores assumes pairwise central interactions, changes in electronic and vibrational specific heats have been neglected, and the co-ordination number is assumed to be independent of composition.

Striking experimental evidence of the importance of the electronic contribution to the energetics of alloy formation has been provided by Hume-Rothery and coworkers[16]. Their discovery of the importance of the electron/atom ratio (e/a) in determining phase equilibria has become a cornerstone of modern theory. Further, Schenck et al[17] have shown that the activity coefficient of carbon in Fe+C+X alloys varies in a highly systematic manner with the valence of the element X in the alloy. Himmler[18] has shown that the activity of hydrogen in copper alloys can be

accounted for qualitatively in terms of changes in the chemical potential of free electrons.

Heat effects associated with the solution of oxygen in common metals and alloys vary from 18 to 43 k cals per gram atom of oxygen. Although the introduction of oxygen into a liquid metal or alloy would considerably distort the electron distribution, it is likely that the electronic contribution to the energetics of solution is small compared with the large ion core interaction energies. The relative importance of the electronic contribution to the heat of mixing of two metals may be due to small ion core interaction energies between metallic ions, when compared with interaction energies between oxygen and metal ions. If this is true, statistical bond models, while unsatisfactory in the treatment of binary metallic systems and in the treatment of carbon, hydrogen and nitrogen in metallic solutions, may be useful in the thermodynamic treatment of dissolved oxygen and sulphur.

STATISTICAL BOND MODELS.

The statistical bond models assume that the total energy of the system can be obtained from the summation of the energies of bonds between pairs of atoms. The forces between atoms are assumed to be short range, so that only nearest neighbour interactions are considered. The energy of a bond between two atoms is assumed to be independent of its environment (or composition of the alloy) and the co-ordination number of atoms is assumed to be constant. The volume and vibrational changes upon formation of the solution from pure components may be neglected.

The simplest chemical bond model is Hildebrand's regular solution model, characterised by a finite heat of mixing and ideal entropy of mixing. The energy of formation of a binary regular solution may be expressed as:

$$\Delta G^{Ex\,M} = \Delta H^{M} \approx N_A N_B Z N \left[E_{AB} - \frac{(E_{AA} + E_{BB})}{2} \right] \quad \ldots\ 1$$

where E_{AA}, E_{BB} and E_{AB} represent the energies of A-A, B-B and A-B bonds, Z is the co-ordination number and N is the Avagadro's number. It has been suggested that the regular solution model lacks internal consistency,

since a finite heat of mixing necessarily implies deviations from ideal entropy. However, if $\Delta H^M < RT$, the deviations from ideal entropy may be negligible. It is possible that in some binary alloys the entropy effect due to deviations from perfect randomness of mixing may be offset by thermal contribution to the entropy of mixing, and the solution conforms to a regular model.

It will be seen from equation 1, that the heat of mixing is perfectly symmetrical with respect to composition. Most metallic systems, however, exhibit non-symmetrical heat of mixing. Kleppa[19] has tried to correlate the assymmetry in the heat of mixing with the valency of the metals forming the alloy. Hardy[20] has suggested the sub-regular solution model, in which the entropy of mixing is considered ideal and the function $ZN\left[E_{AB} - (E_{AA} + E_{BB})/2\right]$ is allowed to vary as a linear function of composition. Although in a few binary metallic systems $\Delta H^M/N_A N_B$ varies linearly with composition, the excess entropy of mixing is rarely zero.

The advantage of the regular solution model lies in its simplicity and the ease with which the treatment can be extended to ternary and multicomponent solutions. Toop[21,22] has shown that the activity coefficient of a component in a ternary regular solution can be expressed in terms of the data on the three binary systems by the equation:

$$\log \gamma_c \text{ (Ternary)} = \left[\frac{N_A}{(1-N_c)} \log \gamma_c(A) + \frac{N_B}{(1-N_c)} \log \gamma_c(B)\right] N_c - (1-N_c)^2 \left[\frac{\Delta G^{Ex}_{A-B}}{4.575\,T}\right] N_A/N_B \quad \ldots\ 2$$

when the composition of component c is close to zero, the above equation reduces to:

$$\log \gamma_c = N_A \log \gamma_c(A) + N_B \log \gamma_c(B) - \frac{\Delta G^{Ex}_{A-B}}{4.575\,T} \quad \ldots\ 3$$

This equation has been derived independently by Darken[23] and Alcock and Richardson[2]. Furthermore if binary A-B is ideal the equation simplifies to:

$$\log \gamma_c = N_A \log \gamma_c(A) + N_B \log \gamma_c(B) \quad \ldots\ 4$$

This expression was derived independently by Wagner[24]. The plot of $\log \gamma_c$

against composition will be linear. Such a behaviour will be referred to as 'ideal' in this thesis.

Alcock[25] has shown that equation 3 is valid even when binary systems C-A and C-B depart significantly from simple regular behaviour. Although this equation does not give a quantitative explanation of the behaviour of oxygen in metallic solutions, it predicts qualitatively the effect of the sign and magnitude of ΔG^{M}_{A-B} on the nature of deviations from 'ideal' linear variation of log γ_C with composition.

The quasi-chemical theory, first introduced by Guggenheim[26], considers the distribution of nearest neighbour pairs as affected by non-zero values of $\left[E_{AB} - (E_{AA} + E_{BB}) / 2\right]$. Applications of this theory to binary and ternary solutions have been reviewed by Oriani[13] and Lupis and Elliot[27]. Oriani has suggested that the application of this model to binary metallic solutions, in which the heats of mixing do not normally exceed a few k cals, is not very helpful. The model leads to free energies of mixing which are little different from those calculated using the regular solution model. The excess entropies predicted by the model are always negative, since only configurational factors are involved. Experimental evidence shows that positive excess entropies are frequent in binary metallic systems with positive heats of mixing. The quasichemical treatment shows that the main source of error in the application of the regular solution model to binary metallic solutions arises from factors other than that due to the neglect of clustering.

Due to the large differences between pairwise interaction energies in solutions of oxygen and sulphur in metals, the error due to the neglect of clustering may become more prominent in the application of the regular solution model to these solutions. Alcock and Richardson[3] have therefore applied the quasichemical model to predict the activity coefficient of oxygen (or sulphur) in binary metallic solutions, using data on the activity coefficient of oxygen in the pure metals and the activity coefficients of metallic components in the binary solution. They postulate a model for the ternary solution in which each atom makes Z nearest-neighbour bonds, and deduce the equation:

$$\left[\frac{1}{\gamma_{o(A+B)}}\right]^{1/Z} = N_A\left[\frac{\gamma_{A(A+B)}}{\gamma_{o(A)}}\right]^{1/Z} + N_B\left[\frac{\gamma_{B(A+B)}}{\gamma_{o(B)}}\right]^{1/Z} \quad \ldots. 5$$

where $N_A + N_B \approx 1$. The number of A and B atoms in the co-ordination shell around each O atom was deduced from the relation:

$$\frac{n\,(B\text{-}O)}{n\,(A\text{-}O)} = \frac{N_B}{N_A} \exp\left(w/zkT\right) \quad \ldots. 6$$

where w/z is the energy change which occurs when a B-O contact is changed to an A-O contact, by exchange of B atom in the co-ordination shell of O atom with an A atom in the body of the melt.

Equation 5 gives only a slight improvement on the regular solution model, when reasonable values of z (8 or 10) are used in the equation. Unreasonably low co-ordination numbers of 2 or 1 have to be assumed[3,28] in order to get reasonable agreement between the measured and predicted activity coefficients.

The significant terms in the quasichemical equation 5 arise from the manner in which the data on oxygen in the two pure metals is combined. The equation is not very sensitive to the way the data on the binary metallic solution is incorporated into the model, since the heat of mixing of metals rarely exceeds 5 k cals and is often lower. Therefore a model which assumes a co-ordination number of 2 for the oxygen atoms and a co-ordination of 8 or 10 for the metal atoms may predict activity coefficients not very different from that calculated from equation 5 with z = 2.

Gokcen[6] has attempted to calculate the activity coefficient of oxygen in a binary metallic solution without the aid of a solution model. From fundamental thermodynamics, Gokcen claims to have derived the equation:

$$\frac{1}{\gamma_{o(A+B)}} = N_A\frac{\gamma_{A(A+B)}}{\gamma_{o(A)}} + N_B\frac{\gamma_{B(A+B)}}{\gamma_{o(B)}} \quad \ldots. 7$$

This equation is identical to Alcock and Richardson's quasichemical

equation with z = 1. An equation based on fundamental thermodynamic relationships would be obeyed by all metallic solutions. The fact that equation 7 does not fit all available data on oxygen in metallic solutions suggests the presence of implicit assumptions in his mathematical treatment.

Belton and Tankins[4] have proposed a model based on the formation of molecular species of the type A-O and B-O between oxygen and metal atoms. The electron affinities and ionisation potentials of oxygen (and sulphur) are such that it is likely that they exist in solution as negatively charged ions. If this is true, the energy of the system would be lowered by the formation of solute-solvent screened dipoles. The authors cite the large heat of solution of oxygen in liquid metals and alloys, and the large depression of the surface tension of liquid metallic solutions by trace amounts of electronegative solutes like oxygen, as evidence for the formation of polar molecules in the liquid. It is argued that as long as the lifetimes of the 'species' are long with respect to the period of vibration they must be treated as separate entities for the evaluation of the entropy of solution. The partial molar entropy of solution of the solute would be given by a combination of the entropies of solution of the two 'species'. Two approximations are considered for the relative concentrations of the 'species': the random and the quasichemical.

In the random case the proportions of the species will be given by:

$$\frac{n\,(A\text{-}O)}{n\,(B\text{-}O)} = \frac{N_A}{N_B}$$

The mole fraction of the species is then

$$N'_{AO} = \frac{N_{AO}}{N_{N_O}} = N_A$$

$$N'_{BO} = \frac{N_{BO}}{N_O} = N_B$$

$$N'_{AO} + N'_{BO} = 1$$

In the quasichemical case,

$$\frac{n\,(A\text{-}O)}{n\,(B\text{-}O)} = \frac{N_A}{N_B} \quad \exp\,(-\Delta E / RT)$$

where ΔE is the exchange energy change that occurs when one B-O species is changed into an A-O species by exchange of a B atom with an A atom in the surrounding solvent. Since the solution of molecular species is considered to be ideal.

$$\frac{\Delta E}{RT} \approx \frac{\Delta H}{RT} = \left(\Delta \bar{H}_{O(A)} - \Delta \bar{H}_{O(B)} - \Delta \bar{H}_{A(A+B)} + \Delta \bar{H}_{B(A+B)}\right) / RT.$$

The mole fractions of the species are given by:

$$N'_{AO} = \frac{N_{AO}}{N_O} = \frac{N_A \beta}{N_B + N_A \beta}$$

$$N'_{BO} = \frac{N_{BO}}{N_O} = \frac{N_B}{N_B + N_A \beta}$$

where $\beta = \exp(-\Delta H/RT)$

The Gibbs Free Energy of solution of oxygen in A-B alloy is given by:

$$\Delta \bar{G}_{O(A+B)} = N'_{BO}\,(\Delta \bar{G}_{O(B)} - \Delta \bar{H}_{B(A+B)} + RT \ln N'_{BO}) + N'_{AO}\,(\Delta \bar{G}_{O(A)} - \Delta \bar{H}_{A(A+B)} + RT \ln N'_{AO}) \quad \ldots\ 8$$

Experimental results for the activity coefficient of oxygen in liquid Cu-Ni and Cu-Co[4,29] alloys and for the activity coefficient of sulphur in Cu-Ag[30] are in reasonable agreement with this theory in the random approximation. In these systems the ratio of the activity coefficients of the solute (oxygen or sulphur) in the two pure metals vary between 3 and 10. The quasichemical version of Belton and Tankins model does not fit any known data.

Formal thermodynamic description of the activity coefficient of oxygen would not be affected by the mechanistics of the association of atoms in solution, and as would be expected equation 8 reduces in the random approximation to equation 3, except for the terms denoting the entropy of mixing of the oxide species.

Presumably the random approximation can be justifiably used only in systems where the ratio of the activity coefficient of oxygen in the

two pure metals is less than 10, i.e. $\Delta\bar{G}_{O(B)} - \Delta\bar{G}_{O(A)} = RT\ (\log \gamma_{O(B)} - \log \gamma_{O(A)}) < RT$. In such a case the difference in energy between an A-O molecule and a B-O molecule is likely to be less than kT, and there is little justification for introducing an entropy term for the mixing of the two oxide species. The apparent agreement between Belton and Tankin's random model and some experimental data referred to earlier must therefore be viewed with caution. Further discussion of the entropy effects on dissolution of oxygen will be presented later in this thesis.

Mathieu et al[31,32] have devised a 'surrounded atom' model for binary solutions. It is derived from Guggenheim's quasichemical model and uses the same basic assumptions. However, the basic entity is no longer the pair of neighbouring atoms, but the atom in the field of force of its z neighbours. This concept is better suited than that of pairwise interaction to the case of the non-central forces to which metallic cohesion is attributed. The potential energy of the solution is taken as the sum of the potential energies of each A and B atom in the field of force of its neighbours. The potential energy of an atom will vary with the composition of its surrounding shell. The authors suggest a parabolic form for the variation of the potential energy with composition. Since the four adjustable parameters required to represent all the thermodynamic properties of a binary system must be deduced from experimental data, the model does not promise well for the prediction of thermochemical values. The model may be useful for the storage of thermochemical data on a binary system in terms of four parameters, and would simplify the use of computers for thermochemical calculations.

Lupis and Elliot[33] have also considered a similar model: the 'central atoms' theory. Their treatment assumes complete randomness of mixing, but the effect of the change in vibrational contribution to the

entropy function is included.

Neither the 'surrounded atom' model nor the 'central atoms' approximation can easily be extended to ternary solutions, but suggest that vibrational contributions to entropy may not be neglected.

EMPIRICAL CORRELATIONS.

Considerable effort has been made to correlate the thermodynamic properties of binary alloys with (1) difference in size of the atoms (2) difference in electronegativity and (3) difference in valency and electron concentration[19,34]. Sufficient data exist to illustrate the importance of all these factors on the thermochemical properties of alloys. For any system the thermochemical properties result from a complex interplay of all the factors and it is difficult to assess the relative importance of each factor.

One of the most important empirical results that has emerged from the study of metallic solutions is the relationship between the heat of mixing and excess entropy of mixing of binary solutions. Kubaschewski[35] has shown that the maximum (or minimum) excess entropies may be approximately related to the maximum (or minimum) heat of mixing in binary alloys by the relationship.

$$\Delta H_{max} = 2300 \cdot \Delta S^{Ex}_{Max} \quad \ldots\ 9$$

Gallagher and Oates[36] have reviewed data on hydrogen in solid metals and have shown an approximately linear relation between the excess partial molar entropy and the partial molar enthalpy of hydrogen. Analysing the existing data in liquid Fe-N-X, Cu-S-X, Fe-H-X, and Al-H-X groups of solutions, Chipman and Corrigan[37] have demonstrated a relationship between the changes in partial molar enthalpy and entropy of the solute (Hydrogen, Nitrogen or Sulphur) on adding a third component X. Such correlations draw attention to the importance of the vibrational contribution to the entropy term.

Richardson[38] found an empirical correlation between the difference

of $\Delta H^{\circ}_{f,25^{\circ}C}$ for FeO and that for many of the oxides of interest in the deoxidation of steel and the effect of the deoxidising element on the activity coefficient of oxygen in molten iron. This rule is useful for very rough estimations, when the difference in the heat of formation of the oxides is large. Pearson and Turkdogan[39] have suggested that in applying Richardson's rule to compare the effect of elements of different valencies, the use of the free energy of formation per gram mole of the compound or per gram atom of a dissolved element is unsatisfactory because it involves the combination of different numbers of atoms. They suggest the use of free energy of formation of oxide per 'mean gram atom'.

REPRESENTATION OF THERMODYNAMIC DATA.

Darken[40,41] has shown that in general the power-series representation[42] of the activity coefficients is inappropriate for binary metallic solutions. For most liquid binary metallic systems there seem to exist two terminal regions in which the thermodynamic behaviour is relatively simple and may be expressed by equations of the form:

Region I: $0 < N_B < N_B'$

$$\log \gamma_A = \alpha_{AB} (1-N_A)^2 \qquad \log \frac{\gamma_B}{\gamma_B^{\circ}} = \alpha_{AB} (N_A^2 - 1)$$

$$\Delta \bar{H}_A = \mathcal{L}_{AB} (1-N_A)^2 \qquad \Delta \bar{H}_B = \Delta \bar{H}_B^{\circ} + \mathcal{L}_{AB} (N_A^2 - 1)$$

Region II: $N_B'' < N_B < 1$

$$\log \gamma_B = \alpha_{BA} (1-N_B)^2 \qquad \log \frac{\gamma_A}{\gamma_A^{\circ}} = \alpha_{BA} (N_B^2 - 1)$$

$$\Delta \bar{H}_B = \mathcal{L}_{BA} (1-N_B)^2 \qquad \Delta \bar{H}_A = \Delta \bar{H}_A^{\circ} + \mathcal{L}_{BA} (N_B^2 - 1)$$

These two composition regions are connected by a central or transition region in which the thermodynamics appear to be more complicated.

This treatment has been extended to ternary solutions[43].

In the vicinity of a single component selected as solvent (A) the excess free energy and the activity coefficients of each component in the ternary solution may be expressed as:

$$\frac{\Delta G^{Ex}}{2.303\,RT} = N_B \log \gamma^{\circ}_B + N_C \log \gamma^{\circ}_C - \alpha_{AB} N_B^2 - \alpha_{AC} N_C^2 - (\alpha_{AB} + \alpha_{AC} - \alpha_{BC}) N_B N_C \quad \ldots\ 10$$

$$\log \gamma_A = \alpha_{AB} N_B^2 + \alpha_{AC} N_C^2 + (\alpha_{AB} + \alpha_{AC} - \alpha_{BC}) N_B N_C \quad \ldots\ 11$$

$$\log \frac{\gamma_B}{\gamma^{\circ}_B} = -2\alpha_{AB} N_B + (\alpha_{BC} - \alpha_{AB} - \alpha_{AC}) N_C + \alpha_{AB} N_B^2 + \alpha_{AC} N_C^2 + (\alpha_{AB} + \alpha_{AC} - \alpha_{BC}) N_B N_C \quad \ldots\ 12$$

$$\log \frac{\gamma_C}{\gamma^{\circ}_C} = -2\alpha_{AC} N_C + (\alpha_{BC} - \alpha_{AB} - \alpha_{AC}) N_B + \alpha_{AB} N_B^2 + \alpha_{AC} N_C^2 + (\alpha_{AB} + \alpha_{AC} - \alpha_{BC}) N_B N_C \quad \ldots\ 13$$

Equation 10 contains five coefficients, four of which are obtainable from the two binary systems. The fifth (α_{BC}) is only obtainable from measurements on the ternary. If the solution is considered regular (i.e. if $\log \gamma^{\circ}_B = \alpha_{AB}$ And $\log \gamma^{\circ}_C = \alpha_{AC}$) equation 10 reduces to

$$\frac{\Delta G^{Ex}}{2.303\,RT} = \alpha_{AB} N_A N_B + \alpha_{AC} N_A N_C + \alpha_{BC} N_B N_C$$

where α_{BC} may be considered to be a characteristic of the binary system B-C.

Wagner[44] and Chipman[45] have suggested the use of interaction parameters defined by:

$$\epsilon^B_C = \lim_{N_A \to 1} \frac{\partial \ln \gamma_C}{\partial N_B} \quad \ldots\ 14$$

$$\epsilon^B_B = \lim_{N_A \to 1} \frac{\partial \ln \gamma_B}{\partial N_B} \quad \ldots\ 15$$

The interaction parameter may be considered as a coefficient in a Taylor series expansion for the logarithm of the activity coefficient

$$\ell n\gamma_C = \ell n\,\gamma_C^{\circ} + \left[N_C \left(\frac{\partial \ell n \gamma_C}{\partial N_C} \right)_{N_A \to 1} + N_B \left(\frac{\partial \ell n \gamma_C}{\partial N_B} \right)_{N_A \to 1} \right]$$

$$+ \left[1/2\, N_C^2 \left(\frac{\partial^2 \ell n \gamma_C}{\partial N_C^2} \right)_{N_A \to 1} + N_C N_B \left(\frac{\partial^2 \ell n \gamma_C}{\partial N_B \partial N_C} \right)_{N_A \to 1} + \ldots \right] \quad \ldots. \; 16$$

If all except the first order terms are neglected, the expansion for the logarithm of the activity coefficient becomes linear with respect to mole fractions of solutes present

$$\ell n\gamma_C = \ell n\gamma_C^{\circ} + N_C \epsilon_C^C + N_B \epsilon_C^B + \ldots\ldots \quad \ldots. \; 17$$

It can be demonstrated from the Gibbs-Duhem equation that

$$\epsilon_C^B = \epsilon_B^C \quad \ldots. \; 18$$

This reciprocity relationship is an important advantage of the Wagner representation. Equation 17 is strictly valid only when the solution is very dilute in B and C. The seriousness of the thermodynamic inconsistency of the ϵ formalism at finite concentrations depends on the system under consideration and on the solute concentrations. If the variation of the logarithm of the activity coefficient of a solute (oxygen) with the mole fraction of each of the alloying elements in a metallic solvent is found to be linear, equation 17 may be used to compute the activity coefficient of the solute in a multicomponent system. At high concentrations of the alloying elements, where the variation of $\log \gamma_{solute}$ with mole fraction is no longer linear, the graphical method of Sherman and Chipman[46] may be used to evaluate the activity coefficient of the solute in a multi-component solution.

Darken's quadratic formalism is expected to represent data over a larger concentration range than the ϵ formalism, unless higher order terms are included in the latter, although the extension of Darken's equation to multicomponent systems has not been developed.

CHAPTER 2

1. REVIEW OF LITERATURE ON OXYGEN IN LIQUID METALS.

Thermodynamic studies of dilute solutions of oxygen in a number of liquid metals of industrial interest (Fe, Ni, Co, Cu, Ag, Pb, and Sn) have been reported. The results are summarised in table I, in terms of the standard free energy of solution per gram atom of oxygen. The standard state of the dissolved oxygen is the 1 at. pct. solution and the reference state is the infinitely dilute solution. Since the metals Fe, Ni and Co have not been included in systems selected for the present study, detailed discussion will not be presented on the behaviour of oxygen in these metals.

Fe, Ni and Co melt above 1450°C and the accuracy of thermochemical measurements at the high temperatures involved does not permit detailed analysis of interactions between atoms in solution. Besides, the activity coefficients of oxygen in liquid Fe, Co and Ni have been studied only over a narrow temperature range (200°C), so that the partial enthalpies and entropies derived there-from are of limited accuracy.

OXYGEN IN SILVER.

Solubility of oxygen in liquid silver has been studied as a function of oxygen pressure and temperature by Sieverts and Hagenacker[55], Donnan and Shaw[56], Parlee and Sacris[57], Diaz et al[58], Baker and Talukdar[59], Block and Stuwe[60], and Fisher and Ackermann[61]. All except the results of Fisher and Ackermann are reasonably concordant, and the best equation for the solubility of oxygen at one atmosphere pressure as a function of absolute temperature is[58]:

$$\log [\text{wt \% O}] = 737.6/T - 1.107$$

This corresponds to $\Delta\bar{H}_0$ of - 3,380 cals per gram atom and $\Delta\bar{S}_0$ of - 1.23 cal deg^{-1} at 1 gram atom %. Oxygen in silver is found to obey Sievert's law upto an oxygen pressure of 1 atm; although at high

TABLE I

Standard Free Energy change for the reaction

$$\tfrac{1}{2}\,O_2 = [O]_{\text{Metal, 1 at \%}}$$

Solvent	ΔG°	Reference
Fe	-27,840 -3.16T	Dastur and Chipman[46]
	-27,890 -3.29T Log to = -0.057 at % O *	Floridis and Chipman[47]
	-16,890 -9.41T	Samarin et al[48]
	-29,570 -2.62T	Gokcen[49]
	-29,700 -2.99T	Belton et al[50]
	-29,090 -2.93T	Fisher and Haussmann[52]
	-43,290 +5.16T	Fisher and Achermann[51]
	-37,700 + 2.35T	Fisher and Janke[52]
	-38,982 +3.14T	Schenck and Gerdom[53]
Ni	-23,270 +1.33T	Fisher and Ackermann[51]
	-18,065 -1.78T*	Bowers[54]
	-18,064 -1.57T	Samarin et al[48]
	-11,920 -4.86T	Belton and Tankins[4]
Co	-23,480 -0.11T	Fisher and Ackermann[51]
	-14,700 -4.91T	Belton and Tankins[4]
Ag	-3,380 +1.23T*	Diaz and Richardson[58]
Cu	-20,317 +1.474T*	Diaz and Richardson[68]
Pb	-28,283 +2.902T*	Alcock and Belford[64] (corrected)
Sn	-43,610 +6.131T*	Alcock and Belford[66] (corrected)

*Selected value.

To obtain the values in the table the following data[69] were used:

$H_2 + \tfrac{1}{2}\,O_2 \rightarrow H_2O$

$\Delta G^\circ = -60,090 + 13.84T$ (Janaf, 1961)

$CO + \tfrac{1}{2}\,O_2 \rightarrow CO_2$

$\Delta G^\circ = -66,560 + 20.08T$ (1700 - 2100°K) (Janaf, 1965)

$\Delta G^\circ = -66,982 + 20.323T$ (1300 - 1800°K) (")

pressures, significant positive deviations are reported[59], even after correcting for the non-ideality of oxygen gas at high pressures. If the activities are plotted on the assumption that the dissolved oxygen is not atomic but is combined as Ag_2O, the activity curves become more ideal.

OXYGEN IN LEAD.

Richardson and Webb[62] have shown that earlier work on the saturation solubility of oxygen in liquid lead, determined by analysing cores of small metal ingots equilibrated with PbO, is in considerable error. At low temperatures the errors arise from inclusion of PbO, small amounts of surface oxidation and the presence of oxidisable impurities such as iron. At high temperatures the ejection of PbO from the metal during cooling and solidification caused the results to be too low.

The loss of or inclusion of oxides during cooling liquid metal containing oxygen is of considerable importance to this study. The loss of oxygen from the liquid metal as oxide is likely to occur on cooling when:

(i) the oxygen content of the metal is greater than the eutectic or monotectic composition. The oxide is then the first phase to separate from the liquid on solidification.

(ii) the temperature of the experiment is very much higher than the melting point of the metal, and

(iii) where the saturation solubility increases rapidly with temperature.

The exact amount of oxygen lost would be a function of the direction and rate of solidification and the geometry of the container. Very rapid quenching can in principle avoid the segregation of the oxide. However, in normal quenching methods, where a sample of the metal is withdrawn into a water cooled compartment, segregation is difficult to avoid.

Solubility of the refractory container in the oxide phase in

equilibrium with the oxygen saturated metal would tend to produce a smaller value of saturation solubility. The effect of crucible materials on the saturation solubility of oxygen in copper, for example, is well illustrated by Kuxmann et al[63].

Inclusion of the oxide phase in the metal during solidification may be detected by following the variation of the activity of oxygen with composition in unsaturated solutions of oxygen in the metal.

When the eutectic composition is very close to the pure metal (as in Pb + O and Sn + O systems) and the saturation solubility increases sharply with temperature, the only reliable methods for determining the saturation solubility are those of Richardson and Webb[62], and Alcock and Belford[64].

Richardson and Webb equilibrated PbO (ℓ) with liquid lead (held in a separate container) via the vapour phase, in a closed assembly, at temperatures from 1000 to 1200°C. An inert gas atmosphere was maintained inside and outside the assembly. After equilibration at the desired temperature, the assembly was cooled and the metal was analysed for oxygen along with the container. All the oxygen that separated from the metal as oxide during solidification would thus be included in the analysis. However, the method is limited to temperatures at which the oxide has appreciable vapour pressure.

Alcock and Belford[64] have measured the saturation solubility of oxygen in Lead from 510 to 700°C by coulombic titration of oxygen into the lead, through a solid electrolyte having an oxygen ion transport number greater than 0.99. The galvanic cell used was:

Pt, Ir, Pb(ℓ) - O / 0.85 ZrO_2 + 15% MgO / Ni-NiO, Pt.

The change in oxygen content of the lead is related to the number of coulombs passed across the cell by

$$q = (2Fm / M)\left[\Delta C / (100 - \Delta C)\right]$$

where ΔC is the change in atom % [O] in Pb, m is the weight of Pb in grms,

and M is the atomic weight of Pb. The saturation solubility is represented by:

$$\log (N [Pb] \text{ at.}\% [O]) = -(5220 \mp 120)/T + (4.53 \mp 0.14)$$

If these results are extrapolated to high temperature, they are in good agreement with the measurements of Richardson and Webb. From the e.m.f. of the cell with unsaturated solutions of oxygen, Alcock and Belford deduced $\Delta\bar{H}_0$ of -28,540 ∓ 630 cals per gram atom and $\Delta\bar{S}_0$ of -3.4 ∓ 0.75 cals deg^{-1} at one atom pct. concentration, using the value of Young and Tomlinson for the oxygen potential of the Ni-NiO reference electrode. More recently Steele[65] has evaluated all the measurements on the free energy of formation of NiO and the best equation has been suggested as:

$$\Delta G^{o}_{T} = -111,930 + 40.58T \text{ cals. per mole of Oxygen.}$$

The selected values of $\Delta\bar{H}_0$ = -28,283 cals/grm. atom and

$\Delta\bar{S}_0$ = -2.902 cal/g atom degree at 1 atom % correspond to measured data of Alcock and Belford and Steele's value for the chemical potential of the reference electrode.

Fisher and Ackermann[61] measured the partial pressure of oxygen over unsaturated solutions of oxygen in lead using the cell;

Pt, air / stabilised ZrO_2 / melt, Pt (?)

and determined the oxygen content of the melts by analysis of suction samples removed from silica sampling tubes. For reasons already mentioned their sampling technique is not suitable for Pb + O solutions. The $\Delta\bar{G}_0$ obtained is 2 k cals higher than that reported by Alcock and Belford and is therefore rejected.

Oxygen in lead is found to obey Sievert's law[64,61].

OXYGEN IN TIN.

Alcock and Belford[66] have measured the activity coefficient and solubility of oxygen in liquid tin from 500 to 750°C using a galvanic cell similar to that used by the same authors in the study of oxygen in lead. Extrapolation of their saturation solubility data to high

temperatures agrees very well with the measurements of Carbo[67] from 900 to 1100°C, using a technique similar to Richardson and Webb. After correcting for the chemical potential of the reference electrode, Alcock and Belford's results at 1 at % oxygen may be expressed by

$$\Delta\bar{G}_O = -43{,}610 + 6.131T \quad \text{cals/gr. atom.}$$

Fisher and Ackermann[61] report a value of $\Delta\bar{G}_O = -46{,}060 + 7.98T$ cals/gr. atom, while Block et al[60] obtain $\Delta\bar{G}_{O,\ 1200^oC} = -35{,}200$ cals/gr.atom. These results are in fair agreement with Alcock and Belford's data. Since both these authors analysed metal specimens removed from silica sampling tubes, it must be concluded that the segregation of the oxides of tin during solidification is less significant than in the case of lead. This may partly be due to the lower solubility of oxygen in tin.

All the authors suggest that Sieverts Law is obeyed till saturation.

OXYGEN IN COPPER.

Previous work on the thermodynamics of oxygen in liquid copper has been reviewed by Diaz and Richardson[68], who have recommended the best equation for the standard free energy change of the reaction:

$$CO_2 = CO + [O]_{Cu}$$
$$\Delta G^o = +46{,}665 - 18.849T$$

The best equation for the standard free energy of formation of carbon dioxide is[69]:

$$CO + \tfrac{1}{2}O_2 = CO_2$$
$$\Delta G^o = -66{,}982 + 20.323T \qquad (1300 - 1800^oK)$$

combining the above equations,

$$\tfrac{1}{2}O_2 \rightarrow [O]_{Cu}$$
$$\Delta G^o = -20{,}317 + 1.474T.$$

Sano and Sakao[70], Young and Tomlinson[29], Diaz and Richardson[68], Rickert and Wagner[71], Osterwald et al[72] have shown that oxygen, in copper deviates negatively from Sievert's Law, although these authors do not agree on the exact magnitude of the deviation. Belton and Tankins[4],

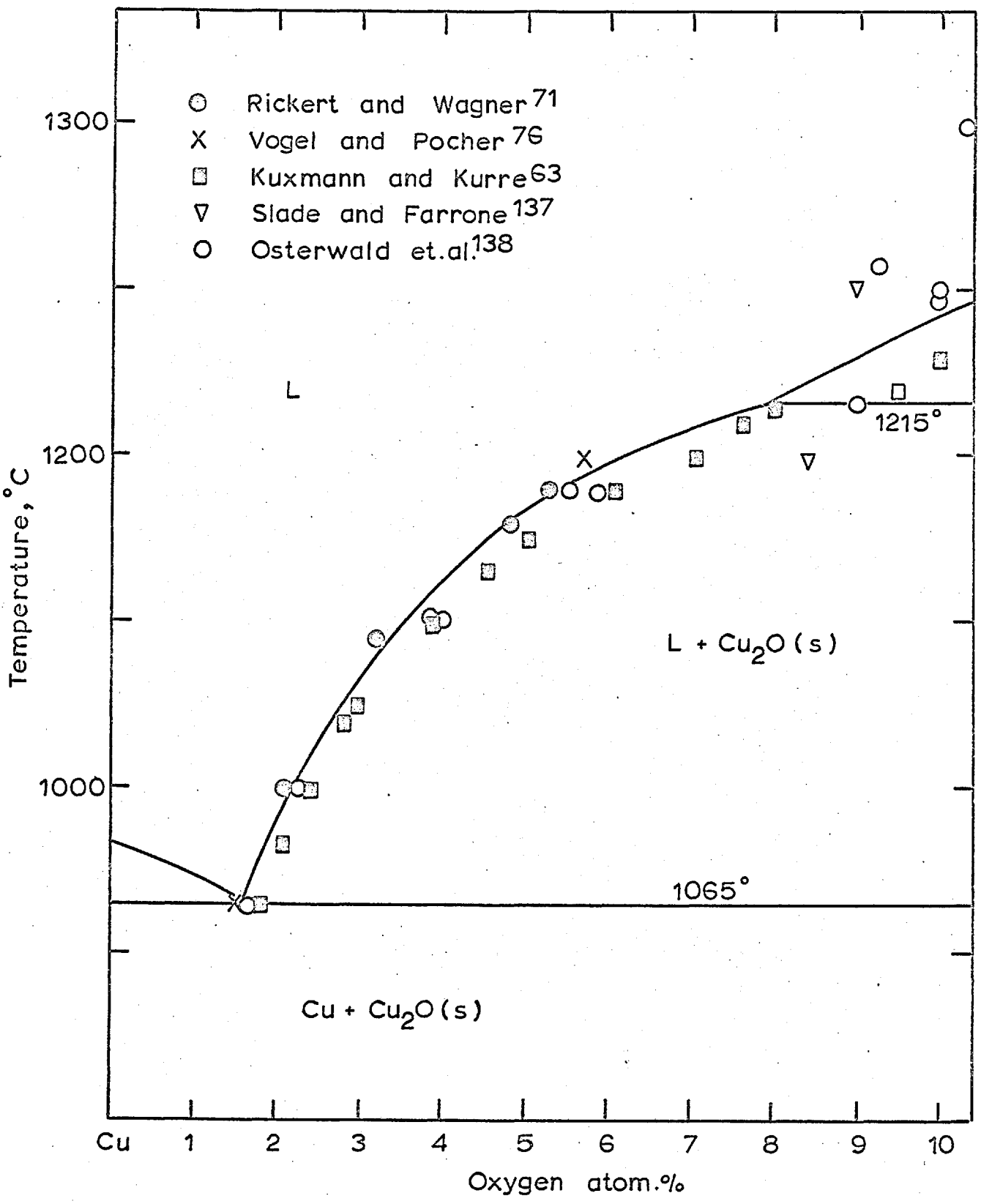

Fig.1. SATURATION SOLUBILITY OF OXYGEN IN LIQUID COPPER

Fisher and Ackermann[51], Pluschkell and Engell[73], Fruehan and Richardson[28], Wilder[74], and Kozuka et al[75], on the other hand, report that oxygen in liquid copper obeys Sievert's law. The saturation solubility of oxygen calculated from thermodynamic data does not agree with measured values, unless deviation from Sievert's Law are taken into consideration.

Data on the saturation solubility of oxygen from 1000 to 1300°C is presented in Fig 1. In evaluating the best curve through the experimental points, greater weight has been given to Rickert and Wagner's[71] coulombic titration method, and the thermal analysis of Vogel and Pocher[76]. Other investigators quenched copper in equilibrium with copper oxide at high temperatures and analysed the copper for oxygen. They failed to ensure that the oxide phase was not trapped in the metal during the quench.

The correlation between the heat of solution and entropy of solution of oxygen in liquid Ag, Cu, Pb, and Sn is shown below:

Solvent	$\Delta \bar{H}_0$ at 1 at %	$\Delta \bar{S}_0$ at 1 at %	$-\Delta H^\circ_{298}$ oxide kcals/gr. at 0
Ag	- 3,380	- 1.23	- 7.42
Cu	- 20,317	- 1.474	- 40.30
Pb	- 28,283	- 2.902	- 51.94
Sn	- 43,610	- 6.131	- 61.40

The data on oxygen in Fe, Ni, and Co (Table 1) does not agree with this pattern of behaviour. As mentioned earlier, the 'second law' evaluation of heats and entropies above the melting point of these metals may not be sufficiently accurate to permit detailed discussion of the causes for this departure. Nonetheless, it is quite possible that the bonding and configurational effects of oxygen in the metals of the 8th group differ from those for the metals of the first four groups of the periodic table.

2. REVIEW OF LITERATURE ON OXYGEN IN BINARY ALLOYS.

Due to the technological importance of understanding the various equilibria in the refining of iron, numerous investigations have been carried out on the effect of a third element on the activity coefficient of oxygen in liquid iron. The selected results are summarised in Table 2. Table 3 includes data on oxygen-additive interactions in other metallic solvents. Very few experiments are reported on the variation of the activity coefficient of oxygen with temperature in metallic alloys.

The techniques used for the study of the activity coefficient of oxygen in alloys may be classified as follows:

(a) Equilibration Techniques.

In this method the alloy is equilibrated with a CO/CO_2 or H_2/H_2O gas mixture at the required temperature. The alloy is quenched or sampled after equilibrium is attained and the oxygen in the metal subsequently analysed. Many early studies using this technique suffered from thermal segregation in the gas mixture. If precautions are taken to avoid thermal segregation, the partial pressure of oxygen over the metallic solution can be defined with an accuracy of $\mp$ 1% when favourable gas ratios are used. Often the components of the alloy have appreciable vapour pressures at the temperature of the experiment. Reaction between incoming gas mixture and the metal condensed on the cooler zones of the reaction tube can alter the gas ratios and lead to significant error. Reaction between the gas mixture and the alloy specimen during quenching can alter the oxygen content of the alloys. For this reason, the replacement of the reactive gas mixture with an inert gas is often recommended before quenching or sampling.

The main difficulty of this technique is in obtaining samples that truly represent quenched in high temperature equilibrium. With low oxygen concentration in the alloy, significant errors may occur in sampling and analysis. The accuracy of this technique is generally

TABLE II

Effect of Additives on the activity coefficient of oxygen in liquid iron at 1600°C.

$$e_O^x = \left(\frac{\partial \log \gamma_O}{\partial \text{ wt \% } x}\right)_{N_{Fe} \to 1}$$

$$\epsilon_O^x = 230 \frac{Mx}{M_{Fe}} e_O^x + \frac{M_{Fe} - M_x}{M_{Fe}}$$

Element (x)	$e_O^x \cdot 10^2$	Range of validity, wt.%	References
Al	- 100		77
Au	- 0.5	0 - 30% Au	47
C	- 44.5	0 - 6% C	79 to 85
Cb (Nb)	- 14	0 - 15% Cb	86
Co	+ 0.77	0 - 15% Co	47, 87 to 89
Cr	- 4.0	0 - 12% Cr	88, 89, 90-92, 95, 96
Cu	- 1.1	0 - 15% Cu	47, 78
Mn	- 2.6		45, 93, 96
Mo	+ 0.3	0 - 20% Mo	47, 88, 97
N	- 14		98 to 101
Ni	+ 0.55	0 - 20% Ni	88, 89, 92, 102
P	+ 3.0	0 - 4% P	83, 105-109
Pt	+ 0.45	0 - 20% Pt	47
S	- 12	0 - 4% S	45, 83
Sb	- 2.3	0 - 15% Sb	95
Si	- 16		104, 110
Sn	- 1.2	0 - 10% Sn	88, 95
Ti	- 18.7		103
V	- 11	0 - 1% V	89, 95, 96
W	+ 0.85	0 - 20% W	47, 88, 95, 97

TABLE III

Effect of additives on the activity coefficient of oxygen in liquid metals

Solvent	Additive (x)	ϵ_O^x	Temp.	Ref.
Ni	S	- 12	1600°C	111
	Fe	- 5.5	1600°C	111
	Co	- 1.0	1600°C	111
	Cu	- 1.8	1500°C	4, 29
Co	S	- 17	1600°C	111
	Fe	- 3.3	1600°C	111
	Ni	- 0.46	1600°C	111
	Cu	- 1.95	1550°C	4, 29
Cu	Pt	+ 8.2	1200°C	29
	Au	+ 3.8	1200°C	29
	Ag	- 3.8	1200°C	29
		- 0.95	1200°C	60
		+ 1.7	1200°C	28
	Ni	- 7.45	1200°C	29, 112
		- 2.8	1500°C	4, 29
	S	- 18.5	1206°C	70
	Co	— 62.8	1200°C	112
		- 10	1500°C	4, 29
	Sn	- 3.4	1200°C	60,70
		- 145	1200°C	28
	Fe	- 552.7	1200°C	112

Continued...

Solvent	Additive (x)	ϵ_0^x	Temp.	Ref.
Ag	Pd	11,930/T - 1.43		113
		6,945/T + 2.52		114
	Pt	8,480/T + 0.66		113
		8,203/T + 1.61		114
	Au	6,907/T + 1.78		113
		5,989/T + 2.62		114
	Cu	-267,690/T + 166.42		115
	Sn	- 44	1200°C	60
Sn	Ag	+ 4.1	1200°C	60
	Cu	+ 3.0	1200°C	60

about $\mp$ 10% in the activity coefficient, although in some cases accuracies of $\mp$ 2% have been attained. The technique is of limited use if gas ratios of the order of 1000 : 1 need to be used to establish the desired oxygen potential.

(b) Solubility Measurements.

In principle an element which lowers the activity coefficient of oxygen in the solvent, will increase the saturation solubility of oxygen in the solvent, and vice versa. Therefore determination of the effect of the additive on the saturation solubility of oxygen in the solvent enables the activity coefficient to be calculated. The method is however not applicable to alloys where the additive forms more stable oxides than that of the solvent, or where mixed oxides form over alloys saturated with oxygen.

(c) Determination of Deoxidation Equilibria.

When the additive forms a very much more stable oxide than the solvent, as in the Fe-Al-O system, the concentration of oxygen in the alloy in equilibrium with the stable oxide (Al_2O_3) may be determined as a function of the additive (Al) concentration. From the equilibria:

$$Al_2O_3 = 2[Al] + 3[O]$$

it follows that,

$$\log K = 2 \log [\%Al] + 3 \log [\% O] + 2 \log f^{Al}_{Al} + 3 \log f^{Al}_{O}$$

The first two terms on the right may be called $\log K'$ and this quantity, representing experimental results, is plotted as a function of pct. Al. From the slope of the line ϵ_O^{Al} may be evaluated provided f^{Al}_{Al} is known from the activity data on binary Fe-Al. In general this technique is of limited applicability. For example, if the phase in equilibrium with oxygen saturated Fe-Al alloys was Iron Aluminate, rather than Al_2O_3, knowledge of the composition of the slag phase and the activity coefficient of Al_2O_3 in the aluminate would be necessary. Small errors in analysis of dissolved elements result in large

discrepancies in the computed activity coefficients.

(d) Solid Oxide Galvanic Cell Techniques.

Solid oxide galvanic cells can be used to determine the oxygen potential in solution of oxygen in metals and alloys. In order to obtain the activity coefficient of oxygen, samples of the metal must be analysed for oxygen, and comparable problems are involved as in gas equilibration techniques. However, solid oxide galvanic cells can be used to measure oxygen potentials where inconvenient ratios of CO/CO_2 or H_2/H_2O would be involved.

Fruehan and Richardson[28] have shown that solid oxide galvanic cells can be used to measure the effect of additives on the activity coefficient of oxygen in liquid metallic solvents, without analysing the alloy for oxygen, provided the activity coefficient of oxygen in the solvent metal is known and certain experimental conditions are satisfied. If an alloying element is added to an unsaturated solution of oxygen in the solvent metal in the cell:

$$\text{Pt, Ni-NiO / Solid Electrolyte / } [O]_{\text{Solvent}}\text{, Pt}$$

the change in e.m.f. constitutes a direct measure of the change in the activity coefficient, provided the concentration of oxygen in solution has not been altered by the addition.

$$\text{Log } f_0^i = - \frac{n F \Delta E}{4.6.\ R T}$$

If the alloying addition is free of oxygen, part of the change in e.m.f. would be due to the dilution of the original solution. The e.m.f. change due to the change in oxygen concentration must then be subtracted from the total change in e.m.f. to obtain ΔE in the above equation. The oxygen concentration in solution after the alloying addition may be calculated from mass balance provided:

(a) There is no exchange of oxygen between the metal, the inert atmosphere, refractory container and conductory lead. This may be

indicated by the constancy of the e.m.f. over prolonged periods at all compositions.

(b) The addition of the alloying element does not result in the formation of an oxide phase, solid, liquid or gaseous. In many cases, it is possible to calculate from known thermochemical data, the oxygen potentials at which the oxide phase would form. Formation of a solid solution between an oxide and the refractory container or the solid electrolyte can enhance the feasibility of oxide formation.

Discussion of the requirements of solid electrolytes for use in galvanic cells will be presented in the next chapter.

RESEARCH PROGRAMME.

Part I: In order to understand the behaviour of oxygen in binary metallic solutions more fully, it was considered preferable to choose systems and experimental temperatures where the activity coefficient of oxygen could be determined over the whole range of compositions between the two pure metals. To permit comparison of the measured activity coefficients with the equations derived on the basis of various models, the thermodynamic data on the mixing of the two metals should be accurately known. Since thermochemical properties can be measured with good accuracy up to 1300°C, and since the activity coefficient of oxygen over the whole range of Cu-Ag[28,29,60], Cu-Sn[28,60], Cu-Ni[4,29] and Cu-Co[4,29] alloys have been determined, it was decided to start studies on oxygen in alloys of Copper with Silver, Tin, Phosphorus and Lead at 1100°C. There are discrepancies in the reported data on Cu + Ag + O and Cu + Sn + O systems and hence a reinvestigation of these systems was considered to be useful. As tin is a major alloying element in copper, the deoxidation equilibria for tin in copper would be of practical interest.

Phosphorus is commercially used as a deoxidiser in copper-making, and data on oxygen - phosphorus interaction would be of interest to

industry, even though the investigations had to be restricted to fairly low concentrations of phosphorus in copper. A number of workers have determined the concentrations of oxygen and phosphorus in liquid copper in equilibrium with copper phosphate slags. The activity coefficient of oxygen in Cu + P alloys obtained in this study can therefore be used to calculate the activity of Cu_2O in copper phosphate.

Before commencing the study of oxygen in Cu-Ag, Cu-Sn, Cu-P and Cu-Pb systems, measurements were planned on Cu + O system, to resolve the conflicting reports in literature on deviations from Sievert's Law. The reliability of the apparatus was to be checked by comparing the measured oxygen potential over a mixture of Cu and Cu_2O from 600 - 1200°C with accurately known data. The e.m.f. of the cell:

$$Pt,\ Ni\text{-}NiO\ /\ CaO - ZrO_2\ /\ [O]_{Cu},\ CO - CO_2,\ Cermet,\ Pt$$

was also to be compared with the e.m.f. calculated from thermochemical data.

Although a number of previous investigations[28,68,112] have shown that $CaO - ZrO_2$ electrolytes with chromium cermet leads were satisfactory for use in liquid copper, their suitability for studies of oxygen in lead rich solutions had to be evaluated. It was therefore decided to measure the oxygen potentials over a mixture of Pb + PbO from 600 to 1120°C, accurate data being available for comparison on the standard free energy of formation of PbO up to its melting point. The results of this study could be used to solve the discrepancy in the data on liquid PbO. Further, it was decided to check the reliability of the activity coefficient of oxygen in lead obtained from the extrapolation of Alcock and Belford's results to 1100°C.

Since accurate data on $\Delta\bar{S}_O$ in binary metallic solutions would be very useful in testing the validity of the various solution models, oxygen activity coefficients in Pb + Sn solutions were considered for study, from 550 to 1100°C. Reliable data on $\Delta\bar{S}_O$ in a binary metallic solution is not available and its determination would considerably

advance the present understanding of the behaviour of oxygen.

The electron - atom ratio (e/a) does not vary with composition in Sn + Pb and Cu + Ag alloys, whereas the changes in e/a ratio with composition would be similar in Cu - Pb and Cu - Sn alloys. The ratio of the activity coefficients of oxygen in the two pure metals is 9.4 in Cu + Pb + O system and 513 in Cu + Sn + O system. Since the changes in e/a ratio with composition in Ag - Pb alloys would be similar to the other Gr. I - Gr. IV alloys of this study, and the ratio of the activity coefficients of oxygen in the pure metals is 8137, it was decided to study the behaviour of oxygen in Pb - Ag alloys. This would permit the evaluation of the effect of the variation of the ratio of oxygen activity coefficients in pure metals on the nature of deviations of the activity coefficient from 'ideal' behaviour (defined by equation 4) to be made.

Although deviations from Sievert's Law are very small in solutions of oxygen in metallic solvents, it is of great interest to study the activity coefficient of oxygen at very low concentration, since no interaction would then occur between oxygen atoms themselves. Techniques involving the analysis of oxygen in solution would not be sufficiently sensitive when oxygen concentration is very small (At. pct $O < 0.01$). The e.m.f. technique of Fruehan and Richardson has therefore been selected in this study.

Part II. Recently Wilder[116] has suggested the use of galvanic cells to measure the concentration of the most reactive metal in engineering alloy systems. For example, the concentration of Zn in molten brass may be obtained from the e.m.f. of the cell;

Pt, Ni - NiO / ZrO_2 + Ca O / Zn (in molten brass) ZnO, Ta.

provided the activity coefficient of Zn is known. For the design of commercial probes incorporating this principle, it is necessary to know the time required to attain equilibrium between reactive metal

and its oxide. Binary Pb-Ag system was chosen to study the time to attain equilibrium, when the composition of the alloy in equilibrium with PbO is varied by additions of Ag. The data obtained would also be of use in models for predicting the activity coefficient of oxygen in these alloys.

Activities in Ag + Pb alloys have been measured recently using galvanic cells incorporating liquid lead silicate electrolyte. Some doubts have been raised[117] about the suitability of this electrolyte, apparently due to the presence of electronic conduction. The results of this study on Pb + Ag alloys would enable an estimation of the errors involved in the use of lead silicate electrolyte to be made.

CHAPTER 3

1. ELECTROCHEMISTRY OF GALVANIC CELLS WITH SOLID ELECTROLYTE.

Since the pioneering work of Kiukkola and Wagner[118] solid mixed oxide electrolytes, which have a defect structure in the anion sublattice, have been used increasingly for measuring chemical potential of oxygen at high temperature. Steele[65] has demonstrated that the reversible e.m.f. of a galvanic cell incorporating the electrolyte solid solution,

$$Pt^{I}, O_2\ (\mu' O_2)\ /\ \underset{(L, M)\ O_2}{\text{Solid Electrolyte}}\ /\ O_2\ (\mu'' O_2), Pt^{II}$$

may be expressed by

$$E = \Delta\mu O_2 / 4F \qquad \ldots. 19$$

provided certain conditions are satisfied. The quantities $\mu' O_2$ and $\mu'' O_2$ represent the relevant chemical potentials of O_2 established at the electrodes by appropriate partial pressures of the gaseous component (O_2) or by condensed phase equilibria represented by the typical reactions:

$$[A]_B + \tfrac{1}{2} O_2 = AO$$
$$2C + \tfrac{1}{2} O_2 = [C_2O]_{DO}$$

where $[A]_B$ represents an alloy of metals A and B and $[C_2O]_{DO}$ represents a solution of the compounds C_2O and DO. When these components are present at the electrodes, the cations of metals A, B, C and D may dissolve in the solid electrolyte.

The conditions under which equation 19 is obeyed may be summarised as follows[65],

(a) when negligible dissolution of electrode components takes place, the transport number of electrons must be zero; but no conditions are attached to the relative values of the transport numbers of the ionic constituents of the electrolyte material.

(b) when there is significant dissolution of electrode components, the transport number of the ionic species to which the two electrodes are reversible must be unity.

(c) If a reaction occurs at the electrode - electrolyte interface, resulting in the formation of an intermediate compound, the transport number of the O^{2-} ions in the intermediate compound must be unity.

When there is finite electronic conduction the e.m.f. would be given by

$$E = \frac{1}{4F} \int_{\mu'_{O_2}}^{\mu''_{O_2}} t_{ion} \, d\mu_{O_2} \qquad \ldots\ldots 20$$

Equation 20 is valid irrespective of the relative values of the transport numbers of the ionic constituents, provided A, B, C and D do not dissolve in the electrolyte. When there is significant dissolution the equation is valid only if $(t_{O^{2-}} + t_e)$ is unity.

2. CHOICE OF ELECTROLYTE.

Zirconia and Thoria based electrolytes have been widely used to measure the oxygen potential at high temperatures. Zirconia based electrolytes are known to have better thermal shock resistance and are therefore more useful in practical applications than Thoria based electrolytes. Besides, Zirconia electrolytes are cheaper and commercially available in a wide variety of forms. For these reasons Zirconia electrolytes were provisionally selected for use in this study.

At low partial pressures of oxygen, the excess electron conduction becomes significant in Zirconia electrolytes. It is therefore necessary to evaluate all the data on the conduction properties of this electrolyte, in order to delineate the regions of oxygen pressure and temperature over which $t_e < 0.01$. Large number of investigations have been done on Calcia stabilised Zirconia, this being reviewed in the next section.

3. ELECTRICAL CONDUCTIVITY OF CALCIA STABILISED ZIRCONIA.

Stabilised Zirconia exhibits ionic conductivity because of its CaF_2 - type structure with a high ionic defect concentration. Lattice

Parameter and density [119-121] measurements indicate that Ca^{2+} ions can substitute directly on Zr^{4+} sites. Several studies have shown that at high temperatures and over a wide range of oxygen partial pressures, Calcia stabilised Zirconia (CSZ) behaves as an ionic conductor ($t_{ion} > 0.99$).

Total conductivity σ_T ($ohm^{-1} - cm^{-1}$) of a material with n independently migrating species is given by:

$$\sigma_{Tot} = \sum_{i=1}^{n} q_i C_i B_i = \sum_{i=1}^{n} \sigma_i \qquad \ldots\ 21$$

where q_i is the charge (coulombs / particle), C_i the concentration (particles / cm^3), B_i the absolute mobility (particles - cm^2/sec-volt-coulomb) and σ_i the partial conductivity of the i species. Important carrier species in CSZ are assumed to be V_O, $\oplus$ and $\ominus$, where V_O is a vacant oxygen ion site, $\oplus$ represents positive holes and $\ominus$ represents excess electrons. Conductance due to the migration of cation defects is negligible. Addition of CaO to ZrO_2 greatly increases the partial anion vacancy conductivity, relative to electronic conductivity, so that σ_T remains constant over wide range of pO_2 at high temperatures.

The pO_2 dependences of the partial excess electron conductivity $\sigma_\ominus$ and the partial positive hole conductivity $\sigma_\oplus$ are dictated by local equilibria

$$\tfrac{1}{2} O_2 + V_O + 2\ominus = O_L \qquad \ldots\ 22$$

$$\tfrac{1}{2} O_2 + V_O = 2\oplus + O_L \qquad \ldots\ 23$$

where O_L is an oxygen ion on its lattice site. Now, $[V_O] = [Ca_{Zr}]$, where the square brackets indicate the concentration of fully ionised, dissociated species. V_O is established by the concentration of the dopant and therefore changes only slightly with O_2. The equilibrium constant for reactions 22 and 23, therefore, yield $C_\ominus \propto pO_2^{-\frac{1}{4}}$ and $C_\oplus \propto pO_2^{\frac{1}{4}}$, if a dilute solution of defects obeying 'Henry's Law' is visualised. If, however, association of dopant cations and anion vacancy defects takes place, deviations from the above $pO_2^{-\frac{1}{4}}$ and

$pO_2^{\frac{1}{4}}$ dependences of σ_θ and $\sigma_\oplus$ would occur.

Under constant pO_2 the conductivity may be expected to obey an Arrhenius type relationship:

$$\sigma = \sigma_0 \exp\ (-Q / RT)$$

or

$$\sigma_{Tot} = \sigma^{o}_{ion} \exp\ (-Qion / RT) + \sigma^{o}_{\oplus}\ pO_2^{\frac{1}{4}} \exp\ (-Q_\oplus / RT)$$
$$+ \sigma^{o}_{\theta}\ pO_2^{-\frac{1}{4}} \exp\ (-Q_\theta / RT) \qquad \ldots\ 24$$

In the region where CSZ exhibits pure ionic conduction σ_{ion} would be greater than $\sigma_\oplus$ or σ_θ by a factor of at least 100. The boundaries of this region may be defined by the following equations:

$$\sigma_{ion} = \sigma_\oplus \cdot 100$$

$$\sigma^{o}_{ion} \exp\ (-Qion / RT) = 100\sigma^{o}_{\oplus} \exp\ (-Q_\oplus / RT)$$

$$\log pO_2 = 4 \log \frac{\sigma^{o}_{ion}}{100\sigma^{o}_{\oplus}} - 4\left(\frac{Qion - Q_\oplus}{2.303\ R}\right) \cdot \frac{1}{T} \qquad \ldots\ 25$$

similarly

$$\log pO_2 = -4 \log \frac{\sigma^{o}_{ion}}{100\sigma^{o}_{\theta}} + 4\left(\frac{Qion - Q_\theta}{2.303 \cdot R}\right) \frac{1}{T} \qquad \ldots\ 26$$

Equations 25 and 26 define the boundary conditions between which CSZ may be used as a solid electrolyte. It it seen that these lines may be readily extrapolated even if direct measurements have established their positions only over limited ranges of pO_2 and T, provided Q_{ion}, $Q_\oplus$ and Q_θ remain constant. Exceptions will include materials in which more than one mechanism for σ_{ion}, $\sigma_\oplus$ or σ_θ is possible. Such cases will not be discussed here, but if conductivity studies show such a behaviour, the corresponding boundaries can easily be delineated.

EXPERIMENTAL METHODS TO DETERMINE THE BOUNDARY DATA.

Classification of these methods is based on reviews by Patterson[122] and Alcock[123].

(a) Conductivity Studies.

Total conductivity (a.c.) measurements will indicate the pO_2 and T

conditions where electronic conduction begins to overpower predominantly ionic conduction. At constant temperature, termination of the pO_2 independent range by the rising σ branch is observed at the pO_2 where electronic conduction begins to overpower the pO_2 independent ionic conductivity.

This method does not permit the evaluation of precise transport numbers of the mobile species to be made.

(b) Combination of Conductivity and Diffusion Data.

In principle, ionic contributions to the total conductivity of an oxide can be obtained from self-diffusion studies through the Nernst-Einstein equation:

$$\sigma_i = \frac{N_i / e_i / D_i}{kT} \qquad \ldots\ 27$$

The electron transport number can be obtained by subtracting the ionic contributions for all the ions from measured values of total conductivity. As the result obtained incorporates the errors of all the measurements, an accuracy better than $\pm$ 0.03 in transport number is seldom achieved.

If defect complexes exist, the possibility of ionic migration under an electric field will decrease, although self-diffusion will not be affected.

(c) Polarization Studies.

D.C. polarization techniques may be used to determine t_e when t_{ion} is approximately unity. The trace electronic conductivity is measured as a function of pO_2 and T. The results are then combined with the total conductivity measurements to determine the conditions where $\sigma_{ionic} = 100 \cdot \sigma_{electronic}$

A d.c. voltage is applied to a cell of the type,

Reversible Electrode (M - MO) / Solid Oxide / Non-reversible electrode (Au, Pt)

to transfer oxygen to the reversible electrode. Because the noble metal non-reversible electrode cannot provide oxygen, the oxygen

activity at the solid oxide - noble metal electrode interface is greatly reduced in a short time due to oxygen ion depletion. When a steady state is reached, the oxygen concentration gradient in the solid oxide balances the applied voltage and net charge transport by oxygen ions is reduced to zero. The current through the cell under these conditions can be analysed to obtain $\sigma_{\oplus}$ and $\sigma_{\ominus}$.

(d) Permeability Studies.

By applying Wagner's analysis[134] to the permeability of oxygen through CSZ both at high and low pO_2, approximate values for $\sigma_{\oplus}$ and $\sigma_{\ominus}$ can be evaluated. Permeability at high pO_2 is due to positive hole conduction. The flux of oxygen through a tube wall is given by:

$$n_O = \frac{A}{L} \frac{4.186\ RT}{2\ Z_O^2\ F^2} \int_{P'_{O_2}}^{P''_{O_2}} \frac{\sigma_{ion}\ \sigma_{elect.}}{\sigma_{ion} + \sigma_{elect.}} \frac{dpO_2}{pO_2} \quad \ldots\ 28$$

$\frac{A}{L}$ is a geometric factor, F is Faraday's constant (96,000 coul./equiv.), Z_O is the valence of oxygen ions, R is the gas constant (1.987 $cal/_{mole\ deg\ K}$) and T is the absolute temperature. The constant 4.186 converts calories to joules so that conductivities may have units of $(ohm\text{-}cm)^{-1}$.

(e) Direct e.m.f. Measurements.

In this method the measured e.m.f. of a galvanic cell,

pO'_2 / solid Electrolyte / pO''_2

is compared with the e.m.f. calculated from equation 19. The partial pressure of oxygen at the two half cells may be fixed by an element and its oxide. The conditions under which the measured e.m.f. is smaller than the calculated directly signals the onset of electronic conductivity. Among all the methods listed, this technique is the most direct, sensitive and reliable.

EVALUATION OF THE COMPLETE IONIC CONDUCTION REGION OF C.S.Z.

From diffusion data of Carter et al[124-126] ionic conductivity of O^{2-}, Ca^{2+} and Zr^{4+} ions can be calculated for CSZ at 1000°C and compared with the measured total conductivity to show that $t_{O^{2-}}$ is virtually unity at an oxygen pressure of 1 atm. Weissbart and Ruka[127]

observed that Faraday's laws were obeyed for reversible transfer of oxygen from cathode to anode in the cell

$$O_2\ (P_1),\ Pt\ /\ Zr_{0.85}\ Ca_{0.15}\ O_{1.85}\ /\ Pt,\ O_2\ (P_2)$$

The electronic contribution to the total conductivity was found to be less than 0.5% at about 1000°C in oxygen atmosphere. Since Faraday yield techniques are not sufficiently sensitive to detect trace electronic conduction, greater emphasis may be placed on the e.m.f. and d.c. polarization techniques, which suggest that $t_{elec} \approx 0.001$, although the precise value would be a function of temperature and pO_2.

(a) Low pO_2 boundary.

Baker and West[128], Fisher and Janke[52], Fruehan[8], Schwerdtfeger[129], Schmalzried[130], and Tretyakov[131] have used e.m.f. cells to determine the partial pressure of oxygen for the onset of excess electron conduction. The results are compared in figure 2. The results of Fruehan[8] and Schwerdtfeger[129] at 1600°C are approximately three orders of magnitude below that reported by Baker et al[128] and Fisher et al[52]. Tretyakov employed coulombic titration through a CSZ tube to remove oxygen from the inside chamber of the tube. After each titration the remaining oxygen established an oxygen pressure in the enclosed volume. The reliability of this technique is doubtful. Besides, his results for the low pO_2 boundary for ionic conduction in ThO_2 + 15% $YO_{1.5}$ are only slightly below that for CSZ, in marked contrast to the large volume of evidence of a much lower pO_2 boundary for this material[65].

A.C. conductivity measurements of Steele[132] indicate a limit about 3 orders of magnitude higher than the selected values. However, a.c. conductivity measurements are not sufficiently sensitive for the determination of the boundary for complete ionic conduction. Greater weight has therefore been assigned to the values of Patterson et al[135], who used a combination of d.c. polarization and a.c. conductivity studies. Line AC in fig. 2, represents a conservative estimate of

Fig.2. TEMPERATURE & pO_2 CONDITIONS FOR PURELY IONIC CONDUCTION IN C.S.Z.

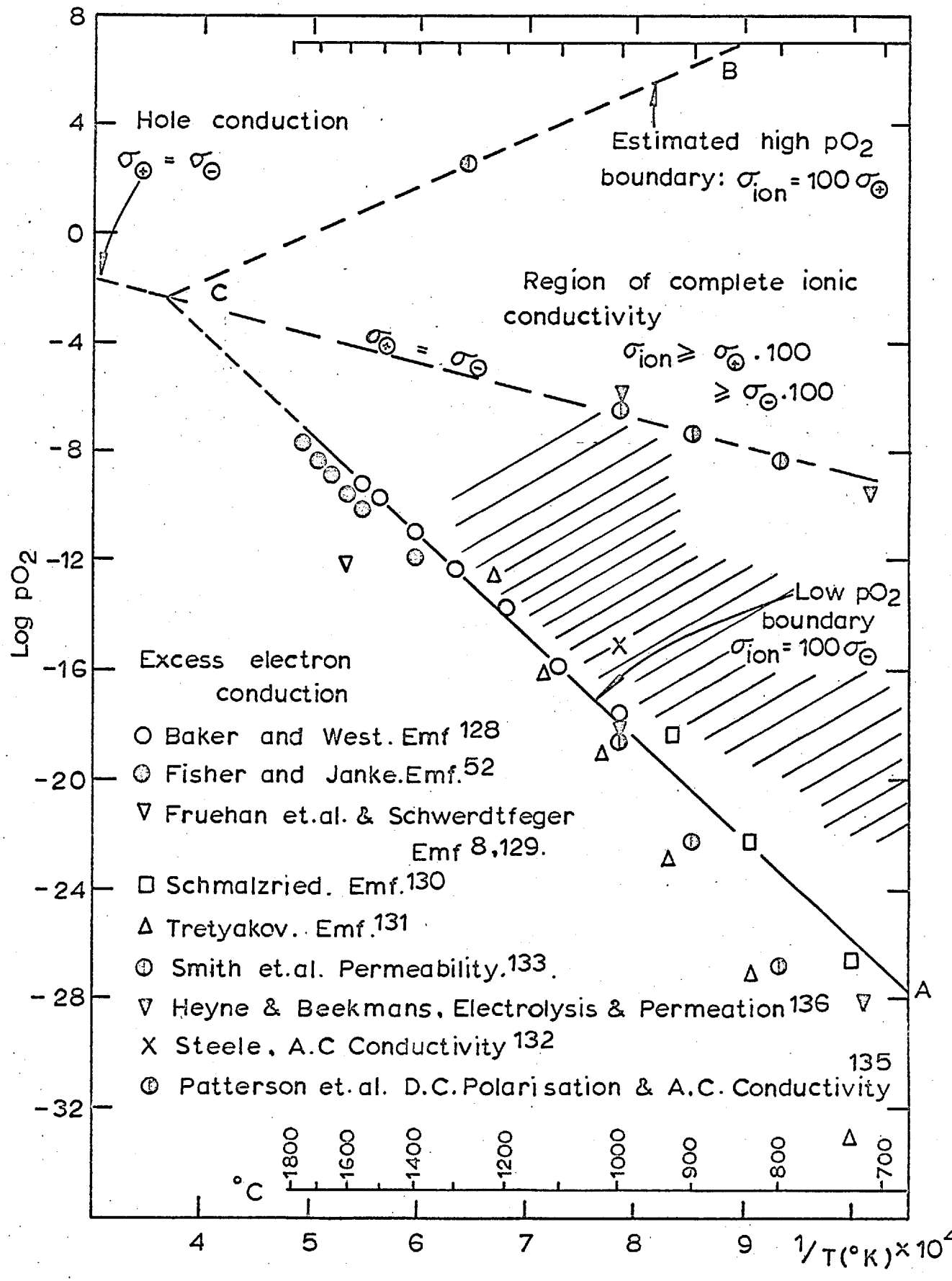

the low pO_2 boundary, which may be used in predicting the performance of solid galvanic cells with CSZ solid electrolyte. The scatter between the results of the various authors may be partly due to differences in the quality of the electrolyte used.

(b) <u>High pO_2 boundary</u>.

Smith et al[133] have measured the high temperature oxygen permeability of CSZ tubes over the pO_2 range from 10^{-4} to 1 atm. According to Wagner's scaling rate theory[134], their results may be interpreted quantitatively in terms of positive hole conduction and the results used to establish the high pO_2 electrolytic boundary. Patterson[122] has calculated the high pO_2 boundary at 1275°C as 2.65 atm., using the results of Smith et al[133]. From the activation energy for permeation and the known activation energy of 29 k cal/mole for oxygen ion conduction in CSZ[135], the slope of the high pO_2 boundary has been calculated as + 23 k cal/mole.

Point C in figure 2, where the high and low pO_2 boundaries for complete ionic conduction meet, must lie on the straight line along which the positive hole and excess electron conductivities are equal. From the d.c. polarization studies of Patterson et al[135] it is possible to obtain, at 800, 900 and 1000°C, the oxygen pressures where the two conductivities are equal. These points are shown in fig. 2.

The best estimate of the high pO_2 boundary, considering all these data, has a slope of 18 k cal/mole and is represented by line BC. The difference of 5 k cal/mole between the slope of this line and that calculated from permeability data is considered to be within the accuracy of all the data used in the calculations.

The selected values yield an activation energy for p-type conduction in CSZ of 49 k cals/mole, while this energy has a value of 25 k cal/mole in Thoria based electrolytes[123]. This difference is reflected in the values for the positive hole conductivity of the

two electrolytes: $\sigma_{\oplus}$ in CSZ is approx. an order of magnitude lower than in Thoria - Yittria electrolytes at 1000°C and pO_2 of 10^{-10} atm. for the same concentration of anionic vacancies[135].

The shaded area in fig 2 represents the pO_2 - T region covered in the present study. It is clear that CSZ electrolytes adequately meet the requirements for use in galvanic cells in this region

4. REFERENCE ELECTRODE.

A mixture of a metal and its lowest stable oxide is generally used as an oxygen reference electrode. The metal - metal oxide systems used in this study were chosen for the following reasons:

(a) Solid solubility of the metal oxide in the solid electrolyte should be as small as possible. NiO is found to have practically no solubility in CSZ up to 1300°C, while FeO penetrates the electrolyte. The extend of penetration is a function of temperature and time.

(b) The e.m.f. of the cell using the selected reference electrode should be as small as possible. Although trace electronic conductivity invariably present in CSZ would not cause any measurable lowering of the e.m.f., it can provide an internal 'short-circuiting' path which allows oxygen to be transfered from one electrode to the other in the direction of the oxygen potential gradient. This flux of oxygen may distrub the equilibrium at the electrode - electrolyte interface unless the relevant chemical reactions and mass transfer processes are sufficiently rapid.

(c) The chemical potential in the reference electrode should be accurately known.

Ni - NiO was chosen as the optimum reference electrode. In some systems involving low oxygen potentials a Fe - FeO electrode was used. When used at 1200°C the duration of the experiment had to be less than 6 to 8 hours to prevent significant penetration of CSZ by FeO.

5. POLARISATION PHENOMENON.

Diaz and Richardson[68] have reported significant polarization of the Ni - NiO reference electrode. To obtain true e.m.f.'s, the reference electrode had to be depolarized by the passage of an external current. Abraham[112] has reported that no polarization occurred when the measured chemical potential of oxygen was below that corresponding to the Ni - NiO electrode. Since more than twenty different investigators have used this reference electrode without observing polarization, it was decided to verify the conclusion of Diaz et al.

6. CONDUCTING LEAD.

A number of investigators[28,68] have found that chromium cermet (72% chromium, 28% alumina and small amounts of silica) was a satisfactory conducting lead in liquid copper. A protective layer of Cr_2O_3 on the surface prevents further oxidation of the cermet. For this reason chromium cermet was initially selected as a conducting lead in this study.

CHAPTER 4

EXPERIMENTAL WORK.

(1) APPARATUS.

The apparatus used in this study was based on that employed by various other investigators[28,68,112].

The alumina reaction tube, 35.5 mm o.d., 28.5 mm i.d., and 820 mm long, was suspended in a vertical platinum furnace, the temperature of which was controlled to better than ∓ 1.5°C by a Kelvin-Hughes proportional type controller operating a mercury relay which interrupted the current through the winding. The control Pt. - Pt. 13% Rh. thermocouple was placed beside the furnace winding. To minimise temperature fluctuations, a kanthal resistance ($\frac{1}{4}$ th the resistance of the windings of the furnace) wire, wound round a refractory brick, was connected to the mercury switch so that it would be in series with the furnace when the switch was off. The overall effect was that the power supply to the furnace in the 'off' position of the control system was approximately 80% of that in the 'on' position. The temperature of the system was measured using a Pt. - Pt. 13% Rh. thermocouple (N) placed just below the crucible containing the liquid metal. The furnace had an even temperature zone (∓ 1.5°C) of 5 cms.

Electrical shielding was effected by means of a nimonic tube or kanthol Al ribbon would round the reaction tube from end to end and maintained at ground potential. The brass head of the cell and the exterior casing of the furnace were also electrically grounded. In experiments above 1100°C, nitrogen was passed between the furnace and reaction tubes to protect the kanthal Al winding.

The alumina crucible containing the liquid metal was supported in the centre of the reaction tube by means of a closed end alumina tube coming from beneath. The lower end of the reaction tube was closed with a water cooled brass cap through which the alumina tube supporting the crucible passed. An entrance for the argon gas used

Fig.3. BRASS HEAD OF THE REACTION TUBE

(Scale 1:2)

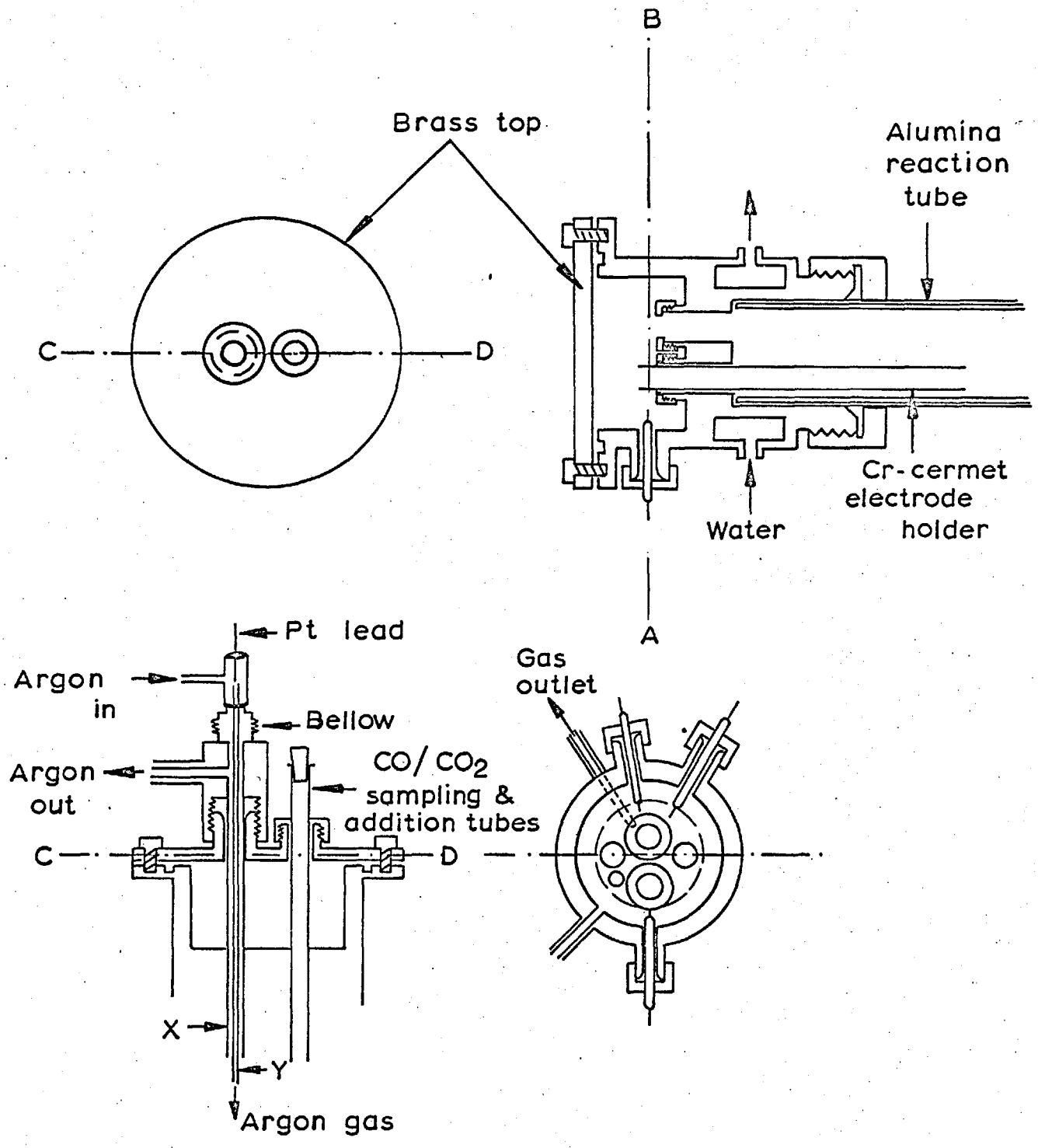

to flush the reaction tube was provided in this cap.

Figure 3 shows the water cooled brass head which closed the top of the reaction tube, held the different tubes going into the cell and permitted gas and electrical connections. All the tubes were held by 'O' rings. The large number of inlets for tubes and leads for electrical connections facilitated the use of a wide variety of cell designs. Section C - D in Fig. 3 shows the assembly of the alumina tube (Y) through which argon gas is passed to flush the Ni-NiO reference electrode. The alumina tube was secured with "Araldite" to the brass argon inlet, which was inserted in a bellow sitting on the top of the argon outlet.

Equimolar mixtures of 'spec pure' nickel and nickel oxide powders were sintered inside the round bottomed solid electrolyte tubes with the platinum lead embedded in the mixture. A similar procedure was used when Fe-FeO reference electrodes were employed. The open end of the 154 mm long solid electrolyte tube was attached to a tight fitting alumina tube (X), 300 mm long, using high temperature alumina cement. This was done to separate the two half cells more completely so that the transport of oxygen and other gaseous species via the gas phase between the two half cells could be completely avoided.

The conducting lead of chromium cermet, about 35 mm long, was pre-oxidised before the experiments in air at 1200°C. A protective layer of oxide prevents further oxidation of the cermet when dipped in liquid metals containing oxygen. The platinum lead was wound round a groove cut at one end of the cermet rod. A tight fitting alumina tube was inserted over this end of the cermet rod, and the joint was sealed with alumina cement to prevent metal vapours attacking the Pt. lead.

When tungsten conducting leads were used in liquid Cu + P alloys, the alumina tube was inserted over most of the length of the tungsten rod, as shown in Fig. 6C. The e.m.f. of the cells was measured with a Vibron electrometer (E.I.L. Model 33 B - 2) of input resistance

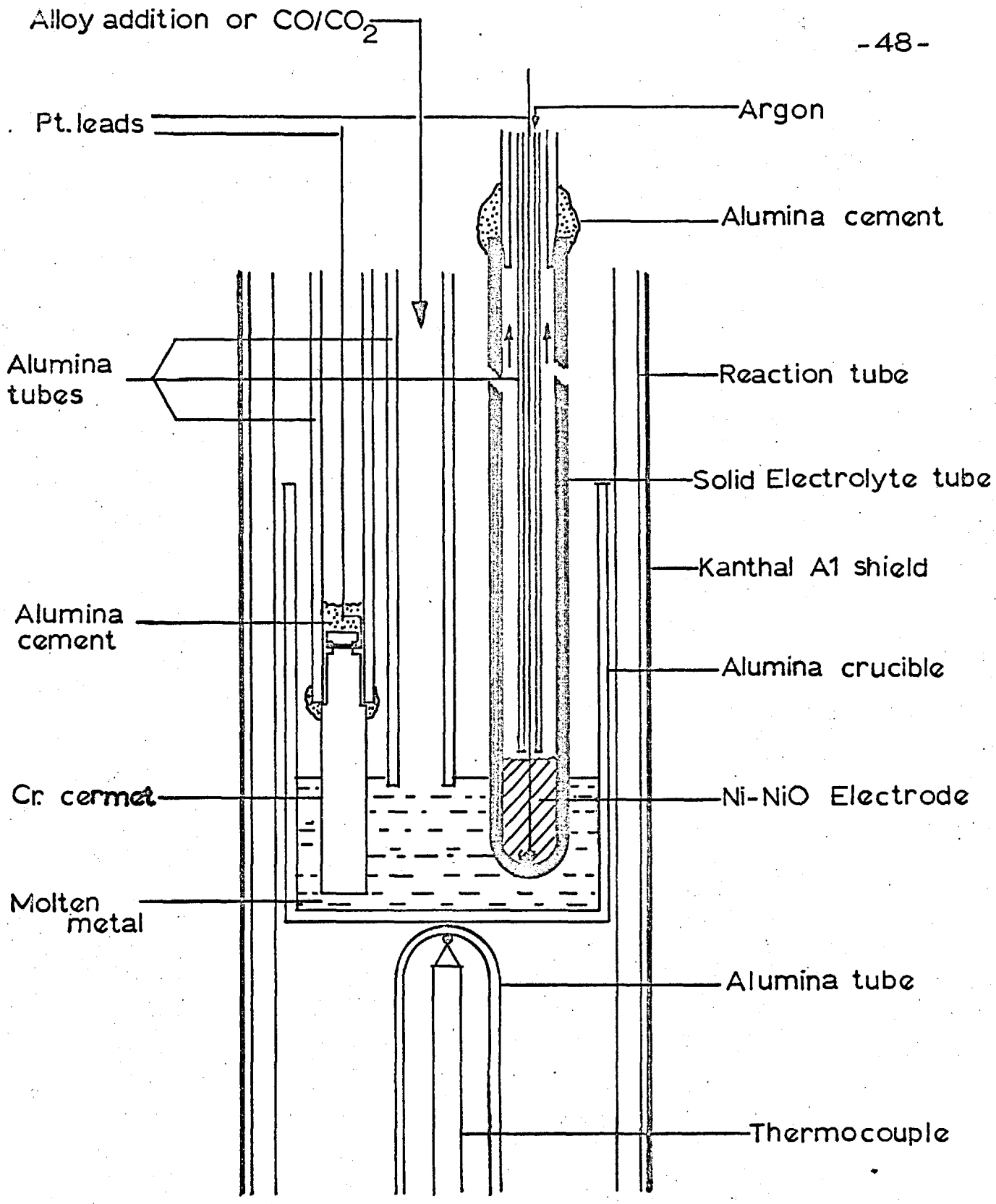

Fig 4 Cell used for measuring e.m.fs in liquid metals (Scale: 2:1)

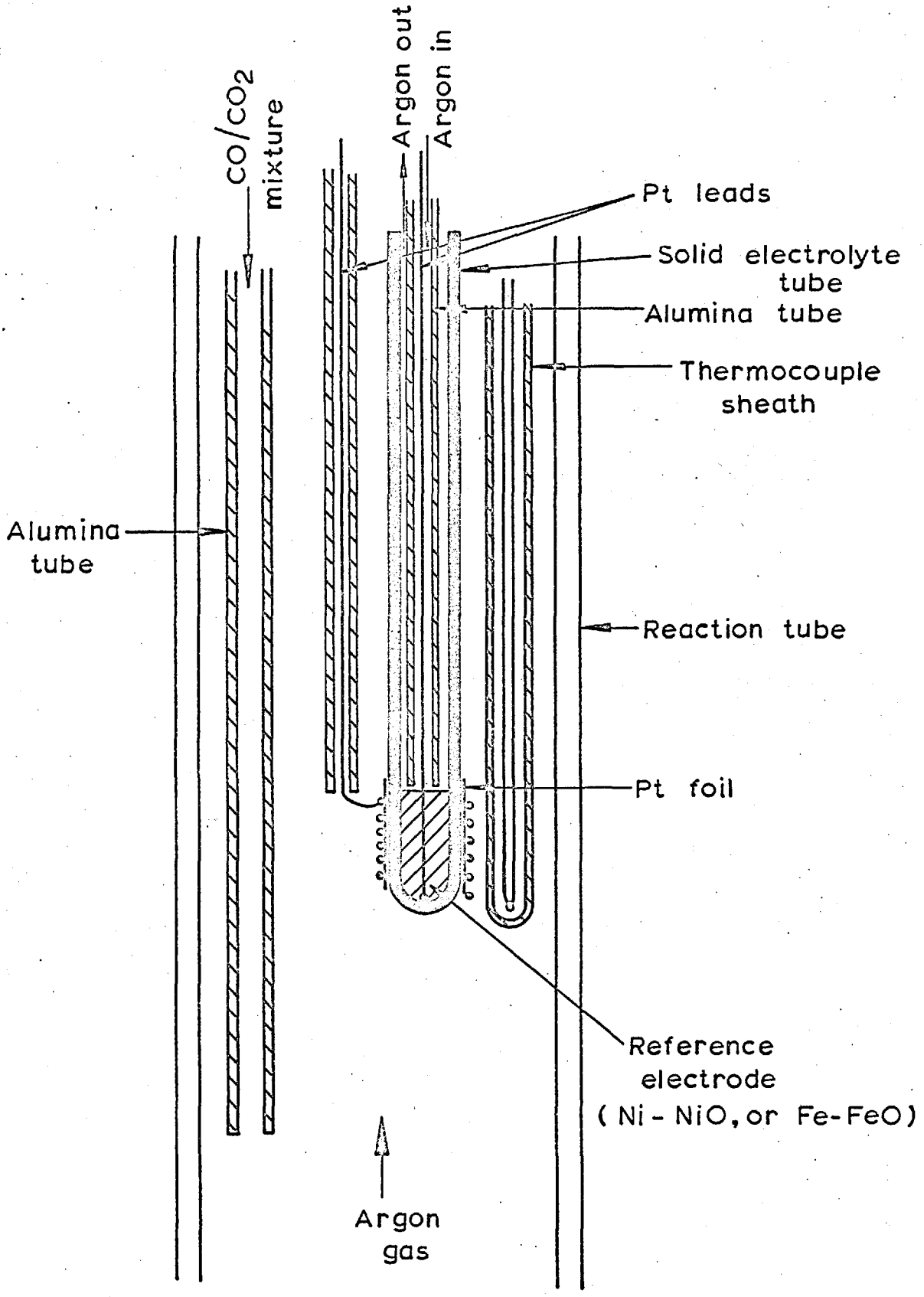

Fig.5. CELL USED FOR MEASURING OXYGEN POTENTIALS IN GASES

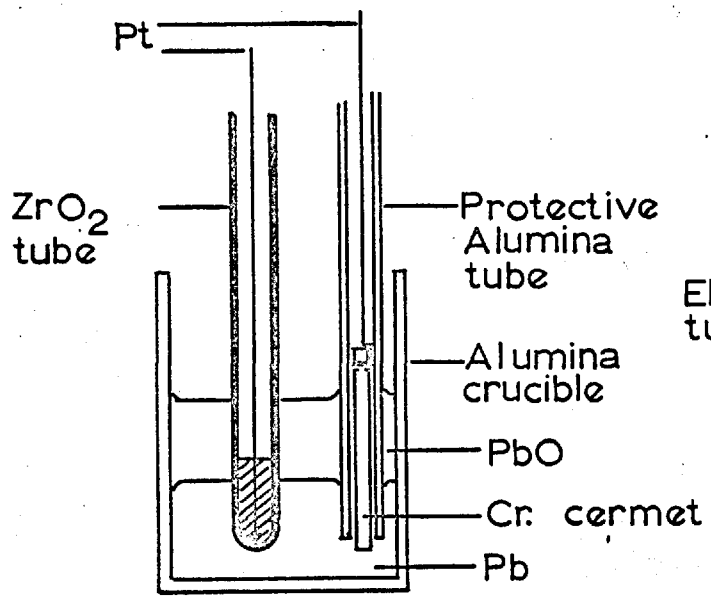

(a)

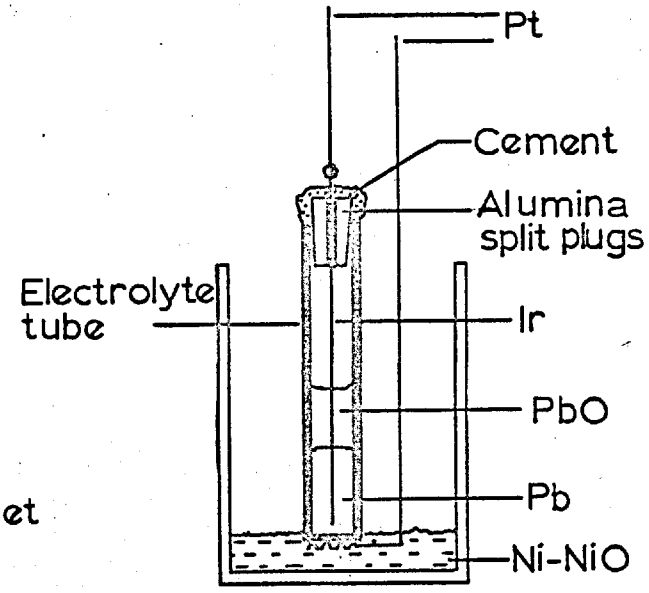

(b)

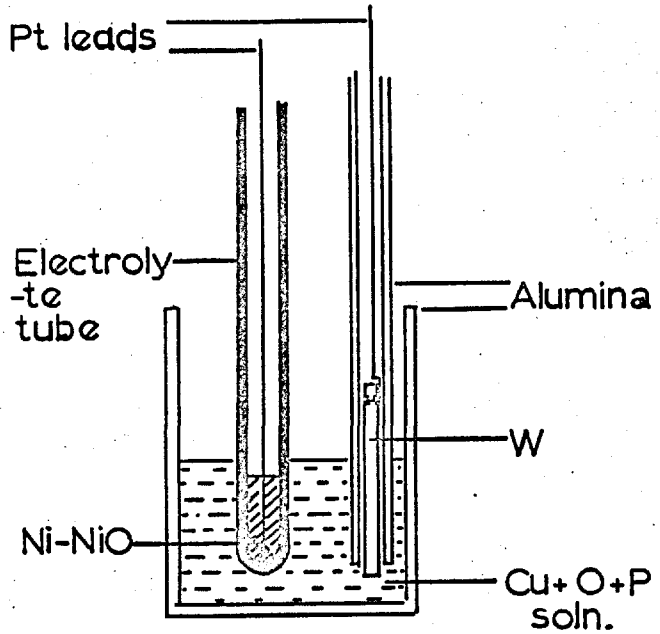

(c)

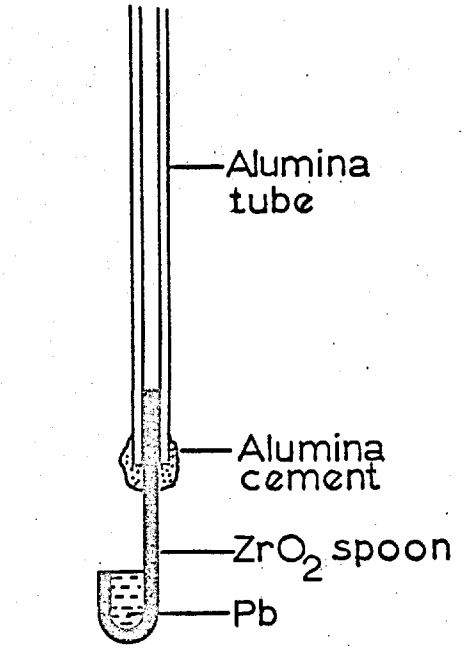

Sampling spoon

(d)

Fig. 6

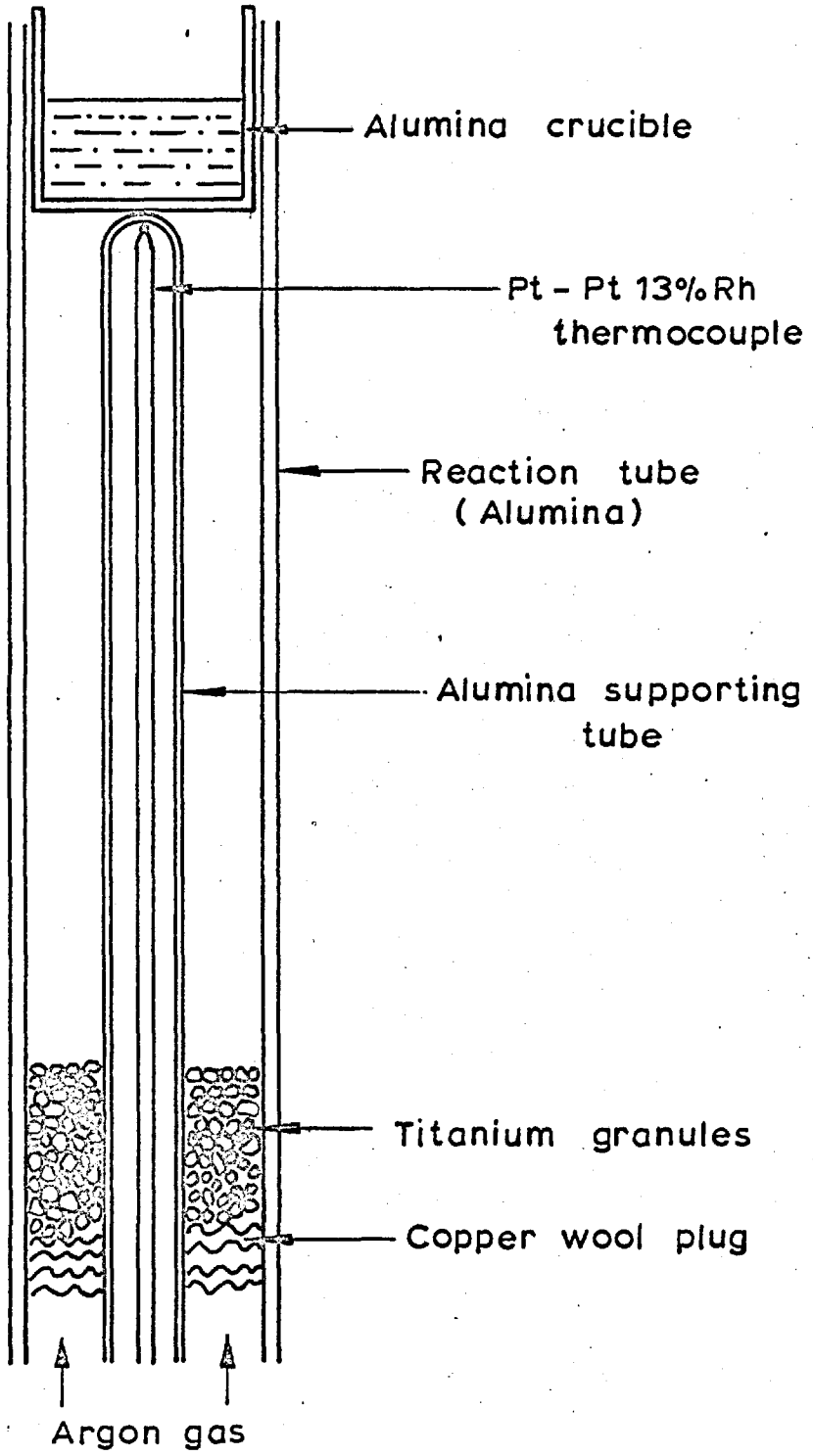

Fig.7. ARRANGEMENT OF TITANIUM INTERNAL GETTER IN THE REACTION TUBE (Scale 1:1)

10^{17} ohms. The accuracy of the instrument is better than 1 pct. of the full scale. The instrument is provided with a 'back-off' circuit, which applies a potential opposite to the input potential. This permits small variations in relatively large potentials to be measured. The output of the instrument was connected to a Honeywell potentiometric recorder, through a potential divider of total resistance of 1.5 k ohms. The reference electrode (Ni-NiO or Fe-FeO) was connected to earth. The platinum wire leading from the cermet was connected to the 'high' terminal on the electrometer using screened non-microphonic co-axial cable.

The approximate resistance of the cells were measured using a Wayne Kerr Universal Bridge (B221A), across the two platinum leads.

Gas cells of the type

$$Pt, Ni\text{-}NiO \;/\; CaO + ZrO_2 \;/\; CO - CO_2, Pt$$

were used in this work. Fig. 5 shows the details of the electrode arrangement in these cells. A similar cell was used to measure the partial pressure of oxygen in the argon gas. It was found that partial pressures of oxygen below 10^{-12} atm. could not be achieved in the reaction tube by purification of the argon gas before admission into the reaction tube. To obtain lower partial pressures of oxygen, internal 'getters' had to be used in some experiments. A column of titanium granules, supported on copper wool, was placed in the vertical reaction tube, 10 to 20 cms below the crucible containing the liquid metal, where the temperature was approximately 850°C. With this arrangement partial pressures of the order of 10^{-17} could be obtained inside the reaction tube. This arrangement is shown in Fig. 7.

(2) GAS TRAIN.

The gas trains are shown diagramatically in Figure 8. Initially the high purity argon gas from the cylinder was dried by silica gel

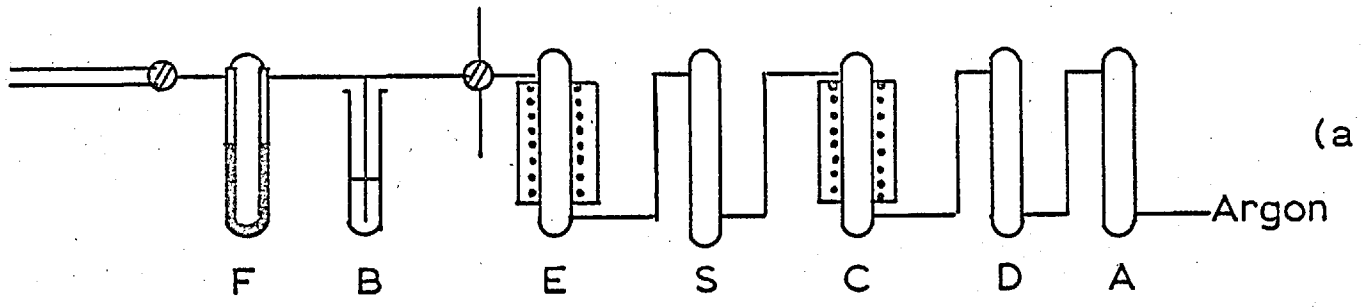

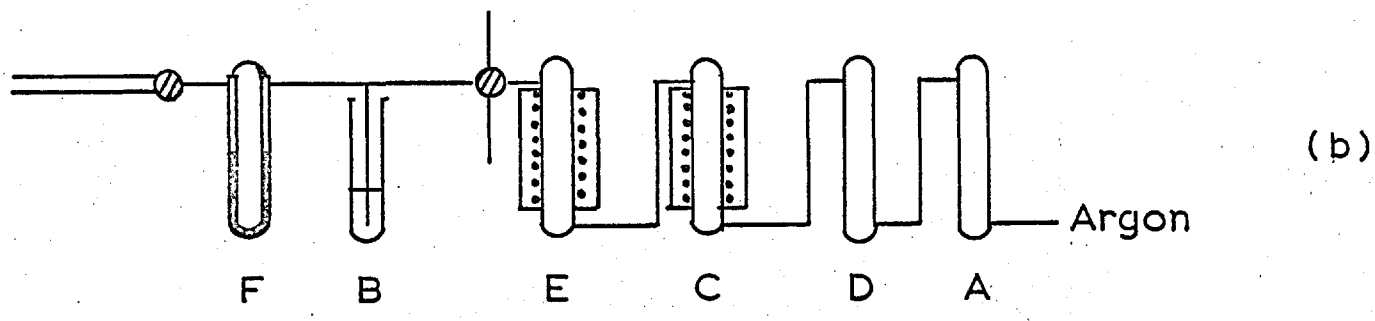

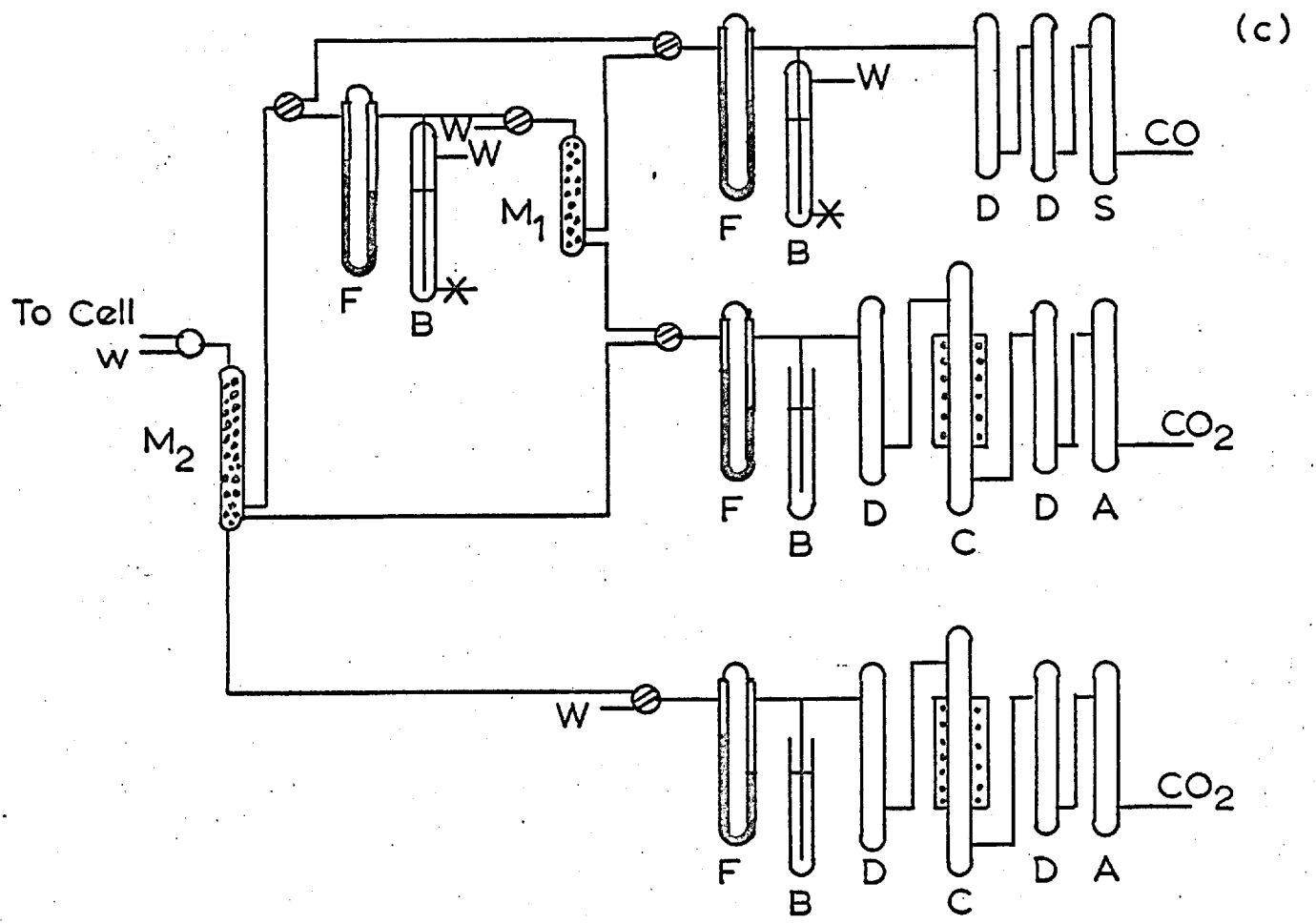

Fig 8. Gas Train.

Fig.8 - Gas Train

A. Silica gel tower.

B. Dybutyl phthalate bolw-off.

C. Copper gauze furnace.

D. Magnesium perchlorate tower.

E. Titanium chips furnace.

F. Flowmeter.

M. Mixer.

S. Sofnolite.

and magnesium perchlorate and passed through a kanthal furnace containing copper at 450°C to remove oxygen. The gas was then passed through sofnolite (sodium hydroxide plus an indicator supported on an inert base) to remove CO_2 and drying towers containing magnesium perchlorate. The argon was further purified by passing through a furnace containing Ti grannules at 900°C, and metered by conventional capillary flowmeters containing dibutyl phthalate. The capillary flowmeter was later removed from the gas train, since the inclusion of the vapours of dibutyl phthalate in the inert gas could produce CO or CO_2 in the hot zone of the reaction tube. The flow rate of argon gas was measured intermittently by passing the gas through the capillary flowmeter to the exit bubbler. The gas train used is shown in Fig 8a. During the course of this study it was realised that the simpler gas trains shown in Figure 8b were adequate.

The carbon monoxide was guaranteed to be not less than 99.2% pure and the maximum impurity contents were 0.6% N_2 and 0.2% CO_2. This gas was passed through a column containing sofnolite to remove CO_2 and drying towers containing magnesium perchlorate.

The 'analytical grade' CO_2 used contained 30 p.p.m. of H_2O, 15 p.p.m. of N_2 and 5 p.p.m. of O_2. This gas was first dried and then passed through copper gauze at 450°C to remove oxygen. The CO_2 then passed through magnesium perchlorate. The gases from the purification trains were maintained at constant pressure by means of the 'blow-offs', metered by capillary flowmeters, and mixed in mixing chambers as shown in Fig. 8c. Gas ratios larger than 100 : 1 are difficult to obtain with accuracy in a system of two flowmeters. Double dilution was employed to get higher ratios. The CO_2 - CO mixture from mixer M_1 was metered by means of a third flowmeter and diluted with more CO_2 from an independent CO_2 line in mixer M_2. The gases were taken to the cell through all-glass lines.

(d) ANALYSIS.

(a) Oxygen in Copper and Copper - Silver alloys.

Oxygen in copper can be readily reduced by hydrogen. The water evolved can be measured gravimetrically or manometrically. Oxygen can also be determined by measuring the loss in weight of a sample after hydrogen reduction. This method has been used by a number of investigators[29,139,140] who found that the results obtained compare favourably with that from vacuum fusion and Baker's method[141].

In this study, oxygen in copper was analysed by the 'loss in weight' technique. The apparatus consisted of a vertical alumina tube surrounded by an electric resistance furnace capable of maintaining a hot zone at 950°C. Pyrex glass cones were joined to the ends of the alumina tube with "Araldite", these joints being protected with water cooling coils. Samples for analysis were held in a jig shown in Fig 9. The jig was constructed from iron wire and copper wire gauze was used for the jig platform. The jig was suspended on an alumina rod which slid through a rubber bung fitting in a glass tube extending vertically from the top of the alumina tube. Argon for flushing the furnace and hydrogen for reduction were dried by passing through silica gel.

The analytical procedure was to weigh the copper sample containing the oxygen on a semi-micro balance. Upto 12 samples were loaded on the jig which was then lowered into the cold zone formed by the glass extension of the reduction tube. The tube was flushed with argon for 30 min. Hydrogen was then introduced into the tube at 50 ml min^{-1}. The jig was lowered into the maximum temperature zone for two hours, although 40 minutes were sufficient for complete reduction. The temperature variation in the hot zone, shown in Fig 9, was found not to affect the reduction. The jig was then withdrawn to the cold zone and allowed to cool before flushing with argon for 20 min. and removing the samples for reweighing.

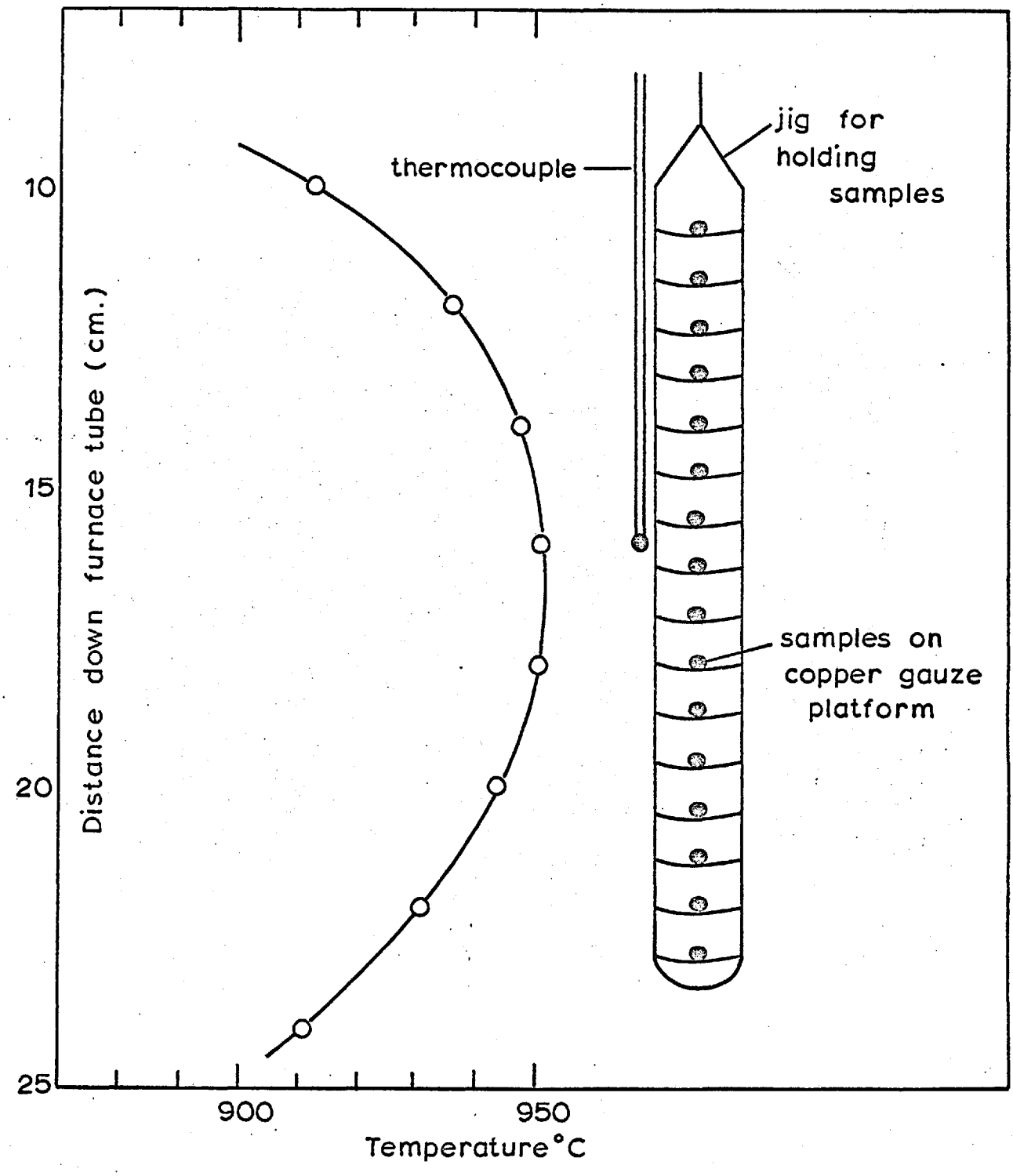

Fig.9. ARRANGEMENT OF OXYGEN CONTAINING COPPER SAMPLES IN THE HYDROGEN REDUCTION FURNACE

When Cu - Ag alloys were analysed for oxygen, the temperature of the furnace was kept at 750°C, and reduction times upto 5 hours were used. The alloy samples were supported on small alumina discs placed on the copper platform to avoid the diffusion of Ag into the copper mesh.

The samples, about 2 to 3 g in weight, could be weighed to ∓ 0.005 mg. The probable error in the oxygen analysis would therefore be 0.1 to 1 pct. for oxygen contents from 2 to 0.2 atom pct. The maximum loss in weight due to vaporization could be calculated at 950°C as 4×10^{-8} g./hr. The gain in weight of copper due to solubility of hydrogen is too small to be detected on the semi micro-balance.

(b) Oxygen in Lead.

Baker's method was used to determine the oxygen content of the lead samples. The lead sample (contained in a Zirconia spoon) was heated in a closed static system filled with hydrogen at reduced pressure. The water vapour formed is condensed at - 80°C in a trap cooled with a mixture of solid CO_2 and acetone. The condensed water was then vaporised in a previously evacuated and known volume and the pressure measured by a mercury manometer. This method has been successfully employed by Richardson and Webb[62] to analyse oxygen in lead. Carbo[67] has given a detailed description of the apparatus and the analytical procedure used.

(c) Phosphorus in Copper.

Practically all the methods for the determination of phosphorus require its preliminary separation as ammonium phosphomolybdate. It is difficult to get the ideal composition of this compound and numerous procedures for the subsequent treatment of phosphomolybdate, precipitate have been proposed.

In this study phosphorus was determined gravimetrically as magnesium pyrophosphate after preliminary separation as ammonium phosphomolybdate. The procedure followed was that described by Vogel[142].

(d) Lead in Copper.

Lead was determined gravimetrically as $PbSO_4$. Approximately 3 g of Cu - Pb alloy was sampled from liquid solution using a silica tube. The entire sample was dissolved in 1 : 1 nitric acid. An aliquot portion of this solution was evaporated three times with sulphuric acid until dense white fumes were evolved. This ensured the complete removal of nitric acid and conversion of the lead salt into the sulphate. After cooling and dilution, the solution was allowed to stand for one hour. The precipitate was then filtered off as lead sulphate through a weighed porous bottomed porcelain crucible. The precipitate was washed three times with 1% (by volume) sulphuric acid, saturated with $PbSO_4$. The crucible was dried at 100°C for 1 hour and then in an electric muffle furnace at 500°C.

(4) MATERIALS.

The following materials were used in this investigation:

Copper: spectrographically standardised copper rods, supplied by Johnson Matthey Chemicals Ltd., were used. The most important impurities were Ag 5 ppm, Fe 2 ppm and Si 2 ppm.

Lead: The lead used in this study was supplied by Goodlass Wall and Lead Industries Ltd., and the main impurities were:

Bi	.. ..	0.0005 pct.
Ag	.. ..	0.0004 pct.
Sn	.. ..	0.0001 pct.
Sb	.. ..	0.0002 pct.
Cu	.. ..	0.0004 pct.
As	.. ..	0.0001 pct.
Fe	.. ..	0.0001 pct.

Tin: Tin supplied by Capper Pass and Sons Ltd. was 99.999% pure. The main impurities were:

Sb	.. ..	0.0003 pct.
Pb	.. ..	0.0003 pct.
Bi	.. ..	0.0001 pct.
Fe	.. ..	0.0001 pct.
As	.. ..	0.0001 pct.
Ir	.. ..	0.0001 pct.

Silver: The silver used in this study was supplied by Johnson Matthey Chemicals Ltd., and contained less than 0.001 pct. total impurities, the most important being Fe 5 ppm and Cu 2 ppm.

'Spec pure' powders of Nickel, Nickel Oxide, Iron, Ferrous Oxide, Lead Oxide and Cupric Oxide were supplied by Johnson Matthey Chemicals Ltd. The maximum impurity content of these materials did not exceed 10 ppm.

Chromium cermets used contained 72% Cr, 28% Al_2O_3 and small amounts of silica, and were supplied by Morgan Refractories Ltd., under the name Metamic 612, in the form of rods approximately 4 mm diameter. The reaction tube and crucibles containing the metal were made of 'Purox' recrystallised alumina and were supplied by Morgan Refractories Ltd.

The lime - zirconia and yttria - zirconia tubes were manufactured commercially. The 'fully stabilised' lime - zirconia contained 15 mole pct. CaO and the 'partially stabilised' variety contained 7.5 mole pct. CaO. The yttria stabilised material contained 4.5 mole pct. of yttria. The tubes $\frac{1}{4}$ in. o.d. and 6 in. long were supplied by the Zirconia Corporation of America. The wall thickness was about 1 mm and they were guaranteed as suitable for high vacuum work.

(5) PREPARATION OF OXYGEN FREE METALS.

Oxygen free metals were prepared by reduction under hydrogen at 900°C for 8 hours. The high purity hydrogen used was further purified by passing through palladium on alumina at 120°C, sofnolite, silica gel magnesium perchlorate and phosphorus pentoxide.

The metal was held in an alumina cricible in the centre of a vertical

reaction tube, which was suspended in a vertical furnace. The reaction tube was flushed with hydrogen entering from the lower end. A separate stream of hydrogen was bubbled through the metal. Specimens of Cu and Ag of the required weight and dimensions were cut from rods before reduction. In the case of Pb and Sn small specimens were cut from the reduced ingots with a steel blade, 2 to 3 minutes prior to each addition. The metals were stored under argon in a desiccator.

When a solid electrolyte tube and a cermet conducting lead were lowered into liquid tin after reduction under hydrogen for 5 hrs. the e.m.f. obtained corresponded to an oxygen concentration of 4×10^{-5} atom pct. However, the e.m.f. decreased with time, probably due to electronic conduction in the solid electrolyte under hydrogen atmosphere.

(6) PREPARATION OF Cu-P MASTER ALLOYS.

Copper was melted in a high purity carbon crucible under hydrogen in an induction furnace. The carbon crucible was supported at the centre of a 2 in. diameter silica tube. The upper and lower ends of the silica tube were closed by means of tight fitting rubber bungs with openings for gases and sampling tubes. The top section of the silica tube was water cooled.

After 50 min. of reduction, the hydrogen atmosphere in the reaction tube was replaced by argon, which was purified by passage through copper at 450°C and titanium at 900°C. Weighed quantities of Copper Phosphide, enclosed in a copper foil were then added to the molten copper. Samples of Cu-P alloy were withdrawn in silica tubes, allowed to solidify in the water cooled section of the reaction tube, and quenched in water. The alloy samples were etched in hydrofluoric acid to remove any possible silica adhering on the surface. When eight one gram samples cut from the same Cu-P alloy rod were analysed for Phosphorus the results agreed within 3 pct. The segregation of Phosphorus in the alloy was therefore insignificant. Before use in the e.m.f. cells, the surface of the alloy rods were cleaned by filing.

(7) PROCEDURE

(a) Measurement of oxygen potential in gases.

The galvanic cell

Pt, Ni-NiO / 7.5% CaO + ZrO_2 / CO-CO_2, Pt .... Cell 1

was assembled as shown in figure 5. The Ni-NiO mixture was sintered inside the 18 in long Zirconia tube with a platinum lead embedded in this mixture. A stream of argon gas flushed this electrode. The atmosphere inside the electrolyte tube was separated from that in the reaction tube by 'O' ring seals as shown in section C-D of fig 3. The reaction tube was flushed with argon gas at 50 mls min^{-1} and the furnace was heated to 1200°C. CO-CO_2 gas mixture was introduced into the cell at 200 mls min^{-1}. Reasonably constant e.m.f.s were obtained 15 to 20 minutes after changing the ratio of CO/CO_2 in the gas.

When the chemical potential of oxygen in the reaction tube was less than that in the Ni-NiO reference electrode, the e.m.f. of the cell did not vary with time. The reversibility of the cell was tested by passing small currents (2 micro amps) in both directions through the cell, using the circuit shown in fig. 10. When the external current transferred oxygen to the Ni-NiO electrode the e.m.f. of the cell returned to the original value in 10 mins. after the removal of the external potential. After passing the external current in the reverse direction, approximately 30 mins. were required for the e.m.f. to return to the initial value. The measured e.m.f.s were approximately 2 mv higher than those calculated from thermochemical data.

When the chemical potential of oxygen in the reaction tube was higher than that in the reference electrode by the equivalent of 100 mv, the e.m.f. of the cell decreased by approximately 3 mv per hr. Constant e.m.f.s could be obtained only after removing oxygen from the reference electrode by external currents (50 to 100 micro amps for 15 min.). The steady e.m.f.s obtained were consistently 3% below those

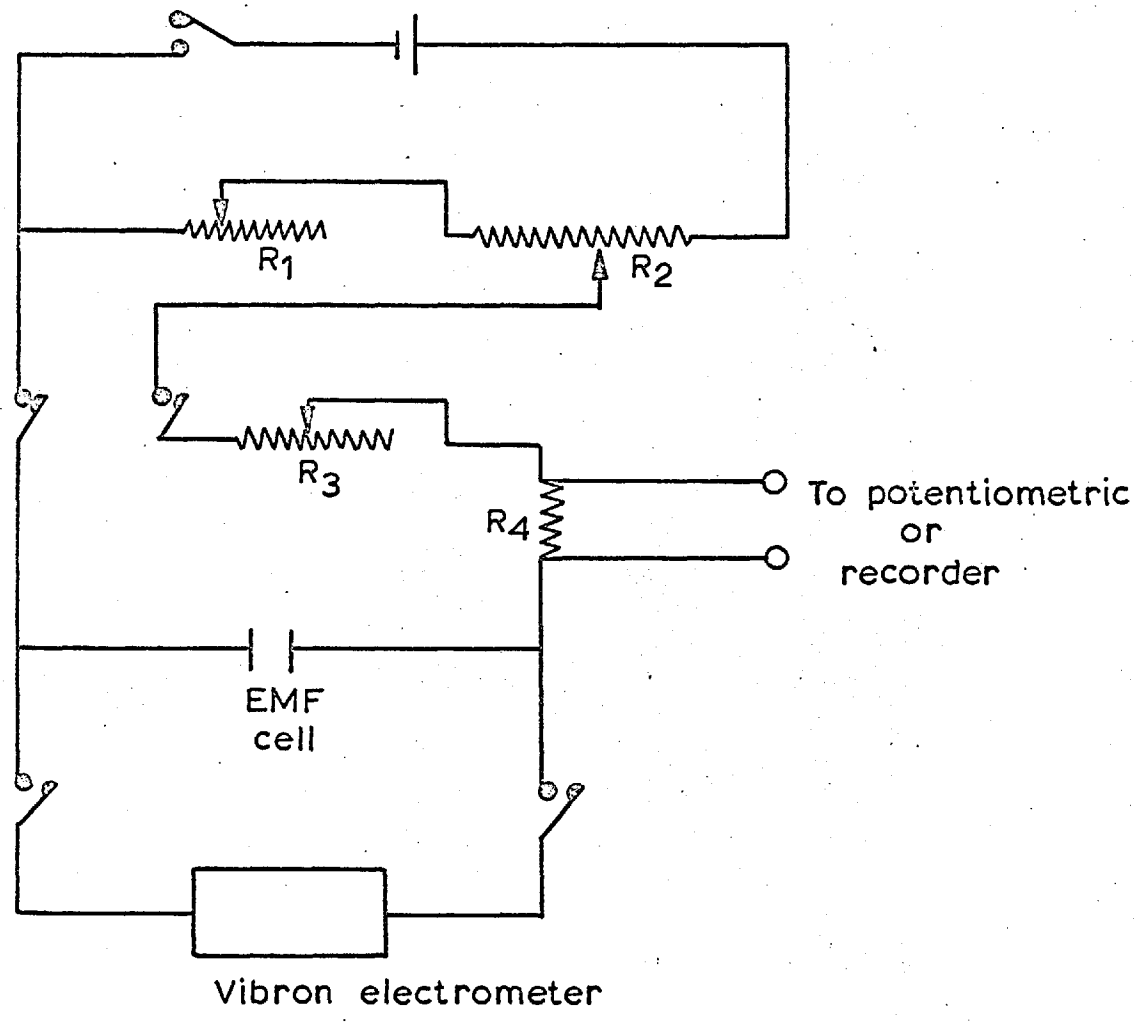

R_1, R_2, R_3 are variable resistors .(10^6 ohms)

R_4, Standard resistance (100 or 500 ohms)

Fig.10. ELECTRICAL CIRCUIT FOR COULOMETRIC TITRATIONS

calculated from thermochemical data. The fair agreement between the calculated and measured e.m.f.s suggested that the cells are capable of monitoring low oxygen pressures in the gas phase.

The galvanic cell

Pt, Ni-NiO / 7.5% CaO + ZrO_2 / O_2 (Argon), Pt .... Cell 2

was assembled as described above to measure the oxygen potential in the argon atmosphere. The furnace was heated to 1100°C. The e.m.f. obtained fluctuated $\mp$ 8 mv, and indicated a mean oxygen pressure of 1.3×10^{-12} atm. in the argon gas. This pressure of oxygen was approximately independent of the flow rate of argon gas in the range 50 to 200 mls min^{-1}. On introducing Ti getters into the reaction tube, the oxygen partial pressure was reduced to 10^{-17} atm; the e.m.f. varied by $\mp$ 17 mv and was sensitive to the flow rate of argon gas. Lowest oxygen pressure was observed with flow rates of 50 to 75 mls min^{-1}.

(b) Cu + O system.

About 60 grams of copper were taken in an alumina crucible in each run. The metal was cut from 5 mm diameter 'specpure' copper rods with shears exclusively used for this purpose. The copper was etched in nitric acid and washed with water and alcohol. The following cells were assembled as shown in fig 4.

Pt, Ni-NiO / 15% CaO + ZrO_2 / $[O]_{Cu}$, CO-CO_2, Cermet, Pt .... Cell 3

Pt, Fe-FeO / 15% CaO + ZrO_2 / $[O]_{Cu}$, CO-CO_2, Cermet, Pt .... Cell 4

The assembly was tested for gas tightness. The reference electrodes and the reaction tube were flushed with purified argon for 2 hours before heating the cell. The thermocouple was checked against the melting point of copper in each run.

Once the experimental temperature had been reached the electrometer was connected to the system and the run started. Oxygen was gradually added to the molten copper by increasing the CO_2/CO ratio in stages.

The gas mixture flow rate was generally kept at 250 mls min^{-1}. The time required to reach equilibrium was 15 to 20 min when the gas mixture was bubbled through the melt. When the gas mixture passed over the melt without bubbling 2 to 4 hrs were required to attain equilibrium. The flow rate of the gas mixture was varied from 100 to 400 mls min^{-1} without any effect on the e.m.f. of the cell.

The behaviour of cell 3 was similar to that of cell 2. Cell 4 produced very reversible e.m.f.s. After coulometric titration of oxygen in either direction the e.m.f. returned to a constant value in 5 min. During the course of the experiment, the $CO-CO_2$ mixture was replaced by purified argon. No change in e.m.f. was observed.

Experiment 6 consisted of measurements on the cell;

Pt, Ni-NiO / 15% CaO - ZrO_2 / $[O]_{Cu}$, Cermet, Pt .... Cell 5

The cell was assembled as in the previous experiment, except for the $CO-CO_2$ inlet. The e.m.f. of the cell (172 mv) decreased by 2 mv in 30 min. Constant e.m.f.s were obtained only after passing large external currents (50 to 150 micro amp) for 5 to 20 min. to depolarize the reference electrode. At the end of the experiment, the argon stream flushing the reference electrode was stopped, and the narrow alumina tube carrying argon to the reference electrode and the associated inlet and outlet connections above the brass head were removed. A 2 cm length was broken away from the top of tube X (fig 3) and the opening in the brass top closed with a rubber bung. With this arrangement no further polarization of the reference electrode was observed even when the e.m.f. was 193 mv and the cell left overnight. This suggested that the observed polarization was at least partly due to oxygen entering the argon stream over Ni-NiO electrode through small leaks invariably present in the complex assembly shown in section C-D of fig 3. It was therefore decided to use the modified arrangement in subsequent experiments. The Ni-NiO electrode was

not flushed with argon, but was allowed to establish its equilibrium partial pressure of oxygen in the gas phase above it. The upper end of tube X (fig. 3) was below the brass top and exposed to the argon atmosphere in the brass head.

In experiments 7 and 8, cell 5 was assembled using the modified arrangement. The oxygen content of liquid copper was varied by adding solid CuO or spec pure Cu through the addition tube. After adjusting the oxygen content to the desired level, the alumina addition tube was replaced by a silica sampling tube, the lower end of which was kept 1 to 2 in. above the liquid copper. The upper end of the silica tube was connected to the exhaust. The argon gas flowing up the reaction tube flushed the silica tube. When a constant e.m.f. was obtained, the silica tube was lowered into the melt and a sample of about 5 grms of copper was drawn into the tube by a syringe attached to the upper end. In initial experiments the sampling tube was immediately removed and quenched in distilled water. However, more concordant results were obtained when the metal in the sampling tube was first allowed to solidify in the water cooled brass head under argon before quenching in distilled water. Samples were taken at various oxygen concentrations between 0.2 and 1.8 atom pct. at 1100 and 1300°C, and the corresponding e.m.f.s recorded. After each experiment the reaction tube and other ceramic components of the cell were cleaned with 1 : 1 HNO_3.

The metal samples were removed from the silica tubes, and etched in hydrofluoric acid overnight to remove any adhering silica film. Lengths of about 8 mm were cut off from either end of the sample, the central portion then being analysed for oxygen. To check for segregation of oxygen in copper, two large samples (8 - 10 gm in weight) were obtained. After removing 1 cm length from either end, each sample was divided into four equal sections and analysed for oxygen. The oxygen content in all the four sections of a sample agreed closely,

indicating that no significant segregation of oxygen had occurred during solidification.

(c) Free Energy of formation of Cu_2O

The e.m.f. of the cell

Pt, Ni-NiO / 7.5% CaO + ZrO_2 / Cu-Cu_2O, Cermet, Pt .... Cell 6

was measured as a function of temperature from 600 to 1200°C. About 30 grams of Cu and 10 grams of Cu_2O were taken in an alumina crucible and the cell assembled as in previous experiments. The cell was maintained at each temperature for more than 2 hrs. The reversibility of the cell was periodically checked by passing external currents in both directions. No polarization of the reference electrode was observed. When the cell was taken through a temperature cycle, reproducible e.m.f.s were obtained.

(d) Pb + O system.

The e.m.f. of the cell

Pt, Ni-NiO / 7.5% CaO + ZrO_2 / $[O]_{Pb}$, cermet, Pt .... Cell 7

was measured as a function of the concentration of oxygen in liquid lead at 1100°C. In this experiment the argon gas used to flush the reaction tube was introduced through the brass head and made to flow down the reaction tube.

Yellow PbO powder was melted in a zirconia crucible and cooled rapidly to obtain a compact solid. This compact was broken up into small grannules, which were added to lead in the cell to increase the oxygen concentration. At a constant temperature the e.m.f. varied with time indicating a loss of oxygen from the solution, when the oxygen content was higher than 0.05. 'Spoon' samples were taken from the melt at three oxygen concentrations. The design of the sampling 'spoon' is shown in fig. 6d. After filling the spoon with the melt the sampler was raised into the water cooled brass head and allowed to cool under argon. The spoon was broken off from the alumina tube

and the lead in the zirconia spoon was analysed for oxygen using Baker's method. The e.m.f.s just before sampling were recorded.

(e) Free Energy of formation of PbO.

The e.m.f. of the cell

Pt, Ni-NiO / 7.5% CaO + ZrO_2 / Pb-PbO, Cermet, Pt .... Cell 8

was studied as a function of temperature from 475 to 1140°C. Since PbO melts at 897°C, and chromium oxide dissolves in liquid PbO, the cermet conducting lead was protected from liquid PbO by an alumina tube as shown in fig 6a. The cell e.m.f.s were reproducible on repeated temperature cycling in the range 500 to 850°C; however, once the cell was heated above 850°C, the e.m.f.s in this range could not be reproduced. On dismantling the cell the PbO was found to be greenish-yellow in colour and qualitative analysis indicated the presence of chromium in PbO. Besides, PbO was found to have penetrated the sides of the alumina crucible.

The cell construction was modified in a subsequent experiment, and Iridium was used as a conducting lead. Iridium has been found to have negligible solubility in lead[62, 117] and at the partial pressures of oxygen prevailing in the cell Iridium oxides are unstable. The arrangement of the cell

Pt, Ni-NiO / 7.5% CaO + ZrO_2 / Pb-PbO, Ir, Pt .... Cell 9

is shown in fig. 6b. The Iridium lead consisted of a strip of metal 50 mm long, 3 mm wide, and 0.3 mm thick. The upper end of the 40 mm long zirconia tube containing a mixture of Pb and PbO was closed with a split alumina plug, which allowed the Ir lead to pass through it. The small gaps between the alumina plug, the Ir lead, and the zirconia tube were closed with high temperature alumina cement.

The e.m.f.s obtained from this cell agreed with the reproducible e.m.f.s of cell 6 in the temperature range 500 to 850°C. However, above 850°C the e.m.f.s were considerably higher than those from cell 6. The e.m.f.s at all temperatures were reversible and were

reproducible when equilibrium was approached from higher and lower temperatures.

(f) Activity Coefficient of Oxygen in Cu-Ag alloys at 1100°C.

Cell 5 was assembled and the oxygen content adjusted to the required level (approximately 0.02 atom pct in experiments 13 and 14 and 0.3 atom pct in experiment 15) by adding reagent grade CuO through an alumina tube. This alumina tube was then replaced by another clean tube. Although no CuO was found to adhere to the sides of the additional tube, this precaution was taken to prevent the possible pick up of oxygen by silver samples which were subsequently dropped into the melt. This procedure of using different tubes to add oxides and metal samples was followed in all the experiments reported in this thesis.

After testing the constancy of the e.m.f. for 3 hours, an oxygen free silver sample of known weight was added to the Cu + O solution in the cell. The e.m.f. of the cell became constant in 10 to 25 min. after each addition. The constant e.m.f. was recorded. Further additions of Ag were made and the procedure repeated.

In experiment 15, suction samples were taken from the Cu + O solution before adding Ag and from Cu + Ag + O solution at the end of the experiment. These samples were analysed for oxygen.

(g) Activity Coefficient of Oxygen in Cu + Sn alloys at 1100°C.

'Specpure' copper rods were etched in dilute nitric acid to remove surface contamination and subsequently reduced in hydrogen at 900°C before use in cell 5, which was assembled as described earlier. In experiment 17, titanium internal 'getters' were used to ensure that no oxygen was transferred to the liquid metal from the gas atmosphere. The electrolyte in experiment 17 was Y_2O_3 + ZrO_2 rather than lime-zirconia. The oxygen content in copper was adjusted to approximately 0.004 atom pct in experiment 16 and 0.002 atom pct in experiment 17

by adding CuO. The cell was kept at a constant temperature for 3 hours to ensure that the e.m.f. did not vary with time. When oxygen free copper was dropped into the Cu + O solution, the change in e.m.f. of the cell indicated that the added copper was free of oxygen. Samples of oxygen free tin of known weight were then added to the Cu + O solution and the constant e.m.f.s obtained after each addition were recorded.

In experiment 16, after a few additions of tin, oxygen free copper was added to decrease the tin concentration. This was followed by further additions of tin to make the composition of the alloy the same as before. If there was an exchange of oxygen between the melt and atmosphere around it, the activity coefficient of oxygen computed from the two e.m.f. readings at the same composition would not be the same.

When the composition of tin in solution exceeded 50 atom pct., the e.m.f. varied with time indicating loss of oxygen from solution. However, when the cell was left overnight at the end of experiment 16, the e.m.f. of the cell decreased by only 2 mv.

When experiments starting with Sn + O solutions in the cell were attempted, drifting e.m.f.s were obtained, even when the oxygen content was below 0.005 atom pct.

(h) Activity Coefficient of Oxygen in Cu + Pb alloys at 1100°C.

Cell 5 was assembled with 7.5% CaO + ZrO_2 electrolyte and oxygen in liquid copper was adjusted between 0.003 and 0.008 atom pct. by adding CuO. In experiment 19 constant e.m.f. could not be obtained. However, when the solid electrolyte tube was withdrawn and replaced by another tube, constant e.m.f. was obtained. This indicated that some tubes were faulty, probably due to the presence of micro-cracks. When tested the faulty tube was found to be incapable of maintaining a vacuum at 600°C.

Cell 7 was assembled using 'specpure' lead previously reduced under hydrogen. The oxygen content was then adjusted between 0.04 and 0.004 atom pct. by adding PbO. In experiment 21 when the cell was left overnight the e.m.f. decreased by only 2 mv. When a known weight of oxygen free lead was added to the Pb + O solution in the cell, the change in e.m.f. indicated that the added metal was free of oxygen. Known weights of oxygen free copper were added to this solution and the constant e.m.f.s obtained after each addition were recorded.

In experiment 21, spoon samples were taken from the Pb + O solution before adding Cu and from Pb + Cu + O solution at the end of the experiment. These samples were analysed for oxygen by Baker's method.

Experiments were also done starting with Pb + O solutions at 950 and 750°C into which oxygen free copper samples were added.

(i) Effect of phosphorus on the activity coefficient of oxygen in liquid copper.

Phosphorus was added to Cu + O solution in cell 5 in the form of Cu-P master alloys containing 2.74 wt. pct. phosphorus, and the constant e.m.f.s obtained after each addition were recorded. The oxygen content of the solution was approximately 0.0003 at. pct. at 1200°C and 0.0006 at. pct. at 1300°C.

Initial runs using chromium cermet leads gave surprising results. The activity coefficient of oxygen decreased rapidly with increasing phosphorus content upto 0.05 wt. pct. phosphorus. The activity coefficient was approximately independent of phosphorus content at higher concentrations. Careful examination of the cell components indicated the occurance of a reaction on the surface of the cermet. When a section of the cermet was scanned under the electron probe microanalyser, the phosphorus concentration in the oxide layer on the surface of the cermet was found to be approximately three times larger than that in the liquid solution. This suggested the formation

of a compound, probably a phosphate, on the surface of the cermet. When samples from Cu + P + O solution in the cell were analysed for phosphorus, the results were 8 to 10 pct. lower than the value calculated on the basis of the mass balance.

When tungsten conducting leads were used, the logarithm of the activity coefficient of oxygen was found to vary linearly with phosphorus concentration. Analysis of suction samples indicated that no phosphorus was lost from the solution. When oxygen free copper was added to Cu + O solution in experiment 31, the change in e.m.f. indicated that the added metal contained no oxygen.

At the low oxygen concentrations used in these experiments, the e.m.f. of the cell decreased (15 - 25 mv in 8 hrs.) with time, indicating an increase in the oxygen content of the solution. Titanium internal 'getters' were therefore used to reduce the partial pressure of oxygen in the argon gas. However, the drift in e.m.f. of the order of 10 to 12 mv in 8 hrs. persisted. The rate of decrease of e.m.f. was lower when a larger quantity of Cu + O solution was used.in the crucible.

Transport of oxygen from the Ni-NiO reference electrode through the electrolyte to the solution due to finite electronic conductivity was a possible reason for the observed decrease in e.m.f. To test this hypothesis an external potential slightly larger than the cell e.m.f. was applied to the terminals of the cell. The applied potential opposed the cell e.m.f. and the small resultant current (approximately 1 micro amp) transferred oxygen from the solution to the Ni-NiO electrode. When the external potential was removed, the cell e.m.f. obtained was the same as that before applying the external potential.

Currents upto 1 micro amp did not polarize the Ni-NiO electrode at temperatures above 1200°C. At 1150°C, however, small polarisation of Ni-NiO electrode was observed due to the applied potential. The

change in the oxygen concentration of the solution due to the passage of a current of 1 micro-amp for 8 hr. is insignificant.

The experiment demonstrated that the transfer of oxygen to the solution from the reference electrode because of finite electronic conductivity in the electrolyte could be prevented by an externally applied potential. During the course of the experiments using Ni-NiO reference electrode, an external e.m.f. was applied to the terminals of the cell except when e.m.f. readings were being taken.

When Fe-FeO reference eledtrode was used, the chemical potentials of oxygen in the two half cells were approximately equal. The decrease in e.m.f. was approximately 3 mv in 8 hr. This was considered to be tolerable when compared with the changes in e.m.f. on adding phosphorus. Therefore no external e.m.f. was applied to the cell when Fe-FeO reference electrode was used. However, the penetration of the electrolyte by FeO limited the useful lifetime of these cells to 8 - 10 hr.

(j) Activity Coefficient of Oxygen in Sn + Pb alloys from 550 to 1100°C.

Oxygen free tin was added to Pb + O solution maintained at a constant temperature in the cell,

Pt, Fe-FeO / 7.5% CaO + ZrO_2 / $[O]_{Pb}$, Cermet, Pt .... Cell 10

and the constant e.m.f.s obtained after each addition were recorded. The experiments were done at 750, 950 and 1100°C. The oxygen content of the solution was less than 0.001 at.pct. at 750, 0.0025 at.pct. at 950, and 0.002 at. pct. at 1100°C. At 550°C the oxygen concentration in lead rich solutions had to be below 0.00005 at. pct. to prevent the formation of SnO_2. Constant e.m.f.s could not be obtained at this low concentration. At 1100°C, when the concentration of tin in solution was higher than 60 at. pct., drift in e.m.f. was observed, suggesting loss os oxygen from the melt.

Experiments starting with Sn + O solutions, using the cell

Pt, Fe-FeO / 7.5% CaO + ZrO_2 / $[O]_{Sn}$, Cermet, Pt .... Cell 11

were done at 750 and 950°C. At 550°C, Fe-FeO reference electrode could not be used due to the disproportionation of Wüstite at 575°C. Ni-NiO reference electrode was used instead of the Fe-FeO electrode. When Sn reduced under hydrogen at 900°C for 5 hr. was dropped into liquid Sn + O solution at 750°C, the change in e.m.f. showed that the added metal contained no oxygen.

(k) Activity Coefficient of Oxygen in Ag-Pb alloys at 1000°C.

Known weights of oxygen free silver were added to lead containing less than 0.02 at. pct. oxygen in cell 7 at 1000°C and the constant e.m.f.s obtained after each addition were recorded.

Similarly, oxygen free lead was added to Ag containing approximately 0.001 at. pct. oxygen and the constant e.m.f.s after each addition were recorded. When oxygen free Ag was added to Ag + O solution, the change in e.m.f. of the cell,

Pt, Ni-NiO / 7.5% CaO + ZrO_2 / $[O]_{Ag}$, cermet, Pf .... cell 12

indicated the added metal was free of oxygen.

(l) Activities in Ag-Pb Alloys.

The cell,

stainless steel, Ir, Pb-PbO / $\overset{CaO +}{ZrO_2}$ / Pb-PbO, Ir, Stainless steel

.... cell 13

was assembled as shown in fig 6b, except that CaO + ZrO_2 crucible was used instead of an alumina crucible, and instead of Ni-NiO weighed quantities of Pb and PbO were placed in the crucible. Ir strips 50 mm long were spot welded to stainless steel wires, which were protected by thermocouple sheaths. The cell produced zero e.m.f. (∓ 0.1 mv) for over 10 hours at 827°C. Weighed quantities of silver were then added to the lead in the crucible, and the e.m.f. of the cell followed as a function of time. Times varying from 45 to 70 min. were required to attain constant e.m.f. after each addition. The small e.m.f.s measured with the vibron electrometer

were checked against a Tinsley portable potentiometer (type 3184 D). The cell e.m.f.s were recorded for 1 hr. after attaining constant values.

In experiment 55, the cell was assembled with 30 g. of Pb-Ag alloy containing 20 at. pct. Ag in equilibrium with PbO in the crucible. The e.m.f. of this cell was recorded after successive additions of Pb.

In experiments 56 to 60, cells were assembled using alloys containing 50, 60, 70, 80, and 90 at. pct. Pb respectively in the zirconia crucible. The e.m.f. of these cells were measured as a function of temperature from the liquidus to 830°C. The e.m.f.s were reversible and reproducible on repeated temperature cycling.

(m) Resistance Measurements.

The total resistance across the platinum leads from the cell was measured in experiments 18 and 19 as 80.7 and 78.5 ohms at 1100°C. When the resistance was measured between the platinum wires attached to two different cermet leads dipping in liquid copper at 1100°C, a value of 16 ohms was obtained.

CONTAMINATION OF Pt CONTACTS.

Both Ni-NiO and Fe-FeO electrodes contaminated the platinum wire in contact with them. The contaminated portions of the Pt wire were not used in subsequent experiments. Although protected by an alumina tube and cement, the platinum wire was found to be contaminated at the junction with the chromium cermet.

It was possible for a thermal e.m.f. due to the different composition of the contacts to be included in the readings. In order to assess the magnitude of this error, the e.m.f. of a junction made from the contaminated Pt wires was measured as a function of temperature. The highest e.m.f. obtained was 0.1 mv.

CHAPTER 5.

R E S U L T S.

(a) Measurement of Oxygen potential in gases.

The e.m.f. of cell 1 is tabulated as a function of CO/CO_2 ratio at 1200°C in table 4 and plotted in fig. 11. The observed polarization of the Ni-NiO electrode and the small descrepancy between the calculated and measured values will be discussed in the following section.

(b) Cu + O system.

The e.m.f. of cells 3 and 4 at different CO/CO_2 ratios is compared with that calculated from thermochemical data[65,69] in figs. 11 and 12 and tables 5 and 6 at 1200°C. The e.m.f. of cells 1 and 3 are almost identical. Better agreement between the measured and calculated e.m.f.'s is obtained when the Fe-FeO reference electrode is used, except at high CO/CO_2 ratios. On dismantling the cell a small amount of carbon was found to have been deposited in the upper part of the reaction tube (exit side), where the temperature was below 950°C. Since the deposit was on the exit side and away from the reaction zone, the deposition of carbon according to the reaction

$$CO_2 + C = 2CO$$

did not apparently alter the CO/CO_2 ratio over liquid copper appreciably. The increasing descrepancy between the calculated and measured e.m.f. at higher CO/CO_2 ratios is probably due to the increasing significance of this reaction. When the experiment was repeated at 1100°C, the measured e.m.f. was 8 to 20 mv lower than that calculated from thermochemical data, and the carbon deposit was found very close to the crucible containing liquid copper.

When the $CO-CO_2$ gas mixture was bubbled through liquid copper, equilibrium was attained in 15 to 20 min. When the gas mixture was passed over the surface of the melt, 2 to 4 hours were required to obtain constant e.m.f. No change in e.m.f. was observed when $CO-CO_2$

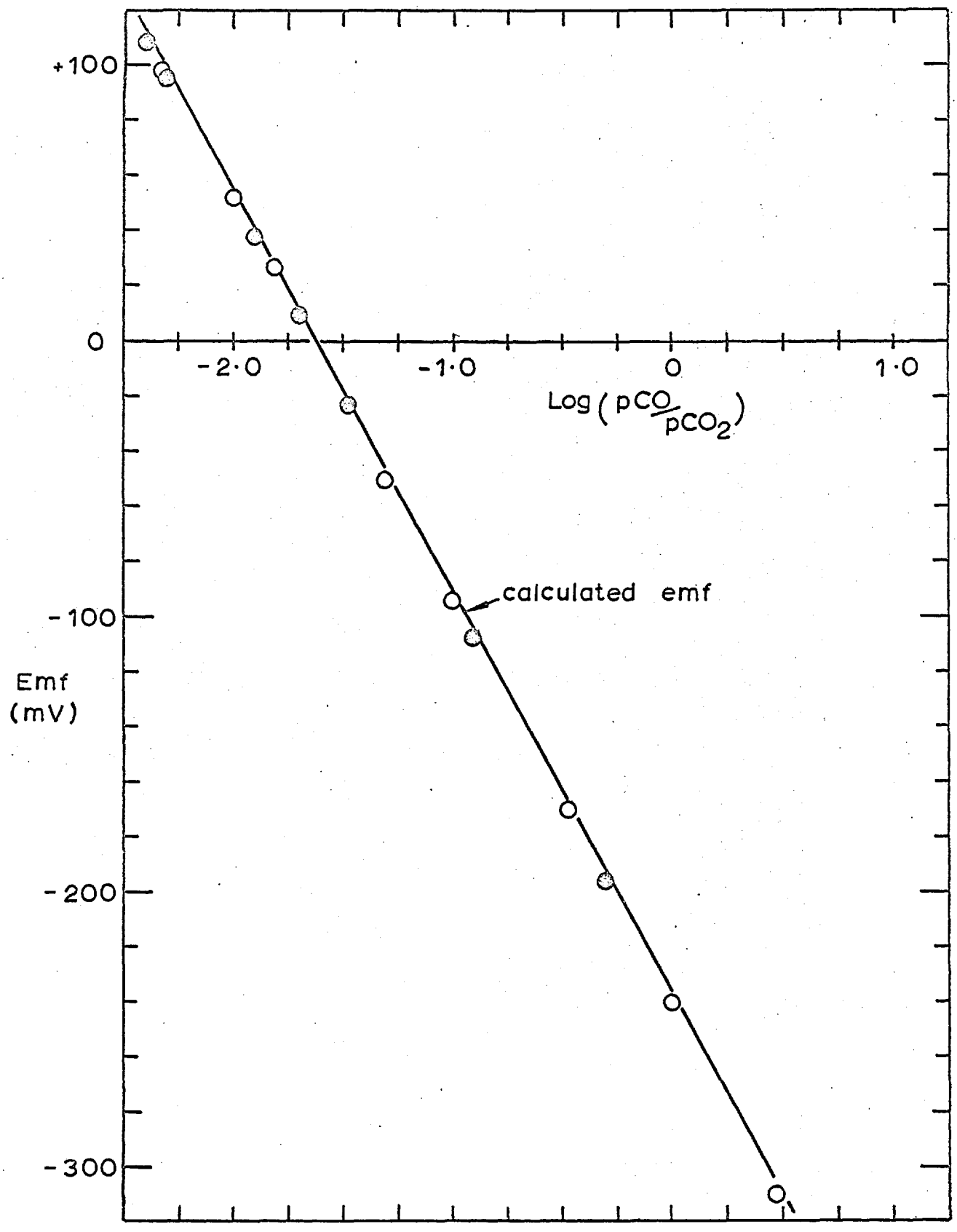

Fig. 11 VARIATION OF EMF WITH CO/CO_2 RATIO

⊙ Ni-NiO/S.E/$[O]_{Cu}$ $CO-CO_2$

O Ni-NiO/S.E/CO/CO_2

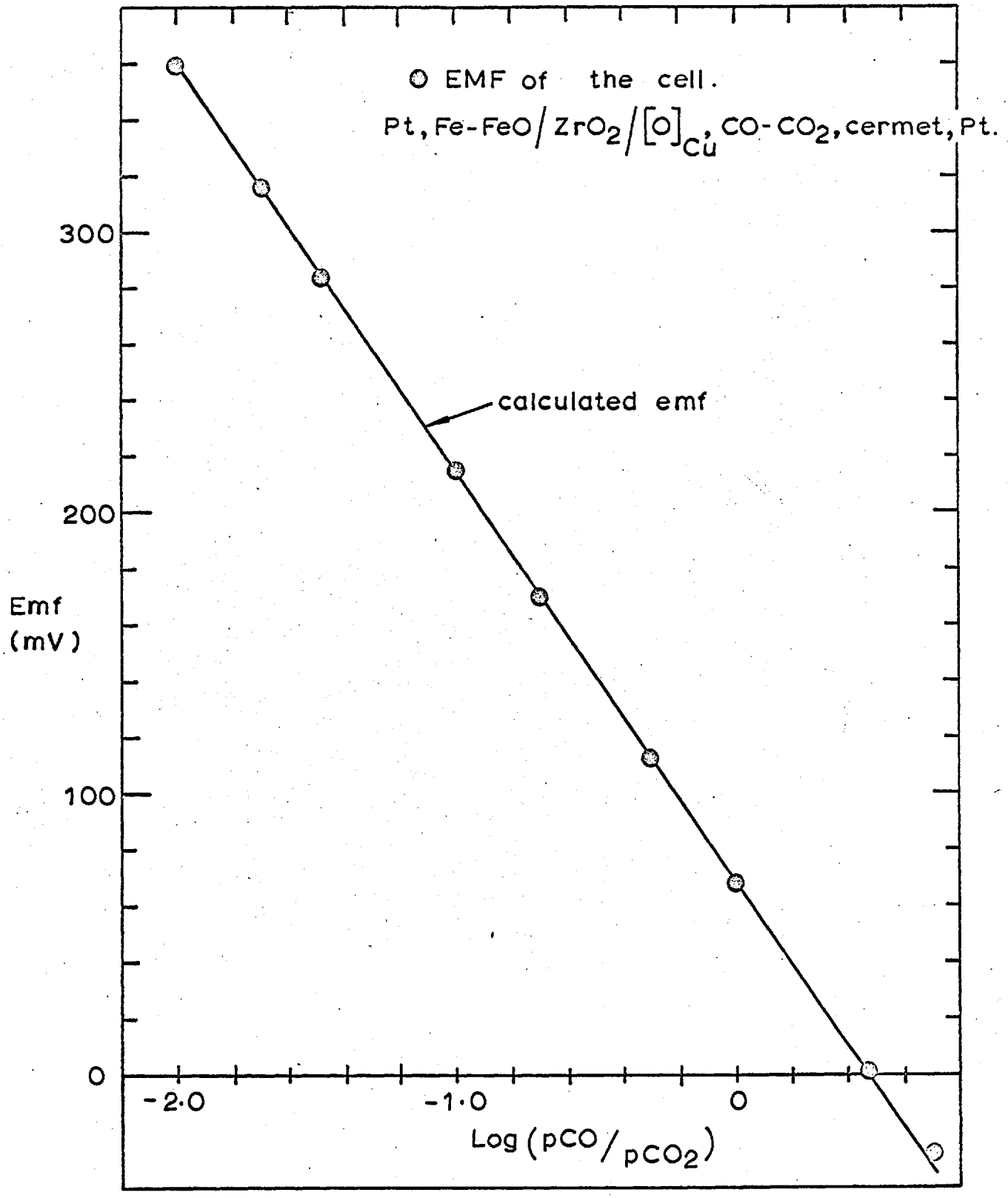

Fig. 12 VARIATION OF EMF WITH CO/CO_2 RATIO

TABLE 4.

E.m.f. of Cell 1 as a function of CO/CO_2 ratio at 1200°C.

pCO/pCO_2	E, mv measured	E, mv calculated
1/210	98	101.7
1/100	52	54.6
1/65	26.5	27.3
1/20	- 49	- 47.5
1/10	- 93.5	- 91.5
1/8	- 108	- 105.7
1	- 240	- 237.6
3	- 310	- 307.3

The following data were used to calculate the e.m.f. of the cell.

$CO + \frac{1}{2} O_2 \rightarrow CO_2$

$\Delta G^\circ_{1200^\circ C} = -37{,}038$ cals (Janaf.)

$2Ni + O_2 \rightarrow 2NiO$

$\Delta G^\circ = -111{,}930 + 40.58T$ (Steele)

TABLE 5.

E.m.f. of Cell 3 as a function of CO/CO_2 ratio at 1200°C.

pCO/pCO_2	E, mv measured	E, mv calculated
1/250	108	112
1/200	96	98.6
1/80	38	40.4
1/50	10	10.6
1/30	- 23	- 21.8
1/3	- 170	- 167.9
1/2	- 196	- 193.6
1/6.5	- 121	- 118.8

TABLE 6.

E.m.f. of Cell 4 as a function of CO/CO_2 ratio at 1200°C.

pCO/pCO_2	E, mv measured	E, mv calculated
1/100	360	361
1/50	317	317.0
1/30	284	284.6
1/10	214	215.0
1/5	170.5	171.0
1/2	112	112.0
1	67.5	68.8
3	1.5	- 0.9
5	- 28.5	- 33.3

$$1.9\ Fe + O_2 \longrightarrow 2\ Fe_{0.95}O$$

$$\Delta G^\circ = -126{,}470 + 31.26T \qquad \text{(Steele}^{65}\text{)}.$$

mixture was replaced by an argon atmosphere after steady state is attained.

Polarization of the Ni-NiO electrode is probably related to small leaks in the argon stream flushing the reference electrode. The oxygen in argon would preferentially oxidise the nickel at the interface between the electrode and electrolyte, and give rise to a higher oxygen potential at the interface, if the transport of oxygen through NiO is slow. Moreover, no polarization was observed when the argon stream flushing the reference electrode was removed and the electrode was allowed to establish equilibrium oxygen potential under a static argon atmosphere. The higher oxygen potential at the electrode - electrolyte interface explains the descrepancy between calculated and measured e.m.f. when Ni-NiO reference electrode was used. The fact that Fe-FeO electrode did not become polarised under identical conditions suggests that diffusion of oxygen is faster in FeO, and therefore the electrode is more reversible.

The analytical results for oxygen in samples withdrawn from Cu + O solution under argon atmosphere are presented in table 7, along with the observed e.m.f. The partial pressure of oxygen over Cu + O solution is calculated from the e.m.f. and the free energy of formation of NiO, using the relationship,

$$E = \frac{RT}{nF} \ln \frac{pO_{2\ I}}{pO_{2\ II}} \qquad \ldots\ 29$$

where E is the e.m.f. in volts, F = 23063 cals per v equivalent, n = 4, R is the gas constant in calories, T is degrees Kelvin, $pO_{2\ I}$ is the oxygen potential in Cu + O solution and $pO_{2\ II}$ is the oxygen potential in equilibrium with nickel and its oxide at temperature T°K.

The 'equilibrium constant' for the reaction

$$\tfrac{1}{2} O_2 = [O]_{Cu}$$

$$K' = \frac{\text{atom pct. oxygen}}{(pO_2)^{\frac{1}{2}}}$$

TABLE 7.

E.m.f. of Cell 5 as a function of oxygen concentration.

T = 1100°C.

E.m.f., mv	at. pct. Oxygen	log K'
124.6	0.2101	2.8822
130.0	0.2455	2.9098
146.8	0.2843	2.8506
145.9	0.3067	2.8898
154.6	0.3499	2.8829
179.0	0.5103	2.8682
189.2	0.5692	2.8504
208.7	0.8363	2.8643
212.1	0.8478	2.8452
218.5	0.9609	2.8526
225.8	1.0313	2.8296
227.8	1.1438	2.8603
229.8	1.1480	2.8466
234.9	1.1898	2.8249
238.4	1.2900	2.8347
235.2	1.3004	2.8610
246.1	1.4299	2.8228
243.3	1.4303	2.8430
249.3	1.4805	2.8141
245.1	1.4989	2.8502
251.0	1.5374	2.8183
252.0	1.6248	2.8348

T = 1300°C.

E.m.f., mv	at. pct. Oxygen	log K'
24.5	0.1921	2.4679
36.3	0.2363	2.4828
54.8	0.2907	2.4541
68.3	0.3714	2.4738
74.6	0.3998	2.4653
79.7	0.4203	2.4547
85.5	0.4800	2.4748
99.4	0.5447	2.4410
102.1	0.5863	2.4552
115.1	0.7216	2.4622
121.8	0.8185	2.4744
131.4	0.8821	2.4453
133.6	0.8906	2.4354
138.1	0.9905	2.4526
145.5	1.0574	2.4333
145.6	1.1079	2.4532
157.2	1.2926	2.4450
162.4	1.3007	2.4147
165.4	1.3900	2.4244
167.6	1.4626	2.4328
170.9	1.5675	2.4415
176.6	1.6020	2.4144
176.0	1.6407	2.4288
178.4	1.6793	2.4231

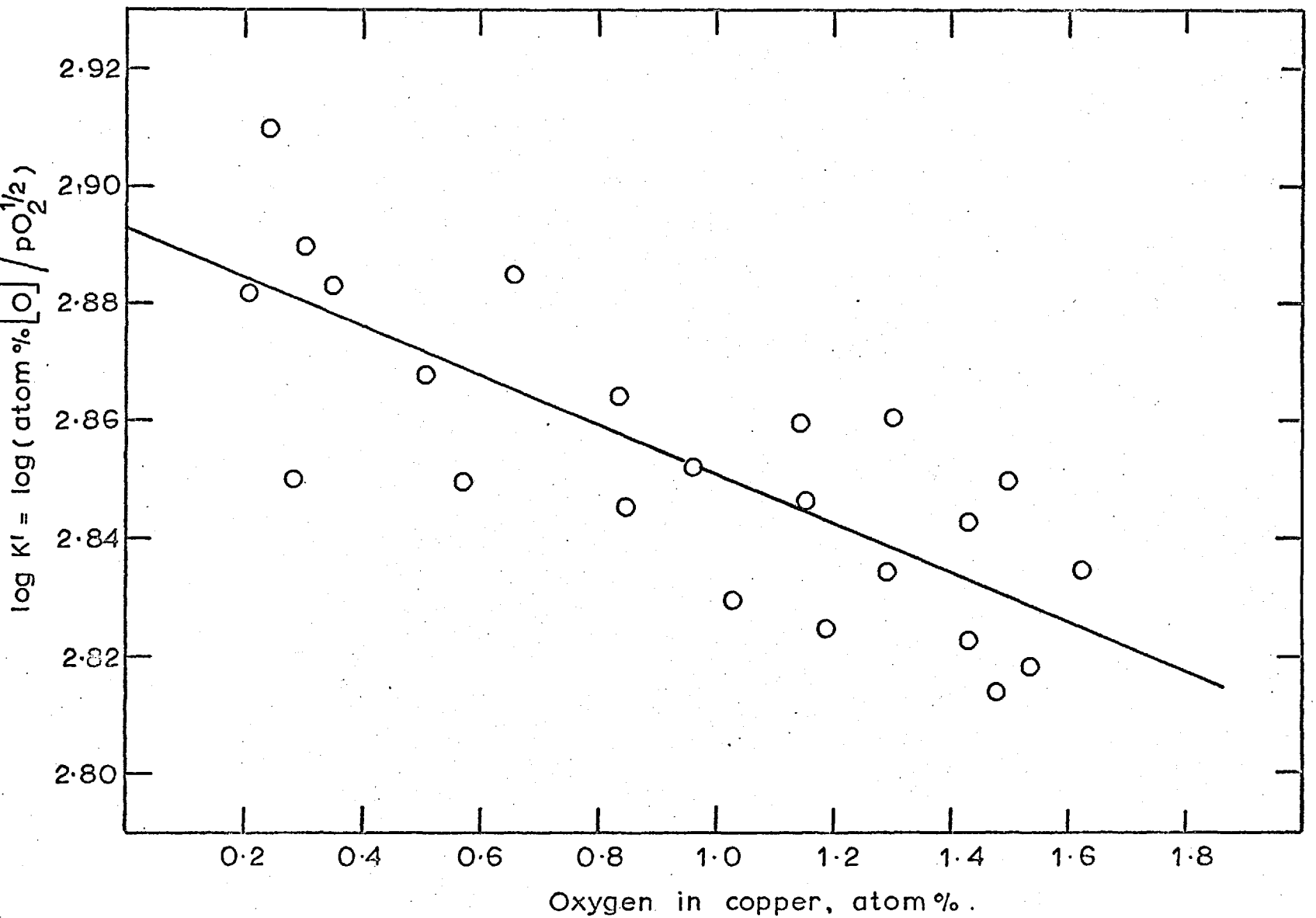

Fig. 13 RELATIONSHIP BETWEEN LOG K' & OXYGEN CONTENT AT 1100 °C

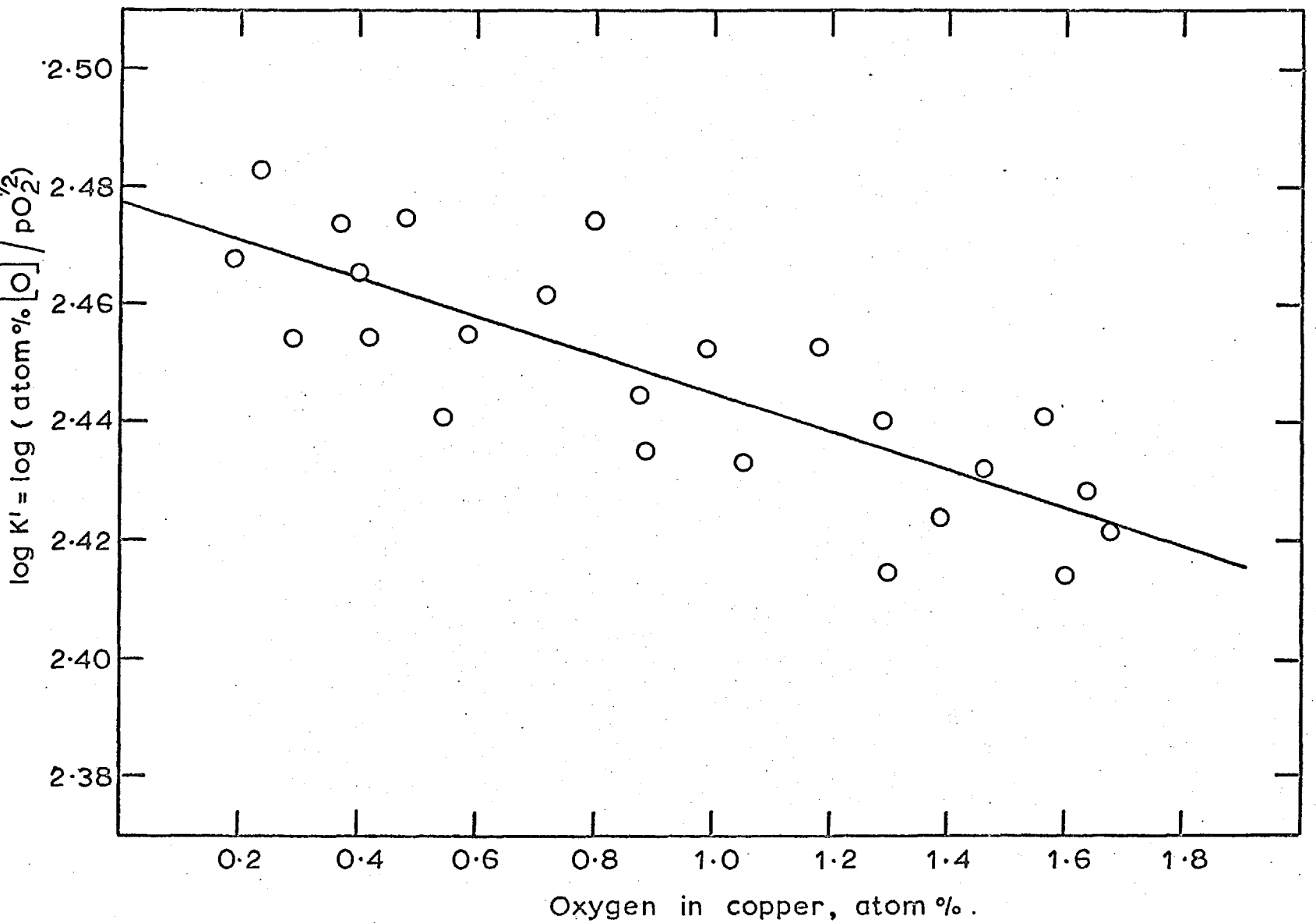

Fig. 14 RELATIONSHIP BETWEEN LOG K' & OXYGEN CONTENT AT 1300 °C.

was found to be a function of oxygen concentration (figs. 13 and 14), indicating that Sieverts' law is not obeyed by oxygen in copper. The best equations for the variation of log K' with concentration are:

$$\log K' = 2.8930 - 0.042 \text{ (at. pct. O)} \qquad (1100^\circ C)$$

$$\log K' = 2.4778 - 0.0324 \text{ (at. pct. O)} \qquad (1300^\circ C)$$

The 'Henrian activity coefficient' of oxygen in Cu + O solutions at 1100 and 1300°C are:

$$\log f_O^O = - 0.042 \text{ (at. pct. O)}$$

$$\log f_O^O = - 0.0324 \text{ (at. pct. O)}$$

The variation of $\log f_O^O$ with temperature can be expressed by the relationship:

$$\log f_O^O = (- 103.99/T + 0.03374) \text{ atom \% O}$$

(c) Free Energy of formation of Cu_2O.

E.m.f. of cell 6 is shown in table 8 as a function of temperature. The e.m.f. may be expressed as a linear function of temperature from 600 to 1065°C.

$$E, \text{ mv} = 344.4 - 0.06888T \qquad \ldots\ 30$$

The standard free energy change for the reaction

$$Ni(s) + Cu_2O(s) = 2Cu(s) + NiO(s)$$

may be calculated from the e.m.f. from the relationship,

$$\Delta G^\circ = - n F E \qquad \ldots\ 31$$

where n = 2, E is the e.m.f. in volts and F = 23063 cals per volt equivalent.

$$\Delta G^\circ = - 15,886 + 3.177 T \text{ cals} \quad (600 - 1065^\circ C)$$

Combining this with the standard free energy of formation of NiO reported by Steele, the standard free energy change for the formation of Cu_2O from oxygen and solid copper is obtained as

$$\Delta G^\circ_{f,Cu_2O} = - 40,079 + 17.113 T \text{ cals/gr. mole} \qquad \ldots\ 32$$

Above the eutectic temperature (1065°C) the e.m.f. does not vary

TABLE 8.

E.m.f. of Cell 6 as a function of temperature.

Temp. °C	E.m.f., mv	Temp. °C	E.m.f., mv
610	283.0	813	269.5
658	280.5	1015	256.0
703	276.9	1030	254.7
752	274.3	1050	253.8
807	270.2	1060	252.5
850	267.0	1100	254.0
903	263.5	1130	257.2
952	262.2	1149	257.5
1003.5	256.0	1187	259.0
1047	253.2	1200	260.0
923	262.3	1172	258.8
875	256.2	1100	253
832	268.2	1081	253
781	271.5	1072	252.3
731	274.8	1094	252.7
680	279.3	1173	256.7
625	282.5	1200	259.2
581	285.2	1180	257.8

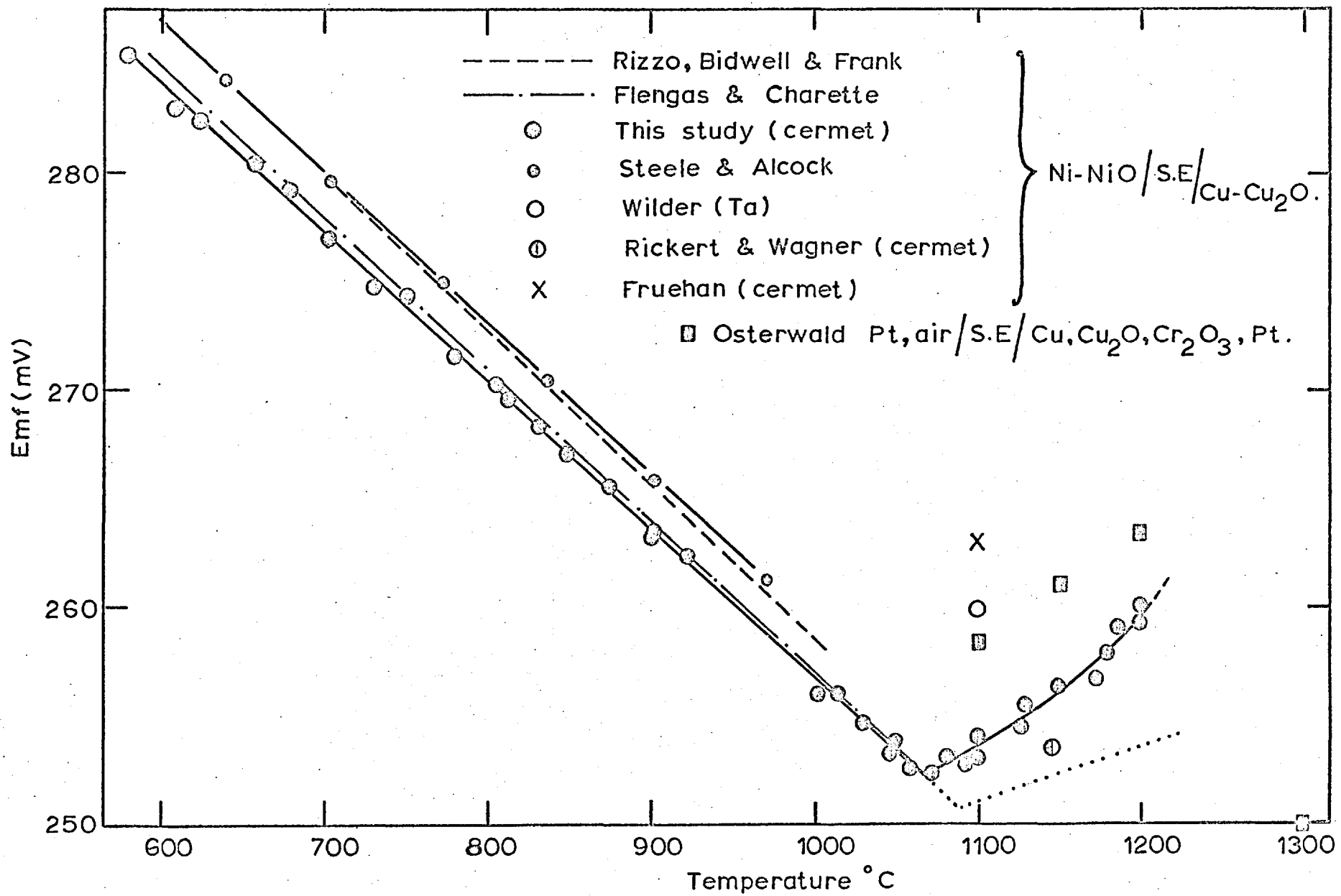

Fig. 15 TEMPERATURE DEPENDENCE OF EMF FOR THE SYSTEM Ni, NiO - Cu, Cu_2O.

linearly with temperature (fig. 15), probably due to the significant solubility of oxygen in liquid copper, which increases with temperature. The activity of copper in Cu + O solution in equilibrium with Cu_2O can be calculated from the saturation solubility data (fig. 1) and the activity coefficient of oxygen through the relationship,

$$\log \gamma_{Cu} = \frac{-(N_O)^2 \epsilon_O^O}{4.606} \quad \ldots\ 33$$

which will be derived in appendix 1. N_O is the saturation solubility of oxygen expressed in mole fraction, and $\epsilon_O^O = (\partial \ln f_O^O / \partial N_O)$. It is assumed that $\log f_O^O$ varies linearly with oxygen concentration upto saturation. From the e.m.f.'s above 1065°C, the calculated activity of Cu in Cu + O solutions in equilibrium with Cu_2O and data on NiO, the standard free energy of formation of $Cu_2O(s)$ from liquid copper and oxygen gas may be calculated and expressed by the relation,

$$\Delta G^\circ_{f,\ Cu_2O} = -45{,}907 + 21.40\ T \qquad (1065 - 1200^\circ C) \quad \ldots\ 34$$

The side of the alumina crucible containing liquid copper was discoloured, suggesting either a small solubility of Cu_2O in alumina or formation of copper aluminate. However, since an excess of Cu_2O was present in the crucible, the activity of Cu_2O could not have been reduced by this dissolution or reaction.

(d) Pb + O system.

The e.m.f. of cell 7 and the oxygen concentration in liquid lead obtained from the analysis of 'spoon samples' are shown in table 9. The square root of the partial pressure of oxygen over Pb + O solution, calculated from the e.m.f. is plotted as a function of oxygen content in Fig. 16. The uncertainty (shown in fig.) in the analysis of oxygen and the restricted number of experiments do not permit any conclusions to be drawn regarding deviations from Sievert's law.

The standard free energy of solution of oxygen can be calculated:

$$\tfrac{1}{2} O_2 = [O]_{Pb}$$

TABLE 9.

Free Energy of solution of oxygen in lead at 1100°C.

E.m.f.	$pO_2^{\frac{1}{2}}$ (Pb^2+ O)	atom % O (analysis)	log K *	ΔG°_{cal} *
- 29.9	2.021×10^{-5}	0.1420	3.8467	24163
+ 36.6	6.2312×10^{-5}	0.4137	3.8221	24008
+ 71.8	1.130×10^{-4}	0.8214	3.8614	24255

* For the reaction $\frac{1}{2} O_2 = [O]_{Pb}$

$$K = \frac{\text{atom pct. Oxy.}}{pO_2^{\frac{1}{2}}}$$

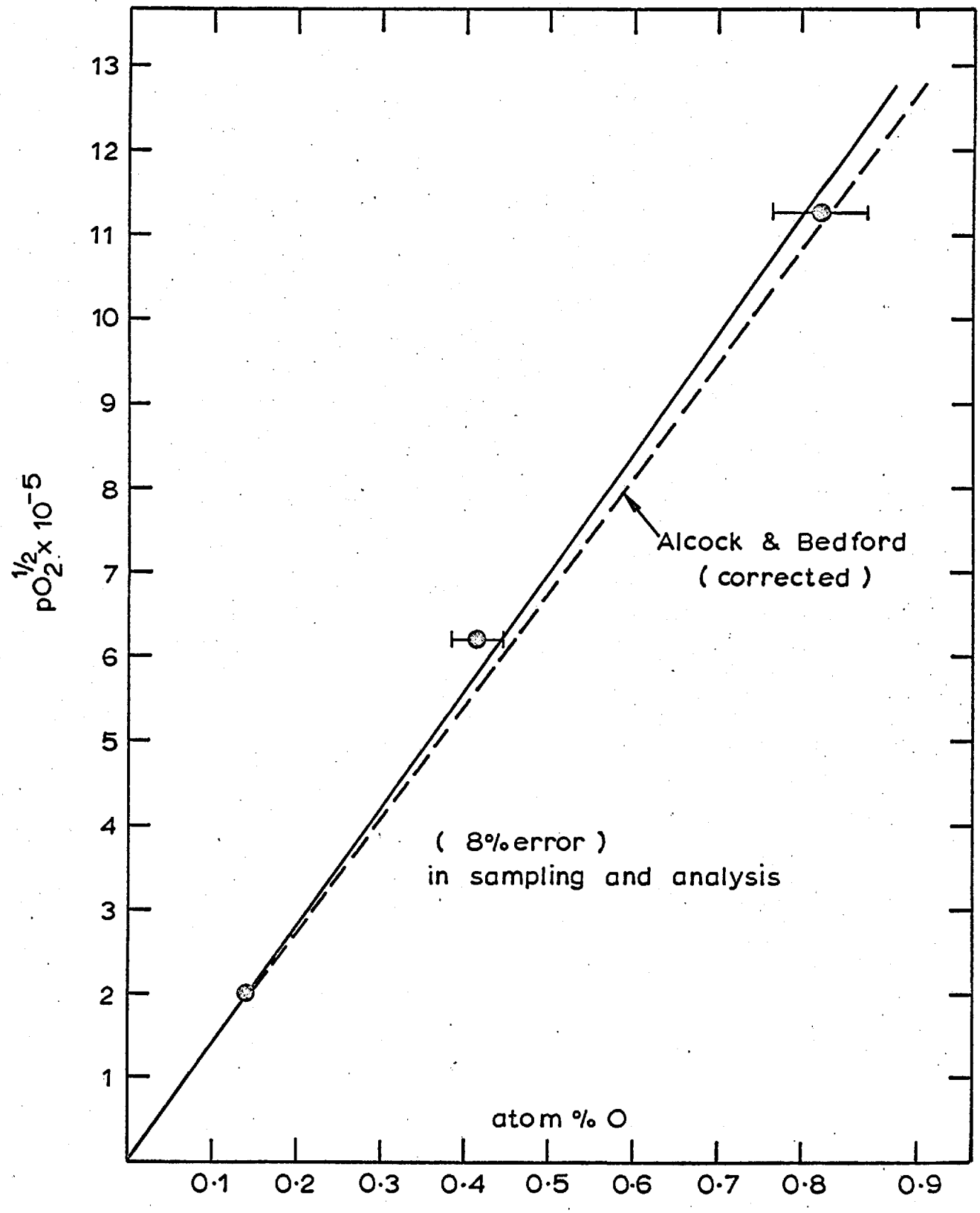

Fig. 16 ACTIVITY OF OXYGEN IN LIQUID LEAD AT 1100 °C

$$\Delta G^{\circ} = -RT \ln K = -4.575\, T \log \left(\frac{\text{at. pct. O}}{p O_2^{\frac{1}{2}}} \right)$$

The average value for ΔG° obtained from the three experimental points is - 24,142, while a value of - 24,298 was selected in chapter 2. In view of the good agreement, Alcock and Belford's (corrected) expression for the free energy of solution of oxygen in Pb may be used from 500 to 1100°C.

(3) Free Energy of formation of PbO.

With chromium cermet conducting lead (fig. 6a), cell 8 gave reproducible e.m.f.s, when temperature was varied in the range 500 to 850°C. Above this temperature the reproducibility of the e.m.f. deteriorated (∓ 2 mv) and in general decreased by 1 or 2 mv when kept under isothermal conditions for periods in excess of 2 hours. When the temperature was reduced below 850°C, the e.m.f. obtained was much higher than that obtained before 'melting' PbO. The results are summarised in table 10. On dismantling the cell, the PbO was found to be greenish-yellow in colour, and qualitative analysis indicated the presence of chromium in PbO. Because of the convex meniscus of Pb, and the penetration of alumina by PbO, a thin film of PbO was found between the Pb and the crucible on all the sides and between the metal and alumina tube protecting the cermet from PbO. The continuous film of PbO around the cermet and the protecting tube probably facilitated the transfer of Cr_2O_3 from the cermet to the PbO phase.

When iridium was used as a lead (fig. 6b) the e.m.f. of cell 9 was reproducible on repeated temperature cycling from 475 to 1130°C. The results are shown in table 10 and fig. 17. Due to the appreciable vapour pressure of PbO, experiments were not attempted above 1130°C. The e.m.f. s below 850°C agreed with those from the cell using cermet lead before 'melting' PbO. However, e.m.f.s above 850°C were 1 to 8 mv higher than those from the cell using cermet lead. This suggests that

TABLE 10.

E.m.f. of Cell 8 as a function of temperature.

Temp. °C	E.m.f., mv	Temp. °C	E.m.f., mv
700	154	900	162.5
625	148	1000	154.0
525	141	1102.5	145.0
674	150.5	830	166.0
823	163	710	170.0
700	153.5	650	165
597.5	146.5	845	166
780	159.5	894	161
825	163	1050	147
850	165	1100	143

E.m.f. of Cell 9 as a function of temperature.

Temp. °C	E.m.f., mv	Temp. °C	E.m.f., mv
675	152	983	158
738	156.7	1044	155
776	159.1	1137	150.8
474.5	137.2	1100.5	152.5
511.5	140.4	1024	157
600	146.8	963	160
801	161.3	850	165
837	164.0	627	148.3
863.5	164.7	550	143.2
924.5	161.7	892	163.2

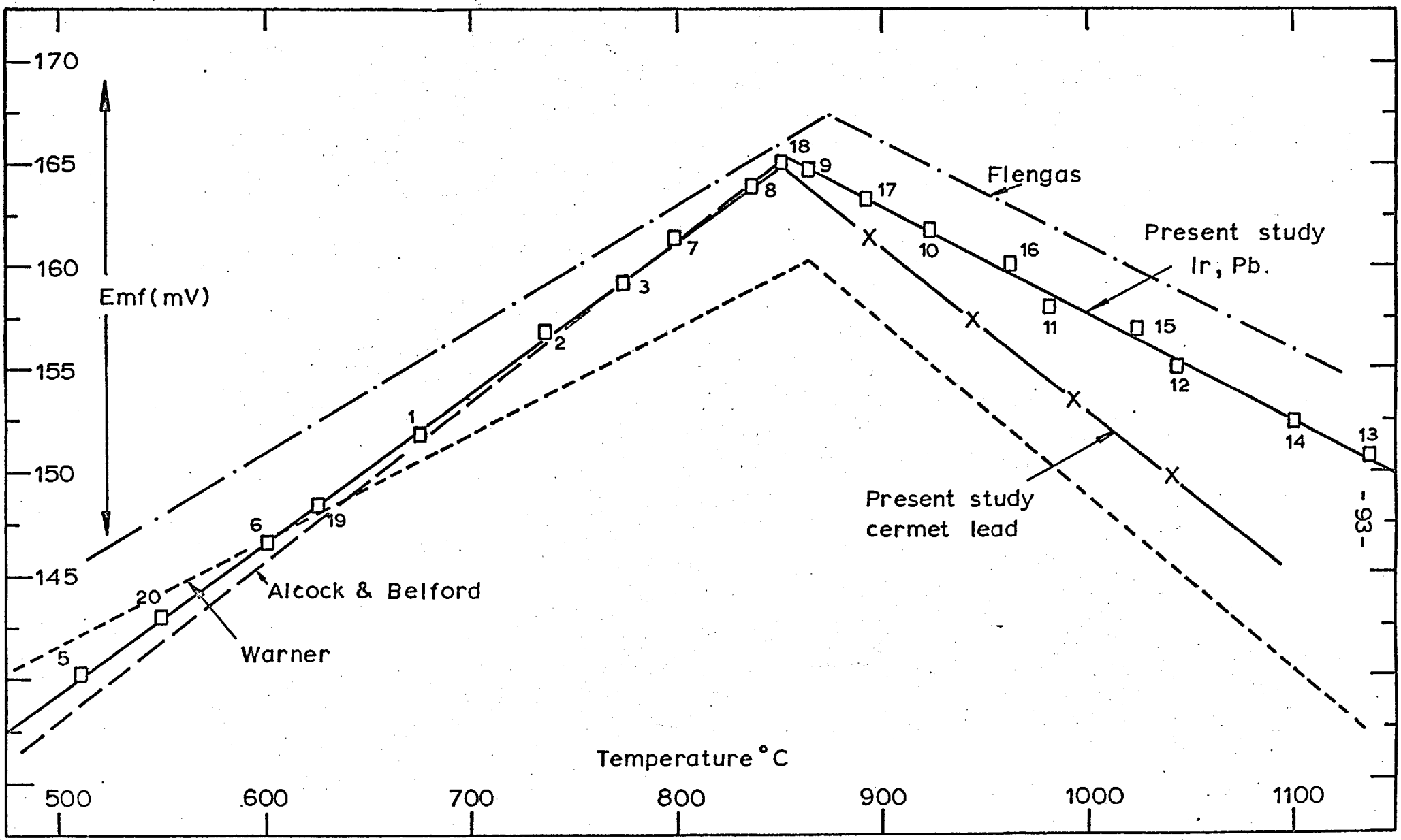

Fig.17 VARIATION OF EMF OF CELL Pt, Ir, Pb-PbO / $CaO.ZrO_2$ / Ni, NiO, Pt WITH TEMPERATURE

the activity of PbO had been lowered by the dissolution of Cr_2O_3 when the cermet was used. For this reason, the results from cell 8 were considered unreliable.

E.m.f. of cell 9 can be expressed by the following equations.

$E = 83.2 + 0.0725\ T$, mv $\quad (475 - 857^{\circ}C)$

$E = 223.65 - 0.05175\ T$, mv $\quad (857 - 1150^{\circ}C)$

From the e.m.f. and data on the reference electrode the standard free energy change for the following reactions can be obtained, using equation 31.

$Pb\ (l) + \frac{1}{2} O_2\ (g) = PbO\ (yellow, s)$

$\Delta G^{\circ} = -52{,}127 + 23.635\ T$ cals $\quad (475 - 857^{\circ}C)$ 35

$Pb\ (l) + \frac{1}{2} O_2\ (g) = PbO\ (l)$

$\Delta G^{\circ} = -45652 + 17.903\ T$ cals $\quad (857 - 1150^{\circ}C)$ 36

According to the Pb - O phase diagram[143,144] a metal rich 'oxide' phase is in equilibrium with liquid Pb above 850°C, the monotectic temperature. The melting point of PbO is 897°C [69] and Pb lowers the melting point by 47°C.

(f) Activity Coefficient of Oxygen in Cu + Ag alloys at 1100°C.

The e.m.f. of cell 5 can be related to the amount of dissolved oxygen and the activity coefficient of oxygen in the solution. If the activity coefficient of oxygen, f_O, is based on the reference state of the infinitely dilute solution of oxygen in pure liquid copper and the concentration is in atom pct., the equilibrium constant for the reaction,

$$\frac{1}{2} O_2 = [O]_{Cu + Ag}$$

is given by

$$K = \frac{(\text{atom pct. } O) \times f_O}{(pO_2)^{\frac{1}{2}}} \quad \text{.... 37}$$

The equilibrium constant (or the standard free energy change for the reaction) is obtained from studies on the Cu + O system. The activity coefficient of oxygen, f_O, may be expressed as the product of two

contributions.

$$f_O = f_O^O \cdot f_O^{Ag} \quad \ldots\ 38$$

where f_O^O is the coefficient for a binary Cu + O solution of the same oxygen concentration and f_O^{Ag} is the contribution of the alloying element (silver). Chipman and coworkers have found that f_O^X is a function of the concentration of the additive, but is wholly or nearly independent of the concentration of oxygen. When equations 37 and 38 are combined, and the numerical values of K, the partial pressure of oxygen in the reference electrode, and f_O^O are substituted, one obtains the relationship;

$$\log f_O^{Ag} = 7.3432\ E - \log (\text{at. pct. O}) - 1.5816 + 0.042\ (\text{at. pct.O}) \quad \ldots\ 39$$

When the concentration of oxygen in the alloy is less than 0.05 at. pct., deviations from Sievert's law are small enough for the last term in the above equation to be neglected. (i.e. $f_O^O = 1$).

The results of the three experiments at 1100°C on copper rich alloys are summarised in tables 11, 12 and 13. The constant e.m.f.s obtained after each addition of silver to the solution are tabulated. From the weight of silver added and the weight of copper in the crucible, the composition of the solution can be computed. The amount of oxygen in Cu + O solution before the addition of Ag may be calculated from the e.m.f. The concentration of oxygen in Cu + O + Ag solution is obtained from the mass balance on the assumption that the added Ag is free of oxygen.

The e.m.f. after each addition of Ag attained a constant value in 10 to 25 mins, depending on the weight of Ag added. The constancy of the e.m.f. over prolonged periods (upto 8 hrs.) indicates that there is no gain or loss of oxygen from the solution.

To verify this conclusion, the Cu + O solution in expt. 15 was sampled for oxygen analysis before adding Ag, and again at the end of

TABLE 11.

Experiment 13:

Cell 5

wt. of Cu in crucible = 23.2773 g.

Temperature = 1100°C.

wt. of Ag added at each stage (g)	Mole fraction of Ag in solution (N_{Ag})	E.m.f. mv	at. pct. O	Log f_O^{Ag}
-	0	- 17.5	0.01950	0
1.5361	0.0373	- 19.9	0.01877	- 0.0010
1.5434	0.0722	- 22.5	0.01809	- 0.0041
2.8308	0.1301	- 25.3	0.01696	+ 0.0031
3.1315	0.1862	- 27.3	0.01587	+ 0.0174
3.7789	0.2449	- 28.6	0.01472	+ 0.0405
5.6398	0.3184	- 30.4	0.01329	+ 0.0714
6.7038	0.3891	- 28.3	0.01191	+ 0.1345

TABLE 12.

Experiment 14.

Cell 5

weight of Cu in crucible = 36.2656 grms.

Temperature = 1099°C.

wt. of Ag added at each stage (g)	Mole fraction of Ag in solution (N_{Ag})	E.m.f. mv	at. pct. O	Log f_O^{Ag}
-	0	- 10.6	0.02192	0
0.4232	0.00683	- 11.2	0.02177	- 0.0016
1.1294	0.02459	- 12.9	0.02138	- 0.0062
1.1718	0.04238	- 14.3	0.02099	- 0.0085
1.5089	0.06432	- 16.5	0.02051	- 0.0146
1.3707	0.08342	- 18	0.02009	- 0.0165

TABLE 13.

Experiment 15

Cell 5

wt. of Cu in crucible after taking a 'suction sample' = 46.312 g.

T = 1101°C.

wt. of Ag added at each stage (g)	Mole fraction of Ag in solution (N_{Ag})	E.m.f. mv	at. pct. O	Log f_O^{Ag}
-	0	164.8	0.4437	0
6.0018	0.05564	159.2	0.4123	- 0.0101
9.0824	0.1398	155.1	0.3723	+ 0.0020
14.8992	0.2780	153.2	0.3212	+ 0.0499
12.7432	0.3961	154.4	0.2875	+ 0.1058

Analysis of Oxygen:

Oxy. in Cu + O soln. at the beginning of the expt. = 0.4392

Oxy. in Cu + O + Ag soln. at the end of the expt. = 0.2837

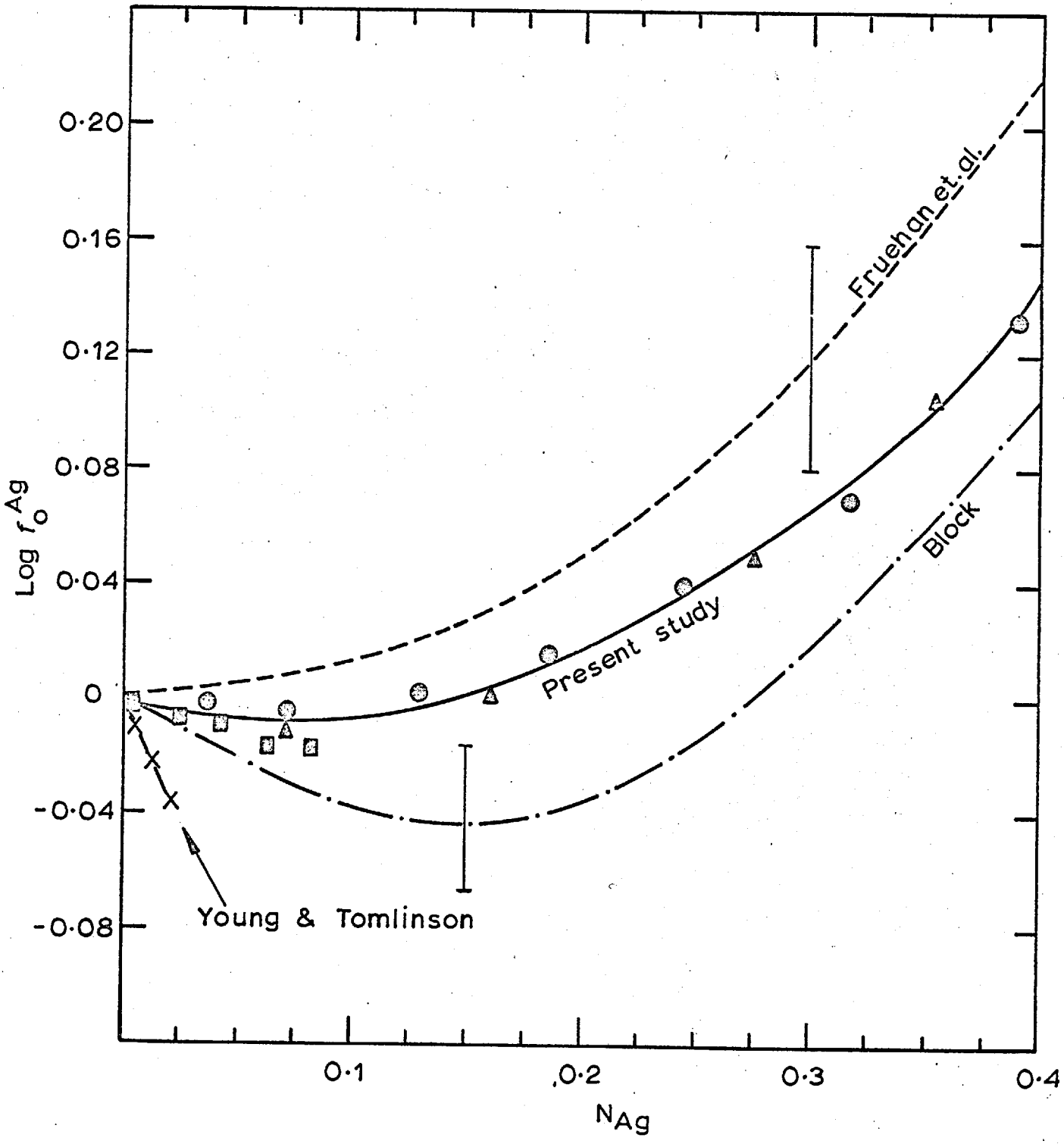

Fig. 18. EFFECT OF SILVER ON THE ACTIVITY COEFFICIENT OF OXYGEN AT 1100°C.

the experiment after several additions of Ag. The analytically determined oxygen concentrations compare favourably with those from the e.m.f. and mass balance (Table 13).

The activity coefficient of oxygen calculated from the results of the three experiments is plotted as a function of silver concentration in fig. 18. Results of each experiment are indicated by a characteristic symbol.

(g) Activity Coefficient of Oxygen in Cu - Sn alloys at 1100°C.

Results of two experiments starting with Cu + O solution are shown in tables 14 and 15. The activity coefficient is calculated using equation 39 and is plotted as a function of the concentration of Sn in figs. 19 and 20.

SnO is reported[145-147] to have a vapour pressure of 7 mm at 1100°C. The possible loss of oxygen from the solution as SnO vapour must therefore be considered. For the reaction

$$2\,Sn(l) + O_2\,(g) = 2\,SnO\,(l)$$

the standard free energy change is given by,

$$\Delta G^\circ = -127{,}240 + 41.70T \text{ cals.}$$

The activity of SnO in the solution can be calculated using this data, and the chemical potential of oxygen in the solution obtained from the e.m.f. at $a_{Sn} = 0.2$, as 0.005. The loss of oxygen as SnO vapour is unlikely at such a low activity of SnO. The constant e.m.f.s obtained over prolonged periods after adding Sn indicates that the loss of oxygen is insignificant. It will be seen from table 14 that the same value for the activity coefficient of oxygen was obtained when the composition of the alloy was approached from higher and lower tin contents during the course of the same experiment. Had there been a gradual loss or gain of oxygen by the solution, differing values for the activity coefficient would have been obtained at the same composition.

TABLE 14.

Experiment 16.

Cell 5

wt. of Cu in the crucible = 30.0482 g.

Temperature = 1100°C.

When 7.0490 grams of oxygen free copper was added to the Cu + O solution in the cell the e.m.f. decreased from - 97 to - 109.5 mv.

wt. of Sn added at each step (g)	Mole fraction of Sn in solution (N_{Sn})	E.m.f. mv	at. pct. O x 10^3	Log f_O^{Sn}
-	0	- 97	5.086	0
-	0	-109.5	4.120	0
2.1340	0.0299	-119.7	3.997	- 0.0618
2.3705	0.0611	-129.0	3.868	- 0.1159
3.2530	0.1007	-143.7	3.705	- 0.2050
7.5933	0.1813	-188.6	3.373	- 0.4938
6.3527	0.2468	-232.5	3.103	- 0.7801
18.2804[*]	0.1800	-211.3	2.263	- 0.4874
10.8601	0.2450	-256.9	2.084	- 0.7865

[*] Oxygen free Cu sample containing no tin.

TABLE 15.

Experiment 17.

Cell 5

Temperature = 1099°C.

wt. of Cu in the crucible = 26.8610 g.

wt. of Sn added at each stage (g)	Mole fraction of Sn in Soln. (N_{Sn})	E.m.f. mv.	at. pct. O x 10^3	Log f_O^{Sn}
-	0	-150	2.077	0
10.0001	0.1662	-217.7	1.732	- 0.4185
8.9674	0.2743	-299.7	1.507	- 0.9601
6.7499	0.3389	-346.5	1.373	- 1.2624
9.8352	0.4147	-394.5	1.216	- 1.5624

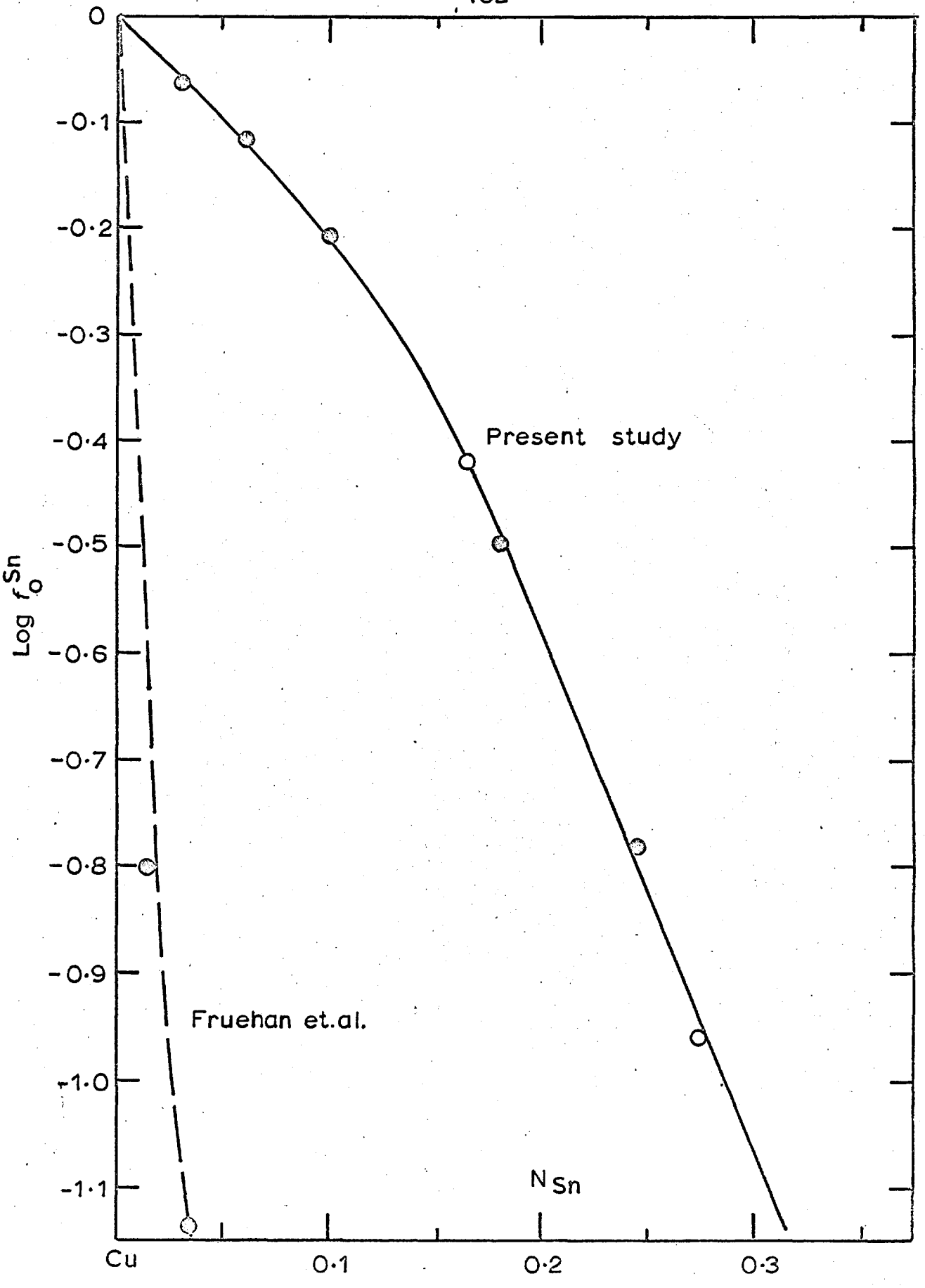

Fig. 19 EFFECT OF TIN ON THE ACTIVITY COEFFICIENT OF OXYGEN IN TIN AT 1100°C.

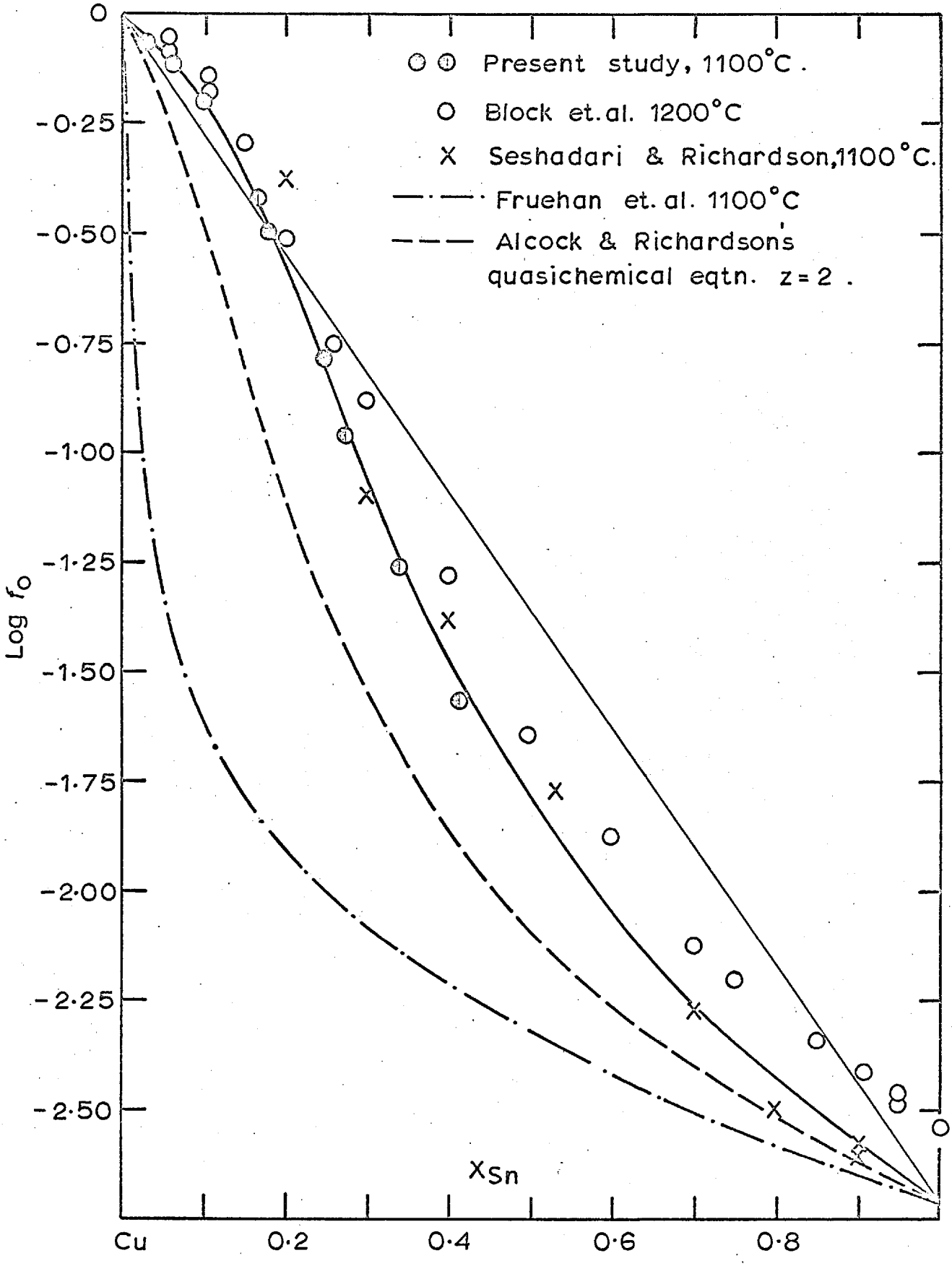

Fig.20 ACTIVITY COEFFICIENT OF OXYGEN IN Cu-Sn ALLOYS

The results of the experiment obtained using $CaO + ZrO_2$ electrolytes agree with those using $Y_2O_3 + ZrO_2$ electrolytes. There was no visual indication of the formation of calcium stannate and when a section of the $CaO + ZrO_2$ tube was examined under an electron probe microanalyser no compounds could be detected.

(h) Activity Coefficient of Oxygen in Cu + Pb alloys at 1100, 900 and 750°C.

The results of the two experiments at 1100°C starting with Cu + O solution are shown in tables 16 and 17. Equation 39 is used to calculate the activity coefficient, which is plotted as a function of lead concentration in fig. 21. From the slope of the plot, the free energy interaction parameter ϵ_O^{Pb} is calculated as - 7.4.

Results of the five experiments starting with Pb + O solution are shown in tables 18 to 22. Three of these experiments were performed at 1100°C and the others at 900 and 750°C. The e.m.f. is related to the activity coefficient and the oxygen concentration as follows;

$\log f_O^{Cu} = 7.3432\ E - 0.6063 - \log (\text{at. pct. O})$ .... at 1100°C.

$\log f_O^{Cu} = 8.5952\ E - 1.3576 - \log (\text{at. pct. O})$ .... at 900°C.

$\log f_O^{Cu} = 9.8555\ E - 2.1140 - \log (\text{at. pct. O})$ .... at 750°C.

Where the standard state for oxygen is its solution in lead at 1 at. pct. These equations are obtained by a procedure similar to that used to derive equation 39. Alcock and Belford's corrected value for the standard free energy change for the solution of oxygen in pure lead is used to obtain the above relations. The activity coefficient of oxygen at the three temperatures is plotted as a function of copper concentration in fig. 22. The interaction parameter ϵ_O^{Cu}, obtained from the limiting slope of these curves as $N_{Pb} \rightarrow 1$, is equal to - 2.3 at 1100°C, - 3.13 at 900°C and - 4.25 at 750°C. ϵ_O^{Cu} is plotted against 1/T in fig. 23. The best line through these points may be

TABLE 16.

Experiment 18.

Cell 5

Wt. of Cu in crucible = 24.0407 g.

Temperature = 1100°C.

wt. of Pb added at each stage (g)	Mole fraction of Pb in solution (N_{Pb})	E.m.f. mv	at. pct. O	Log f_O^{Pb}
-	0	- 69	0.008163	0
0.7533	0.00952	- 73	0.008085	- 0.0270
1.1422	0.0236	- 80	0.007970	- 0.0707
1.8285	0.0454	- 91	0.007792	- 0.1429
2.2844	0.0712	- 104	0.007589	- 0.2255
2.3797	0.0967	- 117	0.007374	- 0.3085
2.2616	0.1196	- 127	0.007187	- 0.3744
2.9637	0.1479	- 139	0.006955	- 0.4475
7.2498	0.2102	- 164	0.006447	- 0.5951
7.7081	0.2671	- 183	0.005983	- 0.7044
9.2254	0.3252	- 199	0.005508	- 0.7852
9.0766	0.3741	- 213	0.005109	- 0.8553

TABLE 17.

Experiment 19.

Cell 5

Temperature = 1101°C.

wt. of Cu in crucible = 26.1446 g.

wt. of Pb added at each stage (g)	Mole fraction of Pb in solution (N_{Pb})	E.m.f. mv	at. pct. O	Log f_O^{Pb}
-	0	- 123	0.003256	0
0.5163	0.00601	- 127	0.003236	- 0.0255
0.7740	0.0149	- 131	0.003208	- 0.0526
0.8315	0.0243	- 136	0.003177	- 0.0850
1.0436	0.0358	- 143	0.003139	- 0.1278
1.6719	0.0536	- 151	0.003081	- 0.1818
2.0792	0.0751	- 162	0.003011	- 0.2530
2.9482	0.1037	- 176	0.002918	- 0.3381
3.7034	0.1373	- 192	0.002809	- 0.4389
3.8180	0.1694	- 204	0.002704	- 0.5123
5.2156	0.2096	- 218	0.002574	- 0.5972
7.4078	0.2603	- 235	0.002408	- 0.6930
5.2408	0.2925	- 245	0.002304	- 0.7453

TABLE 18.

Experiment 20.

Cell 7

Temperature = 1101°C.

wt. of Pb in crucible = 20.4393 g.

wt. of Cu added at each stage (g)	Mole fraction of Cu in solution (N_{Cu})	E.m.f. mv	at. pct. O	Log f^{Cu}_{O}
-	0	-227	0.005312	0
0.3814	0.0573	-238	0.005008	- 0.0532
0.4220	0.1132	-247	0.004711	- 0.0951
0.5072	0.1727	-255.5	0.004395	- 0.1246
0.5274	0.2265	-260.5	0.004109	- 0.1352
0.4448	0.2667	-262.5	0.003895	- 0.1260
1.3163	0.3645	-268.5	0.003376	- 0.1089
1.3205	0.4395	-271.5	0.002977	- 0.0744
2.1566	0.5426	-273	0.002495	- 0.0101
2.6316	0.6076	-275.5	0.002085	+ 0.0503
4.9144	0.6998	-273.3	0.001595	+ 0.1823
3.4665	0.7426	-274.2	0.001367	+ 0.2428
3.1279	0.7719	-274.2	0.001212	+ 0.2953

Lead in solution at the end of the expt. (Analysis) = 21.2 at. pct.

TABLE 19.

Experiment 21.

Cell 7

Temperature = 1099°C.

E.m.f. of cell was constant at - 115.9 mv.

A 'spoon sample' was taken from Pb + O solution.

wt. of Pb in crucible after sampling = 24.2010

Constant e.m.f. after adding 4.8097 g. of oxygen free Pb = - 122.2 mv.

wt. of Cu added at each stage (g)	Mole fraction of Cu in solution (N_{Cu})	E.m.f. mv	at. pct. O	Log f_O^{Cu}
-	0	-115.9	0.03759	0
-	0	-122.2	0.03136	0
1.2187	0.1206	-142.5	0.02758	- 0.0958
1.3836	0.2265	-154.5	0.02426	- 0.1263
2.1821	0.3497	-162	0.0204	- 0.1047
1.7602	0.4239	-165	0.01807	- 0.0749

Oxygen Analysis (Baker's method)

Oxygen content of Pb + O soln. at the start of expt. = 0.03645 at. pct.

Oxygen content of Cu + O + Pb soln. at the end of the expt. = 0.0175 at.pct.

Lead in Cu + O + Pb soln. at the end of the expt. = 55.4 at. pct.

TABLE 20.

Experiment 22.

Cell 7

Temperature = 1100°C.

weight of Pb in crucible = 23.7638 g.

wt. of Cu added at each stage (g)	Mole fraction of Cu in soln. (N_{Cu})	E.m.f. mv	at. pct. O	Log f_O^{Cu}
-	0	-121	0.009823	0
1.4031	0.1615	-219	0.008236	- 0.1310
1.1868	0.2624	-228	0.007246	- 0.1420
1.4653	0.3574	-233.5	0.006312	- 0.1209
1.5030	0.4327	-235	0.005572	- 0.0760
3.1717	0.5450	-237	0.004469	+ 0.0051
2.5977	0.6085	-237.5	0.003845	+ 0.0649
4.5907	0.6859	-237	0.003085	+ 0.1653
4.4602	0.7366	-236.5	0.002588	+ 0.2454
4.9777	0.7768	-236	0.002193	+ 0.3217

Lead in solution at the end of the expt. = 21.4 at. pct.

TABLE 21.

Experiment 23.

Cell 7

Temperature = 900°C.

wt. of Pb in the crucible = 65.7429 g.

wt. of Cu added at each stage (g)	Mole fraction of Cu in solution (N_{Cu})	E.m.f. mv	at. pct. O	Log f_O^{Cu}
-	0	- 36	0.02143	0
0.2265	0.0111	- 38.5	0.02119	- 0.0147
0.3324	0.0270	- 41.9	0.02085	- 0.0371
0.4530	0.0477	- 45.7	0.02041	- 0.0604
0.4084	0.0657	- 48.7	0.02002	- 0.0778
0.5630	0.0895	- 52.2	0.01951	- 0.0966
0.6562	0.1157	- 56.2	0.01895	- 0.1185
0.4452	0.1326	- 59.2	0.01859	- 0.1359
0.6069	0.1548	- 61.0	0.01811	- 0.1400
0.6234	0.1763	- 65.5	0.01765	- 0.1475

TABLE 22.

Experiment 62.

Cell 7

Temperature = 751°C.

Wt. of Pb in the crucible = 55.2151 g.

wt. of Cu added at each stage (g)	Mole fraction of Cu in Soln. (N_{Cu})	E.m.f. mv.	at. pct. O	Log f_O^{Cu}
-	0	88.5	0.05735	0
0.2603	0.0151	85	0.0565	- 0.0280
0.2836	0.0311	82	0.0556	- 0.0511
0.3171	0.0484	78	0.0546	- 0.0822
0.3703	0.0678	75.2	0.0534	- 0.1004

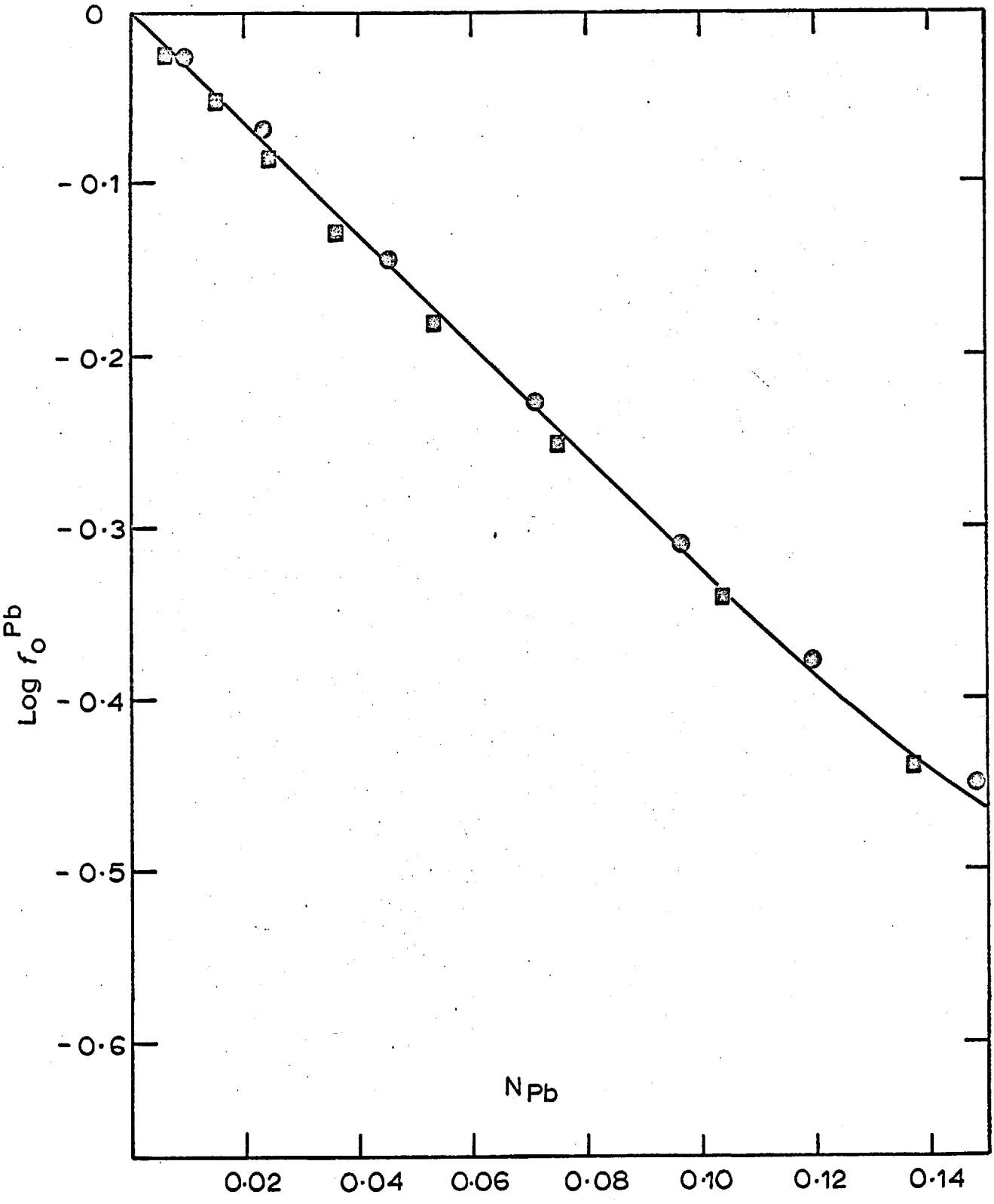

Fig. 21 | EFFECT OF LEAD ON THE ACTIVITY COEFFICIENT OF OXYGEN IN LIQUID COPPER AT 1100°C.

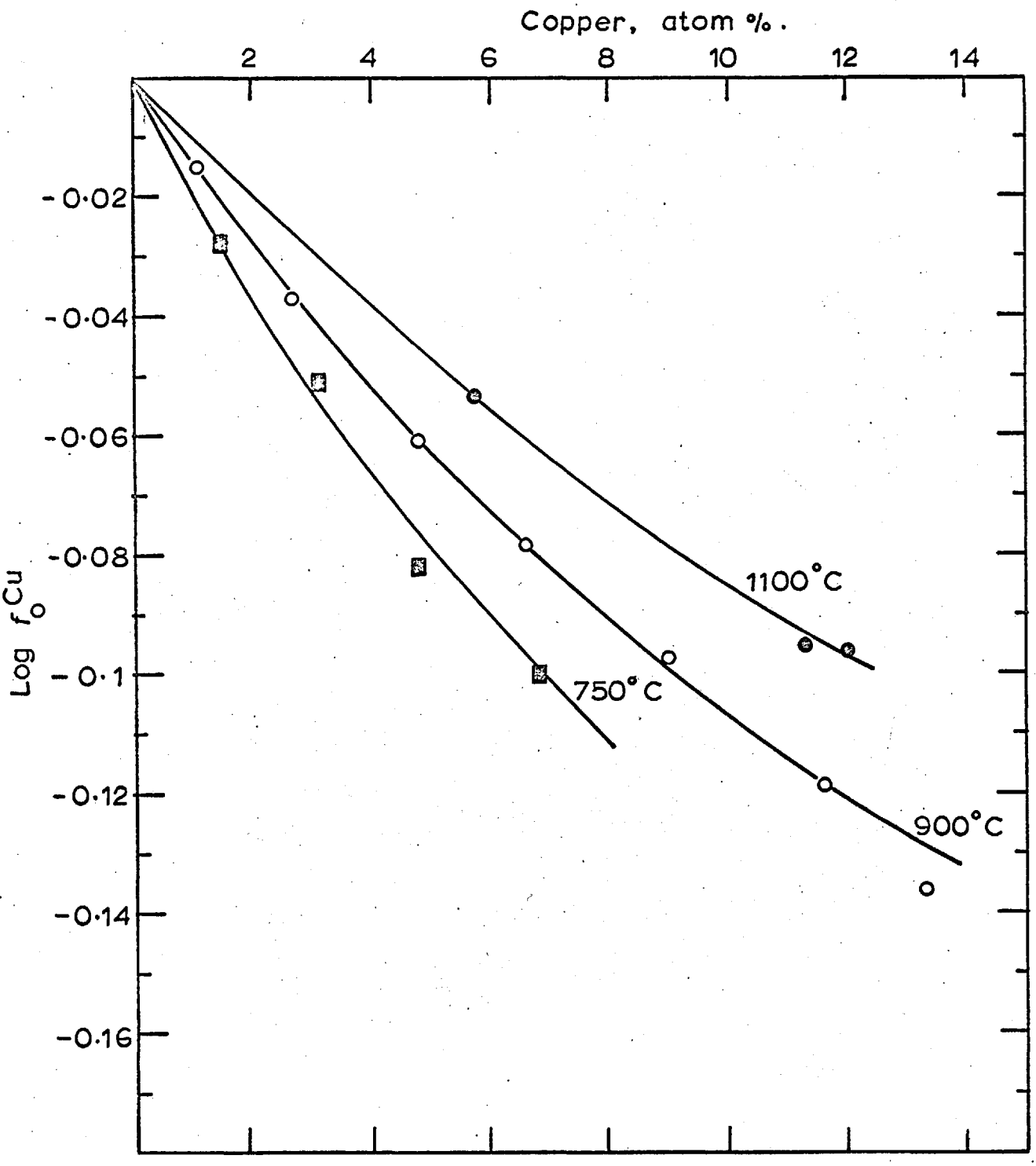

Fig. 22 EFFECT OF COPPER ON THE ACTIVITY COEFFICIENT OF OXYGEN IN LIQUID LEAD AT 1100, 900, & 750°C.

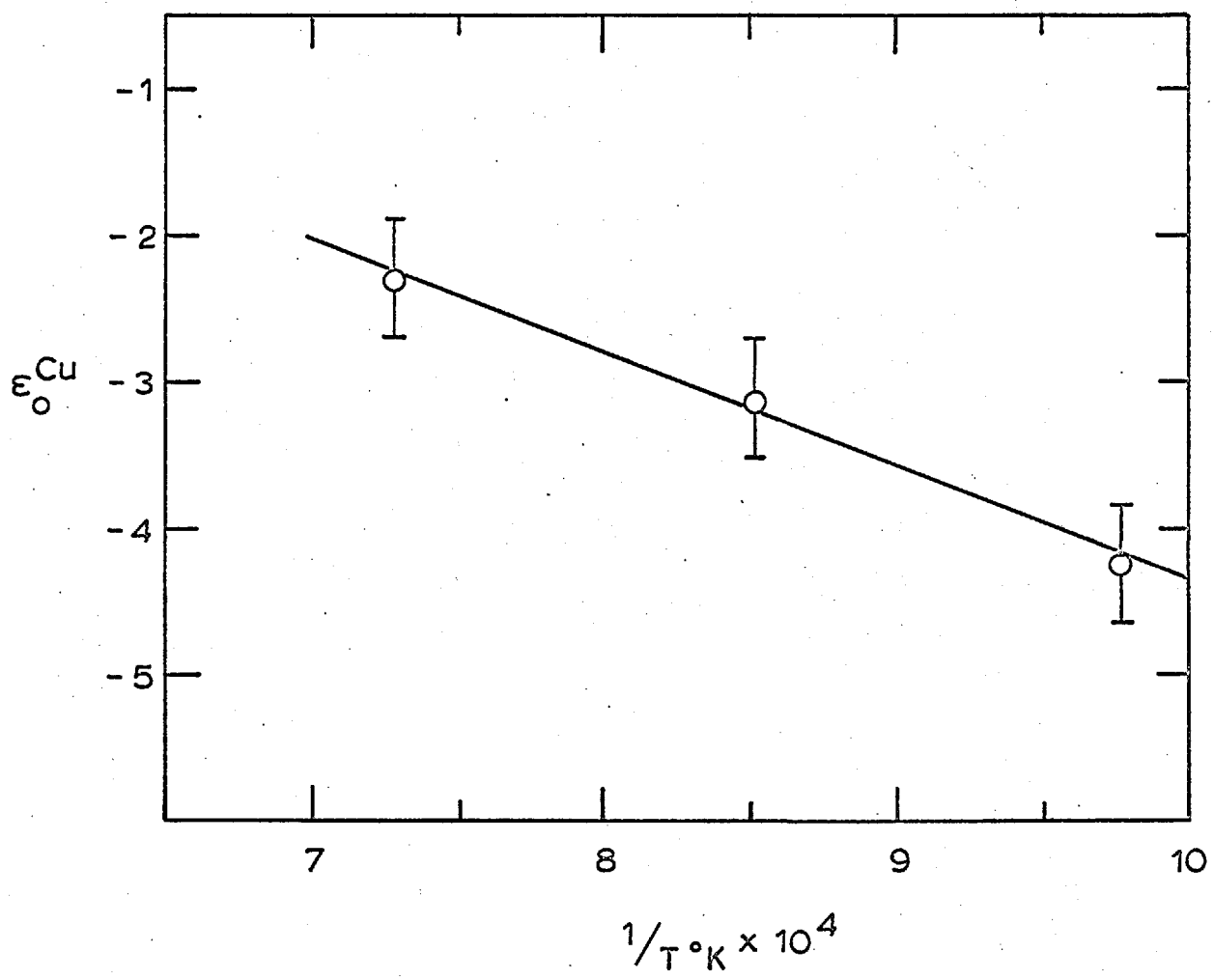

Fig.23 EFFECT OF TEMPERATURE ON THE INTERACTION COEFFICIENT BETWEEN OXYGEN & COPPER IN LIQUID LEAD

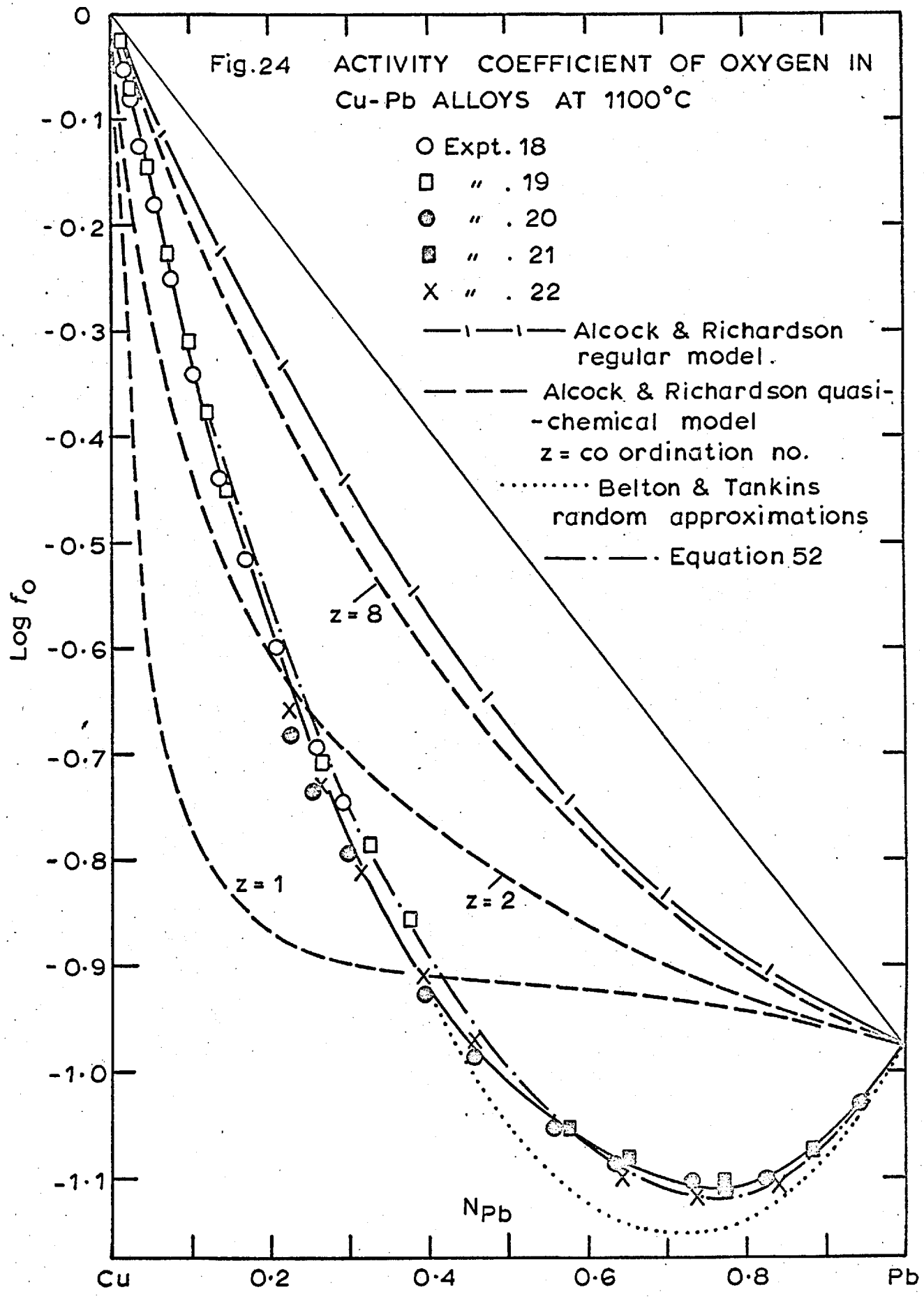
Fig.24 ACTIVITY COEFFICIENT OF OXYGEN IN Cu-Pb ALLOYS AT 1100°C
O Expt. 18
□ " . 19
⊙ " . 20
▣ " . 21
X " . 22
Alcock & Richardson regular model.
Alcock & Richardson quasi-chemical model
z = co ordination no.
Belton & Tankins random approximations
Equation 52
z = 8
z = 2
z = 1
Log f_O
N_{Pb}
0
-0·1
-0·2
-0·3
-0·4
-0·5
-0·6
-0·7
-0·8
-0·9
-1·0
-1·1
Cu
0·2
0·4
0·6
0·8
Pb

represented by

$$\epsilon_O^{Cu} = -7767/T + 3.42 \quad \ldots\ldots \quad 40$$

The activity coefficient of oxygen in the whole range of Cu - Pb alloys at 1100°C is shown in fig. 24, referred to oxygen in liquid copper. The activity coefficient of oxygen in pure lead is taken from the corrected results of Alcock and Belford. The results of the experiments starting with Cu + O solution and Pb + O solution are in reasonable agreement and indicate the validity of the experimental technique used in this study.

To ensure that there was no loss of oxygen from lead rich solution as PbO vapour, samples from the melt were analysed by Baker's method in expt. 21. The analytical values are in good agreement with those calculated from the e.m.f. and the mass balance, and indicate that an insignificant amount of oxygen was lost from the solution.

(i) Effect of P on the activity coefficient of oxygen in liquid copper from 1150 to 1300°C.

The results of the experiments at 1150, 1200, 1250 and 1300°C are summarised in tables 23 to 30. The e.m.f. of the cell is related to the activity coefficient and concentration of oxygen in solution as follows;

$$\log f_O^P = -3.4962 + 7.0852\,E - \log(\text{at. pct. O})$$
(Fe - FeO reference electrode, 1150°C)

$$\log f_O^P = -3.2736 + 6.8447\,E - \log(\text{at. pct. O})$$
(Fe - FeO reference electrode, 1200°C)

$$\log f_O^P = -1.1762 + 6.8447\,E - \log(\text{at. pct. O})$$
(Ni - NiO reference electrode, 1200°C)

$$\log f_O^P = -1.0037 + 6.6200\,E - \log(\text{at. pct. O})$$
(Ni - NiO reference electrode, 1250°C)

$$\log f_O^P = -0.8421 + 6.4095\,E - \log(\text{at. pct. O})$$
(Ni - NiO reference electrode, 1300°C)

TABLE 23.

Experiment 27.

Pt, Ni-NiO / CaO. ZrO_2 / $[O]_{Cu}$. W, Pt

wt. of Cu in the crucible = 26.0123 g.

Temperature = 1200°C.

Wt. pct. P in the master alloy = 2.74

wt. of master alloy added at each step.	wt. pct. P in soln.	E.m.f. mv	at. pct. O	$\text{Log} f_O^P$
-	0	- 339	0.321	0
1.3012	0.1300	- 353	0.3057	- 0.0778
1.4823	0.2639	- 370	0.290	- 0.1713
1.5099	0.3868	- 390	0.2755	- 0.2859
1.8238	0.5198	- 414	0.2599	- 0.4247
1.7893	0.6364	- 438	0.2462	- 0.5655
2.1263	0.7599	- 450	0.2316	- 0.6210
2.2031	0.8733	- 461	0.2183	- 0.6707

Analysis of Phosphorus:

P in sample obtained from the solution at the end of the expt = 0.87 wt. pct.

TABLE 24.

Experiment 28.

The cell used was the same as that in experiment 27.

wt. of Cu in the crucible = 26.4231 g.

Temperature = 1200°C.

wt. pct. P in the master alloy = 2.74.

wt. of master alloy added at each step.	wt. pct. P in soln.	E.m.f. mv	at. pct. O x 10^3	$\text{Log} f_O^P$
-	0	- 340	0.3123	0
0.3239	0.0332	- 345	0.3085	- 0.0255
0.4729	0.0802	- 351	0.3032	- 0.0589
0.7120	0.1480	- 363	0.2954	- 0.1300
0.9304	0.2316	- 374	0.2859	- 0.1911
1.8060	0.3793	- 396	0.2691	- 0.3150
1.6020	0.4965	- 413	0.2557	- 0.4094
2.6880	0.6690	- 439	0.2360	- 0.5563

Analysis of Phosphorus.

Phosphorus in solution at the end of the experiment = 0.67 wt.%

TABLE 25.

Experiment 29.

Pt, Fe-FeO / 15% CaO - ZrO_2 / $[O]_{Cu}$, W, Pt

wt. of Cu in the crucible = 25.2138 g.

Temperature = 1200°C.

wt. pct. P in the master alloy = 2.74

wt. of master alloy added at each step (g)	wt. pct. P in soln.	E.m.f. mv	at. pct. O x 10^3	$\log f_O^P$
-	0	- 18	0.4012	0
0.3138	0.0337	- 22	0.3963	- 0.0222
0.2987	0.0650	- 26	0.3917	- 0.0444
0.3082	0.0965	- 30	0.3871	- 0.0662
0.6455	0.1602	- 36	0.3777	- 0.0973
0.6049	0.2173	- 43	0.3694	- 0.1353
0.7482	0.2843	- 51.5	0.3596	- 0.1819
1.2390	0.3879	- 65.5	0.3444	- 0.2591
1.3120	0.4885	- 79.5	0.3297	- 0.3359
1.1189	0.5677	- 91.5	0.3181	- 0.4022
2.4829	0.7250	-113.5	0.2950	- 0.5202
2.4038	0.8570	-135.5	0.2757	- 0.6413

Phosphorus in the solution at the end of expt. = (1) 0.845, (2) 0.859 wt. pct.

TABLE 26.

Experiment 30.

The cell used was the same as that in experiment 27.

wt. of Cu in the crucible = 28.3456 g.

Temperature = 1250°C.

wt. pct. P in the master alloy = 2.74.

wt. of master alloy added at each step (g)	wt. pct. P in soln.	E.m.f. mv	at. pct. O x 10^3	$\text{Log} f_O^P$
-	0	-352	0.4631	0
0.5783	0.0548	-360	0.4538	- 0.0443
0.6127	0.1105	-366.5	0.4444	- 0.0781
1.2493	0.2172	-380	0.4264	- 0.1491
1.4321	0.3293	-393	0.4074	- 0.2160
1.5352	0.4390	-410	0.3889	- 0.3081
2.1730	0.5782	-438	0.3654	- 0.4660
2.5263	0.7202	-450	0.3414	- 0.5161
2.0702	0.8234	-462	0.3239	- 0.5730

wt. pct. P in soln. at the end of expt obtained by analysis of samples. } = 0.820 wt. pct.

TABLE 27.

Experiment 31.

The cell used was the same as that in experiment 27.

wt. of copper in the crucible = 23.6123 gm.

When 3.5885 g of oxygen free copper was added to the Cu + O solution in the cell, the e.m.f. changed from - 361.5 mv to -371 mv.

Temperature = 1300°C.

wt. pct. P in the master alloy = 2.74.

wt. of master alloy added at each stip (g)	wt. pct. P in soln.	E.m.f. mv.	at. pct. O x 10^3	$\text{Log} f_O^P$
-	0	-371	0.6012	0
0.5214	0.0515	-376	0.5899	- 0.0237
0.5993	0.1084	-380.5	0.5774	- 0.0433
1.3216	0.2257	-359	0.5517	- 0.1170
1.2982	0.3312	-406	0.5285	- 0.1679
1.4017	0.4356	-416	0.5056	- 0.2124
2.4831	0.5999	-435	0.4696	- 0.3031
2.5038	0.7435	-448	0.4380	- 0.3559
3.5023*	0.6797	-452	0.4005	- 0.3400

* Oxygen free copper sample containing no phosphorus

Analysis of phosphorus in soln. at the end of the expt. = 0.681 wt. pct.

TABLE 28.

Experiment 32.

The cell used was the same as that in experiment 27.

wt. of Cu in the crucible = 26.1020 g.

Temperature = 1300°C.

wt. pct. P in the master alloy = 2.74.

wt. of master alloy added at each step (g)	wt. pct. P in soln.	E.m.f. mv	at. pct. O x 10^3	Log f_O^P
-	0	-373.5	0.5810	0
1.3085	0.1308	-385	0.5533	0.0521
1.3484	0.2531	-398.5	0.5273	0.1178
1.4029	0.3690	-412.5	0.5028	0.1868
1.3369	0.4694	-423.5	0.4815	0.2382

Phosphorus in the sample obtained from the solution at the end of the expt. = 0.473 wt. pct.

TABLE 29.

Experiment 33.

The cell used was the same as that in expt. 29.

wt. of copper in the crucible = 27.1302 g.

Temperature = 1150°C.

wt. pct. P in master alloy = 2.74.

wt. of master alloy added at each step (g)	wt. pct. P in soln.	E.m.f. mv	at. pct. O x 10^3	Log f_O^P
-	0	- 3.6	0.3007	0
1.2138	0.1161	- 20.8	0.3848	- 0.0980
1.5153	0.2479	- 43.8	0.2705	- 0.2386
1.6823	0.3796	- 65.8	0.2562	- 0.3709
1.4318	0.4812	- 76.8	0.2452	- 0.4296
1.3429	0.5688	- 88.8	0.2357	- 0.4979
1.5138	0.6597	-112.7	0.2258	- 0.6488

Analysis of phosphorus in the sample obtained from the soln. at the end of the expt. = 0.66 wt. pct.

TABLE 30.

Experiment 34.

The cell used was the same as that in expt. 29.

wt. of copper in the crucible = 26.4126 g.

Temperature = 1150°C.

wt. pct. P in master alloy = 2.74.

wt. of master alloy added at each step (g)	wt. pct. P in soln.	E.m.f. mv.	at. pct. O x 10^3	Log f_O^P
-	0	- 7.6	0.2817	0
1.1020	0.1097	- 27	0.2704	- 0.1199
1.3265	0.2307	- 44.5	0.2580	- 0.2234
1.8137	0.3792	- 64.6	0.2427	- 0.3386
2.2412	0.5400	- 92.5	0.2262	- 0.5063

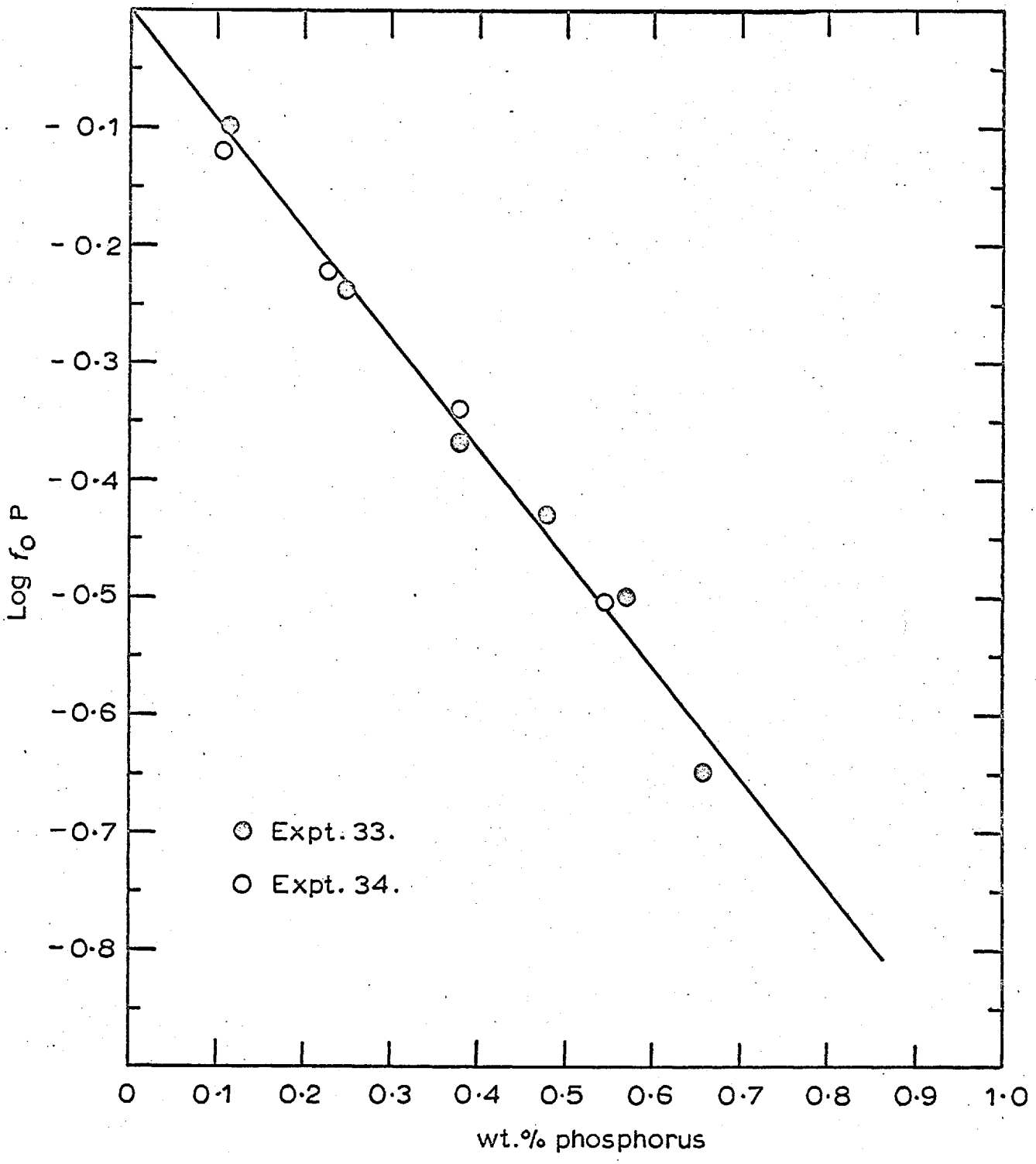

Fig. 25 EFFECT OF PHOSPHORUS ON THE ACTIVITY COEFFICIENT OF OXYGEN IN LIQUID COPPER AT 1150°C

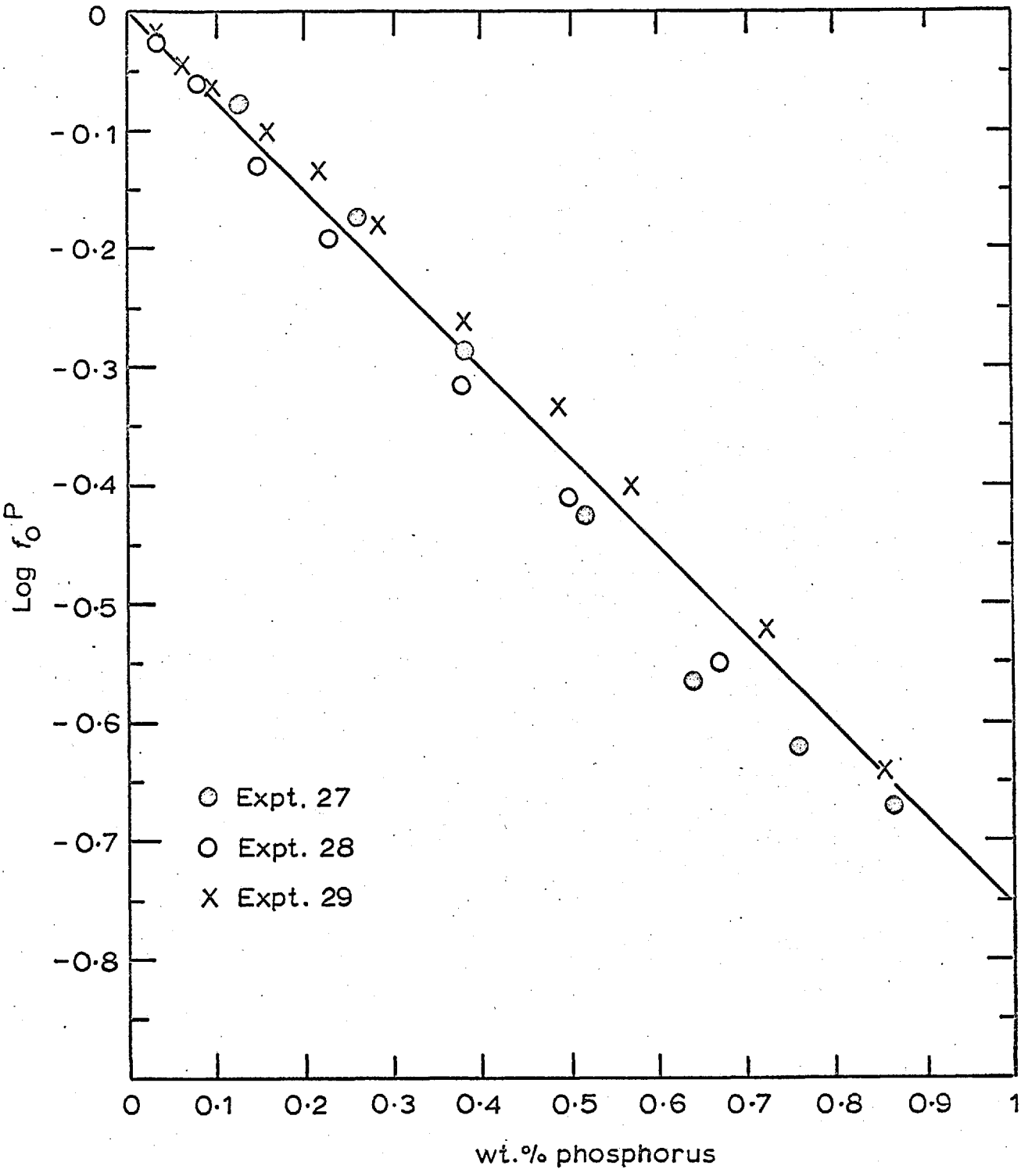

Fig.26 EFFECT OF PHOSPHORUS ON THE ACTIVITY COEFFICIENT OF OXYGEN IN LIQUID COPPER AT 1200°C

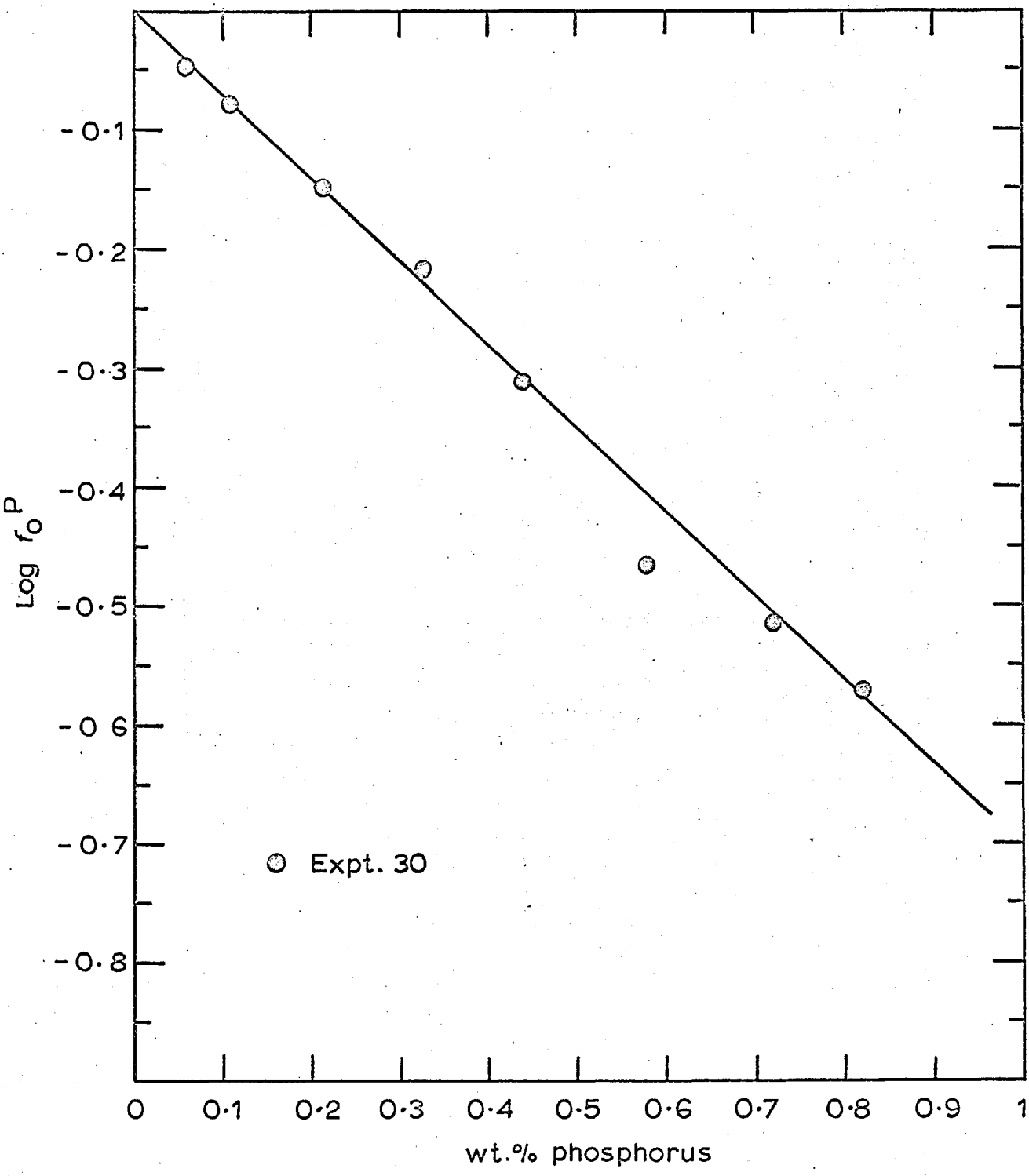

Fig.27 EFFECT OF PHOSPHORUS ON THE ACTIVITY COEFFICIENT OF OXYGEN AT 1250°C.

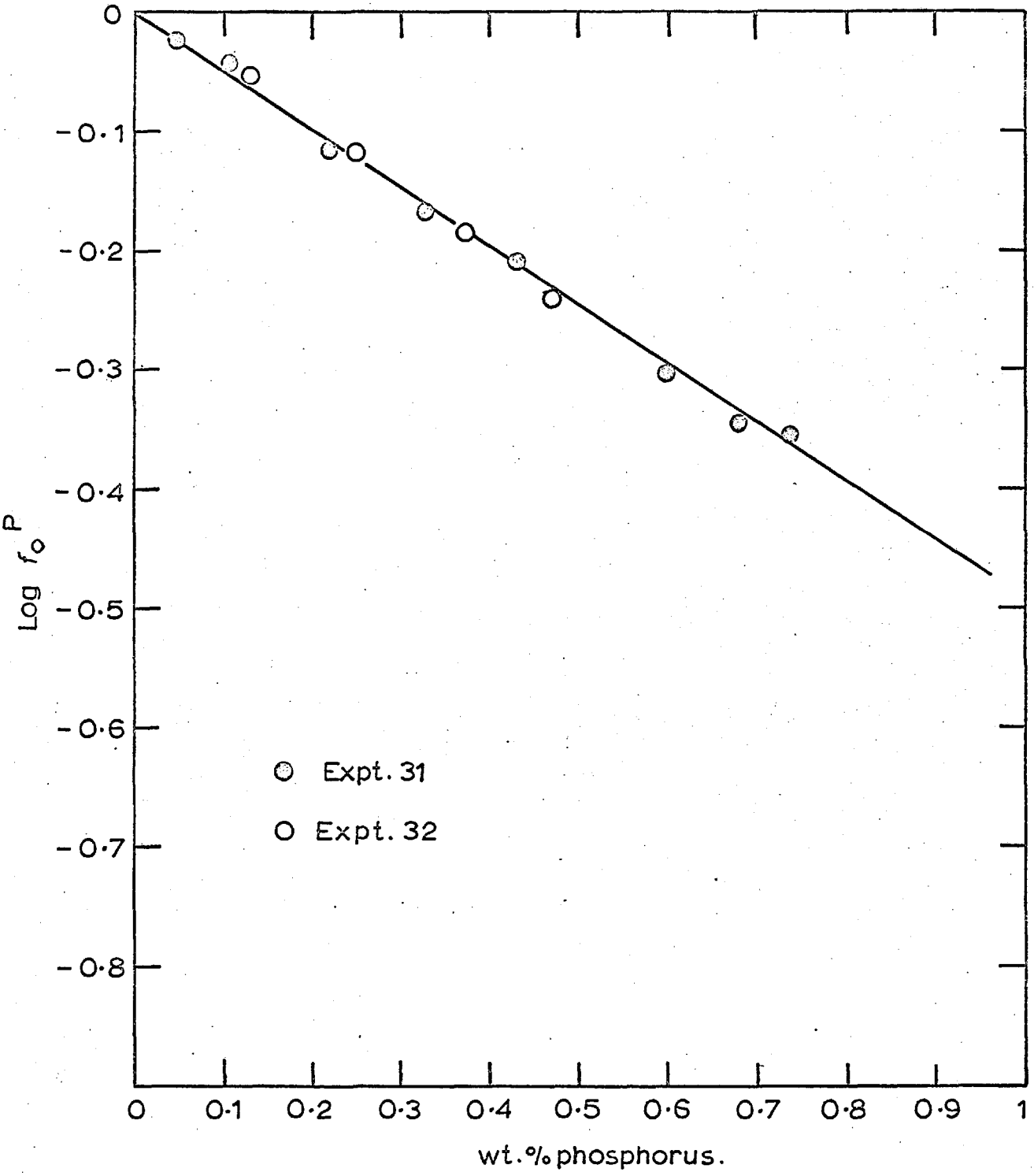

Fig.28 EFFECT OF PHOSPHORUS ON THE ACTIVITY COEFFICIENT OF OXYGEN IN LIQUID COPPER AT 1300°C.

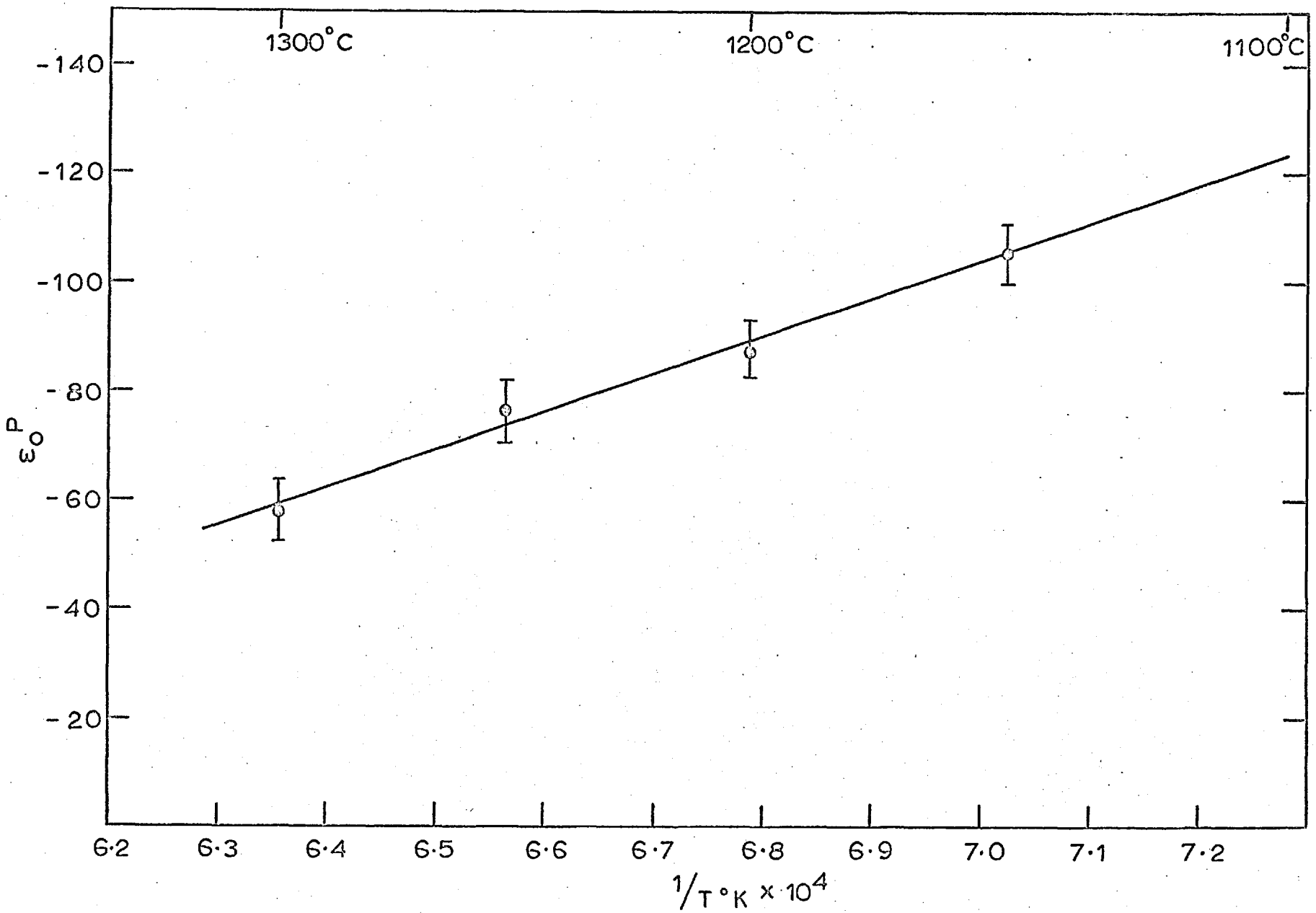

Fig. 29 VARIATION OF THE INTERACTION PARAMETER ε_o^P WITH TEMPERATURE

The values recommended by Steele are used for the chemical potential of oxygen in the reference electrode. The standard state for oxygen is the infinitely dilute solution in copper where the activity is equal to atom pct. The derived activity coefficients at different temperatures are plotted separately in figures 25 to 28. At each temperature the variation of the logarithm of the activity coefficient with concentration may be represented by a straight line. The free energy interaction parameter ϵ_0^P obtained from the slopes of these lines is plotted as a function of 1/T in fig. 29. The least mean squares line through the experimental points may be represented by:

$$\epsilon_0^P = -696{,}371/T + 383.9 \quad \ldots\ 41$$

(j) Activity Coefficient of Oxygen in Pb + Sn alloys from 550 to 1100°C.

The results of experiments at 550, 750, 950 and 1100°C are summarised in tables 31 to 43. In experiments where oxygen free lead was added to Sn + O solution, the following equations may be used to derive the activity coefficients; the standard state for oxygen being taken as 1 pct. solution in tin at the relevent temperature.

$\log f_0^{Pb}$ = 12.2505 E - 0.1865 - log (at. pct. O)
(Ni - NiO reference electrode, 550°C)

$\log f_0^{Pb}$ = 9.8555 E - 2.1169 - log (at. pct. O)
(Fe- FeO reference electrode, 750°C.)

$\log f_0^{Pb}$ = 8.2438 E - 1.4312 - log (at. pct. O)
(Fe - FeO reference electrode, 950°C)

In experiments where oxygen free Sn was added to Pb + O solution the following equation may be used to derive the activity coefficient; the standard state for oxygen being one at. pct. solution in lead at the relevent temperature.

$\log f_0^{Sn}$ = 9.8555 E - 4.6860 - log (at. pct. O)
(Fe - FeO reference electrode, 750°C)

TABLE 31.

Experiment 35.

Cell:

Pt, Ni-NiO / 7.5% CaO + ZrO_2 / $[O]_{Sn}$, Cermet, Pt.

Temperature = 550°C

Weight of Sn in the crucible = 44.4558 g.

wt. of Pb added at each stage (g)	Mole fraction of Pb in soln. (N_{Pb})	E.m.f. mv	at. pct. O x 10^3	Log f_O^{Pb}
-	0	- 239.5	0.7575	0
4.2301	0.0517	- 237.6	0.7184	0.0461
4.0801	0.0967	- 235.5	0.6842	0.0929
4.7034	0.1436	- 233.8	0.6487	0.1368
7.8646	0.2121	- 231.0	0.5969	0.2068
16.9379	0.3276	- 226.4	0.5093	0.3327
11.3672	0.3880	- 223.9	0.4636	0.4049
12.8629	0.4444	- 221.0	0.4209	0.4830
16.9471	0.5044	- 215.4	0.3754	0.6008
3.4096	0.5150	- 215.2	0.3674	0.6113

TABLE 32.

Experiment 36.

The cell used was the same as in experiment 35.

Temperature = 550°C.

weight of Sn in the crucible = 48.6409 g.

wt. of Pb added at each stage (g)	Mole fraction of Pb in soln. (N_{Pb})	E.m.f. mv	at. pct. O x 10^3	Log f_O^{Pb}
-	0	- 230.5	0.9763	0
3.0891	0.035	- 229.0	0.9420	+0.0351
7.5327	0.1113	- 226.4	0.8677	+0.1013
7.3905	0.1749	- 225.3	0.8055	0.1467
14.9710	0.2798	- 220.8	0.7031	0.2614
14.7329	0.3598	- 217.3	0.6250	0.3550

TABLE 33.

Experiment 36.

Cell 11

Temperature = 750°C.

weight of Sn in the crucible = 35.2352 g.

When 6.0475 g of oxygen free copper was added to the Cu + O solution in the cell, the e.m.f. changed from 32.4 mv to 25.4 mv.

wt. of Pb added at each stage (g)	Mole fraction of Pb in soln. (N_{Pb})	E.m.f. mv	at. pct. O x 10^3	Log f_O^{Pb}
-	0	25.4	13.61	0
2.6494	0.0128	26.9	13.10	0.0305
4.3022	0.0336	28.2	12.4	0.0682
4.1450	0.0536	29.9	11.8	0.1055
4.0201	0.0730	31.0	11.25	0.1371
7.5303	0.1093	34.5	10.36	0.2074
7.5654	0.1458	36.7	9.59	0.2626
6.2520	0.1760	37.9	9.04	0.3002
9.5589	0.2221	39.5	8.31	0.3525
6.3505	0.2528	41.5	7.88	0.3951
9.5850	0.2990	43	7.32	0.4430

TABLE 34.

Experiment 37.

Cell 11

Temperature = 749°C.

weight of Sn in the crucible = 38.8162 g.

wt. of Pb added at each stage (g)	Mole fraction of Pb in soln. (N_{Pb})	E.m.f. mv	at. pct. O x 10^3	Log f_O^{Pb}
-	0	19.6	11.93	0
4.4375	0.D614	22.3	11.2	0.0533
3.3087	0.1026	23.7	10.71	0.0874
9.3978	0.2019	27.5	9.52	0.1751
11.0155	0.2936	31.0	8.43	0.2624
11.6847	0.3703	34.9	7.512	0.3509
19.1130	0.4654	39.8	6.377	0.4703
14.3068	0.5196	42.2	5.731	0.5407

TABLE 35.

Experiment 38.

Cell 10

Temperature = 751°C.

weight of Pb in the crucible = 64.5089 g.

wt. of Sn added at each stage (g)	Mole fraction of Sn in soln. (N_{Sn})	E.m.f. mv	at. pct. O x 10^3	Log f_O^{Sn}
-	0	167	0.9116	0
0.2577	0.0070	148.5	0.9052	-0.1792
0.4911	0.0198	126.5	0.8935	-0.3904
0.6492	0.0365	104	0.8783	-0.6046
0.7447	0.0549	85	0.8615	-0.7835
1.3831	0.0871	61	0.8322	-1.0049
1.6007	0.1218	44	0.8005	-1.1556

TABLE 36.

Experiment 39.

Cell 10

Temperature = 750°C.

weight of Pb in the crucible = 52.4417 g.

wt. of Sn added at each stage (g)	Mole fraction of Sn in soln. (N_{Sn})	E.m.f. mv	at. pct. O x 10^3	Log f_O^{Sn}
-	0	163.7	0.8459	0
2.6482	0.0810	66.5	0.7774	-0.9212
2.6297	0.1495	32	0.7194	-1.2274
2.6924	0.2098	8.5	0.6684	-1.4271
2.1066	0.2512	- 5.2	0.6334	-1.5387
2.6345	0.2973	+ 52.5* 39.3	2.346* 2.201	-1.6413
2.0279	0.3292	28.3	2.102	-1.7300
4.9164	0.3955	9.1	1.894	-1.8733

* PbO added to solution to increase the oxygen concentration.

TABLE 37.

Experiment 40.

Cell 10

Temperature = 750°C.

weight of Pb in the crucible = 44.6573 g.

wt. of Sn added at each stage (g)	Mole fraction of Sn in soln. (N_{Sn})	E.m.f. mv	at. pct. O x 10^3	Log f_O^{Sn}
-	0	150.5	0.6269	0
1.6720	0.0614	67.3	0.5884	-0.7923
1.5014	0.1102	37.5	0.5578	-1.0627
1.8506	0.1641	8.8	0.5240	-1.3184
3.3761	0.2473	- 21.5	0.4719	-1.5715
6.1180	0.3620	- 52.5	0.3999	-1.8051
5.7322	0.4419	- 74.0	0.3499	-1.9590
5.5581	0.5022	- 89.9	0.3121	-2.0667

TABLE 38.

Experiment 41.

Cell 11

Temperature = 950°C.

wt. of Sn in the crucible = 41.6639 grms.

wt. of Pb added at each stage (g)	Mole fraction of Pb in soln. (N_{Pb})	E.m.f. mv	at. pct. O x 10^3	Log f_O^{Pb}
-	0	- 90	6.710	0
4.7441	0.0612	- 88.3	6.298	0.0414
5.3360	0.1199	- 86.5	5.806	0.0918
11.8086	0.2313	- 82.7	5.157	0.1745
14.4127	0.3318	- 78.5	4.459	0.2720
13.5833	0.4068	- 74.4	3.979	0.3555
17.1831	0.4797	- 70.1	3.49	0.4479
12.5081	0.5225	- 64.6	3.204	0.5305

TABLE 39.

Experiment 42.

Cell 11

Temperature = 950°C.

wt. of Sn in the crucible = 39.9676 g.

wt. of Pb added at each stage (g)	Mole fraction of Pb in soln. (N_{Pb})	E.m.f. mv	at. pct. O x 10^3	Log f_O^{Pb}
-	0	- 71.4	9.550	0
5.3302	0.0710	- 69.6	8.872	0.0472
5.5674	0.1351	- 68.1	8.260	0.0902
6.8757	0.2030	- 65.6	7.611	0.1462
12.3980	0.3019	- 62.0	6.667	0.2340
15.0818	0.3934	- 58.6	5.793	0.3229
14.2153	0.4602	- 54.9	5.155	0.4038
14.1849	0.5136	- 52.0	4.645	0.4727
14.2144	0.5574	- 49.3	4.226	0.5363

TABLE 40.

Experiment 43.

Cell 10

Temperature = 951°C.

wt. of Pb in the crucible = 53.8133 g.

wt of Sn added at each stage (g)	Mole fraction of Sn in soln. (N_{Sn})	E.m.f. mv	at. pct. O x 10^3	Log f_O^{Sn}
-	0	104.3	2.482	0
1.5898	0.0490	43.7	2.360	-0.4774
1.7660	0.0983	9.8	2.238	-0.7333
1.7456	0.1421	-12.9	2.129	-0.8991
3.5549	0.2192	-40.9	1.938	-1.0892
4.8142	0.3041	-69.6	1.727	-1.2757
7.8202	0.4085	-99.4	1.468	-1.4507
7.5801	0.4837	-118.8	1.282	-1.5518

TABLE 41.

Experiment 44.

Cell 10

Temperature = 951°C.

wt. of Pb in the crucible = 48.7483 g.

wt. of Sn added at each stage (g)	Mole fraction of Sn in soln. (N_{Sn})	E.m.f. mv	at. pct. O x 10^3	Log f_O^{Sn}
-	0	108	2.669	0
0.7407	0.0258	68.9	2.600	-0.3118
0.7679	0.0512	43	2.532	-0.5129
2.0350	0.1126	3.4	2.368	-0.8111
4.6366	0.2265	-41.3	2.664	-1.1200

TABLE 42.

Experiment 45.

Cell 10

Temperature = 1101°C.

wt. of Pb in the crucible = 52.4675 g.

wt. of Sn added at each stage (g)	Mole fraction of Sn in soln. (N_{Sn})	E.m.f. mv	at. pct. O x 10^3	Log f_O^{Sn}
-	0	+ 11.6	2.01	0
0.7739	0.0251	- 14.6	1.96	-0.1817
0.9793	0.0551	- 41.7	1.90	-0.3673
1.7093	0.1033	- 72.7	1.802	-0.5722
1.6416	0.1451	- 95.8	1.718	-0.7210
4.7171	0.2463	-137	1.515	-0.9671

TABLE 43.

Experiment 46.

Cell 10

Temperature = 1099°C.

wt. of Pb in the crucible = 49.7432 g.

wt. of Sn added at each stage (g)	Mole fraction of Sn in soln. (N_{Sn})	E.m.f. mv	at. pct. O x 10^3	Log f^{Sn}_O
-	0	7.4	1.872	0
1.1538	0.0389	- 36.9	1.799	-0.3079
1.4718	0.0844	- 67.8	1.714	-0.5142
2.0868	0.1419	- 99.5	1.606	-0.7184
2.5877	0.2039	-124	1.490	-0.8651
4.2969	0.2893	-152	1.331	-1.0260
7.9766	0.4072	-185	1.110	-1.1848
8.3209	0.4946	-209	0.946	-1.2936
14.8256	0.5998	-240	0.749	-1.4177

TABLE 44.

Experiment 51.

Cell 7

Temperature = 999°C.

wt. of Pb in the crucible = 46.5967 g.

wt. of Ag added at each stage (g)	Mole fraction of Ag in soln. (N_{Ag})	E.m.f. mv	at. pct. O x 10^2	Log f^{Ag}_O
-	0	- 79.2	2.632	0
1.1395	0.0450	- 72.8	2.513	0.0708
1.4800	0.0975	- 64.7	2.375	0.1596
2.9082	0.1854	- 50.1	2.144	0.3196
3.6301	0.2740	- 34.3	1.911	0.4947
5.3282	0.3739	- 14.0	1.648	0.7198
7.5073	0.4755	+ 8.6	1.380	0.9758
8.7915	0.5593	+ 29.7	1.160	1.2183

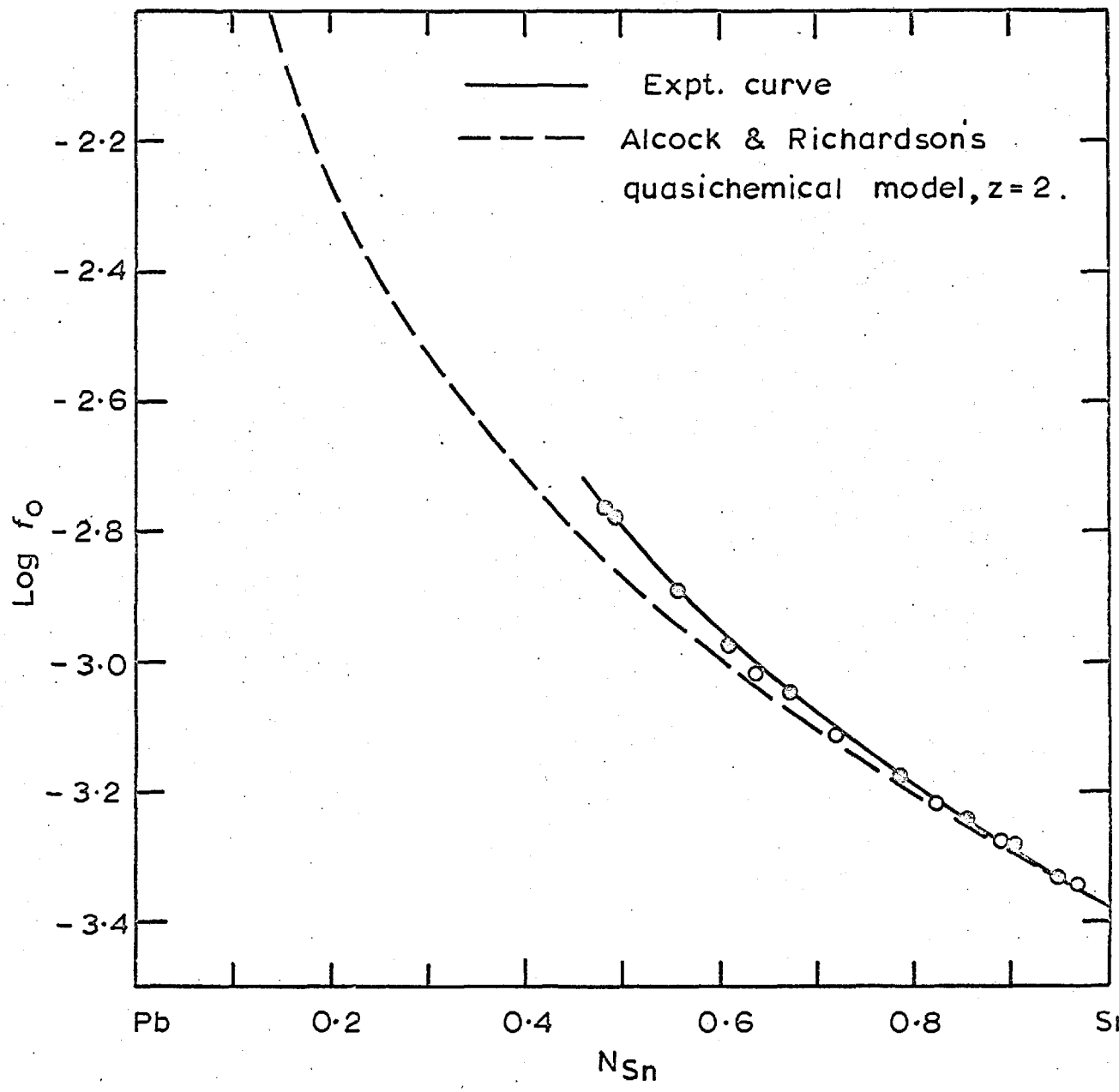

Fig. 30 ACTIVITY COEFFICIENT OF OXYGEN IN Pb-Sn ALLOYS AT 550°C. (STD. STATE FOR OXYGEN IN 1% SOLN. IN LEAD)

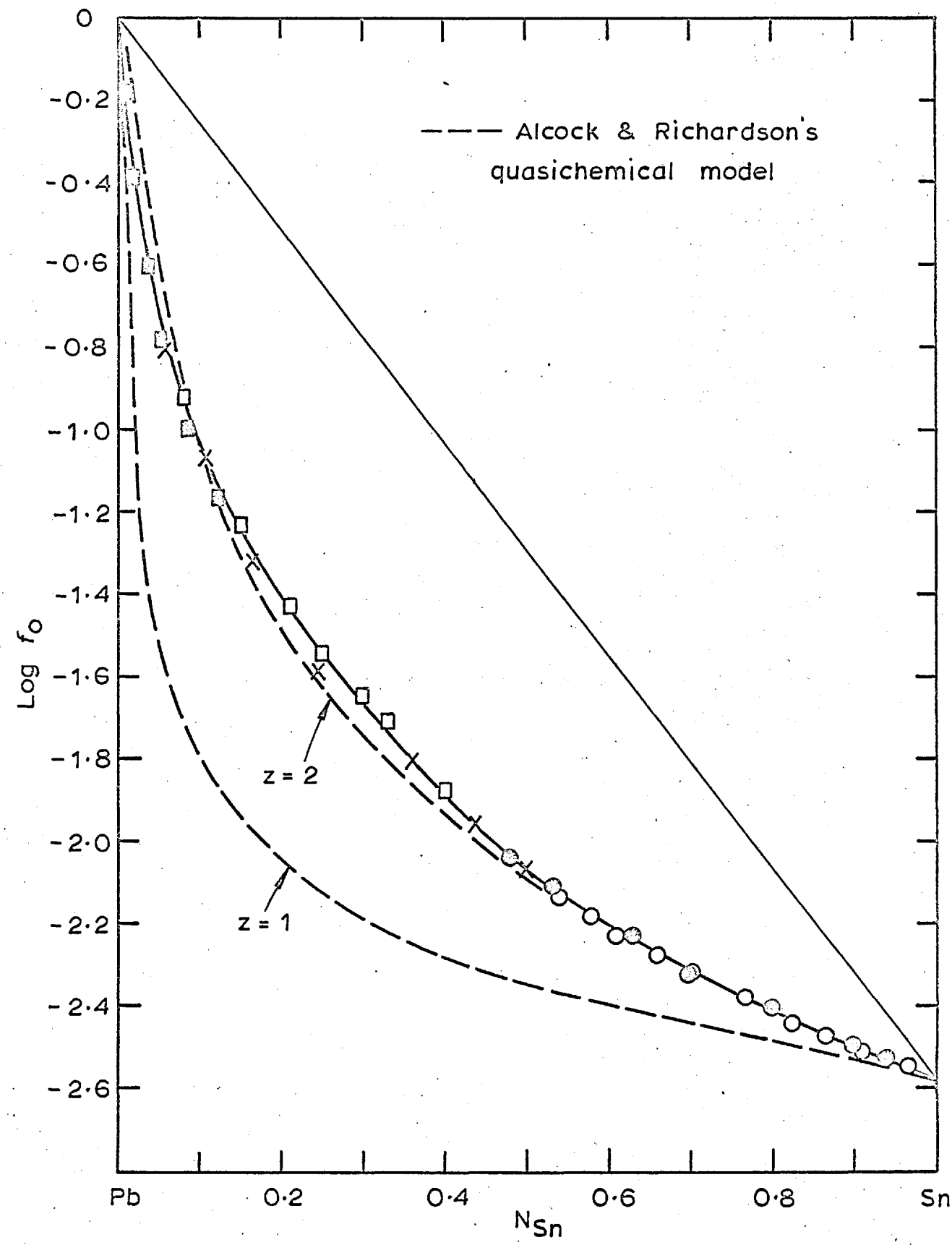

Fig. 31 ACTIVITY OF OXYGEN IN Pb-Sn ALLOYS AT 750°C.

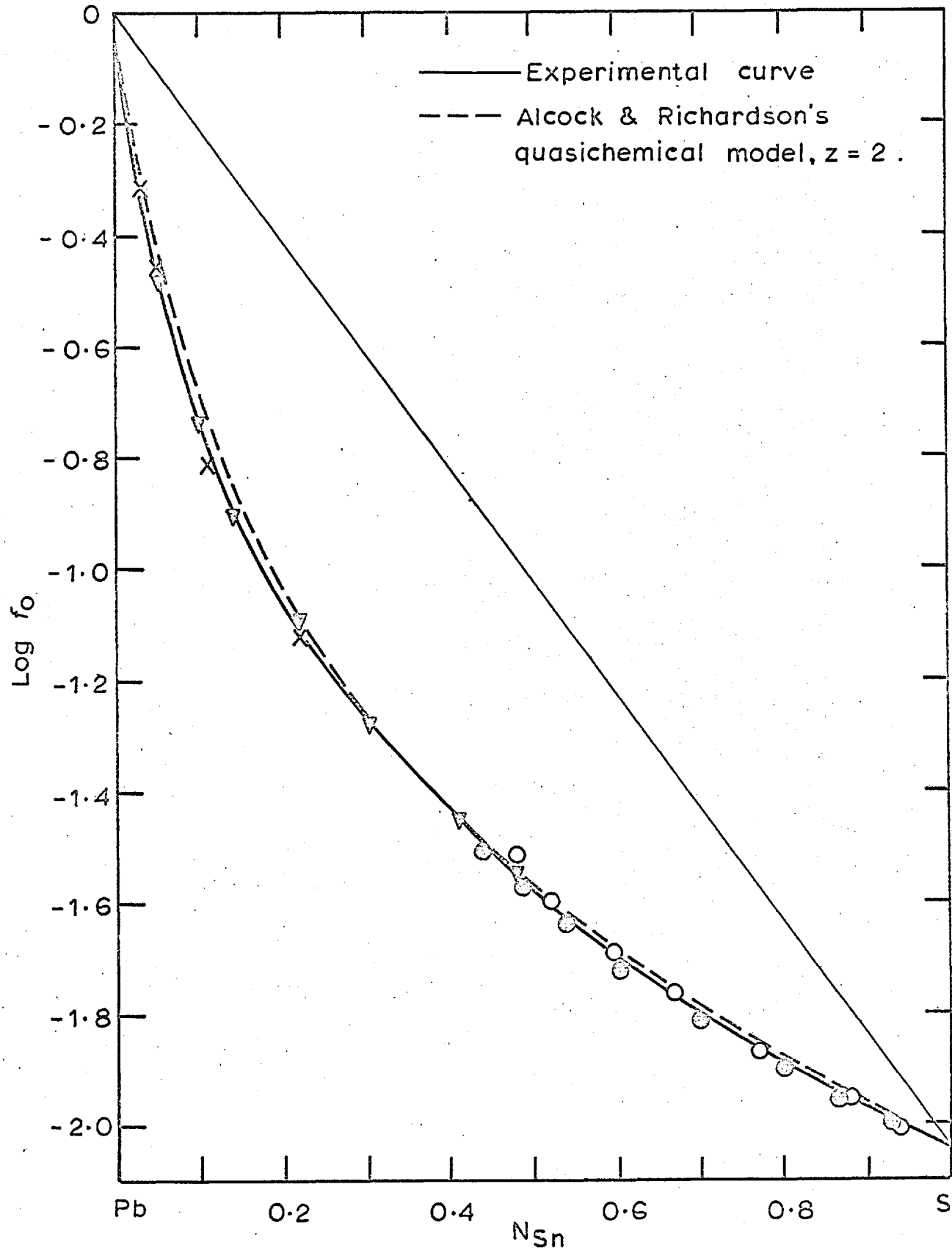

Fig. 32 ACTIVITY COEFFICIENT OF OXYGEN IN Pb-Sn ALLOYS AT 950°C.

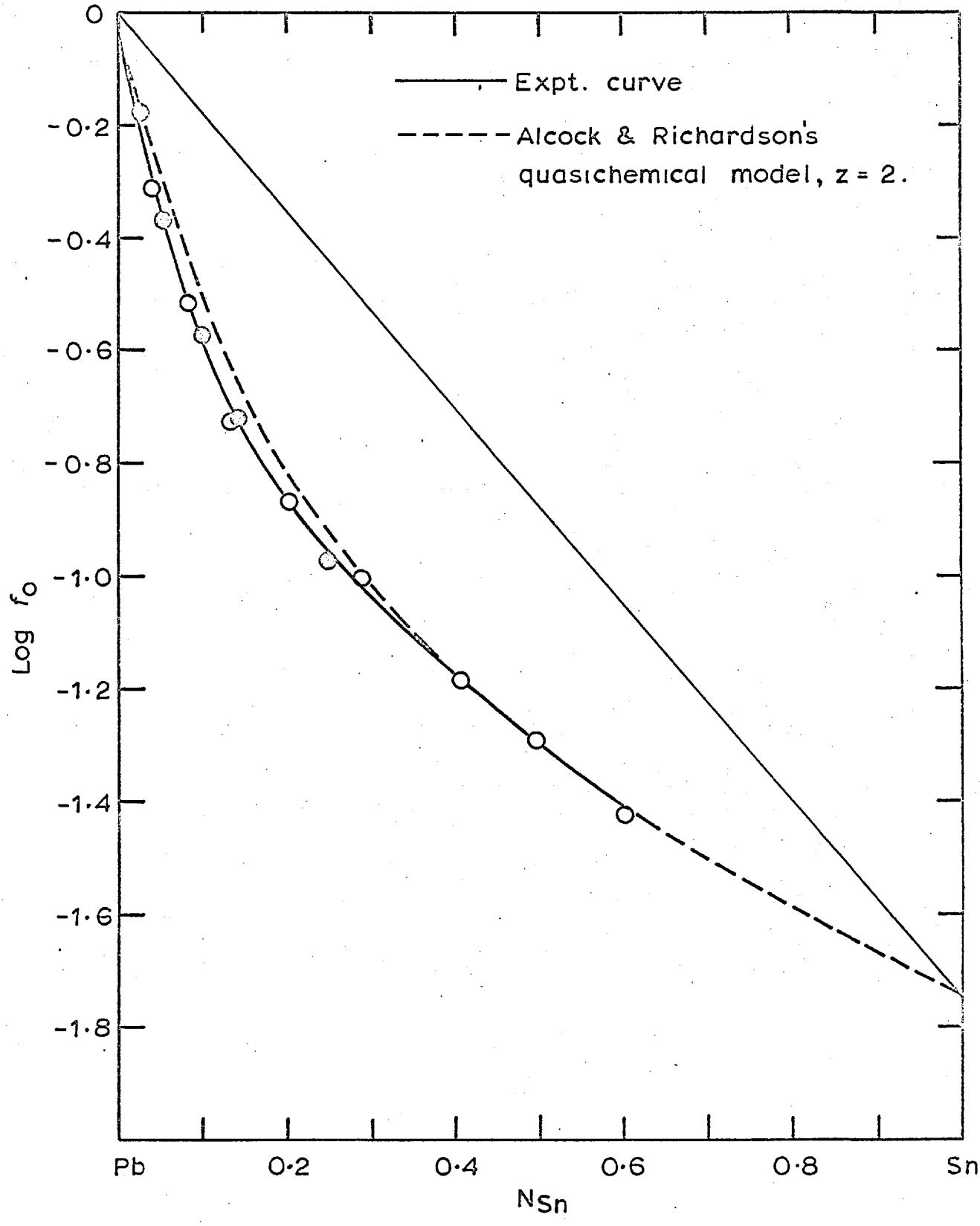

Fig.33. ACTIVITY COEFFICIENT OF OXYGEN IN Pb-Sn ALLOYS AT 1100°C

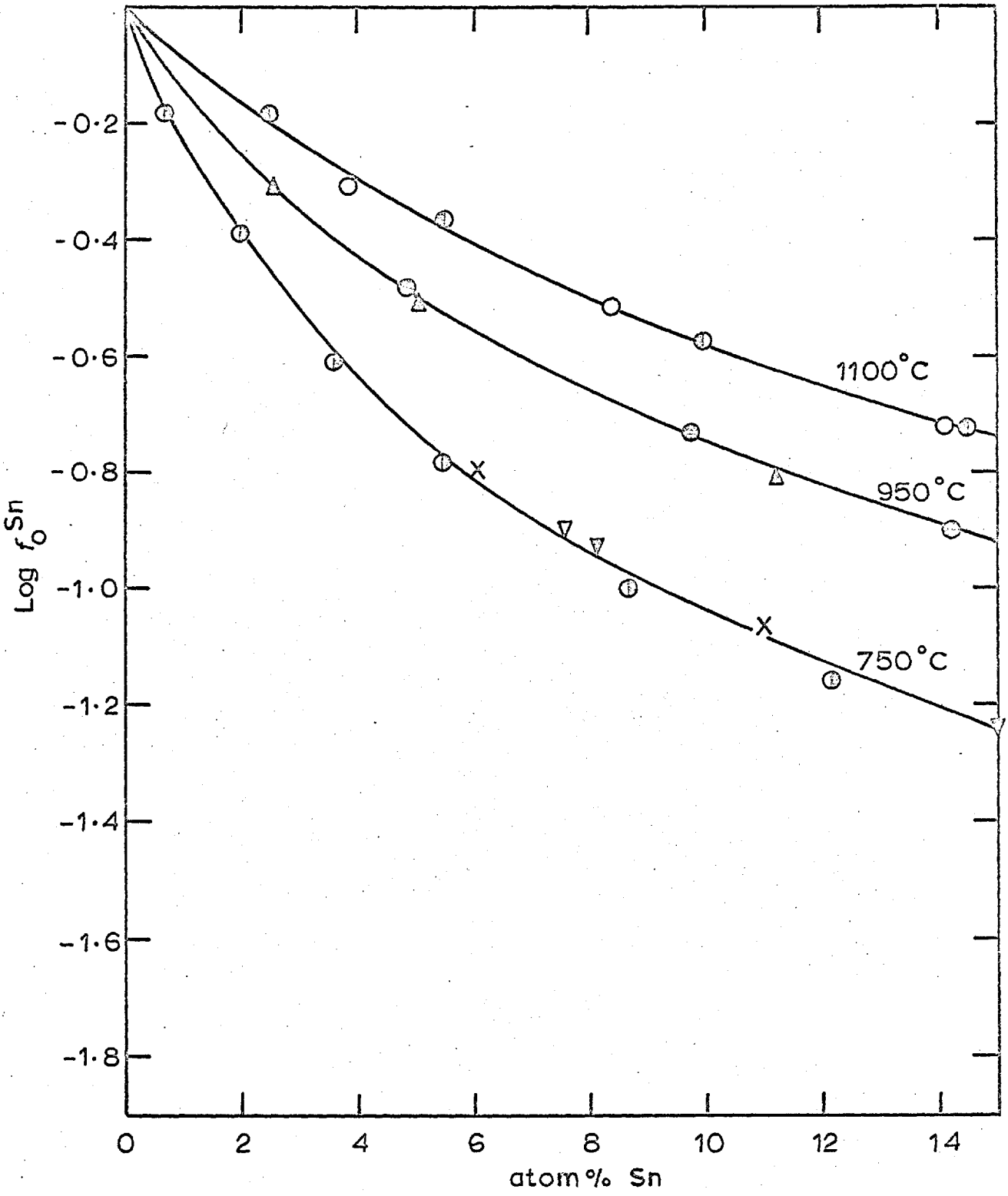

Fig.34 EFFECT OF TIN ON THE ACTIVITY COEFFICIENT OF OXYGEN IN LIQUID LEAD.

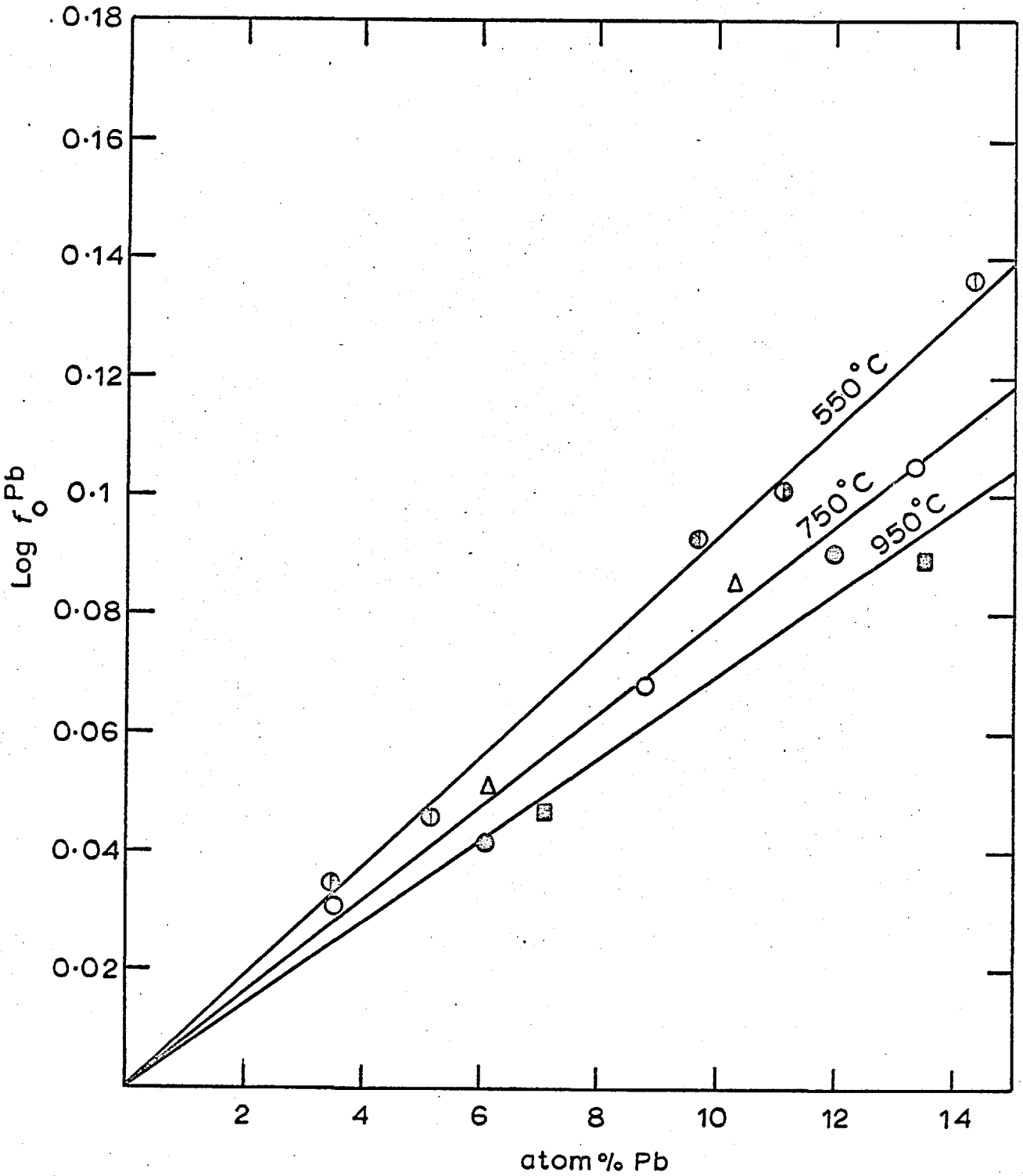

Fig. 35. EFFECT OF LEAD ON THE ACTIVITY COEFFICIENT OF OXYGEN IN TIN.

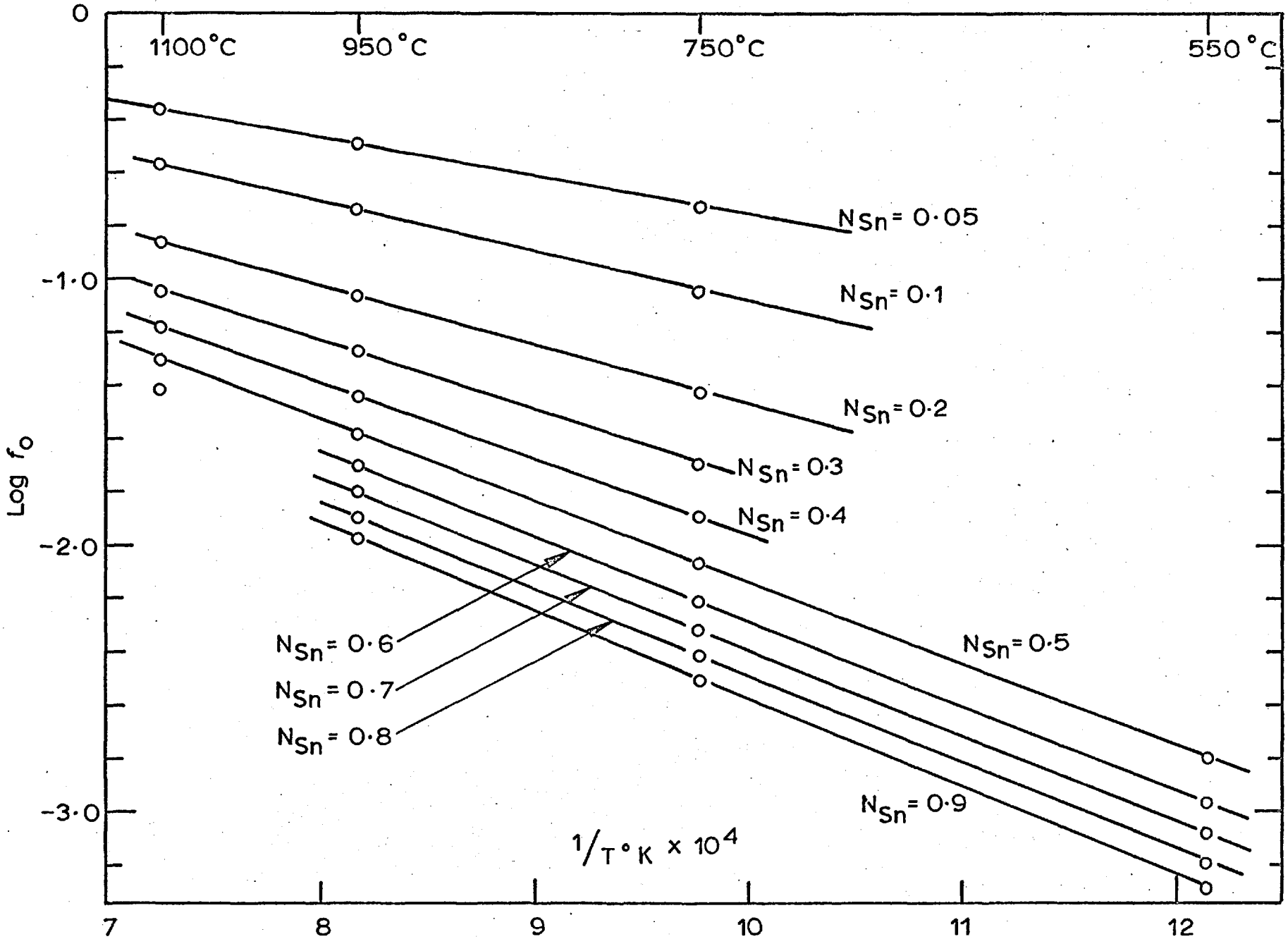

Fig. 36. VARIATION OF THE ACTIVITY COEFFICIENT OF OXYGEN IN Pb-Sn ALLOYS WITH TEMPERATURE. (THE STANDARD STATE FOR OXYGEN IS 1 atom% SOLN. IN LEAD AT THE TEMPERATURE)

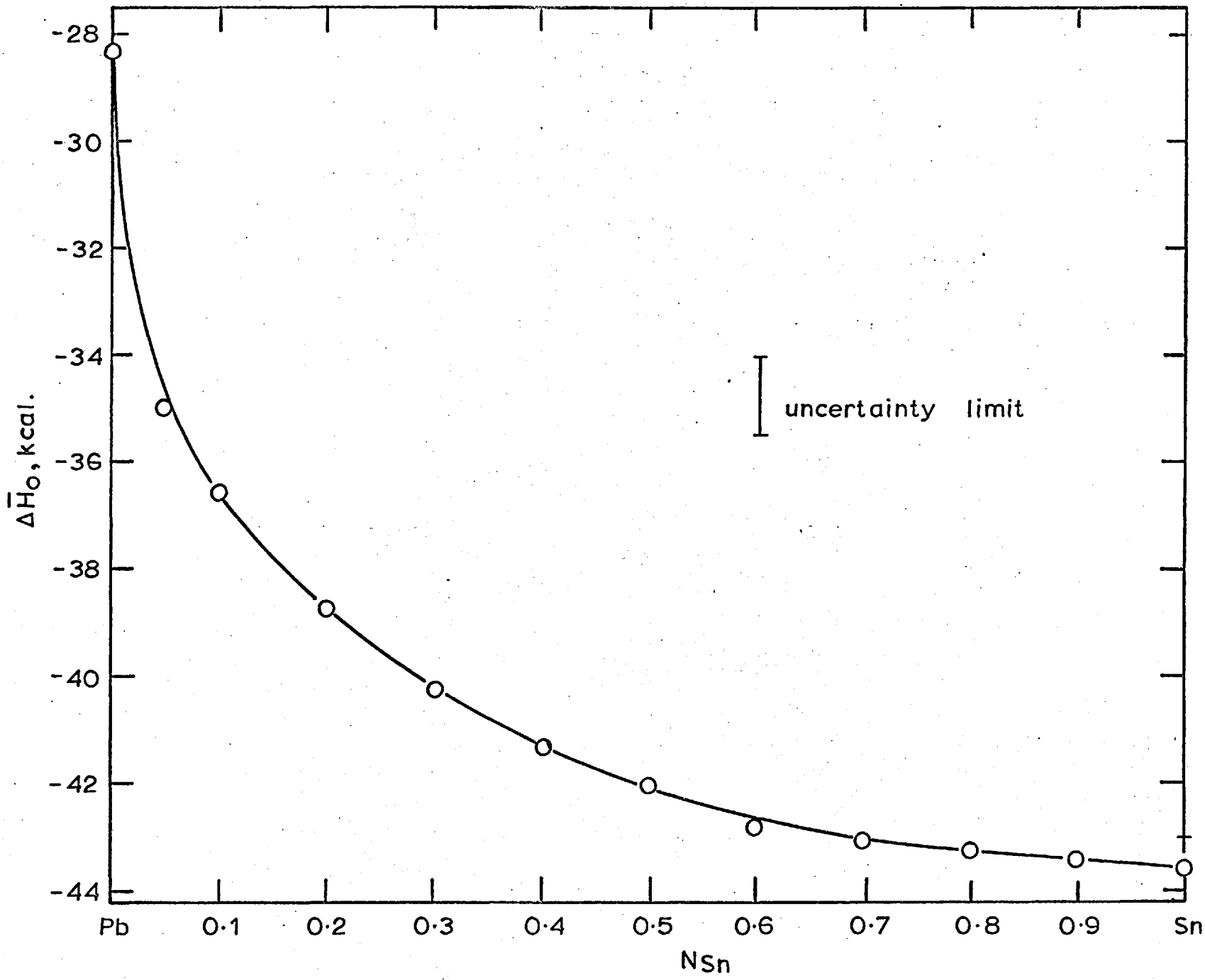

Fig. 37. RELATIVE PARTIAL MOLAR ENTHALPY OF OXYGEN IN Pb-Sn ALLOYS.
(STANDARD STATE IS PURE OXYGEN GAS AT 1 atm. PRESSURE)

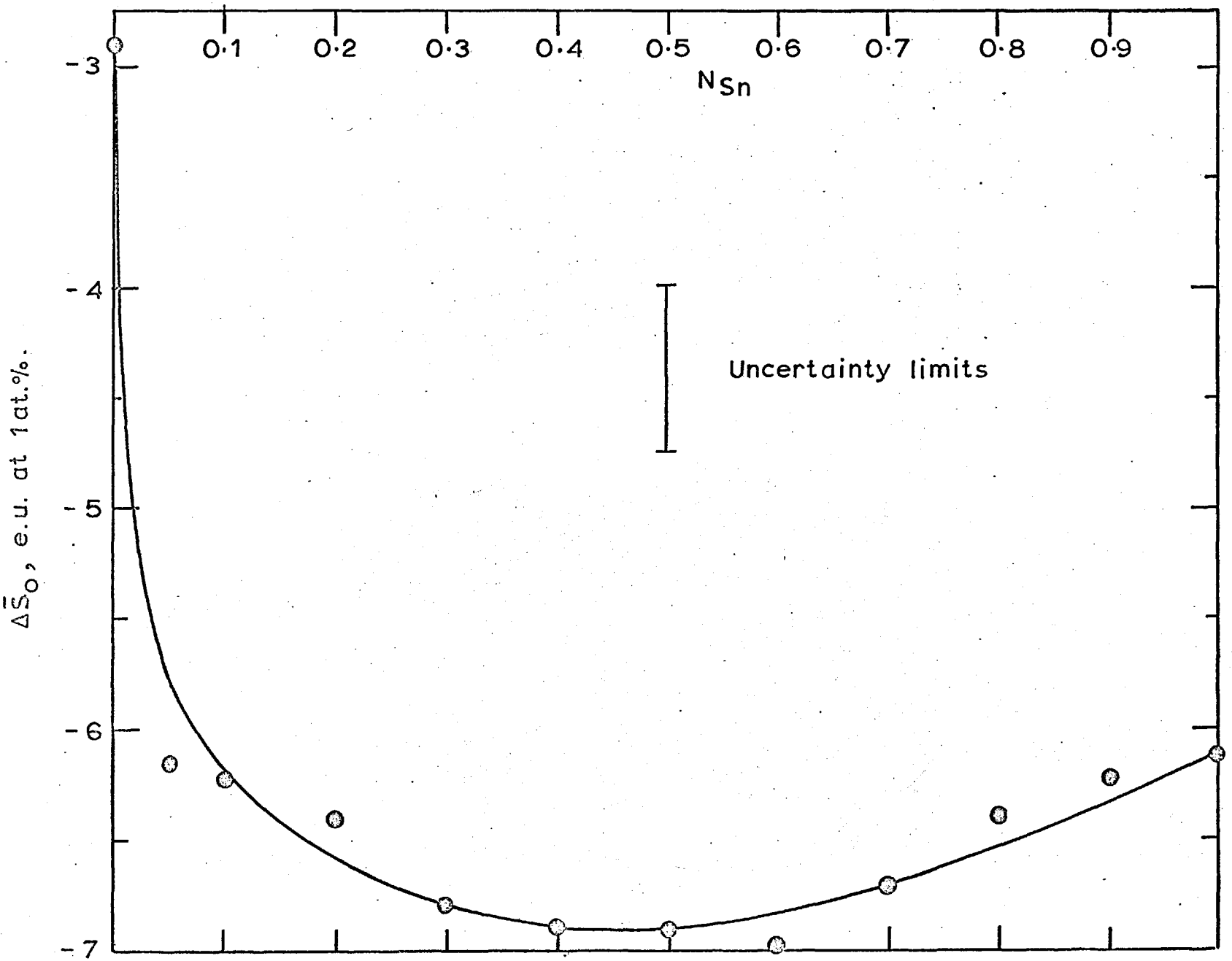

Fig.38. RELATIVE PARTIAL MOLAR ENTROPY OF OXYGEN AT 1atm.%. IN Pb-Sn ALLOYS.

$$\log f_O^{Sn} = 8.2438\ E - 3.4647 - \log (\text{at. pct. O})$$

(Fe - FeO reference electrode, 950°C)

$$\log f_O^{Sn} = 7.3432\ E - 2.7822 - \log (\text{at. pct. O})$$

(Fe - FeO reference electrode, 1100°C)

The results are shown in figures 30 to 33, where the logarithm of the activity coefficient of oxygen with respect to 1 pct. solution in lead as standard state is plotted against the composition of the alloy at each temperature. An enlarged representation of the two terminal regions is provided in figures 34 and 35. The variation of the activity coefficient with temperature is represented in fig. 36. The relative partial molar enthalpy and entropy of oxygen at 1 at. pct. in Pb + Sn alloys may be calculated from the data in this figure, using the equations:

$$\Delta\bar{H}_O = 4.575 \left[\frac{\delta \log f_O}{\delta (1/T)}\right]_{P,\ comp.}$$

$$\Delta\bar{S}_O = \Delta\bar{H}_O / T - 4.575 \log f_O$$

The variation of $\Delta\bar{H}_O$ and $\Delta\bar{S}_O$ at 1 at. pct. with the composition of the alloy is shown in figures 37 and 38.

It is seen from figures 31 and 32 that the results of the experiments with either Pb + O or Sn + O as starting solution are in good agreement. From the known free energy of formation of SnO_2[67] and the activity of Sn in Pb + Sn alloys[12], the e.m.f. of the cell corresponding to Sn - SnO_2 equilibria may be calculated as a function of the activity of Sn in solution and is shown overleaf.

The e.m.f.s in the experiments reported in this section are lower than those shown above for Sn - SnO_2 equilibria. Hence the formation of SnO_2 in solutions during the experiments is unlikely. It can also be shown that due to the low activity of SnO (0.01) loss of oxygen from the lead rich solution as SnO vapour is unlikely.

a_{Sn}	E.m.f., mv 750°C	E.m.f., mv 950°C
0.1	126.8	169
0.2	111.5	151
0.3	102.6	140
0.4	96.3	132
0.5	91.3	126.5
0.6	87.3	122
0.7	83.9	118
0.8	81.0	114
0.9	78.4	111

(k) Activity Coefficient of Oxygen in Pb + Ag alloys at 1000°C.

Results of the two experiments starting with Pb + O solution and one experiment starting with Ag + O solution are shown in tables 44 to 46. The equation

$$\log f_O^{Ag} = -0.9524 + 7.9200\ E - \log (\text{at. pct. O})$$

is used to derive the activity coefficient of oxygen (tables 44 and 45) relative to oxygen in lead. In experiment 53, where oxygen free lead was added to Ag + O solution, the equation employed to derive the activity coefficient (relative to oxygen in silver) is,

$$\log f_O^{Pb} = -4.8629 + 7.9200\ E - \log (\text{at. pct. O})$$

The derived values are shown in figure 39. The results of the three experiments are in good agreement.

(l) Activities in binary Ag + Pb alloys.

The e.m.f. of cell 13 is a direct measure of the activity of Pb in Pb - Ag solutions. The virtual cell reaction may be represented by

$$Pb\ (l) \rightarrow [Pb]_{Alloy}$$

If pure liquid lead is taken as the standard state for lead, then the

TABLE 45.

Experiment 52.

Cell 7

Temperature = 1000°C.

wt. of Pb in the crucible = 40.6987 g.

wt. of Ag added at each stage (g)	Mole fraction of Ag in soln. (N_{Ag})	E.m.f. mv	at. pct. O x 10^2	Log f_O^{Ag}
-	0	-117	1.321	0
1.3169	0.0585	-107.5	1.244	0.1014
1.4068	0.1139	-100.6	1.170	0.1826
2.5074	0.1980	- 86.7	1.059	0.3360
2.8043	0.2750	- 72.8	0.958	0.4898
4.7268	0.3759	- 54.5	0.824	0.6998
6.0933	0.4709	- 34.5	0.699	0.9299
10.3762	0.5798	- 10.7	0.555	1.2185

TABLE 46.

Experiment 53.

Cell 12

Temperature = 1001°C.

wt. of Ag in the crucible = 35.0723 g.

wt. of Pb added at each stage (g)	Mole fraction of Pb in soln. (N_{Pb})	E.m.f. mv	at. pct. O x 10^3	Log f_O^{Pb}
-	0	251.5	1.346	0
2.8457	0.0405	180	1.290	-0.6218
6.4211	0.1210	107	1.183	-1.2345
8.2378	0.2063	42	1.068	-1.7793
13.4906	0.3151	-18	0.921	-2.2145
12.9836	0.3951	-55	0.814	-2.5275

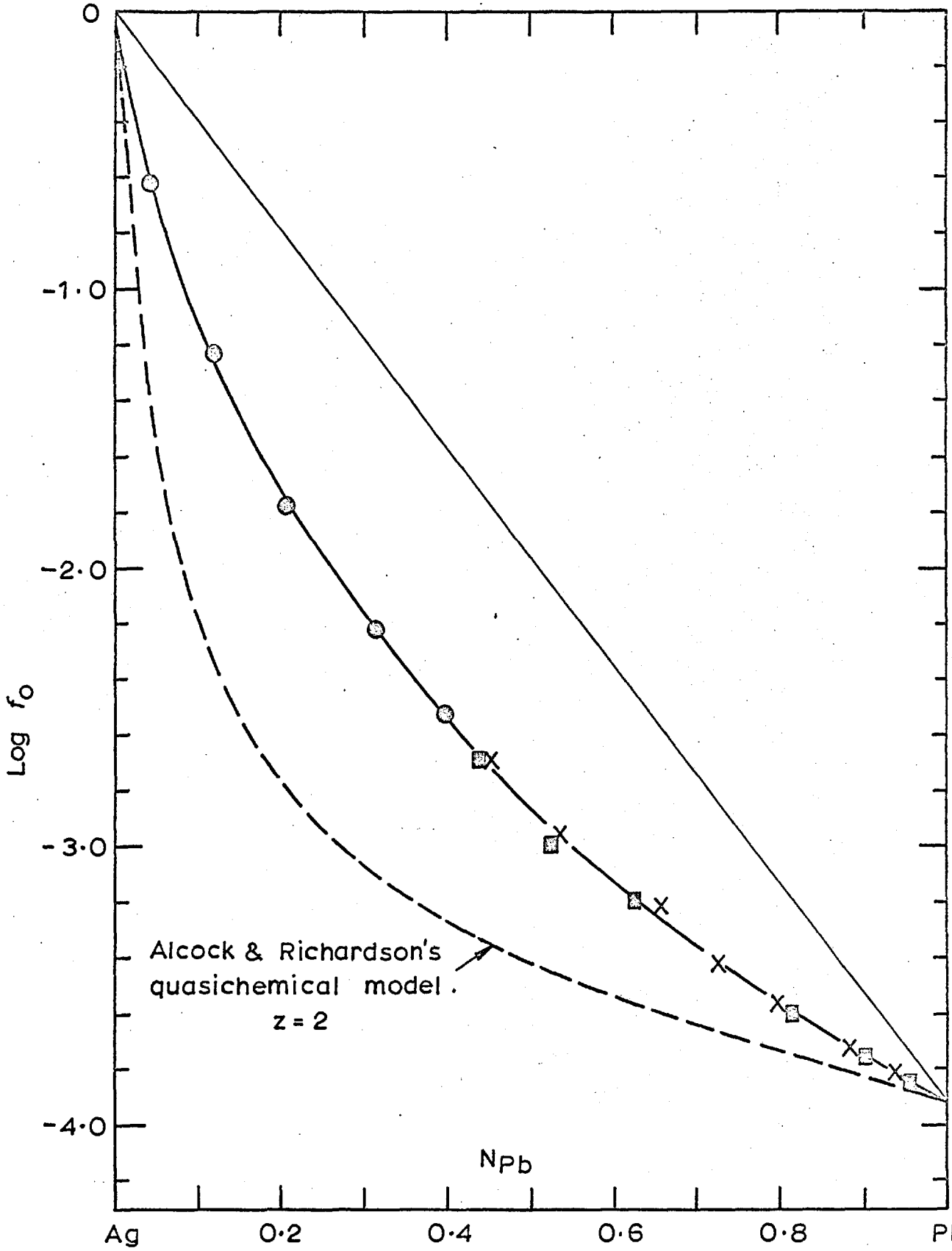

Fig. 39. ACTIVITY COEFFICIENT OF OXYGEN IN Ag-Pb ALLOYS AT 1000°C. (STD. STATE IS 1 atom.%. SOLN. IN Ag)

relative partial molar properties of mixing of lead in Pb - Ag alloys may be calculated directly from the experimental data

$$\Delta\bar{G}_{Pb} = RT \ln A_{Pb} = - nFE$$

$$\Delta\bar{H}_{Pb} = - nF \left[E - T \left(\frac{\delta E}{\delta T} \right)_{N_{Pb}} \right]$$

$$\Delta\bar{S}_{Pb} = nF \left(\frac{\delta E}{\delta T} \right)_{N_{Pb}}$$

The value of n may be taken as 2 since Pb is divalent in PbO, E is the e.m.f. in volts and F is the Faraday equivalent (23,063 cals per volt equiv.).

Results of experiments 54 and 55 are presented in table 47 and calculated activities are plotted in figure 40. The results of experiments 56 to 60 are shown in table 48 and plotted in figure 41. Equations representing the variation of the e.m.f. with temperature and the derived relative partial molar enthalpy of Pb are also shown in table 48.

When α'_{Pb} [equal to $RT \ln \gamma_{Pb} / (1-N_{Pb})^2$], calculated from the smoothed activity cure for lead in figure 40, is plotted against the mole fraction of lead, two linear segments are obtained which intersect at $N_{Pb} = 0.4$. The linear segments may be represented by the following equations at 1100°K;

$$\alpha'_{Pb} = 1355 + 1920\, N_{Pb} \quad (0.4 > N_{Pb} > 0)$$

$$\alpha'_{Pb} = 2000 + 205\, N_{Pb} \quad (1 > N_{Pb} > 0.4)$$

The relative partial molar free energy of silver and the integral excess free energy of mixing of Ag + Pb alloys at 1100°K are obtained by Gibbs-Duhem integration from the data on the relative partial molar free energy of lead;

$$\Delta\bar{G}_{Ag} = RT \ln N_{Ag} - N_{Ag} N_{Pb} \alpha'_{Pb} + \int_0^{N_{Pb}} \alpha'_{Pb}\, d N_{Pb}$$

$$\Delta G^{M,\ Excess} = (1 - N_{Pb}) \int_0^{N_{Pb}} \alpha'_{Pb}\, d N_{Pb}$$

TABLE 47.

Experiment 54.

N_{Pb}	E.m.f., mv	a_{Pb}
0.9498	2.30	0.952
0.9052	4.20	0.915
0.8203	7.95	0.845
0.7512	10.55	0.800
0.6489	15.55	0.725
0.5404	20.30	0.652
0.4008	26.50	0.571
0.3113	36.30	0.465
0.2418	46.45	0.375
0.1693	56.80	0.302

Experiment 55.

N_{Pb}	E.m.f., mv	a_{Pb}
0.200	51.80	0.335
0.352	30.00	0.531
0.498	20.8	0.645
0.621	15.5	0.721
0.799	8.8	0.831

TABLE 48.

Experiment 56.

N_{Pb} = 0.5

Temp. °C	E.m.f., mv
633	14
700	17
754	18.6
800	20.4
822	21.4
833	22
766	19.5
733	17.7
650	15

Experiment 57.

N_{Pb} = 0.6

Temp. °C	E.m.f., mv
617	11.1
700	13.3
800	16.4
817	16.7
833	17.5
750	15.3
667	12.8

Experiment 58

N_{Pb} = 0.7

Temp. °C	E.m.f., mv
567	8.1
650	9.5
750	10.3
804	12.8
834	13.1
767	12.1
750	10.5
700	10.8
600	9.0

Experiment 59.

N_{Pb} = 0.8

Temp. °C	E.m.f., mv.
500	5.5
600	6.5
700	7.5
777	8.0
810	8.9
840	9.0
750	8.3
667	6.9
567	5.7

Experiment 60.

N_{Pb} = 0.9

Temp. °C	E.m.f., mv
467	3.0
500	3.0
650	3.9
750	4.25
830	4.8
800	4.4
700	3.7
550	3.0

N_{Pb}	E.m.f., mv	$\Delta\overline{H}_{Pb}$, cal.
0.9	$E = -0.9 + 0.5 \times 10^{-2}T$	41
0.8	$E = -3.157 + 1.087 \times 10^{-2}T$	146
0.7	$E = -7.263 + 1.833 \times 10^{-2}T$	335
0.6	$E = -13.80 + 2.80 \times 10^{-2}T$	636
0.5	$E = -20.76 + 3.833 \times 10^{-2}T$	958

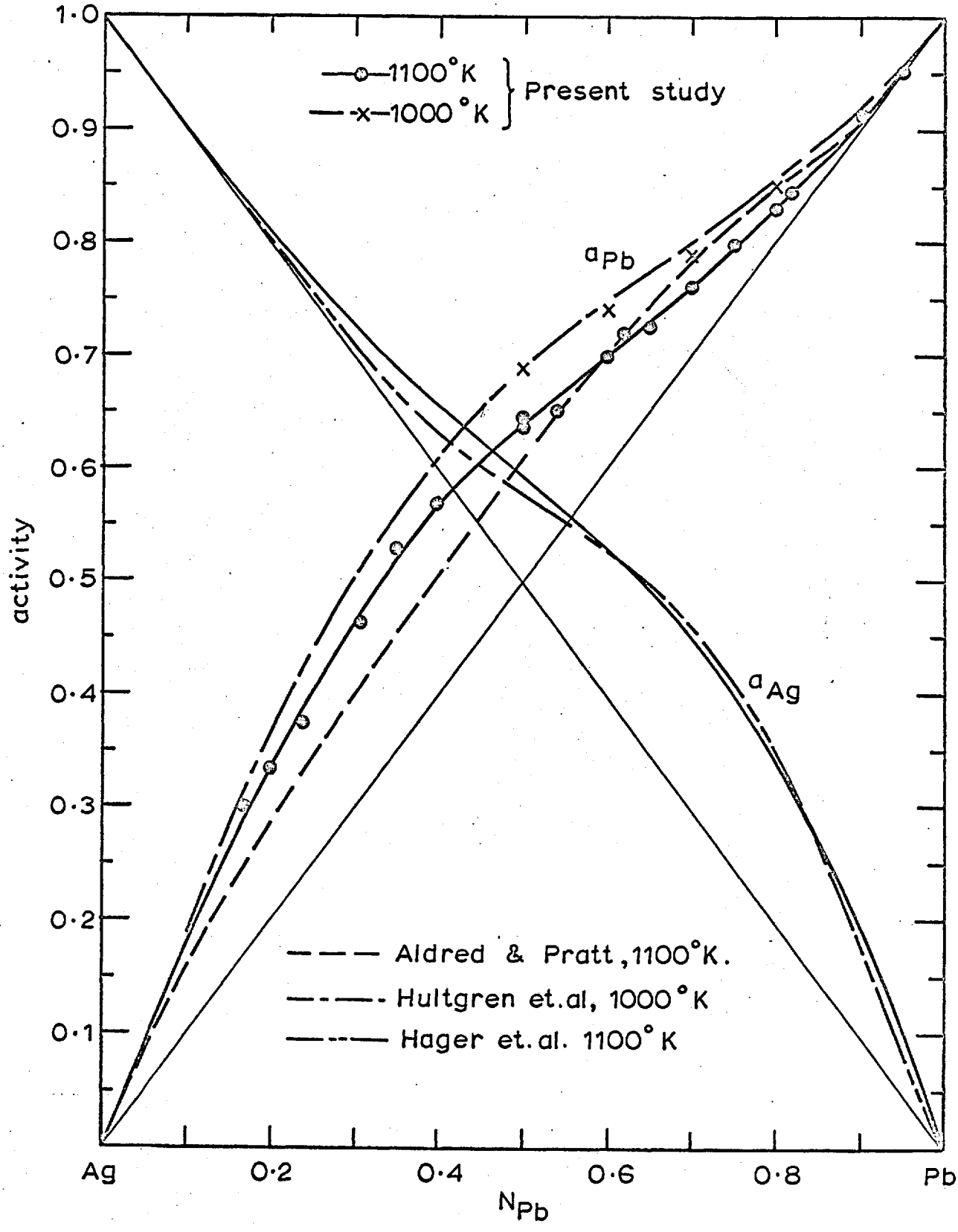

Fig.40. ACTIVITY OF LEAD & SILVER IN Pb-Ag SYSTEM

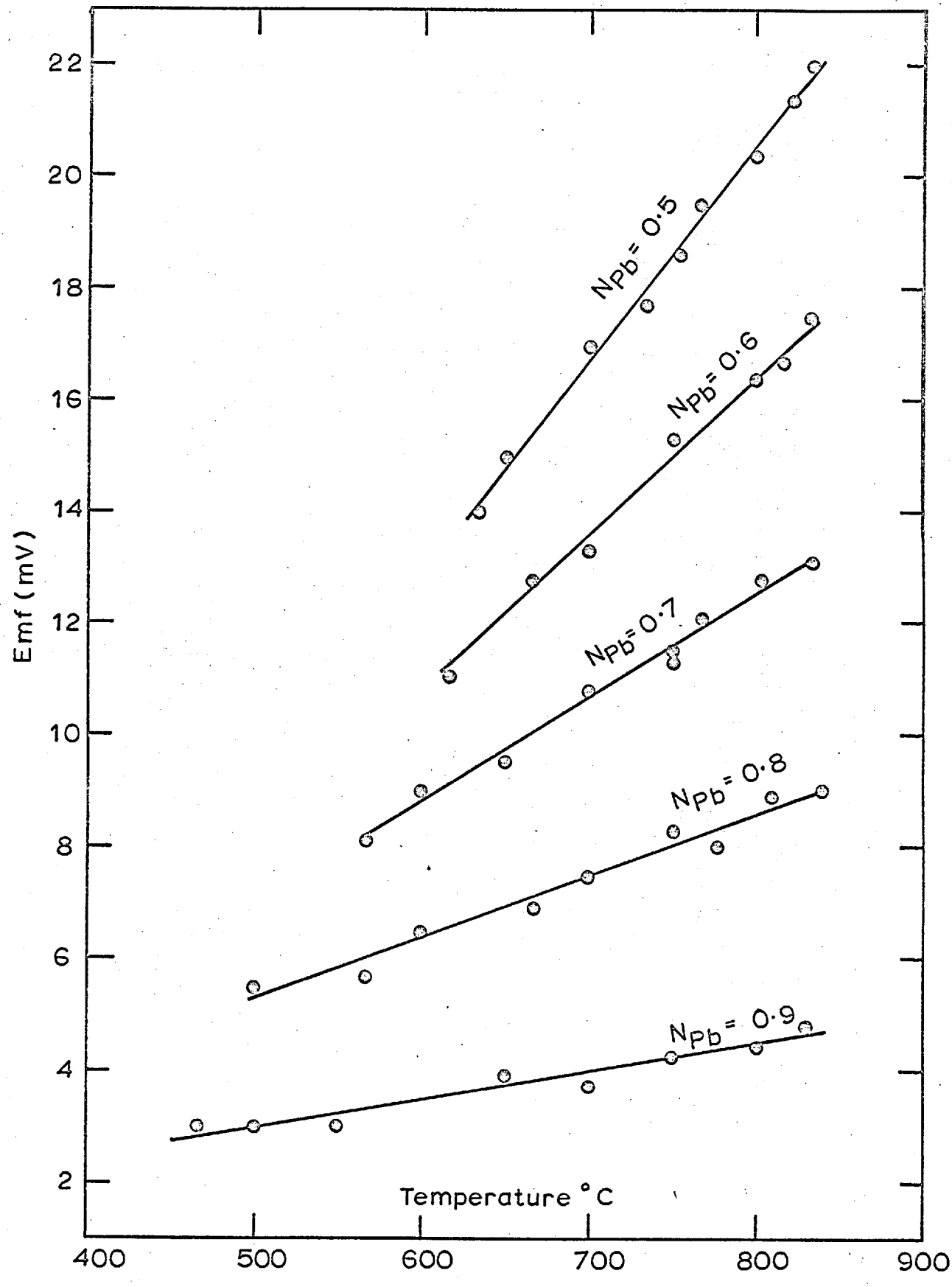

Fig. 41. VARIATION OF THE EMF OF THE CELL, Pt, Ir, Pb-PbO/ ZrO_2/ Ag-Pb-PbO, Ir, Pt. WITH TEMPERATURE

The computed activity of Ag is shown in figure 40. The excess free energies of mixing are shown below:

N_{Pb}	0.1	0.2	0.3	0.4	0.5	0.6	0.7	0.8	0.9
$\Delta G^{M,\ Excess}$ cal	130	248	345	417	453	446	397	306	173

Due to the large difference in the standard free energies of formation of PbO and Ag_2O, displacement reactions of the type

$$2\ Ag\ (alloy) + PbO \rightarrow Pb\ (alloy) + Ag_2O$$

are unlikely to introduce an error greater than 0.1 pct.

The solubility of oxygen in the alloy is a function of composition and temperature. The solubility of oxygen in pure lead is 0.61 at. pct. at 1100°K and the solubility in the alloys would be lower than this value. The lowering of the activity of lead due to oxygen solubility would introduce a maximum error of 11 cals in the relative partial molar free energy of lead. This corresponds to an error of 0.2 mv in the measured e.m.f., and lies within the accuracy of the e.m.f. measurements reported in this study.

CHAPTER 6.

Discussion.

On the basis of measurements on cells 1, 3, 4 and 5 it appears that the polarization of Ni-NiO electrodes can be overcome by the use of techniques that permit good contact to be obtained between the electrolyte and the reference electrode and by ensuring the absence of reaction between the reference electrode and residual oxygen in the atmosphere around it. Approximately 15 pct. of the solid electrolyte tubes used in this study were found to be faulty, probably due to the presence of microcracks. When such tubes are used the transport of oxygen across the electrolyte could lead to polarization, unless the relevant chemical reactions and mass transfer processes at the electrode - electrolyte interface are sufficiently rapid.

Under identical conditions, observed polarization was more severe when oxygen was transported to the Ni-NiO reference electrode due to the oxygen potential gradient than when vice versa. This is probably due to more rapid transport of oxygen through Ni than through NiO - due to the small non-stoichiometric range of NiO, transport of oxygen through it may be expected to be slow. The fact that the Fe-FeO reference electrode does not polarize under those conditions producing polarization in Ni-NiO electrode suggests that the rates of reaction or transport of oxygen in Fe and FeO are considerably higher than with Ni and NiO.

Diaz and Richardson[68] observed severe polarization of Ni-NiO electrodes. They used presintered Ni-NiO pellets which were shaped to fit the electrolyte tube after sintering. With this arrangement contact between the reference electrode and the electrolyte is likely to be poor. Fruehan and Richardson[28] sintered the Ni-NiO mixture inside the solid electrolyte tube to obtain better contact and found that the polarization of the electrode was much reduced. Abraham[112]

did not observe polarization of the electrode when the oxygen content of copper was low enough to cause oxygen to be transported from the reference electrode to liquid copper. All these investigators[28,68,112] used a separate stream of argon to flush the reference electrode.

Rickert and Wagner[71], and Wilder[74] do not report any polarization of Ni-NiO electrode when measuring oxygen in liquid copper using solid oxide galvanic cells. These authors used cell constructions with the inert atmospheres over the two half cells separated, but did not flush the reference electrode with a stream of inert gas. This suggests, in agreement with the observation made in this study, that the performance of the reference electrode is more satisfactory when a static inert atmosphere is maintained over the electrode than when a continuous stream of inert gas is passed over it.

Cu + O System.

Young[29] has measured the oxygen contant of liquid copper in equilibrium with CO/CO_2 mixtures from 1100° to 1500°C. His results can be combined with the standard free energy of formation of CO_2 from CO and O_2[69], to give the following equation for the standard free energy of solution of $\frac{1}{2} O_2$ in liquid copper

$$\Delta G^\circ = -20,542 + 1.723T \text{ cals/gr. atom Oxygen} \quad \cdots\cdot 43$$

More recently Diaz and Richardson[68] have reviewed the literature on the Cu + O system and recommended values shown in table 1 (page 17). The equilibrium constant for the solution of oxygen in copper obtained in this work is compared below with the recommended values:

Temp. °C	log K (This study)	log K (Young)	log K (Diaz and Richardson)
1100	2.8930 ∓ 0.005	2.8936	2.9122
1300	2.4774 ∓ 0.005	2.4778	2.6926

In view of the excellant agreement between the values obtained in this study and those of Young, equation 43 may be used to provide the

best description of the standard free energy of solution of oxygen in copper.

The major source of error in this investigation is likely to be in the determination of oxygen in copper. The probable error is 1 pct. at the lowest oxygen concentrations measured. The fact that the scatter of experimental points is independent of oxygen concentration suggests that the actual source of random error may be in the sampling procedure. Log K is estimated to be accurate to ∓ 0.005.

Young[29] expressed deviations from Sievert's law by the relation:

$$\log f_O^O = - \frac{60.4}{T} \text{ (atom pct. O)}$$

while the results of this study are in good agreement with this equation at 1100°C, the agreement is less satisfactory at higher temperatures. Rickert and Wagner[71] have also shown that the activity of oxygen varies non-linearly with composition. From their plot the activity coefficient at 1145°C may be deduced as:

$$\log f_O^O = - 0.415 \text{ (atom pct. O)}$$

Osterwald[72] has also reported deviations from Sievert's law, which are in good agreement with that obtained in this study. Sano and Sakao[70] report more pronnounced deviations [$\log f_O^O = - 0.053$ (at.pct. O)] The smaller value of log K and increased deviations from Sievert's law reported by these authors can be explained by a non-random error in their CO analysis. Such an error could possibly occur due to some of the CO_2 in the equilibrium gas mixture reacting with copper lost by vaporization from the melt and depositing on the colder parts of the reaction tube.

As the observed deviations from Sievert's law are small, they can be masked by large errors in experimental determinations. The observation of several authors[4,28,51,73-75] that oxygen in copper obeys Sievert's law may arise from lack of sufficient accuracy in their measurements. The magnitude of the deviation is similar to that

reported by Floridis and Chipman (table 1) for oxygen in liquid iron. Besides sulphur in copper and iron is also found to deviate negatively from Sievert's law.

If oxygen and sulphur are assumed to dissolve in metals and alloys as partly ionised species, it is unlikely that they will occupy nearest neighbour positions due to repulsive electrostatic interactions. Deviations from Sievert's law must then be the result of next nearest neighbour interactions. Positive deviations from Sievert's law are to be regarded as due to the effect of repulsive forces between solute atoms, and negative deviations due to attractive forces. Interpretation of observed negative deviations in terms of the tendency of oxygen atoms to cluster together in the next nearest neighbour position, enables a clearer understanding of many metal - metal oxide and metal - metal sulphide phase diagrams which exhibit immiscibility between two liquids, one metal rich, and the other rich in oxygen or sulphur. Further examples of immiscibility between liquid metals and ionic liquids is provided by phase diagrams of metal - metal halide systems.

Free Energy of formation of Cu_2O

The e.m.f. of cell 6 is compared with those reported by Steele and Alcock[149], Rizzo et al[150], and Flengas and Charette[151] in figure 15 (page 87). The results of this study are in excellent agreement with those of Flengas and Charette, but are 2 to 3 mv below those reported by Steele and Alcock, and Rizzo et al. The measured e.m.f.s are compared with those calculated from Kiukkda and Wagner[118] and measured by Rapp and Maak[152], and Sellars and Maak[153] (not shown in fig. 15) in the table overleaf.

All these e.m.f.s below 1065°C are in good agreement, except that calculated from Kiukkala and Wagner at 800°C.

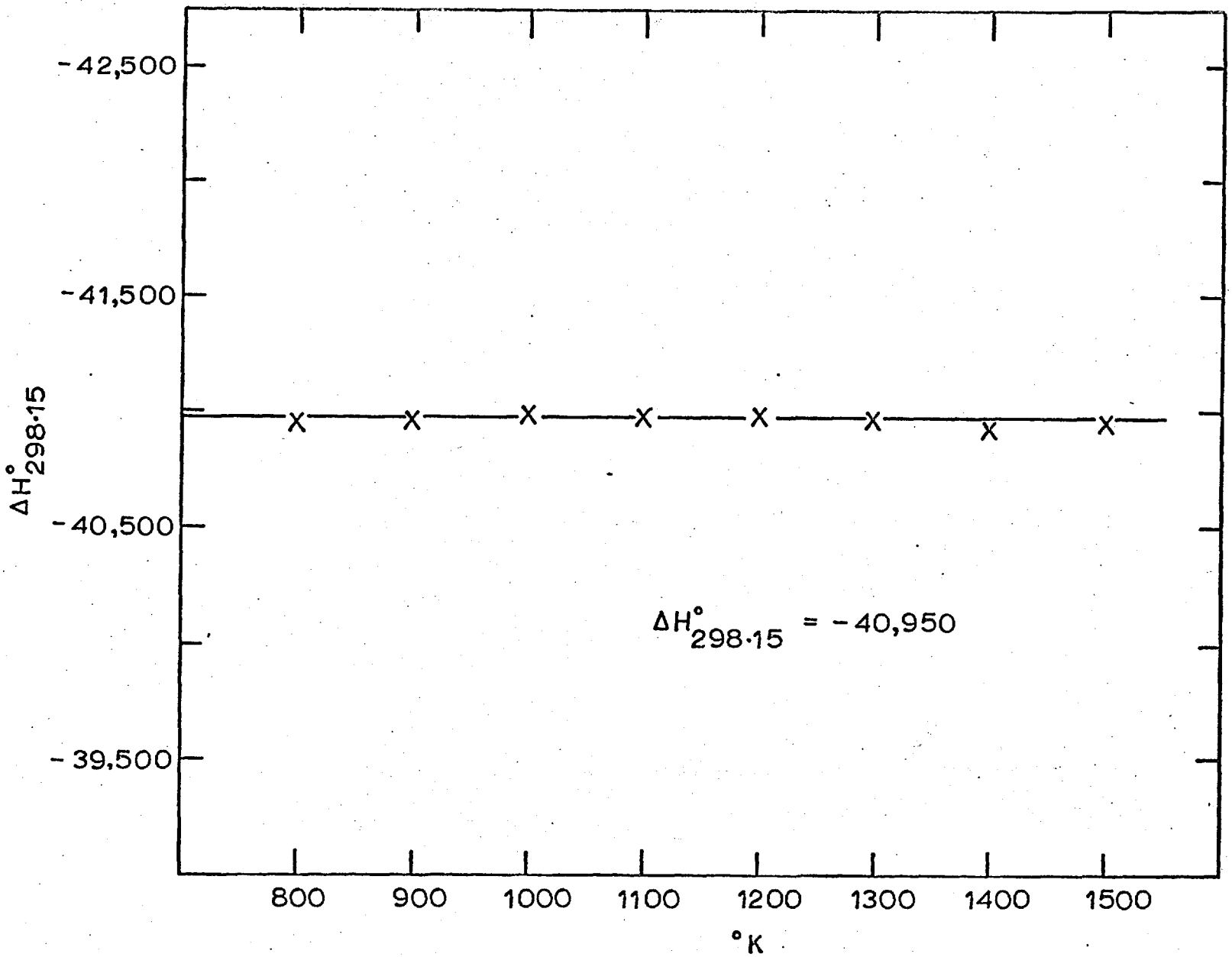

Fig. 42. $\Delta H^{\circ}_{298\cdot15}$ (THIRD LAW) FOR $2Cu + {}^{1}/_{2}O_2 \longrightarrow Cu\cdot O$.

Temp. °C	E.m.f. of cell, Ni-NiO / ZrO_2 / Cu-Cu_2O			
	This study	Kiukkola and Wagner	Sellars and Maak	Rapp and Maak
1000	257 ∓ 0.5	257 ∓ 3	258.4 ∓ 0.5	258
900	263.5 ∓ 0.5	263 ∓ 3	264.4 ∓ 0.5	-
800	270.5 ∓ 0.5	266 ∓ 3	271.5 ∓ 0.5	-

The data obtained above 1065°C by different authors show a spread of 7.5 mv. The e.m.f.s of this study are lower than those of Wilder[74] Osterwald et al[154], and Fruehan et al[28], but are higher than that reported by Rickert and Wagner[71] at 1145°C. The disagreement between the e.m.f. of this study and that of Fruehan et al is surprising, since both measurements have been carried out under very similar conditions. Lack of experimental details makes it difficult to account for the large spread of values.

To evaluate the results, the standard free energy of formation of Cu_2O derived from the e.m.f.s obtained in this study was analysed by a 'third law treatment' using the expression:

$$\Delta H^\circ_{298} = \Delta G^\circ_T - \Delta(H^\circ_T - H^\circ_{298}) + T\left[\Delta S^\circ_{298} + \Delta(S^\circ_T - S^\circ_{298})\right]$$

The calorimetric data $H^\circ_T - H^\circ_{298}$, $S^\circ_T - S^\circ_{298}$ and S°_{298} for Cu_2O were obtained from Mah et al [155]. The corresponding values for copper were obtained from Hultgren et al[12], while those for oxygen are from the compilations of Kelly[156] and Wagman et al[157]. Provided the calorimetric data and the free energy data are correct, a constant value of ΔH°_{298} should be obtained in agreement with the recommended value. The values of ΔH°_{298} obtained by the 'third law treatments' are shown in figure 42, from which it can be seen that the values derived from e.m.f.s are virtually constant throughout the temperature range (600 to 1200°C). A value of - 40,975 ∓ 50 cals is obtained as

the heat of formation of Cu_2O at 298°C. Mah and coworkers[155] calculate a value of - 40,830 ∓ 300 cals based on their calorimetric study and older equilibrium data on the decomposition of CuO to Cu_2O. It can therefore be concluded that the new calorimetric data of Mah et al on the entropy and high temperature heat content of Cu_2O coupled with the high temperature equilibrium data obtained in the study by solid electrolyte e.m.f. studies yield excellent third law correlations for the formation of Cu_2O.

Thermodynamic data on Cu + O solutions and the free energy of formation of Cu_2O can be used to calculate the saturation solubility of oxygen in liquid copper. The calculated values can then be compared with those measured by independent methods. The saturation solubility of oxygen in copper was discussed in Chapter 2 and is shown in fig. 1 (page 22). The selected values are compared below with those calculated from thermochemical data obtained in this study at 1100 and 1200°C.

Temp. °C	Saturation solubility of oxygen in copper, at. pct.	
	Value from phase diagram (fig. 1)	Calculated from thermochemical data
1100°C	2.24	2.40
1200°C	6.20	6.70

The agreement is considered to be reasonable, especially since the calculated phase boundary is very sensitive to small errors in thermochemical data. If oxygen in liquid copper is assumed to obey Sievert's law, then the saturation solubility at 1200°C calculated from thermochemical data would be 30 to 40 pct smaller than that shown in the phase diagram. This provides an additional indication of deviations from Sievert's law.

Pb + O system.

The purpose of the three experiments to determine the partial pressure of oxygen over Pb + O solutions was to check the validity of the standard free energy of solution of oxygen in lead obtained by extrapolation from Alcock and Belford's results at lower temperatures. A value of - 24,140 ∓ 150 cal is obtained for the free energy of solution of $\frac{1}{2} O_2$, which compares with a value of - 24,298 obtained from the relevent equation in table 1 (page 17). The latter value has therefore been used throughout this study. The results are not sufficiently accurate to permit conclusions to be drawn regarding deviations from Sievert's law.

Free Energy of formation of PbO.

The e.m.f. of cell 9 is compared with those obtained by other investigators[64, 151, 158] in figure 17 (page 93). The results of this study are in excellent agreement with those of Alcock and Belford[64] and in fair agreement with those of Flengas and Charette[151], all of whom used iridium leads to make electrical contact with lead in equilibrium with PbO. Both Warner, and Flengas et al used oxygen reference electrode; their results are plotted using Steele's value for the free energy of formation of NiO. The results of Warner are 5 to 12 mv lower than those obtained by other investigators, probably due to the use of an iron conducting lead, protected from PbO by an alumina sheath. In the author's experience this method of protection is ineffective (Chapter 5, section e). A layer of PbO is invariably present between the Pb and the protective sheath, and this film of PbO makes contact with the conducting lead. Solution of iron oxides in PbO could be a possible cause for the lower chemical potential of oxygen measured corresponding to Pb-PbO equilibria. Besides, continuous oxidation of iron in contact with oxygen saturated lead could give a lower oxygen potential in the metal.

The magnitude of this effect will depend on the relative rates of oxidation of iron, decomposition of PbO, and transport of oxygen through the metal.

From the change in slope of the e.m.f. - temperature plot at the monotectic temperature, the heat of fusion of PbO can be calculated and compared with calorimetric data [158, 159]. The monotectic temperature obtained from the discontinuity in e.m.f. temperature plots of different investigators can also be compared with that obtained from the phase diagram [143,144].

	This study	Flengas et al	Warner	Phase diagram	Calorimetry
ΔH_{fusion} cal.	6,475	5,840	7,092	-	6,400[158]
Monotectic Temp. °C	857	877	865	850	

It is seen from the above table that the results of this study are in better agreement with calorimetric measurements and phase diagram data than those of other investigators. The difference in the free energy of formation of PbO obtained in this study and those reported by Sridhar et al[160] suggests that liquid PbO has an electronic transport number of 0.04.

Further, the saturation solubility of oxygen in lead at 1100°C may be calculated as 3.08 at. pct. from the free energy of solution and the partial pressure of oxygen in equilibrium with Pb and PbO, obtained in this study, assuming Sievert's law is obeyed by oxygen in Pb up to saturation. This compares favourably with a value of 2.9 reported by Richardson and Webb[62].

Thermodynamics of Oxygen in Cu + Ag alloys.

The activity coefficient of oxygen in Cu + Ag alloys obtained in this study at 1100°C is compared with that reported by other investigators [28,29,60] in figure 18 (page 98). Young [29] equilibrated beads of Cu + Ag alloy with $CO-CO_2$ mixtures at 1200°C. Because of the high vapour pressure of silver at 1200°C, the beads were found to have lost weight after equilibration. The final composition was obtained from mass balance on the assumption that weight loss was due solely to the vapourization of Ag. Block et al[60] equilibrated 40 grms of Cu + Ag alloy at 1200°C with $H_2 - H_2O$ - Ar mixture and analysed samples obtained from the solution for oxygen, while Fruehan et al [28] used a technique similar to that used in this study. The results of this study are in fair agreement with those of Block et al and Fruehan et al when the uncertainty in their determinations are taken into account, but disagree with those of Young. Surface depletion of beads due to vaporization of Ag and the increase in the concentration of oxygen at the surface of the bead due to surface tension effects probably interfered with the attainment of equilibrium in the experiments of Young, although it is not clear how these factors result in higher oxygen concentration in alloy beads.

The lowering of the activity coefficient of oxygen in copper by silver is surprising since such effects are generally ascribed to attractive forces between the alloying element and oxygen. The attraction between silver and oxygen is less than that between copper and oxygen in view of the activity coefficients of oxygen in the two pure metals and the relative stabilities of the respective oxides. The Cu-Ag system shows marked positive deviations from Raoult's law, indicating that Ag - Cu bond energies are smaller than those of Ag-Ag or Cu-Cu. This effective repulsion between Ag and Cu atoms must in some way account for the effect of Ag in decreasing the activity of oxygen.

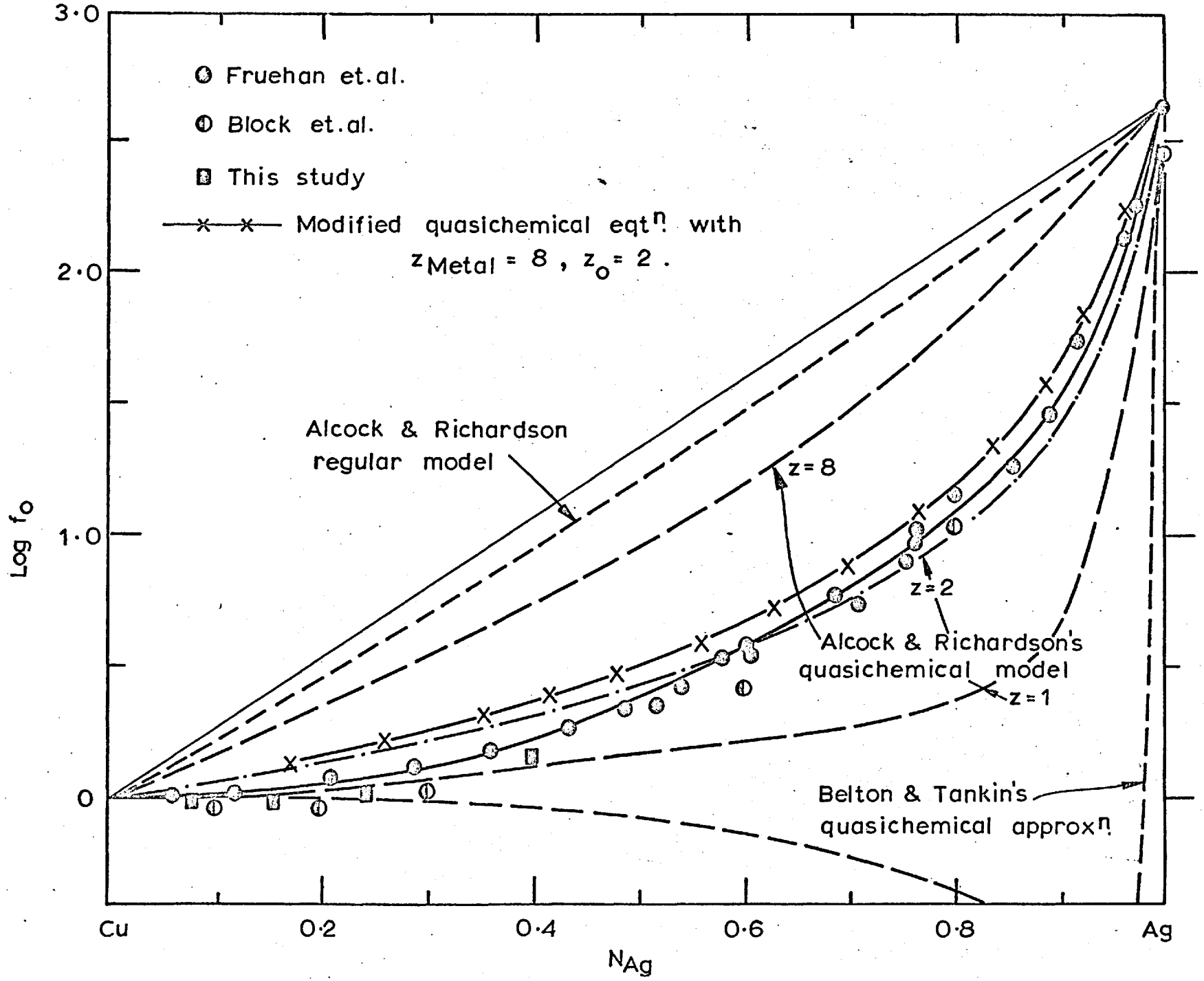

Fi-.43 ACTIVITY COEFFICIENT OF OXYGEN IN Cu-A ALLOYS AT 1100°C

The activity coefficient of oxygen in the whole range of Cu + Ag alloys is shown in fig. 43, compared with the predictions of various models. The binary data on Cu + Ag used in the models is obtained from Hultgren et al[12]. It is clear that Alcock and Richardson's quasichemical model with the coordination number (Z) equal to two gives an adequate representation of the data, especially at the silver rich end. The 'regular' models of Alcock and Richardson, and Belton and Tankins are not strictly applicable to this system since the ratio of the activity coefficient of oxygen in the two pure metals (Ag and Cu) is 444 : 1. It may also be noted that Cu and Ag have the same number of free electrons per metal atom.

Activity Coefficient of Oxygen in Cu-Sn alloys.

The activity coefficient of oxygen obtained in this study is compared with that reported by other investigators[28,60] in figure 20 (page 103). Block et al[60] equilibrated Cu + Sn alloys with H_2-H_2O-Ar mixtures at 1200°C and analysed the alloy samples for oxygen, while Fruehan et al[60] used a technique similar to that used in this study. Fruehan et al added oxygen-free tin to Cu + O solution containing approximately 0.8 at. pct. oxygen. It will be shown later (fig. 44) that the addition of Sn at this oxygen concentration would result in the formation of SnO_2, causing large changes in the e.m.f., these being misinterpreted as an effect of tin on oxygen activity. In addition, SnO has a vapour pressure of approximately 7 m.m[145-147] at 1100°C, so some loss of oxygen as SnO was possible. SnO has since been found to penetrate the CaO - ZrO_2 electrolyte and this phenomenon also could cause the loss of oxygen from the melt when a_{SnO} is greater than 0.04.

The oxygen content of Cu + O solutions prior to Sn addition was maintained at 0.002 and 0.004 at. pct. in this study. At these low oxygen concentrations SnO_2 cannot form, a_{SnO} is maintained below 0.005

and the solid electrolyte is not attacked.

To check the results of the e.m.f. studies, Seshadri and Richardson [161] have measured the solubilities of oxygen in pure tin and copper-tin alloys under a fixed pressure of SnO. Tin silicate slags were equilibrated at 1110°C, via the vapour phase, with beads of pure Sn and Cu-Sn alloys in closed containers under an inert atmosphere. From the ratio of oxygen contants in pure tin and the alloys and knowledge of activity of Sn in Cu-Sn alloys[162], the activity coefficient of oxygen in the alloys is computed, assuming Sievert's law is obeyed by oxygen in Sn and Cu-Sn alloys. The derived activity coefficients are shown in fig. 20, in good agreement with the results obtained in this study.

The free energy interaction parameter, $\epsilon_O^{Sn} = -4.61$ obtained at 1100°C from this study compares favourably with the results of Block et al who obtained a value of - 3.4 for ϵ at 1200°C, and of Sano and Sakao[70] who give values of - 3.2 at 1206°C and - 4.2 at 1155°C from experiments on alloys containing up to 5 pct tin using a technique similar to Block et al. It thus appears that the results of Fruehan et al[28] are in error, and this is now thought to be due to the formation of a separate oxide phase in their experiments.

The deoxidation equilibria for tin in copper may be calculated from the data now available. Although liquid SnO is the stable phase in equilibrium with pure Sn at 1100°C[67], SnO_2 can be shown to be the oxide phase in equilibrium with tin in dilute solution in copper. For the calculation, the activity of tin in the Cu + Sn alloys may be taken from Alcodk et al[162]. Their results show that α_{Sn} (equal to $\frac{\log \gamma_{Sn}}{N_{Cu}^2}$) is a linear function of mole fraction up to 30 at. pct. tin and may be expressed as:

$$\alpha_{Sn} = -1.38 + 3.333\, N_{Sn} \qquad (1100°C)$$

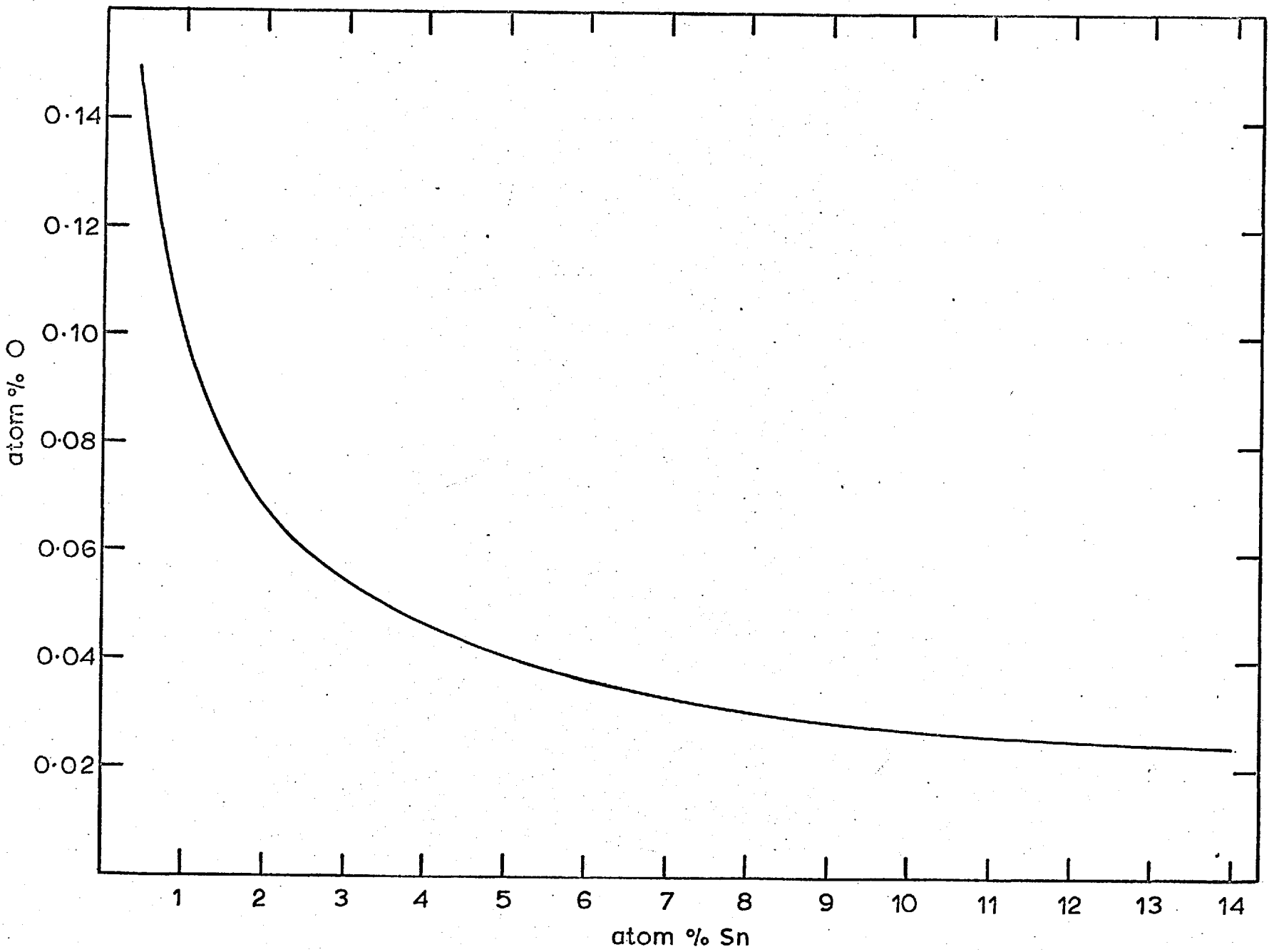

Fig.44 OXYGEN AND TIN CONCENTRATIONS IN LIQUID COPPER IN EQUILIBRIUM WITH SnO_2 AT 1100 °C

The free energy change for the reaction

$$\tfrac{1}{2}\,[Sn] + [O] = \tfrac{1}{2}\,SnO_2 \qquad \ldots\ 44$$

may be calculated from the standard free energy of formation of $\frac{1}{2}\,SnO_2$

$$\Delta G^\circ = -69{,}825 + 25.31\,T \quad \text{cal}$$

and the free energy of solution of oxygen in copper obtained in this study. For reaction 44, then

$$\Delta G^\circ = -49{,}283 + 23.58\,T \quad \text{cal}$$

The equilibrium constant K derived from this equation is then

$$K = \frac{1}{a_{Sn}^{\frac{1}{2}} \cdot \text{at. pct. O.} \cdot f_O^{Sn} \cdot f_O^O}$$

where f_O^{Sn} represents the effect of Sn on the activity coefficient of oxygen and f_O^O denotes the variation of the activity coefficient with oxygen concentration. The a_{Sn} may be taken as equal to $N_{Sn} \cdot \gamma_{Sn} \cdot f_{Sn}^O$, where f_{Sn}^O takes account of the effect of oxygen on the activity of tin. This may be calculated via Wagner's reciprocal relationship[44].

$$\epsilon_O^{Sn} = \epsilon_{Sn}^O$$

The terms f_{Sn}^O and f_O^O are very near to unity and may be neglected without significant error. The calculated deoxidation curve is shown in fig. 44.

The shape of the activity coefficient curve shown in fig. 20 (page 103) is of interest. The marked change in slope which occurs at about 20 at. pct. tin appears at the same composition as the minimum in the heat of mixing curve for Cu + Sn[162]. This is near the composition (25 at. pct. Sn) at which Bever and Floe[163] have reported a sharp discontinuity in the solubility isotherm for hydrogen in the liquid alloys and the composition of intermediate solid phase Cu_3Sn. Magnetic susceptibility data of Honda and Endo[164], the density data of Boremann and Sauerwald[165], electrical resistivity measurements of

Roll and coworkers[166], and the viscosity measurements of Gebhardt et al[167] show discontinuities or rapid changes in slope at about this composition. In addition, Eretnov and Lynbimov[168] have redetermined the viscosities in Cu-Sn alloys from 1100 to 1300°C and found a maximum near 20 pct. Sn. The peculiarities in physical and chemical properties may indicate changes in the chemical potential of the electrons at this composition.

The experimental values for the activity coefficient of oxygen are compared with those computed from Alcock and Richardson's quasichemical model with Z = 2 in figure 20. The experimental curve shows less marked deviations from ideal behaviour than that predicted by the model. The 'regular' models are not strictly applicable since the activity coefficient of oxygen in the two pure metals differs by a factor of 525.

The activity coefficient of Oxygen in Cu + Pb alloys.

The measured activity coefficient of oxygen in Cu-Pb alloys at 1100°C is compared in figure 24 (page 114) with that predicted by various models, using the data of Schurmann et al[169] for binary Cu-Pb alloys. Since the ratio of the activity coefficients of oxygen in the two pure metals (Cu and Pb) is 9.4 : 1, the models based on regular approximations may be used with some justification. It is seen that Alcock and Richardson's regular and quasichemical equations do not fit experimental data. Belton and Tankin's regular approximation gives an adequate representation, especially in copper rich alloys. This model is similar to the 'regular' model of Alcock and Richardson, except for the terms representing the entropy of mixing of oxide 'species'.

The variation of the interaction parameter ϵ_O^{Cu} with the reciprocal of temperature may be compared with that obtained from Belton and Tankin's model. From equation 8 (page 10.) it can be

deduced that

$$\frac{d \in_O^{Cu}}{d(1/T)} = \frac{- \Delta\bar{H}_{O\,(Cu)}}{R} - \frac{\Delta\bar{H}^{o}_{Cu\,(Cu + Pb)}}{R} = 580$$

where the standard state for oxygen is 1 at. pct. solution in lead and $\Delta\bar{H}^{o}_{Cu(Cu + Pb)}$ represents the relative partial molar enthalpy of Cu at infinite dilution in Pb. The value of 580 does not agree with the experimentally determined value of - 7767. The values obtained in this study suggest that the relative partial molar entropy of oxygen in lead is decreased by the addition of Cu, while Belton and Tankin's model assumes an increase in the relative partial molar entropy. Further evidence that the entropy of oxygen in metals is lowered by additives which decrease the activity coefficient of oxygen will be presented in a subsequent section. The apparent agreement between experimental data and Belton and Tankin's random approximation must therefore be viewed with caution.

The effect of copper in decreasing the activity of oxygen in lead is probably due to repulsive interactions between copper and lead atoms in solution, since the Cu-O bond is likely to be weaker than the Pb-O bond. This hypothesis is in line with the observation of Floridis and Chipman[47] that copper lowers the activity of oxygen in liquid iron.

Effect of Phosphorus on the activity coefficient of oxygen in liquid Copper.

Phosphorus lowers the activity coefficient of oxygen in liquid copper. This may be expected since the O-P bond energies are likely to be very much greater than O-Cu bond energies in view of the relative stabilities of the oxides. The large difference in O-P and O-Cu bond energies is partly compensated by the strong attractive interaction between copper and phosphorus atoms.

Despite conflicting reports in the literature, phosphorus is

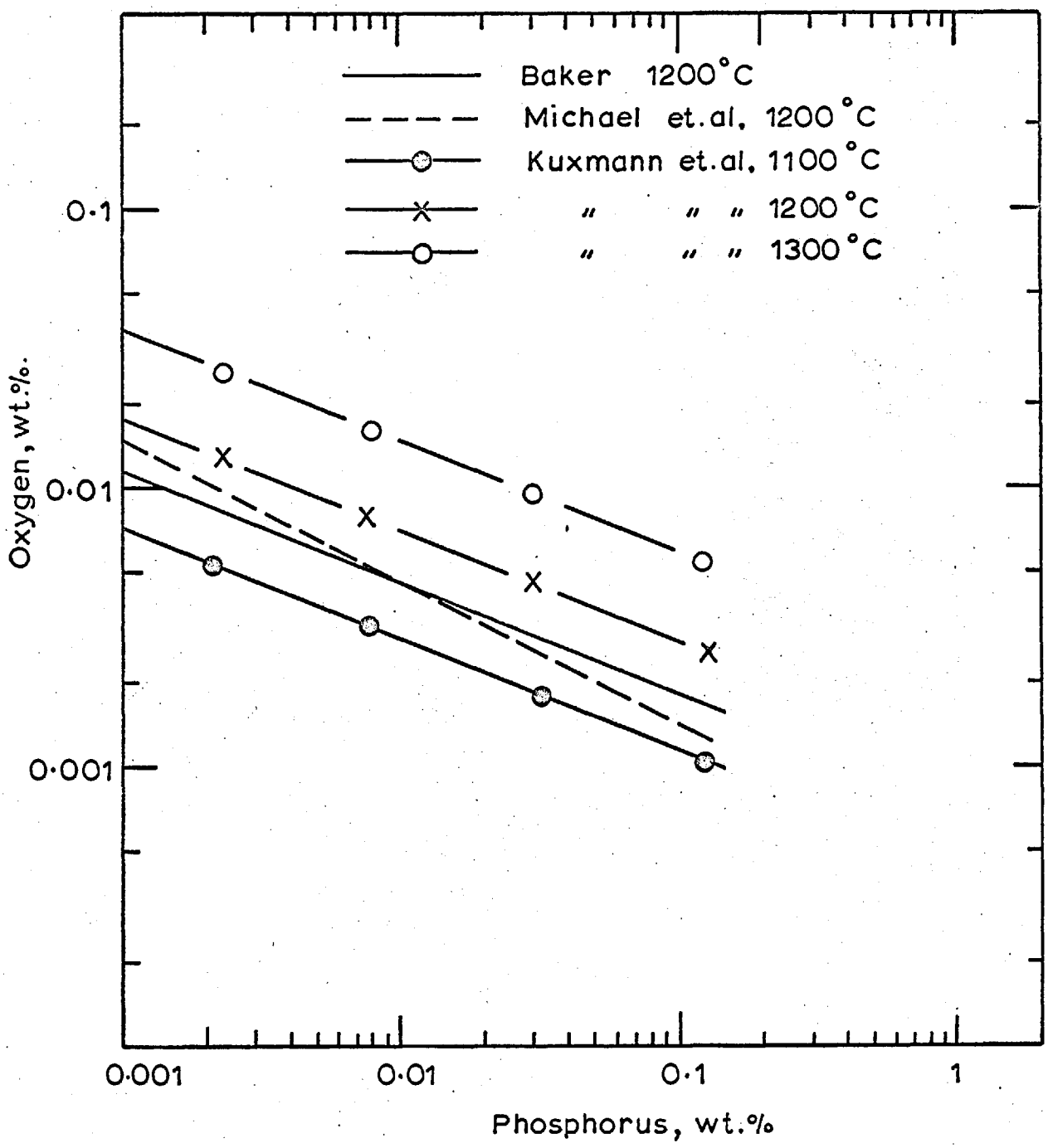

Fig. 45 RELATIONSHIP BETWEEN OXYGEN & PHOSPHORUS CONTENTS OF MOLTEN COPPER IN EQUILIBRIUM WITH COPPER PHOSPHATE SLAGS

considered to increase the activity coefficient of oxygen in liquid iron (table 2). P-O and Fe-O bond energies are probably of comparable magnitude and the increase in the activity of oxygen due to the presence of phosphorus is probably due to strong Fe-P attractive interaction.

Baker[170], Michael et al[171], and Kuxmann et al[172] have measured the oxygen and phosphorus concentrations in equilibrium with copper phosphate slags of known composition. The deoxidation equilibria for phosphorus in copper is shown in fig. 45. It is readily seen from the figure that phosphate slags would not be formed at the low oxygen concentration used in this study. The activity of oxygen in equilibrium with copper phosphate slags may be computed from the oxygen concentration and the interaction parameter ϵ_O^P obtained in this study. Since the mole fraction of copper in solution is greater than 0.99, the activity of copper may be taken to be equal to mole fraction (Raoults law). The activity of Cu_2O in the slag phase can then be readily calculated from the standard free energy of formation of Cu_2O (1). Figure 46 shows the calculated activity of Cu_2O in copper phosphate, compared with the activity of PbO in $PbO - P_2O_5$ melts. No other data is available on activities in binary liquid phosphates. It appears from the figure that copper phosphates are much less stable than lead phosphates.

Recently Ball[173] has proposed a phase diagram for $Cu_2O - P_2O_5$ system in which solid Cu_2O is shown to be in equilibrium with a liquid phase containing 62 mole pct. Cu_2O at 805°C. From the heat of fusion of Cu_2O[155], the a_{Cu_2O} with respect to supercooled liquid as standard state can be obtained at this composition and temperature as 0.12. This value is nearly an order of magnitude higher than that deduced from the results of Baker[170], Michael et al[171], and Kuxmann et al[172]. The validity of the phase diagram is therefore in

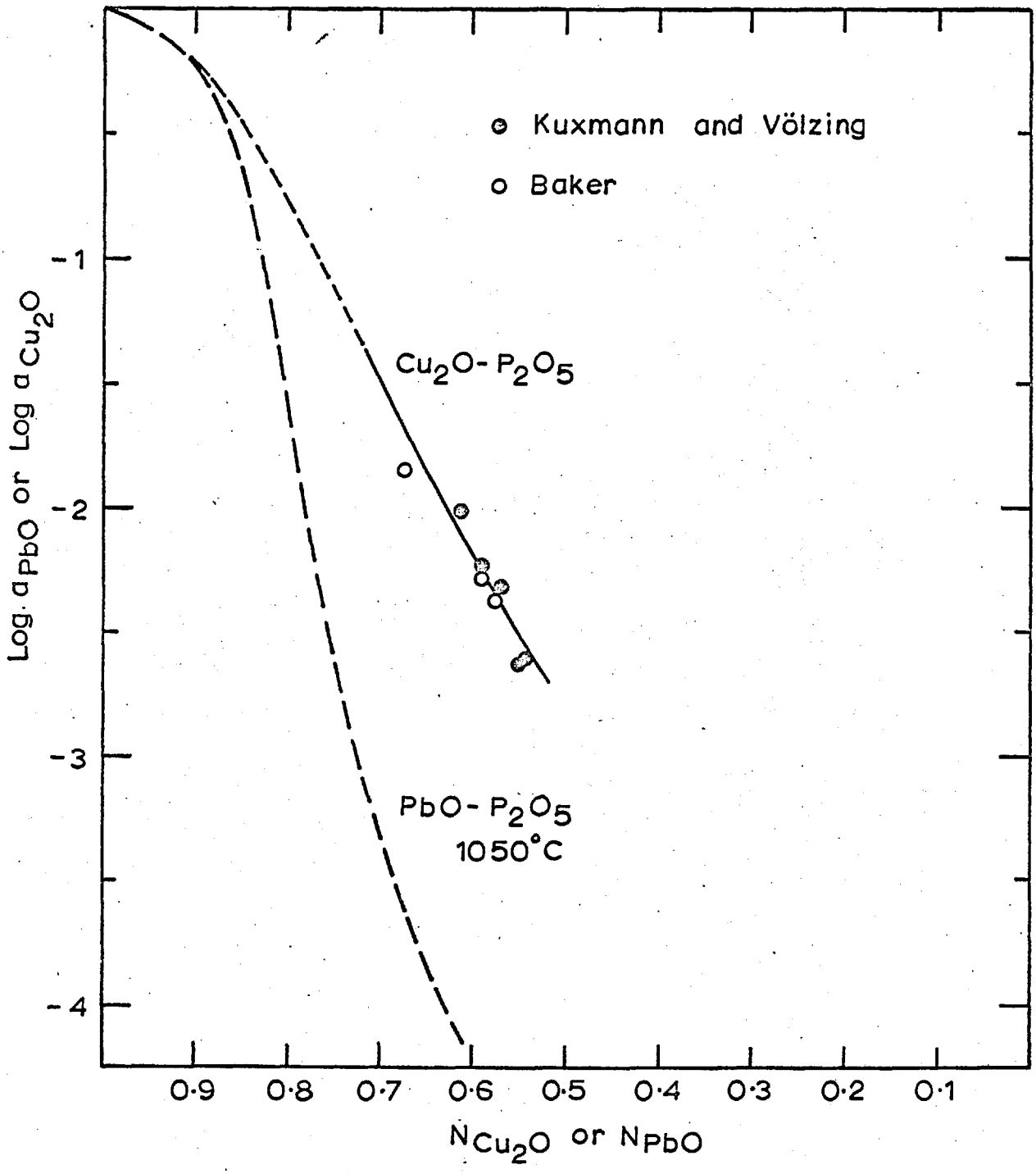

Fig.46 ACTIVITY OF Cu_2O IN LIQUID COPPER PHOSPHATE AT 1200°C

doubt. Ball[173] heated copper (II) phosphate samples under argon on a hot stage microscope and observed the evolution of oxygen on melting. Thereafter repeated raising and lowering of the temperature gave reproducible liquidus and solidus temperatures, which were interpreted as that of the $Cu_2O - P_2O_5$ system. The author failed to verify the final composition of his samples. It is likely that the measured liquidus and solidus temperatures pertain to a pseudo-binary section of the ternary $CuO - Cu_2O - P_2O_5$ system.

The heat of formation of Cu_3P from solid copper and red phosphorus at 298°K is - 31.6 ∓ 2 k cal/mole[11]. The entropy of formation of Cu_3P from solid copper and phosphorus vapour (P_2) can be estimated as - 22 e.u., by analogy with the average values for the entropy changes associated with the following reactions:

$$M_x O_y + 2\,(s) \rightarrow Mx\,Oy\,(s) + O_2\,(g) \qquad \Delta S^\circ = 43.5 \text{ e.u.}$$

$$M_x N_y + 2\,(s) \rightarrow Mx\,Ny\,(s) + N_2\,(g) \qquad \Delta S^\circ = 44.5 \text{ e.u.}$$

where y may be zero. It is therefore possible to estimate the standard free energy of formation of $Cu_3P(s)$ from liquid copper and phosphorus vapour at 987°K as - 36.44 k cal, using heat of fusion of copper and thermodynamic data on the sublimation of red phosphorus[69]. At 987°K (eutectic temperature in Cu + P system) copper containing 15.8 at. pct. P is in equilibrium with solid Cu_3P

$$G^\circ_{Cu_3P} = RT \ln \left[a^3_{Cu} \cdot (p_{P_2})^{\frac{1}{2}} \right]$$

The activity of copper may be obtained from phase diagram data (depression in melting point). The partial pressure of phosphorus over Cu + P solution of eutectic composition at 987°K is estimated to be 3×10^{-8} atmosphere. Loss of P due to vaporization from solution is therefore likely to be insignificant.

The partial pressure of P_2O_5 over Cu + O + P solutions used in this study can be estimated to be below 10^{-9} atmos. at 1200°C.

Loss of oxygen as P_2O_5 is therefore unlikely. According to St. Pierre et al[174] WO_2 is the stable oxide in equilibrium with W above 725°C, and from the standard free energy of formation of WO_2[174,175] it can be shown that at the oxygen potentials prevailing in Cu + O + P solutions in this study WO_2 could not form.

St. Pierre et al[176] have shown that the composition at which the oxygen concentration attains a minimum value in M-X-O systems in equilibrium with an oxide phase of the composition $M_a X_b O_c$ can be predicted through the relation:

$$\frac{N_x^{*}(1 - N_x^{*})}{1 - (1 - a/b)N_x^{*}} = -\frac{1}{\epsilon_x^x + \frac{c}{b}\epsilon_o^x}$$

where N_x^{*} is the mole fraction of the additive (which lowers the activity of oxygen) in solution at the composition corresponding to the minimum in oxygen concentration. Using this equation, ϵ_O^P obtained in this study, an estimated value of ϵ_P^P of 22 from Cu + P phase diagram, and the composition of slags from Baker,[170] Michael et al[171] and Kuxmann et al[172] a minimum in oxygen solubility may be expected at approximately 0.3 wt. pct. P at 1200°C. Although Kuxmann et al[172] restricted their measurements to phosphorus concentrations below 0.2 pct. P, their experimental points at higher phosphorus concentrations tend to indicate an approaching minimum in oxygen concentration. It would be interesting to extend these studies to higher P concentrations to verify the prediction.

Activity Coefficient of Oxygen in Pb-Sn alloys.

It is seen from figures 30 to 33 (pages 139 to 142) that Alcock and Richardson's quasichemical model with Z = 2 gives a good fit to experimental data. The data on binary Pb-Sn alloys is taken from the compilations of Hultgren et al[12], which are based on calorimetric data of Kleppa and e.m.f. measurements by Elliott and Chipman in the

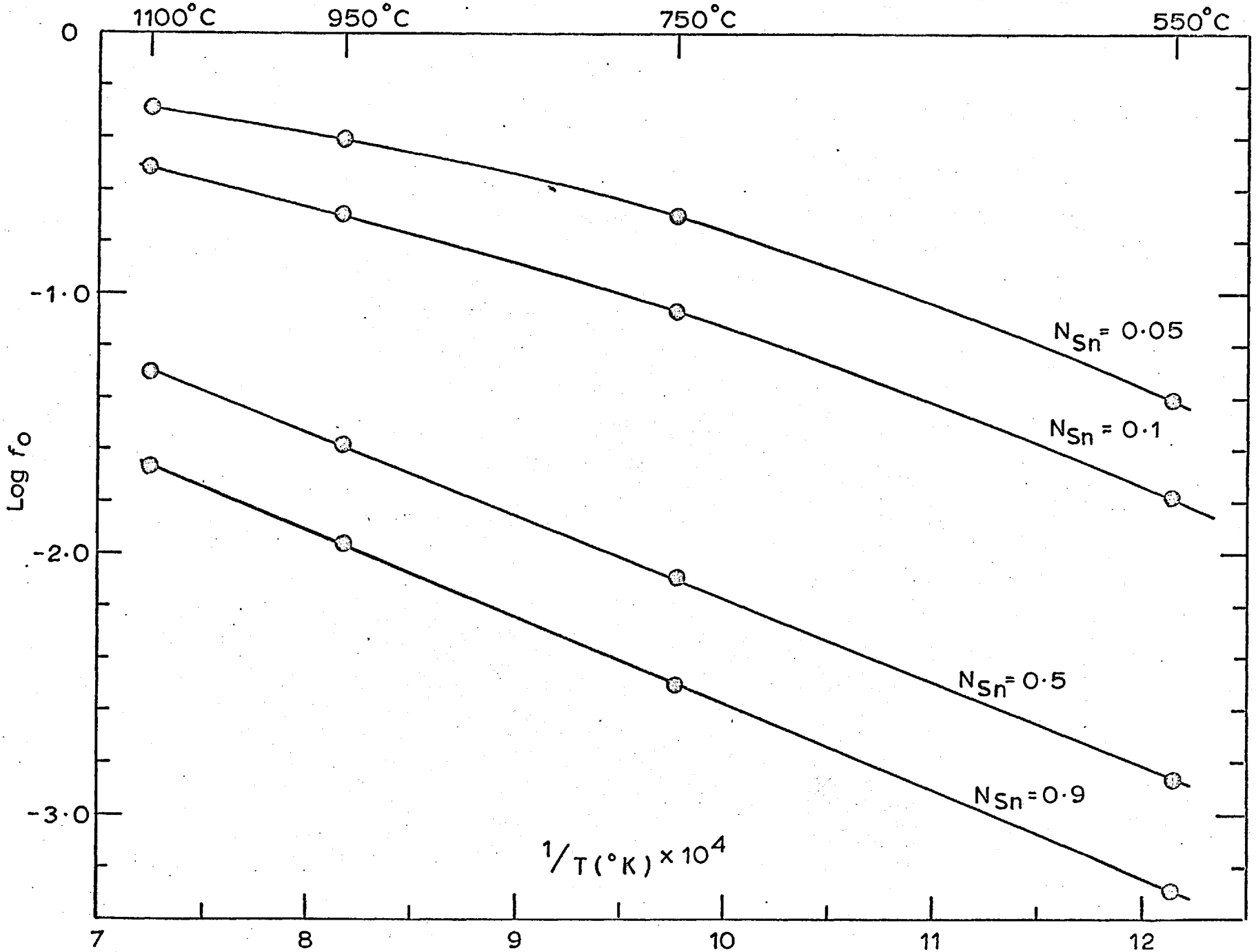

Fig.47 VARIATION OF ACTIVITY COEFFICIENT WITH TEMPERATURE FOR Pb-Sn ALLOYS ACCORDING TO ALCOCK & RICHARDSON'S QUASICHEMICAL MODEL WITH Z=2

ternary Pb-Sn-Cd system. More recently Hawkins and Hultgren[177] have reported measurements on the activity of Pb in Pb-Sn alloys by a torsion effusion method, these showing considerably larger positive deviations from Raoult's law. However, the relative partial molar free energies of lead reported by these authors show a scatter of ∓ 150 cals and slopes of $\Delta\overline{G}_{Pb}$ versus temperature plots do not correspond to the calorimetric data of Kleppa. No great reliance is therefore placed on the activities reported by Hawkins et al. Atarashya et al[178] determined the activity of tin from $H_2 - H_2O$ equilibrium measurements. Although their data show that the thermodynamics of Pb-Sn alloys can best be represented by a sub-regular model, their results are in fair agreement with the data used in this thesis to compute the activity coefficient of oxygen in terms of the quasichemical model.

It is seen from figs. 30 to 33 that the deviations of the activity coefficient from 'ideal' behaviour become less pronounced than that predicted by the quasichemical equation (with Z = 2) as the temperature is decreased and as the difference in the activity coefficient of oxygen in the pure metals is increased.

The logarithm of the activity coefficient of oxygen calculated from Alcock and Richardson's quasichemical model (Z = 2) at various temperatures is plotted against 1/T in fig. 47. The plots are non-linear, especially for lead rich compositions, indicating that the relative partial molar enthalpy ($\Delta\overline{H}_O$) of oxygen varies with temperature. The slope of the curve for $N_{Pb} = 0.1$ in fig. 47 between 950 and 1100°C gives a value of $\Delta\overline{H}_O = -8780$ cals, while the slope of the same curve between 550 and 750°C yields a value of $\Delta\overline{H}_O = -14{,}690$ cals. This variation may be expected since the ratio of Sn-O bonds to Pb-O bonds is obtained through equation 6 (page 8). This ratio would be a function of temperature and therefore the relative partial molar

enthalpy and entropy of oxygen would be temperature dependent. The variation of these properties with temperature is most significant in lead rich solution, where the exchange energy w/z which occurs when a Sn-O bond is changed to a Pb-O bond has the largest value. Although experimental results (fig. 36, page 145) do not show non-linear variation of log f_O with 1/T, the small range of temperatures covered in this study for Pb rich solutions do not permit definite conclusions to be drawn regarding the variation of $\Delta\bar{H}_O$ with temperature.

The $\Delta\bar{H}_O$ is calculated from Alcock and Richardson's model (Z = 2) using the equation

$$\Delta\bar{H}_{O(Pb+Sn)} = N^0_{Pb}\left[\Delta\bar{H}_{O(Pb)} - \Delta\bar{H}_{Pb(Pb+Sn)}\right] + N^0_{Sn}\left[\Delta\bar{H}_{O(Sn)} - \Delta\bar{H}_{Sn(Pb+Sn)}\right]$$

where N^0_{Pb} and N^0_{Sn} are the mole fractions of Pb and Sn in the co-ordination shell around oxygen, and are obtained from equation 6. The calculated values at a mean temperature of 950°C are shown below:

N_{Sn}	0.1	0.2	0.3	0.4	0.5	0.6	0.7	0.8
$\Delta\bar{H}_O$, kcal	9.78	12.20	13.30	13.91	14.31	14.59	14.80	15.00

This is in fair agreement with those obtained in this study. The values of $\Delta\bar{H}_O$ and $\Delta\bar{S}_O$ at 1 at. pct. O obtained in this study (Figs. 37, 38 - Page 146, 147) for Pb-Sn alloys are of the same sign. Thus only a fraction of $\Delta\bar{H}_O$ is available as $\Delta\bar{G}_O$. This is in qualitative agreement with the quasichemical equation. The rapid decrease of $\Delta\bar{S}_O$ at 1 at. pct. oxygen in lead on adding tin may be interpreted as due to the vibrational and configurational effects of clustering of tin atoms around oxygen atoms.

Activity Coefficient of Oxygen in Ag + Pb alloys.

Richardson and Webb[62] have suggested that earlier work on the

vapour pressure of PbO is in error. On the basis of the weight loss of Pb and PbO from their iridium assembly, they suggest a vapour pressure of 5 mm at 1100°C and 1.5 mm at 1000°C.

The activity of PbO in Ag rich solutions in experiment 53 may be calculated from the observed e.m.f.s (table 46), the standard free energy of formation of PbO, and the activity of Pb in Pb + Ag alloys. The maximum value for the a_{PbO} in solution is 0.102 at $N_{Pb} = 0.04$. The pressure of PbO over the solution is therefore 0.15 mm. At higher Pb concentrations the a_{PbO} is lower due to the lower activity coefficient of oxygen. It may therefore be concluded that the addition of Pb could not result in the formation of a PbO phase. The constant e.m.f.s obtained after successive Pb additions indicate that the loss of oxygen as PbO (g) from the melt is insignificant. Besides, the results of the experiments starting with Ag + O solution would not agree with those obtained from experiments starting with Pb + O solution if there had been loss of oxygen from the solution on adding Pb to Ag + O solution.

The logarithm of the activity coefficient of oxygen obtained from these experiments is compared with that predicted by Alcock and Richardson's quasichemical equation with Z = 2 in fig. 39 (page 151). As in the Cu + Sn + O system, the observed deviation from ideal behaviour is less pronounced than that predicted by the quasichemical equation.

Thermodynamics of binary Ag-Pb alloys.

The activity of lead obtained from the e.m.f. of cell 13 and the activity of silver obtained from the Gibbs-Duhem relationship are compared with previous work in figure 40 (page 156). The activities are in reasonable agreement with the phase diagram calculations of Hultgren et al[12] for alloy compositions $N_{Pb} < 0.4$. Data of these authors at higher lead concentrations are based on earlier galvanic

cell measurements using fused salt electrolyte. From the free energies of formation of $PbCl_2$ and AgCl it is seen that these studies are not reliable at low lead concentrations due to displacement reaction between the alloys and the chloride electrolyte.

The vapour pressure measurements of Aldred and Pratt[179] give activities of lead which are much too small compared with the results of this study and the data recommended by Hultgren et al[12]. Vapour pressure measurements generally have an uncertainty of ∓ 100 cals in the relative partial molar free energy and are less reliable than e.m.f. methods.

The activities obtained in this study are in very good agreement with the results of Hager et al[180] who used a galvanic cell incorporating silica saturated lead silicate electrolyte.

Mo, Pb (l) / PbO - SiO_2 (l); SiO_2(s) / Pb - Ag (l), Mo

The small discrepancy between the activities obtained in this study and those of Hager et al is within the uncertainty of their activity measurements.

Results of reliable calorimetric measurements of integral heat of mixing of Ag-Pb alloys are shown in Fig. 48 and these suggest that the heat of mixing increases with temperature. Although small positive deviations from the Neumann-Kopp rule may exist in this system, it is unlikely to cause the large difference shown in fig. 48. It is more likely that the results of Castanet et al [181] are higher by approximately 100 cals due to some unidentified experimental errors in lead rich alloys.

The best values for the heat of mixing are chosen using certain characteristic features in the thermodynamic properties of alloys. If Darken's[40,41] quadratic formalism discussed in chapter 1 is valid, the tangent drawn to the plot of $\Delta H^M/N_{Pb}$ versus N_{Pb} at $N_{Pb} = 1$ must intercept the ordinate at $N_{Pb} = 0$ giving $\Delta\bar{H}^\circ_{Ag}$. Similarly

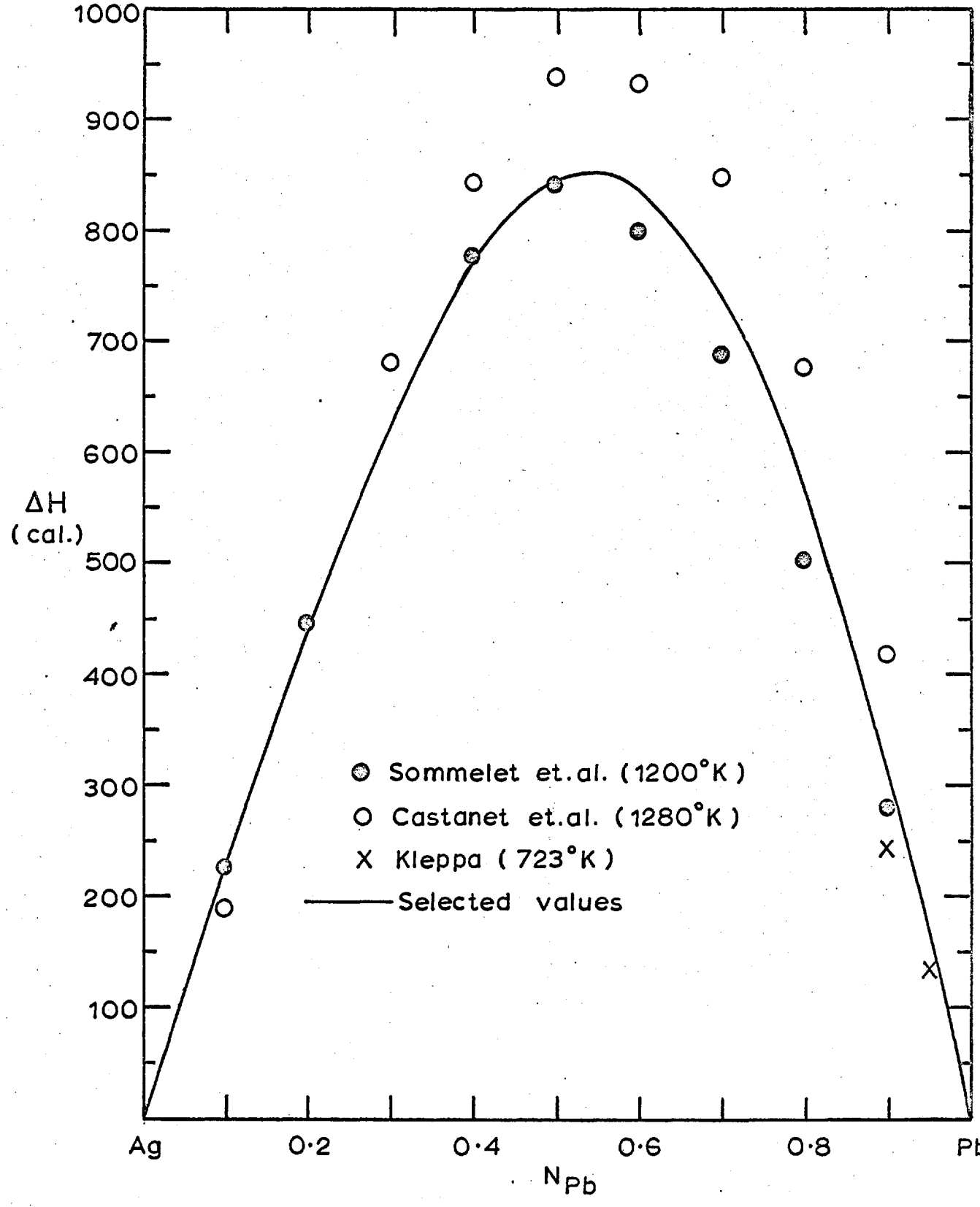

Fig.48 INTEGRAL HEATS OF FORMATION OF SILVER-LEAD ALLOYS

the tangent to the plot of $\Delta H^M/N_{Ag}$ versus N_{Ag} at $N_{Ag} = 1$ must intercept the ordinate at $N_{Ag} = 0$ giving $\Delta\bar{H}^{o}_{Pb}$. These interrelations are used to crosscheck the independent data available and to select the best values shown in fig. 48. Greater emphasis has been placed on the measurements of Kleppa[183] and Sommelet[182], which are in fair agreement. Besides the partial heat of Ag at infinite dilution in lead has been measured by Jena and Bever[184] at 673°K as 2.6 kcals, in good agreement with Kleppa.

The relative partial molar enthalpy of Pb corresponding to the selected integral heats of mixing may be expressed by the following equations:

$$\beta_{Pb} = 2300 + 4562\, N_{Pb} \qquad (0.4 > N_{Pb} > 0) \quad \ldots\ldots \quad 48$$

$$\beta_{Pb} = 3425 + 1167\, N_{Ag} \qquad (1.0 > N_{Pb} > 0.4) \quad \ldots\ldots \quad 49$$

where $\beta_{Pb} = \dfrac{\Delta\bar{H}_{Pb}}{(1-N_{Pb})^2}$

$$\Delta\bar{H}_{Ag} = -N_{Ag} N_{Pb} \beta_{Pb} + \int_0^{N_{Pb}} \beta_{Pb}\, dN_{Pb}$$

and $$\Delta H^M = (1-N_{Pb}) \int_0^{N_{Pb}} \beta_{Pb}\, dN_{Pb}$$

The relative partial molar enthalpies of lead calculated from equations 48 and 49 are compared with those obtained from the temperature coefficients of e.m.f. in this study.

N_{Pb}	0.5	0.6	0.7	0.8	0.9
$\Delta\bar{H}_{Pb}$ (measured)	958	636	335	146	41
$\Delta\bar{H}_{Pb}$ (evaluated from calorimetric data)	1003	622	337	146	35

Although the excellent agreement is fortuitous, it reflects favourably

on the performance of the cell.

The variation of α'_{PbO} and β_{PbO} with N_{Pb} shows a discontinuity at $N_{Pb} = 0.4$, which corresponds to the point of inflection on the liquidus curve for this system. The integral excess properties for the liquid Ag - Pb alloys obtained from the activity measurements in this study and the selected calorimetric data are shown below:

N_{Pb}	$\Delta G^{M,Ex}$ 1000°K	ΔH^{M}	$\Delta S^{M,Ex}$
0.1	130	228	0.089
0.2	248	435	0.170
0.3	345	615	0.245
0.4	417	775	0.325
0.5	453	845	0.356
0.6	446	830	0.349
0.7	397	740	0.312
0.8	306	562	0.233
0.9	173	314	0.128

These values represent the best available data on liquid Ag-Pb alloys. The observed positive excess free energies and heats of formation are not surprising in a system with such a large component size disparity and are generally attributable to a misfit energy. The mixing of atoms of different size may also be expected to reduce the mean vibrational frequency and so give rise to positive excess specific heats and excess entropies. The ratio of the maximum heat of mixing to the maximum excess entropy has a value of 2361°K in good agreement with the empirical correlation of Kubaschewski[35] discussed in chapter 1.

Deviations from perfectly random distribution of atoms can only lead to negative excess entropies. Positive excess entropies must be

due to vibrational contributions. If it is assumed that the distribution of atoms is perfectly random in Ag-Pb alloys and the excess entropies are solely due to vibrational effects, then ΔCp will be defined by the relation

$$\int_0^T Cp\ (\text{alloy}) - N_{Pb}\ Cp\ (Pb) - N_{Ag}\ Cp\ (Ag)\ \frac{dT}{T} = \Delta S^{Ex,Vib.}$$

Although ΔCp will be a function of temperature and cannot be evaluated from the above relation, it is unlikely to have a value greater than 0.12 at $N_{Pb} = 0.9$. Using this high estimate for ΔCp, increase in the heat of mixing may be calculated to be approximately 65 cals when the temperature is raised from 723°K to 1280°K. The selected heat of mixing at 1000°K at $N_{Pb} = 0.9$ is approximately 50 cals above the value reported by Kleppa (fig. 48), which is in agreement with the small positive deviations from the Newmann-Kopp suggested by positive excess entropies.

Effect of Temperature on the Interaction Parameter.

When a third element is added to the dilute solution of oxygen in a metal, the chemical potential of oxygen is increased by an amount

$$\Delta\bar{G}_0^{Extra,x} = \Delta\bar{G}_{0(Ternary)} - \Delta\bar{G}_{0(Binary)} = RT\ \epsilon_0^x\ Nx$$

where $\Delta\bar{G}_0^{Extra,x}$ is the extra partial molar free energy of oxygen occasioned by the addition of component X. It is convenient to define corresponding enthalpy and entropy terms:

$$\Delta\bar{H}_0^{Extra,x} = \eta_0^x\ Nx$$
$$\Delta\bar{S}_0^{Extra,x} = \tau_0^x\ Nx$$

where η_0^x may be designated as the enthalpy interaction parameter, and τ_0^x as the entropy interaction parameter. These parameters are strictly constant only in very dilute solutions. However, ϵ_0^x has been found to be a constant for many systems at finite concentrations, at least within the limits of present-day experimental accuracy.

The parameters are related as follows:

$$RT\,\epsilon_0^x = \eta_0^x - T\,\tau_0^x$$

$$\frac{d\,\epsilon_0^x}{d(1/T)} = \eta_0^x / R.$$

The enthalpy interaction parameter is plotted against the free energy interaction parameter for Cu-O-x systems at 1200°C fig. 49. The data of O-P interactions is obtained from the results of this study (Equation 41). Data on O-Ni and O-Co interactions are deduced from the results of Young[29] and Abraham[112], who measured the free energy parameter at 1500 and 1200°C. A straight line passing through zero point in fig. 49 may be used to represent the data. This relationship between ϵ_0^x and η_0^x is not surprising since chemical interactions which lead to the lowering of the activity also promote a larger negative value for the heat of solution. Provided ϵ_0^x is known at one temperature, η_0^x and therefore the value of ϵ_0^x at any other temperature may be estimated once such correlations are established. However, it must be noted that the slope of the line in fig. 49 is a function of temperature. Chipman and Corrigan[87] have shown that such correlations exist for the following groups of systems: Fe-N-X (l), Fe-N-X (s), Fe-H-X (l), Cu-S-X (l), and Al-H-X (l).

To obtain more fundamental insight into the nature of oxygen additive interactions in liquid metals, the entropy parameter is plotted against the enthalpy parameter in fig. 50, for all ternary systems containing oxygen as a solute for which data is available. As the entropy and enthalpy parameters are obtained from measurements of the free energy parameter over a range of temperatures, the accuracy of the results shown in figure may be poor. However, it is interesting to note the correlation between the two parameters when both have negative values. It seems that the additives which

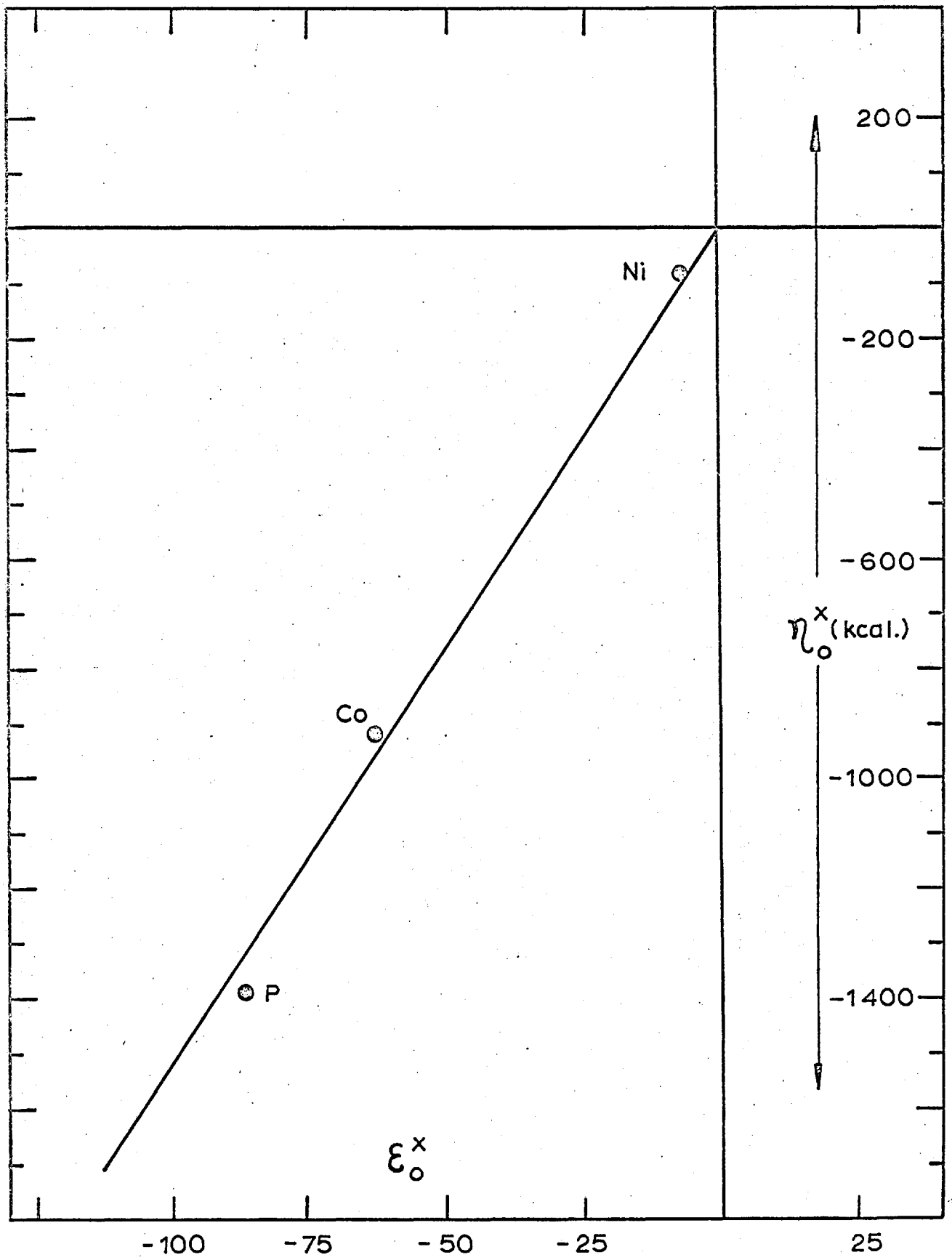

Fig.49 COMPARISON OF ENTHALPY & FREE ENERGY INTERACTION PARAMETERS: OXYGEN IN LIQUID COPPER ALLOYS AT 1200°C.

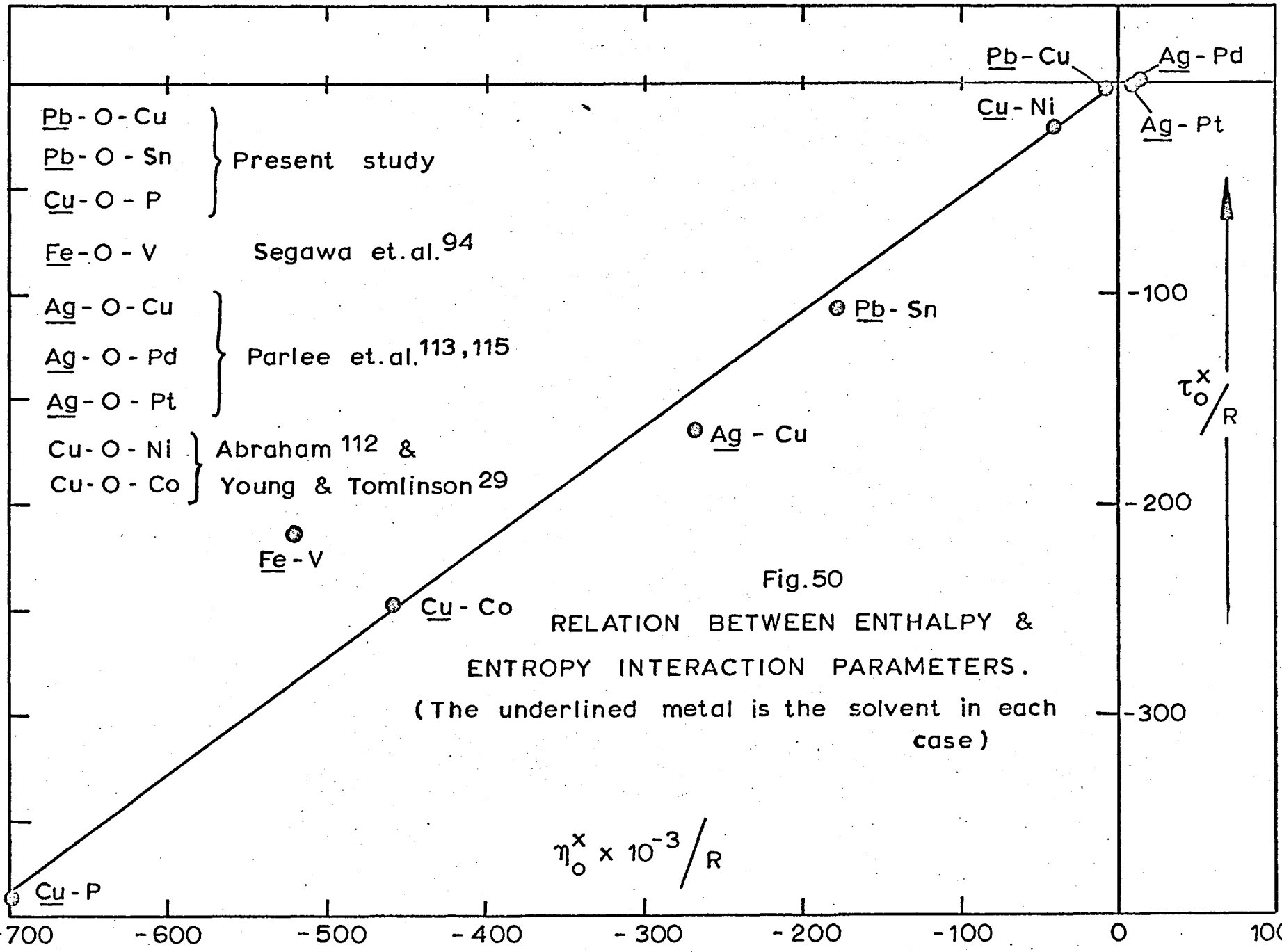

Fig.50

RELATION BETWEEN ENTHALPY & ENTROPY INTERACTION PARAMETERS.

(The underlined metal is the solvent in each case)

lower the activity coefficients also decrease the relative partial molar entropy of oxygen in solution. This suggests that models similar to those proposed by Belton and Tankins which show an increase in the partial entropy of oxygen on alloying are not in accord with the observed behaviour. The activity coefficient of oxygen in Cu-Co alloys was measured by Belton et al[4] over a range of temperature and the partial molar entropy of oxygen in pure metals was shown to increase on adding the third element, in support of their model. The data of Young[29] and Abraham [112] do not support this finding. The temperature coefficient of the activity obtained by Belton et al[4] is probably inaccurate because of some undetected interfering experimental phenomenon which varies in importance with temperature. The relative partial molar enthalpy and entropy of oxygen in liquid copper obtained by these authors is in marked disagreement with that obtained by other workers[28,29,70,72].

The enthalpy and entropy interaction parameters in fig. 50 have the same sign and suggest that at about 1000°K, the extra entropy is approximately half the extra enthalpy. Thus only about half the extra partial molar enthalpy is available as extra free energy.

Applicability of Solution Models.

Alcock and Richardson's regular model[2] and the quasichemical equation[3] with Z = 2 do not in general fit experimental data when the activity coefficients of oxygen (or sulphur) in the two pure metals do not differ by a factor greater than 10. The variation of the logarithm of the activity coefficient with composition in Cu + Pb alloys at 1100°C (Fig. 24, page 114) is a typical illustration of this discrepancy. A similar behaviour of oxygen has been observed in Cu-Ni and Cu-Co alloys[4,29] at 1500°C.

Belton and Tankins' random approximation gives a reasonable fit to data in systems mentioned above. The main drawback of the model lies

in the inclusion of the entropy of mixing of 'oxide species'. Experimental data available at the present time does not support such a hypothesis.

If it is assumed that oxygen in liquid metals and alloys forms 'species' of the type A-O-A, B-O-B and A-O-B and that the ratio of the number of A-O to B-O bonds is equal to the ratio of the mole fractions of A and B (random approximation) then the relative partial molar enthalpy of oxygen in a binary alloy is given by:

$$\Delta\bar{H}_{O(A+B)} = N_A \Delta\bar{H}_{O(A)} - 2\Delta\bar{H}_{A(A+B)} + N_B \Delta\bar{H}_{O(B)} - 2\Delta\bar{H}_{B(A+B)} \quad \ldots\ldots \quad 50$$

The metal atoms attached to the oxygen atom are assumed not to make any other bonds in solution. The equation implies that the heat of solution of oxide 'species' from the vapour phase is independent of the composition of the alloy.

The ideal partial molar entropy of oxygen in solution is $(-R \ln N_O)$. When a solute is present in dilute solution it will be randomly distributed in the solvent medium, and any observed excess entropy of the solute may be attributed to thermal causes. The difference in $\Delta\bar{S}_O$ in pure A and B can therefore be attributed to the difference in the strength of A-O and B-O bonds and the consequent difference in vibrational frequency of oxygen. If the vibrational entropy contribution is allowed to vary linearly with composition, the partial molar entropy of oxygen in the alloy is given by:

$$\Delta\bar{S}_{O(A+B)} = -R \ln N_O + N_A (\Delta\bar{S}_{O(A)} + R \ln N_O) + N_B (\Delta\bar{S}_{O(B)} + R \ln N_O)$$

$$= N_A \Delta\bar{S}_{O(A)} + N_B \Delta\bar{S}_{O(B)} \quad \ldots\ldots \quad 51$$

Unlike Belton and Tankins' model, the entropy of mixing of oxide species is not included in the above equation, since the difference in strength between A-O and B-O bonds is likely to be less than 'kT'. Combining equations 50 and 51

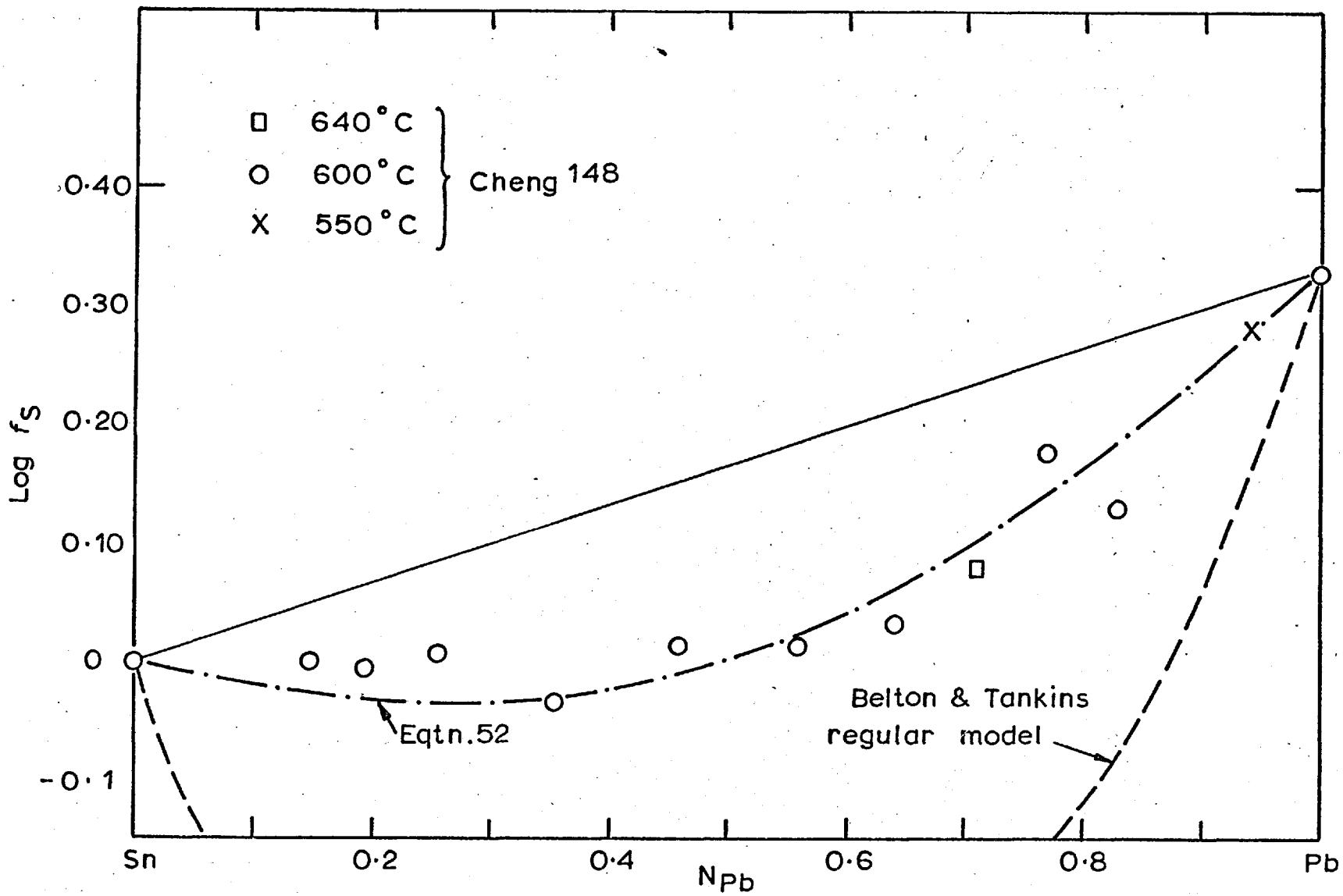

Fig.51 VARIATION OF ACTIVITY COEFFICIENT OF SULPHUR IN Sn-Pb ALLOYS.

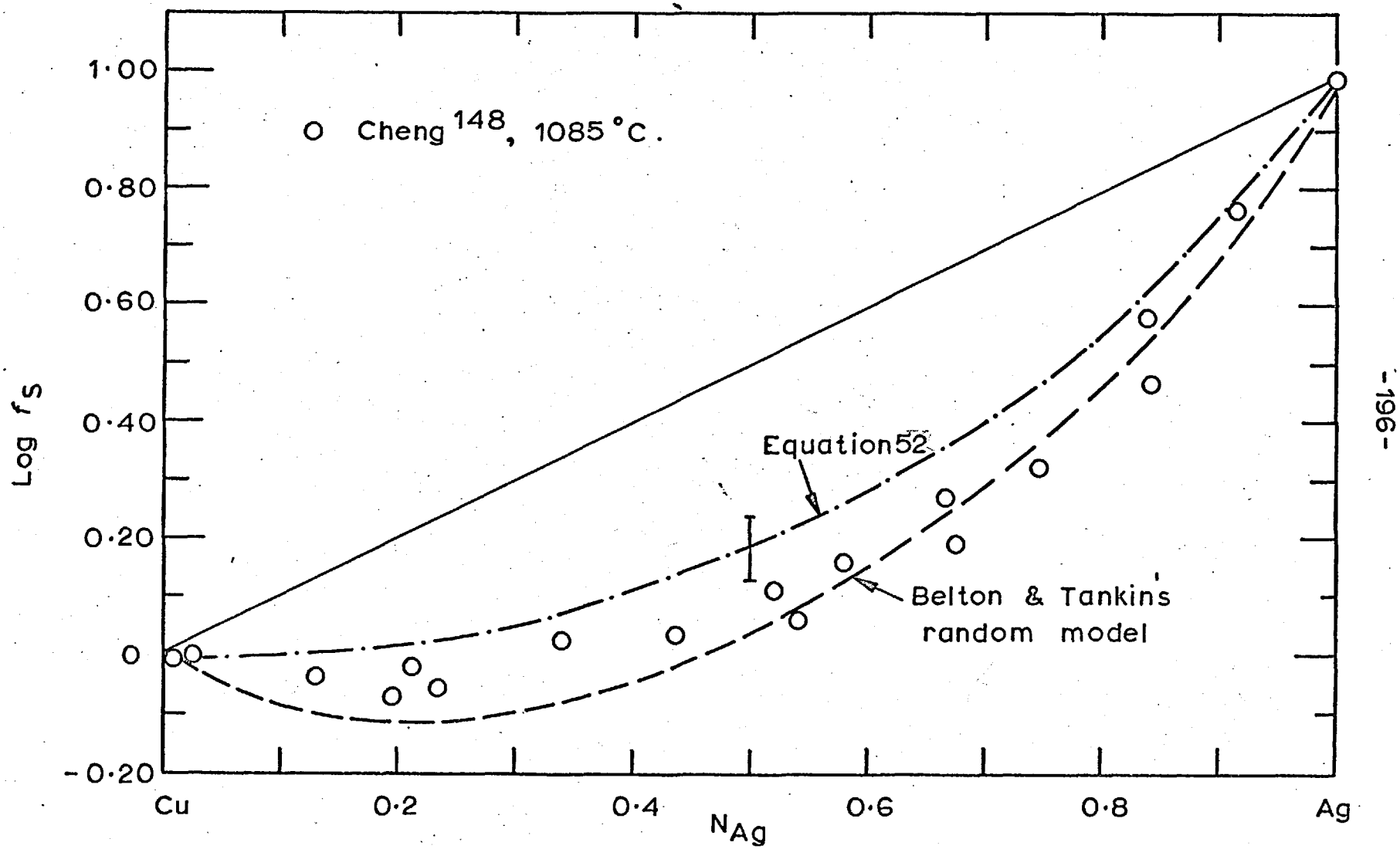

Fig. 52 ACTIVITY COEFFICIENT OF SULPHUR IN Cu-Ag ALLOYS

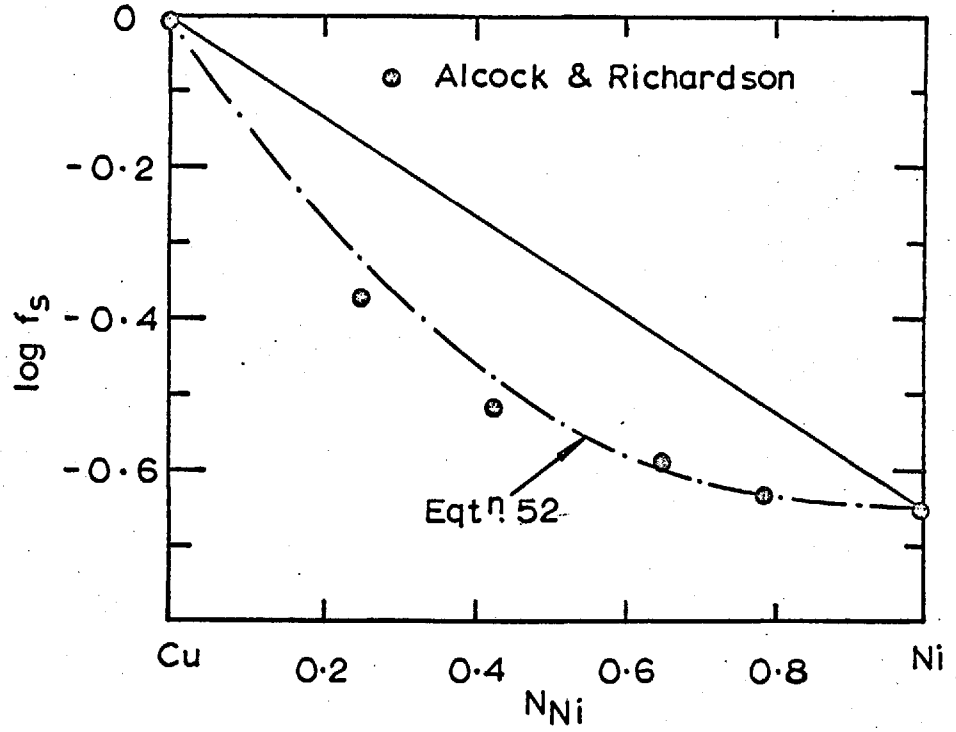

Fig.53a ACTIVITY COEFFICIENT OF SULPHUR IN Cu-Ni ALLOYS AT 1500°C

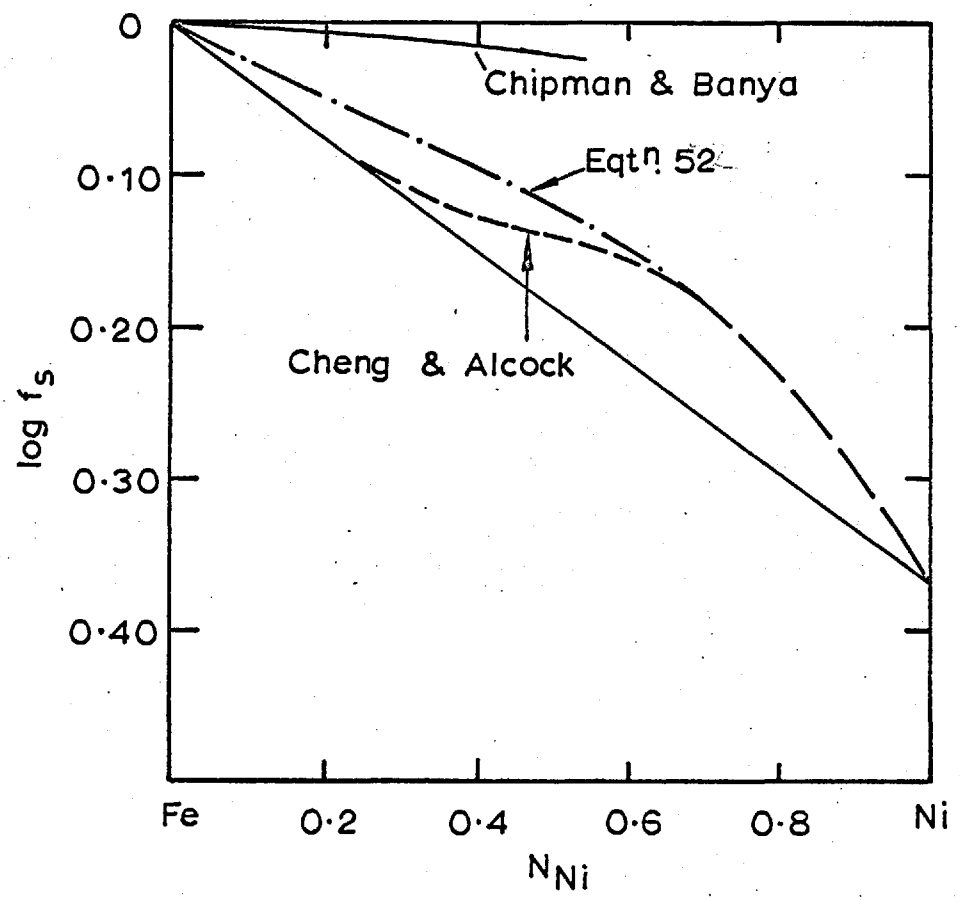

Fig.53b ACTIVITY COEFFICIENT OF SULPHUR IN Fe-Ni ALLOYS AT 1500°C

$$\Delta \bar{G}_{O(A+B)} = N_A \Delta \bar{G}_{O(A)} + N_B \Delta \bar{G}_{O(B)} - 2 \Delta H^M_{(A+B)} \quad \ldots\ldots \quad 52$$

This equation is plotted for the Cu + Pb + O system in figure 24 (page 114) and is found to give a good fit to experimental data. The activity coefficients predicted by this equation are compared with available experimental data on the activity coefficients of oxygen and sulphur in binary metallic solutions in figures 51 to 53. In these systems the difference between the activity coefficient of the solute in the two pure metals is less than 10, and random approximation may be used with some justification. It is seen that the activity coefficient of sulphur in Pb + Sn[148], Cu + Ag[148], Cu-Ni[2], and Fe-Ni[2] systems are adequately represented by equation 52, especially when the uncertainties in the binary data used in the model are considered. In Pb + Sn system the measured activity coefficients are in good agreement with equation 52, but disagree with those predicted by Belton and Tankins' random approximation. Due to discrepancies in the literature on the activity of sulphur in Fe-Ni, Fe-Co and Fe-Cu alloys[148,52] it is not possible to test equation 52 in these systems. The activity coefficients of oxygen in Cu-Ni and Cu-Co alloys[29] are compared with those obtained from the equation in figure 54. The data of Young on oxygen in pure nickel has been adjusted to agree with that of Bowers[54].

The binary data on Cu + Ni alloys is obtained from a recent review by Kubaschewski et al[186]. The only data on liquid Cu + Co alloys is the partial heat of solution of Co in liquid Cu, determined by Dokken et al[187].

$$\Delta \bar{H}_{Co} = \left[8 - 5N_{Co}\right] N_{Cu}^2 \quad \mp \ 3 \text{ k cals /G. atom.}$$

If it is assumed that this relationship is valid over the whole composition range, than

$$\Delta H^M_{(Cu + Co)} = N_{Cu} N_{Co} \left[8 - 2.5 N_{Co}\right]$$

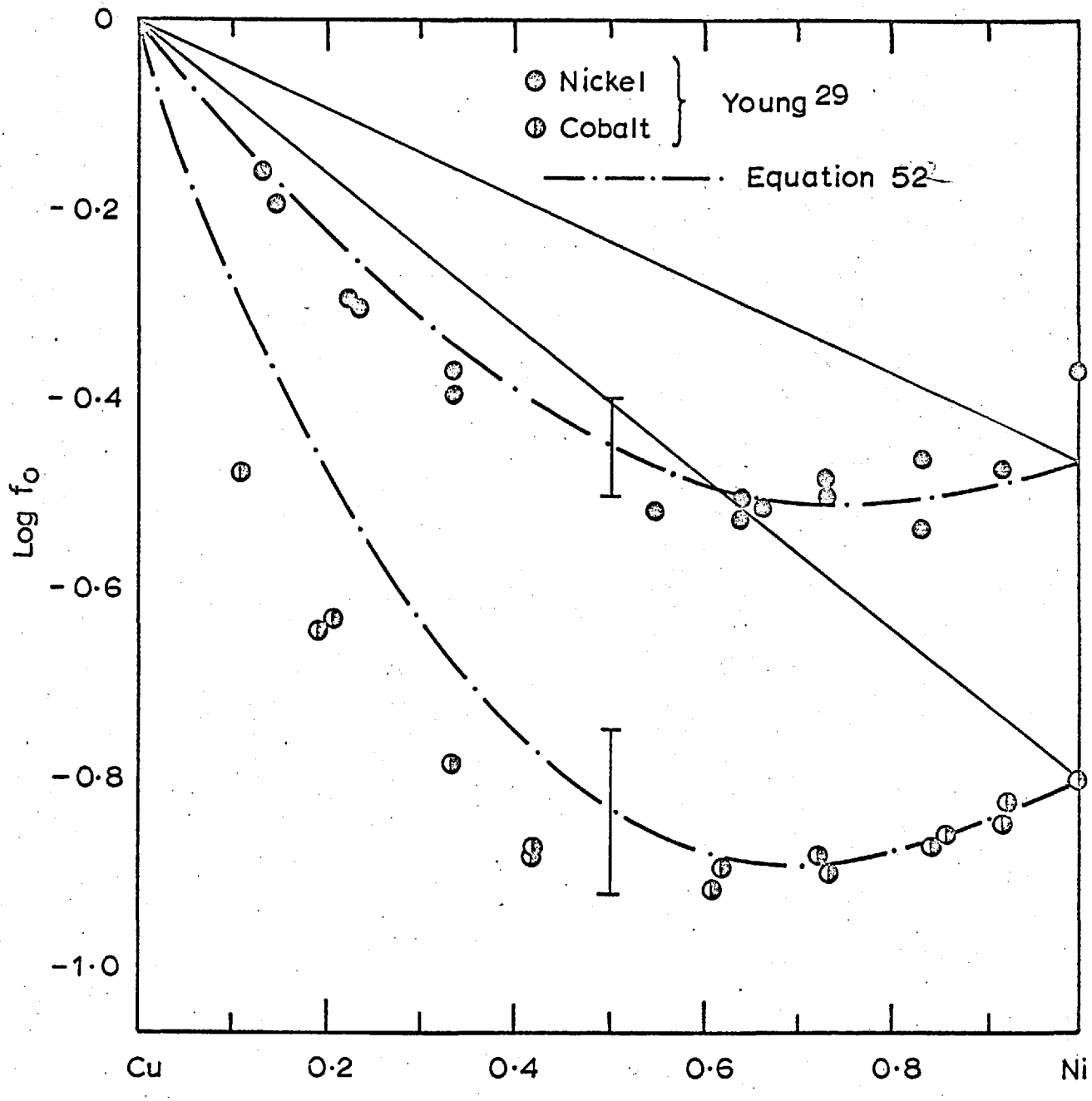

Fig. 54 ACTIVITY COEFFICIENT OF OXYGEN IN Cu-Co & Cu-Ni ALLOYS

The heats of mixing obtained from this equation are used in the model to predict the activity coefficient of oxygen in Cu-Co alloys. Due to large uncertainty in binary data close agreement with experimental values is not to be expected. Binary data on Pb + Sn, Cu + Ag and Fe-Ni alloys are taken from the compilation of Hultgren et al[12].

The close agreement between the measured values and those predicted by equation 52, despite the variation of e/a ratio with composition in some systems, shows that the equation can be used to forecast the behaviour of oxygen and sulphur with useful accuracy for those systems in which the activity coefficients of oxygen in the pure metals differ by a factor less than 10.

When this difference is larger than 10, quasichemical equations are likely to be more useful. It is seen from figures 32 and 43 (pages 141 and 169) that Alcock and Richardson's quasichemical equation with Z = 2, gives a reasonable fit to experimental data. However this equation failed to forecast satisfactorily the behaviour of oxygen in Cu + Sn and Ag + Pb alloys (figs. 20 and 39) where the difference between the activity coefficients of oxygen in the pure metals is larger than in Cu + Ag and Pb + Sn systems. Besides, the e/a ratio is expected to vary with composition in liquid alloys formed between the elements of groups IB and IV B of the periodic table. Data of Block et al on oxygen in Ag + Sn alloys at 1200°C (figure 55) shows a trend similar to that in Cu + Sn and Ag + Pb alloys.

Alcock and Richardson's quasichemical model with Z = 2 is a seemingly unreasonable one with the co-ordination number of all the atoms equal to two. If it is assumed that oxygen atoms have a co-ordination number of two and the metal atoms have a co-ordination number of eight, it can be shown (appendix 2) that

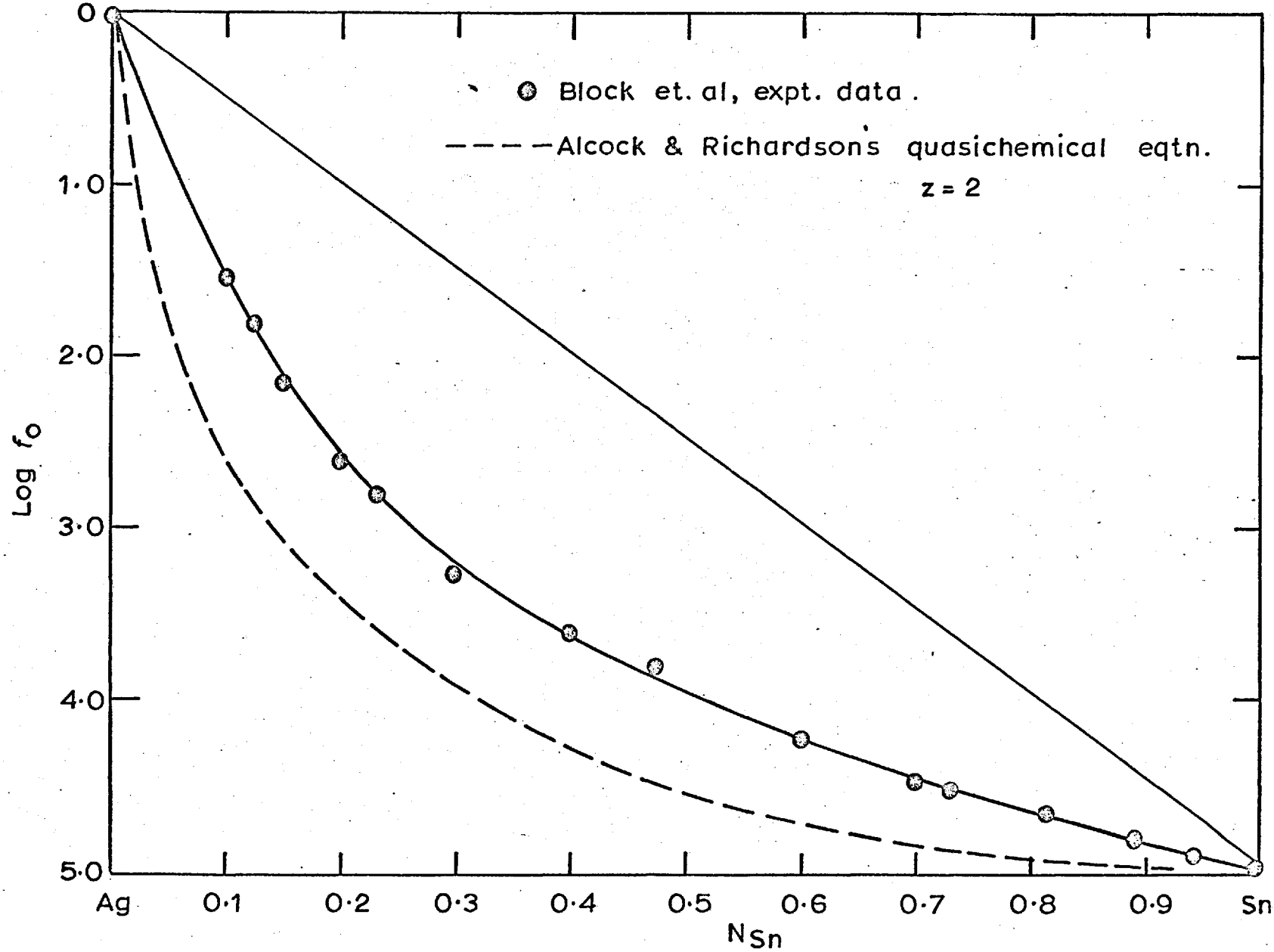

Fig.55 ACTIVITY COEFFICIENT OF OXYGEN IN Ag - Sn ALLOYS AT 1200°C

$$\Delta\overline{G}_{O(A+B)} = N_B^o \left[\Delta\overline{G}_{O(B)} - \tfrac{1}{4}\,\Delta\overline{G}^{Ex}_{B(A+B)} \right] + N_A^o \left[\Delta\overline{G}_{O(A)} - \tfrac{1}{4}\,\Delta\overline{G}^{Ex}_{A(A+B)} \right] + 2RT \left[N_A^o \ln \frac{N_A^o}{N_A} + N_B^o \ln \frac{N_B^o}{N_B} \right]$$

This modified quasichemical equation is plotted in figure 43 (page 169) It is seen that this equation predicts values very close to those obtained from Alcock and Richardson's equation with Z = 2. This is because the equations are not very sensitive to the way the binary data on A-B alloys is incorporated into the model. Provided the co-ordination number of oxygen is kept the same, the predicted activity coefficients of oxygen are approximately the same. It would however be interesting to try to formulate a quasichemical model based on the formation of 'species' of the type A-O-A, B-O-B, and A-O-B in solution, but until this can be done, Alcock and Richardson's quasichemical equation with Z = 2 may be used to make predictions in an empirical manner.

Technological Applications.

The data obtained in this study can be used in calculations on deoxidation equilibria. For example, the deoxidation equilibria for tin in copper was calculated in a previous section (page 172). A useful way of summarising the available data is in terms of free energy - temperature diagrams. For example, in figure 56 the chemical potential of oxygen in Cu + O solutions is plotted as a function of temperature (dashed lines) for various oxygen concentrations. Also shown in the figure are lines corresponding to the standard free energy of formation of pure oxides from oxygen at 1 at. pressure and metal dissolved in copper at 1 at. pct. concentration. The diagram can therefore provide a basis for preliminary estimates of the temperatures at which oxides can form and the extent to which alloying elements

can scavenge oxygen from solution. To enable quantitative predictions to be made, further information on activities of oxide components in slags and the effect of alloying elements on oxygen activity in liquid copper must be available. The results of this study and others of a similar nature[29,112] have provided information on oxygen - additive interactions, which are summarised in figure 57. However, little information is available on the activity of oxides in slags of importance to copper smelting.

The source of data used for the standard free energy of solution of elements in liquid copper (1 at. pct.) are the following: S - ref. 2; Pb - ref 169; Si - ref. 99; Zn and Fe - ref. 12; Sn - ref. 162; Ni, Co and Ag - ref. 12 and 187; Al - ref. 188; Mn - ref. 189.

Conclusions.

Accurate thermodynamic data have been obtained on the activity of oxygen in Cu-Ag, Cu-Sn, Cu-Pb alloys at 1100°C, Pb-Ag alloys at 1000°C and Pb-Sn alloys from 550 to 1100°C, over the whole range of compositions. These together with existing data on oxygen in Cu-Ni and Cu-Co alloys at 1500°C and on sulphur in a number of binary alloys, enable a critical evaluation of the solution models that have been proposed to predict the activity coefficient of oxygen in binary alloys.

It may be concluded that when the ratio of the activity coefficients of the solute in the two pure metals is less than 10, equation 52 and Belton and Tankins' random approximation give a reasonable fit to experimental data. However, Belton and Tankins' random approximation is shown to predict excess entropies of the wrong sign.

When the ratio of the activity coefficient of the solute in the two pure metals is greater than 10, none of the proposed quasichemical equations are in reasonable agreement with measured data in all the systems, although Alcock and Richardson's equation with Z = 2 has

Fig. 56 FREE ENERGY TEMPERATURE DIAGRAM FOR OXYGEN IN LIQUID COPPER & FOR EQUILIBRIA INVOLVING VARIOUS OXIDES. THE STANDARD STATE FOR METAL IS 1 at.%. SOLN. IN COPPER

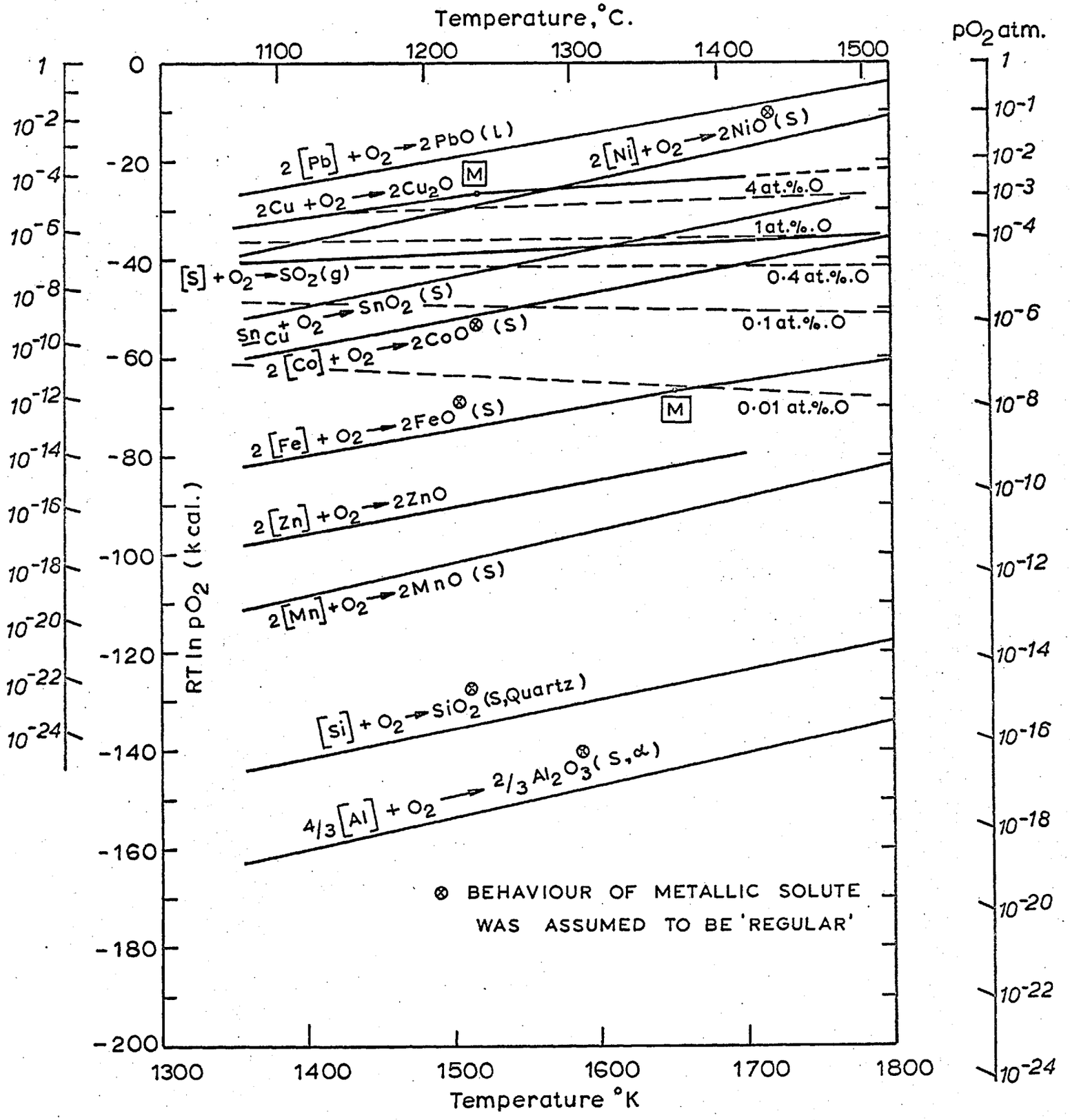

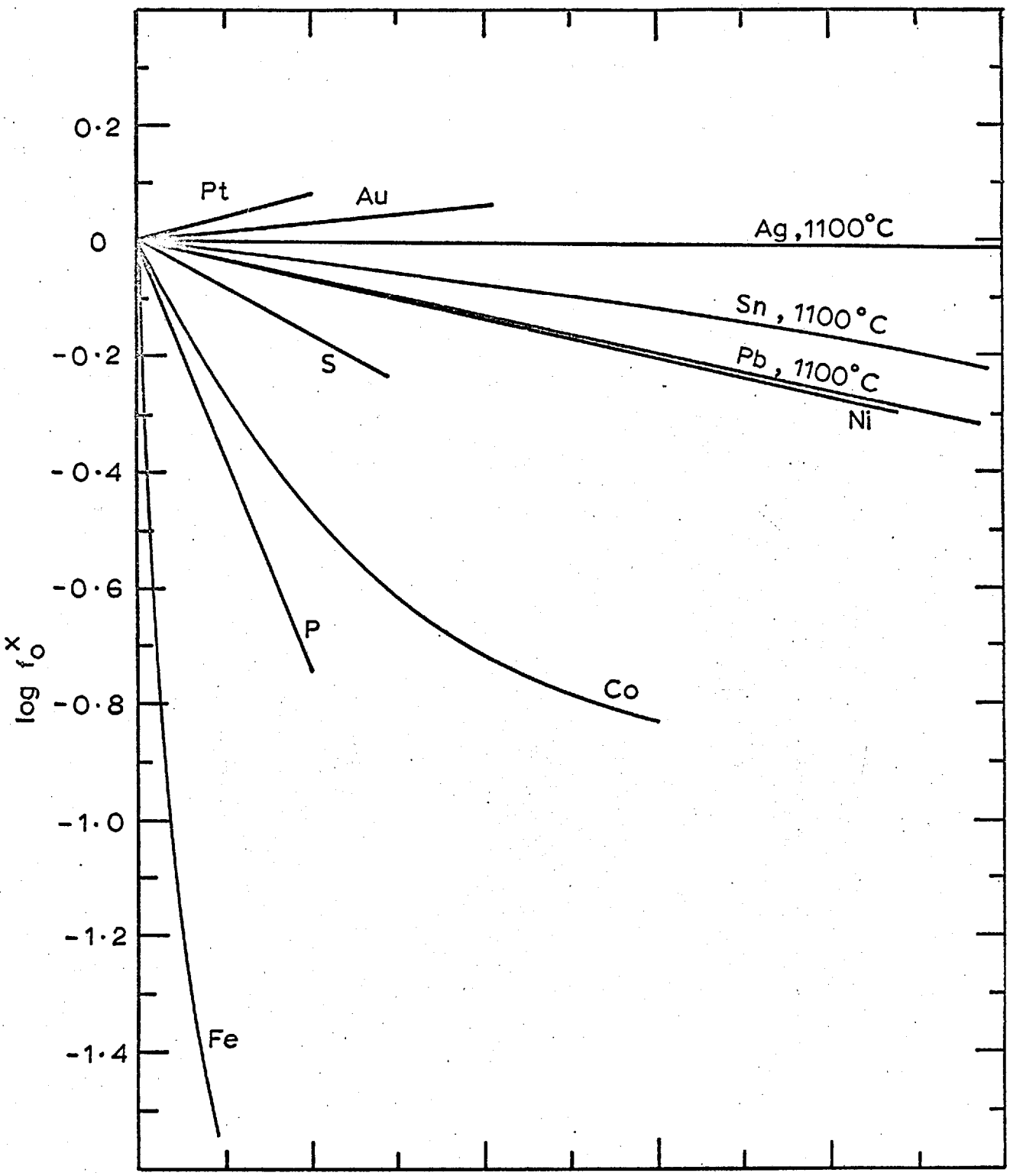

Fig.57 EFFECT OF ADDITIVES ON THE ACTIVITY COEFFICIENT OF OXYGEN IN LIQUID COPPER AT 1200°C.
(Ag, Pb, Sn, P, this study. Pt, Au, Ni. Ref.29-)
(Ni, Co, Fe. Ref.112. S Ref.70.)

been found to forecast accurately the behaviour of oxygen in Pb + Sn and Cu + Ag solutions.

Empirical correlations have been found between the enthalpy and entropy interaction parameters, obtained from the temperature coefficient of free energy parameters. However, enthalpies obtained from the temperature coefficient of free energies are generally inaccurate. Calorimetric studies on the enthalpies associated with oxygen-additive interactions are therefore suggested. The results of such studies can then be combined with the free energy data obtained in this study to obtain more accurate data on entropy parameters.

Acknowledgment

The author wishes to express sincere gratitude to Dr. J.H.E. Jeffes for supervision, suggestions and encouragement received throughout the course of this work. He is also greatly indebted to Prof. F.D. Richardson for helpful discussions and financial support.

Sincere appreciation is extended to the staff and members of the Nuffield Research Group. Thanks are due especially to Dr. J. Carbo-Nover for help in the analysis of oxygen in lead and Mr. R.L. Harvey for reading the manuscript of this thesis and for help in the analysis of oxygen in copper.

REFERENCES.

1) F.D. Richardson, Iron and Coal Trades Review, 1961, Vol.183, p. 1105-1115.

2) C.B. Alcock and F.D. Richardson, Acta Met., 1958, Vol.6, p.385-95.

3) C.B. Alcock and F.D. Richardson, Acta. Met., 1960, vol. 8, p.882-87.

4) G.R. Belton and E.S. Tankins, Trans TMS-AIME, 1965, vol. 233, p. 1892-98.

5) H. Wada and T. Saito, Trans. Jap. Inst. Metals., 1961, vol 2, p.15-20.

6) N.A. Gokcen, Scripta Met., 1969, vol. 3, p.157-64.

7) A. Behr, Light Metals and Metals Industry, 1965, vol. 28, p.58.

8) R.J. Fruehan, L.J. Martonik and E.T. Turkdogan, Trans. TMS-AIME, 1969, vol. 245, p. 1501-1509.

9) J.K. Pargeter, Journal of Metals, 1968, vol. 20, p. 27-31.

10) K.H. Ulrich and K. Borowski, Archiv Eisenhuttenwesen, 1968, vol. 39 p. 259.

11) O. Kubaschewski and J.A. Catterall, Thermodynamic Data of Alloys, Pergamon Press, 1956.

12) R. Hultgren, R.L. Orr, P.D. Anderson and K.K. Kelley, Selected Values of Thermodynamic Properties of Metals and Alloys, John Wiley & Sons, 1963.

13) R.A. Oriani, The Physical Chemistry of Metallic Solutions and Intermetallic Compounds, vol. 1, paper 2A, H.M.S.O. London, 1959.

14) C.B. Alcock and R.A. Oriani, Trans TMS-AIME, 1962, vol. 224, p.1104-15.

15) P. Bolsaitis and L. Skolnik, Trans TMS-AIME, 1968, vol. 242, p.215-25.

16) W. Hume-Rothery, G.W. Mabbott, K.M. Channel-Evans, Phil. Trans. Roy. Soc., 1934, p.233.

17) H. Schenck and M.G. Frohberg, Steelmaking: The Chipman Conference, The M.I.T. Press, 1962.

18) W. Himmler, Z. Phys. Chem. 1950, vol. 195, p.245.

19) O.J. Kleppa, Liquid Metals and Solidification, Am. Soc. Metals, Ohio, 1958, p. 56-86.

20) H.K. Hardy, Acta Met., 1953, vol. 1, p. 202.

21) N.J. Olson and G.W. Toop, Trans TMS-AIME, 1966, vol. 236, p.590-92.

22) G.W. Toop, Trans TMS-AIME, 1965, vol. 233, p. 850-55.

23) L.S. Darken, J. Am. Chem. Soc., 1950, vol. 72, p. 2909.

24) C. Wagner, Zeits. Physik. Chem., 1928, vol. 132, p. 273.

25) C.B. Alcock, Application of Fund. Themody. to Met. Processes, Gorden & Breach, Ed. G.R. Fitlerer, 1967.

26) E.A. Guggenheim, Mixtures, Univ. Press, Oxford, 1952.

27) C.H.P. Lupis and J.F. Elliott, Acta Met., 1966, vol. 14, p.1019.

28) R.J. Fruehan and F.D. Richardson, Trans TMS-AIME, 1969, vol. 245, p. 1721-26.

29) D.R. Young, The thermodynamic study of oxygen in molten copper alloys, Ph.D. Thesis, University of London, 1965.

30) L.L. Cheng, Thermodynamic Studies on sulphur dissolved in liquid alloys, Ph.D. Thesis, University of London, 1959.

31) J.C. Mathieu, F. Durand and E. Bonnier, Jour. de Chimic Physique, 1965, vol. 62, p. 1289-96.

32) P. Hicter, J.C. Mathieu, F. Durand and E. Bonnier, Advances in Physics, 1967, vol. 16, p. 523-33.

33) C.H.P. Lupis and J.F. Elliott, Acta Met., 1967, vol. 15, p.265.

34) J.N. Pratt, Rev. Int. Hautes Temper. et Refract., 1967, vol. 4, p. 97-108.

35) O. Kubaschewski, Thermodynamics, vol. 2, I.A.E.A., Vienna, 1966.

36) P.T. Gallagher and W.A. Oates, Trans TMS-AIME, 1969, vol. 245, p. 179-82.

37) J. Chipman and D.A. Corrigan, Applic. Fund. Thermodyn. Met. Processes, Ed. G.R. Fittcrer, Gordon & Breach, 1967, p. 23-37.

38) F.D. Richardson, J. Iron. Steel Inst., 1950, vol. 166, p. 137.

39) J. Pearson and E.T. Turkdogan, J. Iron. Steel Inst., 1954, vol.176 p. 19.

40) L.S. Darken, Trans TMS-AIME, 1967, vol. 239, p.80-90.

41) E.T. Turkdogan and L.S. Darken, Trans. TMS-AIME, 1968, vol.242, p. 1997-2005.

42) M. Margules, Sitzber. Akad. Wiss. Wien, 1895, vol. 104, p.1243-78.

43) L.S. Darken, Trans TMS-AIME, 1967, vol. 239, p.90-96.

44) C. Wagner, Thermodynamics of Alloys, Addison Wesley Press, Cambridge, 1952.

45) J. Chipman, J. Iron. Steel. Inst. 1955, vol. 180, p. 93.

46) C.W. Sherman and J. Chipman, Trans. TMS-AIME, 1952, vol. 194, p.597.

46a) M.N. Dastur and J. Chipman, Trans TMS-AIME, 1949, vol. 185, p.441: Journal of Metals, August, 1949.

47) T.P. Floridis and J. Chipman, Trans TMS-AIME, 1958, vol. 212, p. 549-53.

48) V.V. Averin, A.Y. Polyakov, A.M. Samarin, Izv. Akad. Nauk. SSSR, Otdelenie Tekn. Nauk No.3, 1955, p.90: No. 8, 1957, p. 120.

49) N.A. Gokcen: Trans TMS-AIME, 1956, vol. 206, p. 1558.

50) E.S. Tankins, N.A. Gokcen, G.R. Belton, Trans TMS-AIME, vol. 230, p. 820-27.

51) W.A. Fisher and W. Ackermann, Archiv. Eisenhuttenwesen, 1966, vol. 37, p. 43-47.

52) W.A. Fisher and D. Janke, Archiv. Eisenhuttenwesen, 1968, vol. 39, p. 89-99.

53) H. Schenck and K.H. Gerdom, Archiv. Eisenhuttenwes., 1959, vol. 30, p. 451-60.

54) J.E. Bowers, J. Inst. Met., 1961-62, vol. 90, p. 321-28.

55) A. Sieverts and J. Hagenacker, Z. Physik. Chem., 1909, vol. 68, p. 115.

56) F.G. Donnan and T.W.A. Shaw, J. Soc. Chem. Ind., 1910, vol. 29, p.987.

57) N.A.D. Parlee and E.M. Sacris, Trans. TMS-AIME, 1965, vol. 233, p. 1918.

58) C. Diaz, C.R. Mason and F.D. Richardson, Trans. Instn. Min. Metallurgy (Section C), 1966, vol. 75, p.C 183-5.

59) E.H. Baker and M.I. Talukdar, Trans Instn. Min. Metallurgy (Section C), 1968, vol. 77, p. C 128-33.

60) U. Block and H.P. Stuwe, Z. Metallkde, 1969, vol. 60, p. 706.

61) W.A. Fisher and W. Ackermann, Archiv. Eisenhuttenwes., 1966, vol. 37, p. 697-700.

62) F.D. Richardson and L.E. Webb, Trans. Instn. Min. Metallurgy, 1955, vol. 64, p. 529-64.

63) U. Kuxmann and K. Kurre, Erzmetall, 1968, p. 199-209.

64) C.B. Alcock and T.N. Belford, Trans. Faraday Soc., 1964, vol. 60, p. 822-35.

65) B.C.H. Steele, Electromotive force measurements in high-temperature systems, I.M.M., London, 1968, p.3-27.

66) C.B. Alcock and T.N. Belford, Trans Faraday Soc., 1965, vol. 61, p. 442-453.

67) J. Carbo Nover, Tin in Silicate slags, Ph.D. Thesis, University of London, 1968.

68) C.M. Diaz and F.D. Richardson, Tran. Instn. Min. Met., Section C, 1967, vol. 76, p C 196- C 203.

69) Janaf Thermochemical Tables, The Dow Chemical Co., Midland, Mich.

70) K. Sano and H. Sakao, Mem. Fac. Engg., Nagoya Univ., 1956, vol. 8, p. 137.

71) H. Rickert and H. Wagner, Electrochimica Acta, 1966, vol. 11, p.83-91.

72) J. Osterwald, G. Reimann, W. Stichel, Z. Physikal. Chem. (Frankfurt), 1969, vol. 66, p. 1-7.

73) W. Pluschkell and H.J. Engell, Z. Metallk., 1965, vol. 56, p.450-2.

74) T.C. Wilder, Trans. TMS-AIME, 1966, vol. 236, p. 1035-40.

75) Z. Kozuka, K. Suzuki, T. Oishi and J. Moriyama, Nippon Kinzoku Gakkai - Si, 1968, vol. 32, p. 1132-1137.

76) R. Vogel and W. Pocher, Z. Metallk., 1929, vol. 21, p. 333-37 and p. 368-71.

77) J.C. d'Entremont, D.L. Guernsey and J. Chipman, Trans TMS-AIME, 1963, vol. 227, p. 14-17.

78) E.S. Tankins, Metallurgical Transactions, 1970, vol. 1, p.538.

79) S. Marshall and J. Chipman, Trans ASM, 1942, vol. 30, p. 695.

80) E.T. Turkdogan, L.S. Davis, L.E. Leak, C.G. Stevens, J.I.S.I, 1955, vol. 181, p. 123.

81) T. Fuwa and J. Chipman, Trans TMS-AIME, 1960, vol. 218, p.887.

82) G.H.T. Bennett, H.T. Protheroe and R.G. Ward, J.I.S.I., 1960, vol. 195, p. 174-79.

83) W.A. Fisher and W. Ackermann, Archiv. Eisenhutt., 1965, vol. 36, p. 965-69.

84) H. Schenck and H. Hinze, Archiv. Eisenhutt., 1966, vol. 37, p.545-50.

85) H. Schenck, E. Steinmetz and M. Gloz, Archiv. Eisenhutt., 1968, vol. 39, p. 69-71.

86) M. Elle and J. Chipman, Trans TMS-AIME, 1961, vol. 221, p. 701.

87) K. Sano and K. Sakao, J. Jap. Inst. Metals, 1959, vol. 23, p. 671.

88) S. Matoba and T. Kuwana, Testu-to-Hagane (Overseas), 1965, vol. 5.

89) W.A. Fisher and M. Haussmann, Archiv. Eisenhutt., 1966, vol. 37, p. 959-61.

90) H.M. Chen and J. Chipman, Trans. A.S.M. 1947, vol. 38, p. 70.

91) E.T. Turkdogan, J.I.S.I. 1954, vol. 178, p. 278.

92) K. Goto, S. Banya and S. Matoba, Testu-to-Hagane (overseas), 1963, vol. 3, p. 184-88.

93) B.V. Linchirskii and A.A. Samarin, Izv. Ak. Nauk. Otdelenine Tekn., 1957, 2.9.

94) K. Segawa, E. Tsunetomi, Y. Nakamura and H. China, Testu to Hagane, 1965, vol. 51, p. 1866-69.

95) H. Schenck and E. Steinmatz, Archiv. Eisenhutt., 1967, vol. 38, p. 871-73.

96) J.K. Pargeter, Canad. Met. Quart., 1967, vol. 6, p. 21 to 31.

97) E.S. Tankins, M.K. Thomas, J.F. Erthal andF.S. Williams, Trans A.S.M. 1965, vol. 58, p. 245-51.

98) R. Pehlke and J.F. Elliott, Trans TMS-AIME, 1960, vol. 218, p. 1096.

99) O. Kubaschewsk, E. Ll. Evans, and C.B. Alcock, 'Metallurgical Thermochemistry', Pergamon Press, 1967.

100) M. Ohtani and N.A. Gokcen, Trans TMS-AIME, 1960, vol. 218, p.533.

101) H. Wada, K. Gunji and T. Wada, Trans. I.S.I. (Japan), 1968, vol. 8, p. 323.

102) H.A. Wriedt and J. Chipman, Trans TMS-AIME, 1956, vol. 206, p.1195.

103) J. Chipman, Trans. TMS-AIME, 1960, vol. 218, p. 767.

104) J. Chipman and T.C.M. Pillay, Trans. TMS-AIME, 1961, vol. 221, p. 1277.

105) J. Pearson and E.T. Turkdogan, J.I.S.I., 1952, vol. 176, p.19.

106) N.P. Levenets and A.M. Samarin, Doklady Akademii Nauk SSSR, 1955, vol. 101, p. 1089.

107) D. Dutilloy and J. Chipman, Trans TMS-AIME, 1960, vol. 218, p.428.

108) K. Sambongi and H. Koizumi, Testu-to-Hagane, 1961, vol. 47, p.1329.

109) S. Banya and S. Matoba, Testu-to-Hagane, 1963, vol. 3, p. 309.

110) N.A. Gokcen and J. Chipman, Trans TMS-AIME, 1952, vol, 194, p. 171; and 1953, vol. 197, p. 1017.

111) W.A. Fisher, Archiv. Eisenhutt., 1967, vol. 38, p. 422-28.

112) K.P. Abraham, Trans. Indian Inst. Metals, 1969, vol. 22, p. 5-7.

113) I.D. Shah and N.A.D. Parlee, Trans. TMS- AIME, 1968, vol. 242, p. 869-75.

114) C.H.P. Lupis and J.F. Elliott, Trans. TMS-AIME, 1968, vol. 242, p. 929-35,

115) N.A.D. Parlee and E.M. Sacris, Trans TMS-AIME, 1967, vol. 239, p. 2005-9.

116) T.C. Wilder and W.E. Galin, Trans TMS-AIME, 1969, vol. 245, p.1287.

117) C.G. Charette and S.N. Flengas, Canad. Met. Quart., 1969, vol. 7, No. 4, p. 191-200.

118) K. Kiukkola andC. Wagner, J. Electrochem. Soc. 1957, vo. 164, p. 379.

119) F. Hund, Z. Phy. Chem., 1952, vol. 199, p. 142.

120) A. Hoffman and W. Fisher, Z. Phy. Chem. (N.F.) 1958, vol. 17, p.30.

121) A. Diness and R. Roy, Solid State Communications, 1965, vol. 3, p.123.

122) J.W. Patterson, 'Conduction Domains in Solid Mixed Conductors', Special Report, Engg. Research Institure, Iowa State University, Iowa, 1969.

123) C.B. Alcock, Electromotive force measurements in high-temperature systems, I.M.M. London, 1968, p. 109-124.

124) R.E. Carter and W.L. Roth, General Electric Rep. No. 63-RL-3479M, 1963, p. 27.

125) L.A. Simpson and R.E. Carter, J. Am. Ceram. Soc., 1966, vol. 49, p. 139.

126) W.A. Rhodes and R.E. Carter, J. Am. Ceram. Soc., 1966, vol. 49, p.244.

127) J.Weissbart and R. Ruka, J. Electrochem. Soc. 1962, vol. 109, p. 723-26.

128) R. Baker and J.M. West, J.I.S.I. 1966, vol. 204, p. 212-16.

129) K. Schwerdtfeger, Trans. TMS-AIME, 1967, vol. 239, p. 1276-81.

130) H.Schmalzried, Z. Elektrochem, 1962, vol. 66, p. 572.

131) J.D. Tretyakov, Neorg Materials (USSR), 1966, vol. 2, p. 501.

132) B.C.H. Steele, Thermodynamic Studies using cells with solid electrolytes; Ph.D. Thesis, University of London, 1965.

133) A.W. Smith, F.W. Mesyars, and C.D. Amata, J. Am. Ceramic Soc., 1966. vol. 49, p. 240.

134) C. Wagner, Z. Physik. Chemic, (B), 1933, vol. 21, p. 25.

135) J.W. Patterson, E.C. Bogren and R.A. Rapp, J. Electrochem. Soc., 1967, vol. 114, p. 752-58.

136) L. Heyne and N.M. Beekerman, Paper presented at the British Ceramic Society Symposium on 'Mass Transport in Non-metallic Solids', 18th Dec., 1969.

137) R.E. Slade and F.D. Farrow, Proc. Royal Socy., (London), 1912, vol. A87, p. 524-534.

138) J.Osterwald, Z. Metallkde, 1968, vol. 59, p. 573-76.
J. Gerlack, J. Osterwald and W. Stichel, Z. Metallkde, 1968, vol. 59, p. 576-79.

139) G.A. Smith, Trans. Inst. Min. and Met., 1963, p. 469-496.

140) G.W. Toop and F.D. Richardson, Advances in Extractive Metallurgy, Pub. by Inst. Min. and Met., 1968, p. 181-205.

141) W.A. Baker, Metallurgia, 1949, vol. 40, p. 188-89.

142) A.I. Vogel, Quantitative Inorganic Analysis, Longmans, 1962, p.635.

143) M. Hansen and K. Anderko, Constitution of Binary Alloys, 1958, and First Supplement 1965, McGraw-Hill Co.

144) E.M. Levin, H.F. McMurdie and F.P. Hall, 'Phase Diagrams for Ceramists', Am. Ceramic Soc., 1964.

145) J.C. Platteeuw, and G. Meyer, Trans. Faraday Soc., 1956, vol. 52, p. 1066-73.

146) B.K. Veselowskii, J. Appl. Chem. USSR, 1943, vol. 16, p. 397-416.

147) R. Colin, J. Drowart and G. Verhaegen, Trans. Farad. Soc., 1965, vol. 61, p. 1364-71.

148) L.L.Cheng, Ph.D. Thesis, University of London, 1959.

149) B.C.H. Steele and C.B. Alcock, Trans. TMS-AIME, 1965, vol. 233, p. 1359.

150) F.E. Rizzo, L.R. Bidwell and D.F. Frank, Trans TMS-AIME, 1967, vol. 239, p. 593.

151) S.N. Flengas and G.G. Charette, J. Electrochem. Soc., 1968, vol.115, p. 796-804.

152) R.A. Rapp and F. Maak, Acta Met., 1962, vol. 10, p. 63.

153) C.M. Sellars and F. Maak, Trans TMS-AIME, 1966, vol. 236, p. 457-63.

154) J. Gerlach, J. Osterwald and W. Stichel, Z. Metallkde, 1968, vol. 59, p. 576-79.

155) A.D. Mah, et al, USBM RI 7026, Sept., 1967.

156) K.K. Kelly, Contributions to the data on theoretical metallurgy XIII. Bulletin No. 584, 1960, U.S. Bur. Mines.

157) D.D. Wagman, et al, N.B. Tech. Note 207-3, Jan. 1968.

158) A.E.M. Warner, Nuffield Research Group, Private Communication.

159) E.N. Rodigina, K.Z. Gomel'ski and V.F. Luginina, Zhur. Fiz. Khim., 1961, Vol. 35, p. 1799.

160. R. Sridhar and J.H.E. Jeffes, Trans. Inst. Min. Met., 1967, vol. 76, p. C 44 - C 50.

161) S.K. Seshadri and F.D. Richardson, Nuffield Research Group, Private Communication.

162) C.B. Alcock, R. Sridhar and R.C.Svedberg, Acta. Met., 1969, vol. 17, p. 839.

163) M.B. Bever and C.F. Floe, Trans TMS-AIME, 1944, vol. 156, p. 149.

164) K. Honda and E. Endo, J. Inst. Metals, 1927, vol. 37, p. 29.

165) F. Sauerwald and K. Boremann, Z. Metallkde, 1922, vol. 14, p. 254.

166) A. Roll and H. Motz, Z Metallkde, 1957, vol. 48, p. 435.

167) E.M. Gebhardt and K. Kostlin, Z. Metallkde, 1956, vol. 47, p.684,

168) K.I. Eretnov and A.P. Lynbimov, Ukrain, Fiz. Zhur., 1967, vol. 12, p. 214.

169) E. Schurmann and A. Kaune, Z. Metallkde, 1965, vol. 56, p. 453-61.

170) W.A. Baker, Am. Soc. Metals, Proceedings of the First World Metallurgical Conference, Cleveland, Ohio, 1952, p. 268-293.

171) A.D. Michael, R.W.Ruddle and A. Cibula, J. Inst. Met., 1956/57, vol. 85, p. 506-517.

172) U. Kuxmann and P. Volzing, Erzmetall, 1969, vol. 6, p. 261-271.

173) M.C. Ball, J. Chem. Soc. (A), 1968, p. 1113-1115.

174) G.R. St. Pierre and W.T. Ebihara, Trans TSM-AIME, 1962, vol. 244, p. 259.

175) F.E. Rizzo, L.R. Bidwell and D.F. Frank, Trans TSM-AIME, 1967, vol. 239, p. 1901.

176) G.R. St. Pierre and R.D. Blackburn, Trans. TSM- AIME, 1968. vol. 242, p. 2-4.

177) D.T. Hawkins and R. Hultgren, 1967, vol. 239, p. 1046.

178) K. Atarashiya, M. Uta, M. Shimoji and K. Niwa, Bull. Chem. Soc. Japan, 1960, vol. 33, p. 706-10.

179) A.T. Aldred and J.N. Pratt, Trans. Faraday Soc., 1961, vol. 57, p. 611-624.

180) J.P. Hager and I.A. Wilkomirsky, Trans. TMS-AIME, 1968, vol. 242, p. 187.

181) R. Castanet, Y. Claire, M. Laffetti, J. Chim, Phys. 1969, vol. 66, p. 1276-85.

182) P.H. Sommelet; University of California, Lawrence Radiation Laboratory, UCRL-16303, 1965.

183) J. Kleppa, J. Physic. Chem., 1956, vol. 60, p. 446.

184) A.K. Jena and M.B. Bever, Trans TMS-AIME, 1967, vol. 239, p.1861.

185) S. Banya and J. Chipman, Trans TMS-AIME, 1969, vol. 245, p. 391.

186) L. Elford, F. Muller and O. Kubaschewski, Berichte der Bunsengesellschaft, 1969, vol. 73, p. 601.

187) R.N. Dokken and J.F. Elliott, Trans TMS-AIME, 1965, vol. 233, p. 1351-8.

188) T.C. Wilder, Trans TMS-AIME, vol. 233, p. 1202.

189) P.J. Spencer, Trans. Farad. Soc., 1968, vol. 64, p. 1470.

APPENDIX I.

The activity coefficient of solute 1 and the activity coefficient of solvent 2 are related by the Gibbs-Duhem relation:

$$N_1 \, d \ln \gamma_1 = - N_2 \, d \ln \gamma_2$$

or

$$\frac{d \ln \gamma_1}{d N_2} = - \frac{N_2}{(1-N_2)} \frac{d \ln \gamma_2}{dN_2}$$

One therefore obtains.

$$\frac{d \ln \gamma_1}{dN_1} = - \frac{d^2 \ln \gamma_2}{d N_2^2}$$

since $dN_1 = - dN_2$ and from L' Hospital's rule

$$\lim_{N_2 \to 1} \frac{d \ln \gamma_1}{dN_2} = \lim_{N_2 \to 1} \frac{d^2 \ln \gamma_2}{d N_2^2}$$

It can also be shown from L' Hospital's rule that

$$\lim_{N_2 \to 1} \frac{\ln \gamma_2}{(1-N_2)^2} = \lim_{N_2 \to 1} \frac{1}{2} \frac{d^2 \ln \gamma_2}{d N_2}$$

Therefore, at low concentration of the solute

$$\frac{\log \gamma_2}{(1-N_2)^2} = - \frac{1}{4.606} \epsilon_1^1$$

APPENDIX II.

If the co-ordination number of metal atom is denoted by Z and that of oxygen is taken as two, then the relative partial molar enthalpy of oxygen in A-B alloys is given by

$$\Delta \bar{H}_{O(A+B)} = N^{\circ}_{B}\left[\Delta \bar{H}_{O(B)} - \frac{2}{Z}\,\Delta \bar{H}_{B(A-B)}\right] + N^{\circ}_{A}\left[\Delta \bar{H}_{O(A)} - \frac{2}{Z}\,\Delta \bar{H}_{A(A+B)}\right]$$

where N°_{b} and N°_{A} are the molefraction of B and A in the co-ordination shells around oxygen atoms, and are obtained from

$$N^{\circ}_{A} = \frac{N_A}{KN_B + N_A} \qquad N^{\circ}_{B} = \frac{K N_B}{KN_B + N_A}$$

where $K = e^{\Delta G^{\ast} / RT}$

where $\Delta G^{\ast}$ is the excess free energy change when a B-O bond is changed to an A-O bond by the exchange of a B atom with an A atom in the surrounding solvent.

$$\frac{\Delta G^{\ast}}{RT} = \ln\left[\left(\frac{\gamma_{O(A)}}{\gamma_{O(B)}}\right)^{\frac{1}{2}}\left(\frac{\gamma_{B(A+B)}}{\gamma_{A(A+B)}}\right)^{1/Z}\right]$$

The partial molar entropy of oxygen at 1 at. pct. O in A-B alloy can be obtained as:

$$\Delta \bar{S}_{O(A+B)} = -2R\left[N^{\circ}_{A} \ln \frac{N^{\circ}_{A}}{N_A} + N^{\circ}_{B} \ln \frac{N^{\circ}_{B}}{N_B}\right] + N^{\circ}_{A}\,\Delta \bar{S}_{O(A)} + N^{\circ}_{B}\,\Delta \bar{S}_{O(B)}$$

$$- \frac{2}{Z} N^{\circ}_{A}\,\Delta \bar{S}^{Ex}_{A(A+B)} - \frac{2}{Z} N^{\circ}_{B}\,\Delta \bar{S}^{Ex}_{B(A+B)}$$

Combining the enthalpy and entropy, relative partial molar free energy of oxygen in A-B alloys is

$$\Delta \bar{G}_{O(A-B} = N^{\circ}_{B}\left[\Delta \bar{G}_{O(B)} - \frac{2}{Z}\,\Delta \bar{G}^{Ex}_{B(A+B)}\right] + N^{\circ}_{A}\left[\Delta \bar{G}_{O(A)} - \frac{2}{Z}\,\Delta \bar{G}^{Ex}_{A(A+B)}\right]$$

$$+ 2RT\left[N^{\circ}_{A} \ln \frac{N^{\circ}_{A}}{NA} + N^{\circ}_{B} \ln \frac{N^{\circ}_{B}}{NB}\right]$$